

This electronic thesis or dissertation has been downloaded from the King's Research Portal at <https://kclpure.kcl.ac.uk/portal/>



Evaluation of the toxicity of the brominated flame retardants, PBDE-47 and HBCD, in neuronal cell lines

Reffatto, Valentina

Awarding institution:
King's College London

The copyright of this thesis rests with the author and no quotation from it or information derived from it may be published without proper acknowledgement.

END USER LICENCE AGREEMENT



Unless another licence is stated on the immediately following page this work is licensed

under a Creative Commons Attribution-NonCommercial-NoDerivatives 4.0 International

licence. <https://creativecommons.org/licenses/by-nc-nd/4.0/>

You are free to copy, distribute and transmit the work

Under the following conditions:

- Attribution: You must attribute the work in the manner specified by the author (but not in any way that suggests that they endorse you or your use of the work).
- Non Commercial: You may not use this work for commercial purposes.
- No Derivative Works - You may not alter, transform, or build upon this work.

Any of these conditions can be waived if you receive permission from the author. Your fair dealings and other rights are in no way affected by the above.

Take down policy

If you believe that this document breaches copyright please contact librarypure@kcl.ac.uk providing details, and we will remove access to the work immediately and investigate your claim.

This electronic theses or dissertation has been downloaded from the King's Research Portal at <https://kclpure.kcl.ac.uk/portal/>

Title: Evaluation of the toxicity of the brominated flame retardants, PBDE-47 and HBCD, in neuronal cell lines

Author: Valentina Reffatto

The copyright of this thesis rests with the author and no quotation from it or information derived from it may be published without proper acknowledgement.

END USER LICENSE AGREEMENT



This work is licensed under a Creative Commons Attribution-NonCommercial-NoDerivs 3.0 Unported License. <http://creativecommons.org/licenses/by-nc-nd/3.0/>

You are free to:

- Share: to copy, distribute and transmit the work

Under the following conditions:

- Attribution: You must attribute the work in the manner specified by the author (but not in any way that suggests that they endorse you or your use of the work).
- Non Commercial: You may not use this work for commercial purposes.
- No Derivative Works - You may not alter, transform, or build upon this work.

Any of these conditions can be waived if you receive permission from the author. Your fair dealings and other rights are in no way affected by the above.

Take down policy

If you believe that this document breaches copyright please contact librarypure@kcl.ac.uk providing details, and we will remove access to the work immediately and investigate your claim.

Evaluation of the toxicity of the brominated flame retardants, PBDE-47 and HBCD, in neuronal cell lines

Valentina Reffatto

Thesis submitted in fulfilment of
the requirements for the Ph.D.
degree

Nutritional Sciences Research Division
King's College London
Franklin-Wilkins Building
Waterloo Campus
London, SE1 9NH

I Abstract

Polybrominated diphenyl ether (PBDE-47) and hexabromocyclododecane (HBCD) are brominated flame retardants (BFRs) commonly used in a wide range of consumer products. They bioaccumulate and persist in the environment, and have been detected in humans and wildlife. Their ability to pass the blood-brain barrier (BBB) and to accumulate in the brain has raised concern about the potential of BFRs to cause neurotoxicity.

Functional genomics was used to investigate the modes of action of PBDE-47 and HBCD in two neuronal cell models namely mouse neuroblastoma (N2A) and neuroblastoma x spinal cord (NSC-19).

It was established that PBDE-47 and HBCD reduce cell viability, increase lactate dehydrogenase (LDH) leakage and cause apoptosis as indicated by increased caspase-3 activity at low micromolar concentrations (1 - 4 μ M). A pre-incubation with the omega-3 fatty acid, docosahexaenoic acid (DHA), mitigated the toxic effect of HBCD in the N2A cell line, with a significant decrease in the LDH leakage. Transcriptome profiling revealed that exposure to PBDE-47 and HBCD affects expression of genes with overlapping functionalities. Both toxicants regulated genes related to calcium homeostasis, endoplasmic reticulum stress and lipid metabolism. Genes involved in thyroid hormone signalling, neurodegenerative diseases and nervous system development were also preferentially regulated. The fatty acid DHA altered the expression of genes that were also regulated by PBDE-47 or HBCD, and HBCD modulated DHA-induced gene expression. It was also established that HBCD exposure affect cellular zinc homeostasis, increasing the level of intracellular weakly bound Zn²⁺. This effect was ameliorated by the antioxidant NAC, suggesting that the [Zn²⁺] increase could have been caused by oxidative stress with release of Zn²⁺ from zinc-binding proteins. This result indicates for the first time that zinc signalling is a potential target of POP toxicity.

In conclusion, we established that PBDE-47 and HBCD have toxicity effects on cells of neuronal origin starting at a concentration of 1 μ M and that exposure to either of these BFRs causes regulation of genes related to many cellular functions, several of which have been observed as BFR phenotypes in animal studies. It was also shown that zinc is a POP toxicity target and that cellular effects of BFRs are modulated by DHA.

II Acknowledgements

I would like to thank all the people that have supported me during my PhD. First of all my supervisor, Professor Christer Hogstrand, for the help during all these years, especially in the writing up phase. A big thank you also to Prof. Israel Sekler and Dr. Michal Hershfinkel that who accepted me in Ben Gurion University and helped me during the time spent in Israel.

Special thanks go to my colleagues at King's, particularly to Dr. Thomas Carroll and Dr. Josef Rasinger, for being always next to me, especially in the difficult times, and for being true friends in all this years.

I would like also to thank all the friends that supported me in this time, especially in the most stressful periods. Thanks for listening for hours and hours, for being there when I needed, for all the understanding, for the English proof-reading and for letting me sleep on your couch/bed/floor anytime I needed.

Vorrei anche ringraziare la mia famiglia, che ha sempre appoggiato la mia scelta di studiare lontano da casa, ma comunque non facendomi mai sentire sola. Un grande grazie anche a tutte le zie, zii e cugini, a cui ho spiegato molte volte cosa ho fatto per gli scorsi tre anni, e che ancora per molti anni continueranno probabilmente a chiederlo.

Grazie anche a tutti gli amici incontrati in questi anni a Londra. Quando si e' lontani da casa le persone che ti circondano diventano un po' come la tua famiglia, e io ho sempre saputo che avrei potuto contare su di voi, e lo so ancora oggi. Un grazie anche a quelli lasciati in Italia, perche' ogni volta che torno a casa, e' come non fossi mai partita.

A voi tutti: grazie...non ce l'avrei mai fatta senza di voi!!!

To all of you: thanks...I wouldn't have made it without you!

III Table of Contents

I Abstract	2
II Acknowledgements	3
III Table of Contents	4
IV List of Figures.....	9
V List of Tables	12
VI List of Equations.....	13
VII List of Abbreviations	14
1.General Introduction	19
1.1 Persistent Organic Pollutants and Brominated Flame Retardants	20
1.2 POPs toxicity in the brain.....	23
1.3 The model contaminants.....	24
1.3.1 2,2',4,4'-tetrabromodiphenyl ether (PBDE-47).....	24
1.3.2 PBDEs in the environment, in biota and in humans	25
1.3.3 PBDE toxic mechanisms	27
1.3.4 1,2,5,6,9,10-Hexabromocyclododecane–HBCD	30
1.3.5 HBCD in the environment, in biota and in humans.....	31
1.3.6 HBCD toxic mechanism	35
1.4 Assessment of toxicology <i>in vitro</i>	37
1.4.1 Mechanistic Toxicology.....	37
1.4.2 Toxicology effects on a genomic scale: gene expression analysis	38
1.5 Projects Aims	41
1.6 Hypothesis and Objectives	42
2.Materials and Methods	44

2.1 Chemicals	45
2.2 Cell Culture.....	45
2.3 Cell viability test	46
2.4 Assessment of Apoptosis.....	47
2.4.1 Caspase-3 assay	47
2.5 Toxicology assay lactate dehydrogenase (LDH) based	48
2.6 Decosahexanoic acid (DHA) effects on HBCD toxicology	50
2.6.1 DHA solubility	50
2.7 Gene Expression Analysis	51
2.7.1 Preparation for Oligonucleotide Array Printing	52
2.7.2 Sample Preparation	53
2.7.3 Microarray.....	58
2.8 Confirmation of differentially expressed genes with Real Time PCR (Q-PCR)..	60
2.8.1 cDNA Synthesis	60
2.8.2 Real time Q-PCR.....	60
2.8.3 Primers tested	62
2.8.4 Housekeeping gene selection	64
2.8.5 Efficiency test.....	65
2.8.6 Analysis of Real Time PCR data.....	66
2.8.7 Agarose gel Electrophoresis.....	66
2.9 Zinc regulation investigation	66
2.9.1 Zinc assay on cells grown on coverslip.....	66
2.9.2 Zinc assay using 96-wells plate.....	67
2.10 Statistical analysis	69
3.PBDE-47 and HBCD cytotoxicity assessment.....	70
3.1 Introduction.....	71

3.1.1 Docosahexaenoic acid (DHA) and lipid regulation	72
3.1.2 Chapter objectives	74
3.2 Methods	74
3.3 Results	74
3.3.1 Effect on cell viability during exposure to PBDE-47 or HBCD.....	74
3.3.2 Assessment of apoptosis in cells exposed to PBDE-47 or HBCD.....	76
3.3.3 Lactate Dehydrogenase (LDH) leakage as a marker of membrane permeability damage in cells exposed to HBCD.....	78
3.3.4 Effect of the fatty acid DHA on LDH leakage caused by HBCD toxicity	79
3.4 Chapter discussion	81
3.5 Chapter conclusion.....	84
4.PBDE-47 and HBCD gene expression profile	85
4.1 Introduction.....	86
4.2 Methods	88
4.2.1 Microarray analysis in cells exposed to PBDE-47 and HBCD	88
4.2.2 Statistical analysis.....	93
4.2.3 Post-analysis: DAVID and IPA.....	93
4.2.4 Chapter objectives	94
4.3 Genes regulated in cells exposed to PBDE-47 of HBCD.....	94
4.3.1 Functional enrichment regulated by PBDE-47 or HBCD	97
4.3.2 Pathways analysis of genes regulated by PBDE-47 or HBCD.....	103
4.4 Confirmation of significant genes regulated by PBDE-47 or HBCD using real- time PCR	107
4.4.1 Q-PCR analysis of genes regulated by PBDE-47	108
4.4.2 Q-PCR analysis of genes regulated by HBCD	111
4.5 General discussion	115
4.5.1 Gene expression profile	116

4.6 Chapter conclusion	129
5. Post-transcriptomics analysis	132
5.1 Introduction.....	133
5.1.1 Zinc and the brain	134
5.1.2 Docosahexaenoic acid (DHA) and the brain	135
5.1.3 Chapter objectives	138
5.2 Methods	138
5.3 Results	138
5.3.1 Intracellular zinc response after exposure of cells to the nitric oxide (NO) donor Nitroprusside.....	138
5.3.2 Intracellular zinc response after cells exposure to HBCD.....	140
5.3.3 Investigation of the mechanism involved in the zinc release caused by HBCD	143
5.4 DHA and HBCD interactions on gene expression.....	146
5.5 Chapter discussion	154
5.5.1 HBCD effects on zinc homeostasis	154
5.5.2 DHA effect on the gene expression	158
5.6 Chapter conclusion.....	163
6. General Discussion	165
6.1 PBDE-47 and HBCD cytotoxicity	166
6.2 Gene expression and functional enrichment terms	168
6.3 Microarray follow-up studies.....	176
6.3.1 HBCD effects on zinc homeostasis	176
6.3.2 DHA effect on gene expression and on HBCD cytotoxicity.....	177
6.4 General conclusion and future prospective	179
APPENDECES	185
Appendix 1.....	185

Appendix 2.....	191
Appendix 3.....	200
References	209

IV List of Figures

Figure 1.1: World capture and aquaculture production.....	23
Figure 1.2: polybrominated diphenil ether (PBDEs) chemical structure (Figure A), 2,2',4,4'-tetrabromodiphenyl ether (PBDE-47) chemical structure (Figure B).....	25
Figure 1.3: Amounts of total PBDEs and the individual PBDE congener, PBDE-47, in food groups from the US.....	27
Figure 1.4: 1,2,5,6,9,10-HBCD chemical structure.....	31
Figure 1.5: Usage of different brominated flame retardants as a percentage of total brominated flame retardant usage.....	32
Figure 1.6: Amounts of HBCD in differing food groups in the USA.....	33
Figure 1.7: 2-colour microarray.....	40
Figure 3.1: Cell viability of N2A cell line (figure A) and NSC19 cell line (figure B) exposed to PBDE-47.....	75
Figure 3.2: Cell viability of N2A cell line (figure A) and NSC19 cell line (figure B) exposed to HBCD.....	76
Figure 3.3: Caspase-3 activity in cells exposed to PBDE-47.....	77
Figure 3.4: Caspase-3 activity in cells exposed to HBCD.....	78
Figure 3.5: LDH leakage from N2A cells exposed to HBCD for 24 hours.....	79
Figure 3.6: Effects of DHA on LDH leakage from N2A cells exposed to HBCD.....	80
Figure 4.1: Visualisation of the spreads of intensities between and within arrays.....	90
Figure 4.2: Comparison of the Log2 fold change between arrays.....	91
Figure 4.3: Fluorescence intensity within array.....	92
Figure 4.4: Commonality in gene expression responses to PBDE-47 or HBCD between N2A and NSC cells.....	96

Figure 4.5: Commonality in gene expression responses from PBDE-47 and HBCD.....	96
Figure 4.6: Lipid methabolism, small molecule biochemistry, cell death pathway.....	104
Figure 4.7: Immunological disease, cancer, connective tissue disorders pathway	105
Figure 4.8: Cellular function and maintenance, cell morphology, cell death pathway.....	106
Figure 4.9: Cellular growth proliferation, cancer, DNA replication, recombination and repair pathway.....	107
Figure 4.10: Log ₂ fold change of genes regulated by PBDE-47.....	111
Figure 4.11: Log ₂ fold change of genes regulated by HBCD in the N2A cell line.....	113
Figure 4.12: Log ₂ fold change of genes regulated by HBCD in the NSC19 cell line.....	115
Figure 4.13: Representation of genes regulated by either PBDE-47 or HBCD linked to neurodegenerative disorders.....	120
Figure 5.1: Preliminary method validation testing the intracellular zinc detection using the dye, Zynpyr1	139
Figure 5.2: Intracellular zinc release in the N2A cell line exposed to a NO donor.....	140
Figure 5.3: Intracellular zinc release detected with the fluorescent dye Zyncpyr1	141
Figure 5.4: Intracellular Zinc in N2A cells exposed to HBCD for 24h.....	142
Figure 5.5: Intracellular zinc in N2A cells exposed to HBCD for 24 hours.....	143
Figure 5.6: Intracellular zinc in the N2A cell line with or without DEDTC.....	144
Figure 5.7: Intracellular zinc in the N2A cell line exposed to HBCD with or without NAC	145

Figure 5.8: Intracellular zinc in the N2A cell line exposed to HBCD with or without L-name	146
Figure 5.9: DHA and HBCD interactions on expression of the App gene.....	148
Figure 5.10: DHA and HBCD interactions on expression of the Bace1 gene.....	149
Figure 5.11: DHA and HBCD interactions on expression of the Hspa5 gene.....	150
Figure 5.12: DHA and HBCD interactions on expression of the Pnpla8 gene.....	151
Figure 5.13: DHA and HBCD interactions on expression of the Homer1 gene.....	152
Figure 5.14: DHA and HBCD interactions on expression of the Tubb2c gene.....	153

V List of Tables

Table 2.1: gene symbol and sequence of the primers tested in Q-PCR Purchased from PrimerDesign.....	62
Table 2.2: gene symbol, QIAGEN ID number and detected transcript of the primers tested in Q-PCR purchased from Qiagen.....	63
Table 2.3: gene symbol and accession number of the primers evaluated as candidate housekeeping genes.....	64
Table 4.1: Number of genes called significantly regulated in cells exposed to PBDE-47.....	94
Table 4.2: Number of genes called significantly regulated in cells exposed to HBCD.....	95
Table 4.3: Enriched Gene Ontology annotation terms among significant genes regulated by PBDE-47 in the N2A cell line.....	98
Table 4.4: Enriched Gene Ontology annotation terms among significant genes regulated by PBDE-47 in the NSC19 cell line.....	99
Table 4.5: Enriched Gene Ontology annotation terms among significant genes regulated by HBCD in the N2A cell line.....	101
Table 4.6: Enriched Gene Ontology annotation terms among significant genes regulated by HBCD in the NSC19 cell line.....	102
Table 4.7: fold change of genes regulated by PBDE-47 in the N2A cell line and confirmed with Q-PCR.....	109
Table 4.8: fold change of genes regulated by HBCD in the NSC19 cell line and confirmed with Q-PCR.....	110
Table 4.9: fold change of genes regulated by HBCD in the N2A cell line and confirmed with Q-PCR.....	112
Table 4.10: fold change of genes regulated by HBCD in the NSC19 cell line and confirmed with Q-PCR.....	114

VI List of Equations

- Equation 2.1:** Frequency of Incorporation (FOI) calculated considering the total pmols/ μ l of Cy dyes incorporated into the c-DNA.....57
- Equation 2.2:** Nucleotide Incorporation (NI) calculated considering the total pmols/ μ l of Cy dyes incorporated into the c-DNA.....58
- Equation 2.3:** primer's Efficiency expressed in percentage calculated from the slop of the Ct values of the 10 fold dilution samples.....65

VII List of Abbreviations

AA	Arachidonic Acid
ACSL4	Acyl-CoA synthetase type 4 for long chain fatty acids
AD	Alzheimer's disease
AhR	Aryl Hydrocarbin Receptor
APP	Amyloid Precursor Protein
A β	Amyloid-beta peptide
BACE1	beta-site APP-cleaving enzyme 1
BACE2	Beta-site APP-cleaving enzyme 2
BBB	Blood Brain Barrier
BFR	Brominated Flame Retardant
BW	Body Weight
Ca ²⁺	Calcium
CACNA1C	Calcium channel, voltage-dependent, L type, alpha 1C subunit
CAMK2D	Calcium/Calmodulin-dependent Protein Kinase II Delta
CAR	Constitutively Active/Androstane Receptor
CGC	Cerebellar granule cells
DL	Dioxin-like
DRE	Dioxin responsive element
CNS	Central Nervous System
DHA	Docosahexaenoic Acid

ECHA	European Chemicals Agency
EDN1	Endothelin 1
EEA	European Union's European Environment Agency
EFSA	European Food Safety Authority
EGR1	Early growth response 1
EPA	Eicosapentaenoic Acid
EPA	Environmental Protection Agency
EPS	Expanded Polystyrene
ER	Endoplasmic Reticulum
FAO	World Food Organisation
FDA	Food and Drug Administration
FASN	Fatty acid synthase
FDR	Benjamini Hochberg False Discovery Rate
FGF2	Fibroblast growth factor 2
FOS	FBJ murine osteosarcoma viral oncogene homolog
GO	Gene Ontology
HBCD	Hexabromocyclododecane
HIP1	Huntingtin interacting protein 1
HOMER1	Homer homolog 1
HSPA5	Heat Shock Protein 5
IC50	Half maximal inhibitory concentration
IP3	Inositol Triphosphate

IPA	Ingenuity Pathway Analysis Software
KEGG	Kyoto Encyclopaedia of Genes and Genomes
KIFAP3	Kinesin-associated protein 3
K _{ow}	Octanol/Water Coefficient
LA	Linoleic Acid
LC50	Half maximal lethal concentration
LDH	Lactic dehydrogenase
MDA	Malondialdehyde
mGluR	Metabotropic glutamate receptor
N2A	Neuroblastoma cell line
NFKB2	Nuclear factor of kappa light polypeptide gene enhancer in B-cells 2
NGFR	Nerve Growth Factor Receptor
NMYC	V-myc myelocytomatosis viral related oncogene, neuroblastoma derived
NSC19	Neuroblastoma and spinal cord cell line
P-450	Cytocrome P-450 Monooxygenase
PAWR	Prostate apoptosis response 4 protein
PBDE	Polybrominated Diphenyl Ethers
PBT	Persistent, Bioaccumulative and Toxic
PCB	Polychlorinated biphenyl
PD	Parkinson's Disease
PINK1	PTEN induced putative kinase 1
PKC	Protein kinase C

PNPLA8	Patatin-like phospholipase domain containing 8
POP	Persistent Organic Pollutants
PRKCA	Protein kinase C, alpha
PUFA	Polyunsaturated Fatty Acid
PXR	Pregnane X Receptor
Q-PCR	Quantitative Polymerase Chain Reaction
RARA	Retinoic acid receptor, alpha
RB1	Retinol binding protein 1
RBP4	Retinol binding protein4
ROS	Reactive Oxygen Species
RyR	Ryanodine Receptor
SIRT1	Sirtuin 1
T3	Triiodothyronine
T4	Thyroxin
TBCB	Tubulin folding cofactor B
TCDD	Tetrachlorodibenzo-p-dioxin
TC-NES	Technical Committee on new and existing substances
TEF	Toxic Equivalency Factor
TG	Thyroglobulin
TRIP6	Thyroid hormone receptor interacting protein 6
TSH	Thyrotropin
TTR	Transthyretin

TUBA1A	Tubulin alpha 1a
TUBB2C	Tubulin, beta 2C
UPR	Unfolded Protein Response
WHO	World Health Organization
XBP1	X-box binding protein 1
XPS	Extruded Polystyrene
Zn ²⁺	Ionic zinc
[Zn ²⁺]	Ionic zinc concentration

1. General Introduction

1.1 Persistent Organic Pollutants and Brominated Flame Retardants

Persistent Organic Pollutants (POPs) are chemical substances that persist in the environment, bioaccumulate through the food chain, and pose a risk of causing adverse effects to human health and the environment (de Wit et al. 2010). POPs are man-made products for commercial and industrial uses, but there is evidence of long-range transport of these substances to regions where they have never been used or produced (de Wit et al. 2010). The consequent threats they cause to the environment of the whole globe, have prompted governments to establish organizations, such as the US's Environmental Protection Agency (EPA), the Food and Drug Administration (FDA), the European Union's European Environment Agency (EEA) and the European Food Safety Authority (EFSA), to evaluate and monitor the impact of POPs on biota and human health.

More important, an international environment treaty named Stockholm Convention on Persistent Organic Pollutants, was signed in 2001 with the aims to control the production and use of persistent organic pollutants. From 2001, the Stockholm Convention banned the intentional production, marketing and use of the 12 POPs of greatest concern (including insecticides such as Aldrin and Dieldrin and pesticides such as DDT), the so-called *dirty dozen*. At the Fourth Conference of Parties in 2009, nine more chemicals were added to the list (Roosens et al. 2010). Among these chemicals were several Polybrominated Diphenyl Ethers, which are also known as Brominated Flame Retardants (BFR).

For most people, dietary sources are the main route of exposure to POPs. Most POPs display low water and high lipid solubility and a resistance to degradation in the environment. Due to their lipophilic characteristics they preferentially bioaccumulate and remain in fatty tissues of animals. Therefore food such as meat, dairy products and fish can contain significant levels of POPs which, over a lifetime of dietary exposure, may lead to toxic levels in humans. Other processes of exposure, including air and dust pollution or occupational exposure, are possible, but they are minor contributions to the general public.

One group of POPs, called Brominated Flame Retardants (BFRs), has recently raised attention especially due to their ubiquitous presence in the biosphere and their

accumulation in human tissue. In fact, in many studies conducted on the US and European populations, they have been detected in serum and breast milk (Darnerud et al. 2009; Schechter et al. 2008)

BFRs are chemical compounds that, in order to meet fire safety regulation, are added or applied to combustible materials to increase their fire resistance (Birnbaum and Staskal 2004a). They have been extensively used since the early 1970s, but in the last decade the demand of BFRs has increased substantially. During the 1990s, market demand was in the order of 145000 tonnes per year, and in 2000 it increased to 310000 per year, and thus, the consumption of BFRs more than doubled, probably due to the increased use of polymeric materials in construction, electronic and computer equipment (Alaee et al. 2003a)

BFRs are produced via direct bromination of organic molecules, or via addition of bromine to alkenes (Alaee et al. 2003b). They can be divided into three groups, based on the different mode of incorporation of bromine into the material: brominated monomers, reactive and additive. Reactive flame retardants are chemically bonded into the plastics. Brominated monomers and additive flame retardants are simply mixed with the polymer; as a result, they can easily leach into the environment after the disposal of the consumer product at the end of its life-cycle (Alaee et al. 2003b).

Recently, concern about BFRs accumulation in fish, and especially in farmed fish, has raised attention about the safety of fish consumption. Several studies reported that concentrations of BFRs are significantly higher in farmed salmon than in wild fish (Foran et al. 2005b; Hites et al. 2004a). The main reason for the difference in contaminant concentration between wild and farmed fish was suggested to relate to the difference in their diets (Hites et al. 2004a). Farmed salmon is fed a diet high in fish oil and fishmeal derived from other marine fish, which are gathered in contaminated waters near the coastline, whilst their wild relatives live and feed in less contaminated open waters. Farmed salmon has particularly raised attention because, as carnivorous fish, it has high probability to be exposed to POPs and to bioaccumulate contaminants. However, in contrast with that reported above, more recent studies conclude that the level of POPs in wild carnivorous fish are comparable in the ones observed in farmed conspecifics (Schechter et al. 2010b; Schechter et al. 2010a).

BFR is only one of several groups of POPs that accumulates in fish. A wide range of chemicals from pesticides and polychlorinated biphenyls (PCBs) to organic compounds

and dioxin, are detected in water and fish, and are considered toxic to aquatic organisms, as well as to humans that eat fish. Contaminant common in fatty fish include the priority substances listed by the Stockholm Convention and it has been suggested that their combined concentrations in fish fillet on the market poses a significant health concern (Foran et al. 2005b; Foran et al. 2005a; Hites et al. 2004a). Metal mercury is also considered one of the main pollutants that accumulate in fish. Mercury can be transported in the atmosphere and fall onto terrestrial and aquatic ecosystems as precipitation or dry deposition. In aquatic systems, mercury may eventually be transformed into monomethyl mercury, a form that is bioaccumulative and can harm fish, wildlife, and humans. Today the detection of BFRs and other POPs in fish remain a serious issue and because of the limited information on their long-term consequences on human health it is difficult to assess the risks of fish consumption.

The demand for fish rose by 21% between 1992 to 2002 to increase further on in the past years (FAO 2004). In the past 50 years fisheries production has registered a low ability to expand where the rate of increase growth achieved a value near to zero in 1990s, indicating that capture fisheries production have reached their maximum potential (FAO 2008). Therefore, to be able to satisfy the increasing demand of fish, World aquaculture has grown extensively during the same 50 years period (FAO 2008), and, as reported in figure 1.1, will keep expanding for the next 20 years (FAO 2008). Salmon farming has dramatically increased in the last decade (Hites et al. 2004a) as, according to FAO, fish in the family of Salmonidae (trout and salmon) are one of the groups with the highest demand (FAO 2004).

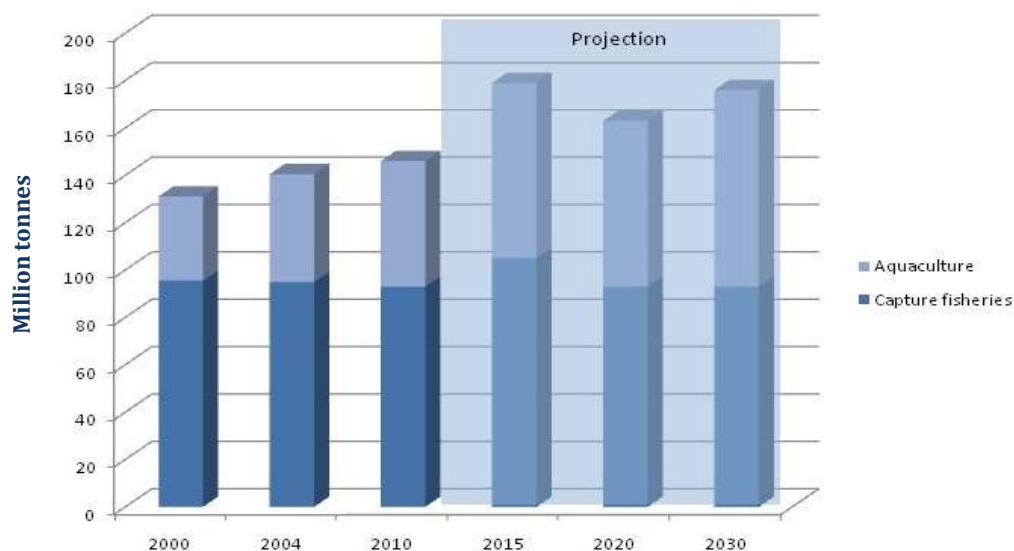


Figure 1.1: World capture and aquaculture production. The graph shows aquaculture production (light blue) and capture fisheries (dark blue) expressed in million tonnes. The past 10 years of production is presented and a prediction for the next 20 years is also reported. From 2000s the increase in growth rate of capture fisheries production achieved a value near to zero, indicating that capture fisheries production have reached their maximum potential. To satisfy the increasing demand of fish, World aquaculture has grown extensively over the same period and will keep growing for the next 20 years (FAO 2008).

1.2 POPs toxicity in the brain

Lipophilic compounds are easily absorbed by the organism and are normally metabolised by processes collectively referred to as biotransformation, to facilitate their excretion by increasing their water solubility. If biotransformation fails, they can get distributed throughout the body and accumulate in fatty tissue. On the other hand, in some cases the metabolites produced during the biotransformation are more toxic than the parent compound (M. M. Dingemans et al. 2008a).

The central nervous system (CNS) is arguably the most critical and sensitive system in the human body. It is also extremely sensitive to a wide range of chemicals and therefore it is essential that the interface between the CNS and the peripheral circulatory system functions as a barrier to potentially harmful molecules (Hawkins and Davis 2005). The capillaries in the brain and in the spinal cord are surrounded by endothelial cells and a collagen matrix that form the Blood Brain Barrier (BBB). The BBB is a physical and metabolic barrier that restricts the passage of substances from the blood to

the brain and helps maintain brain homeostasis (Hawkins and Davis 2005). The BBB is impermeable for many compounds except small lipophilic substances, which can easily cross to the brain by diffusion (Hawkins and Davis 2005).

Despite the BBB protection, various POPs still manage to penetrate into the brain by diffusion, and therefore to accumulate. *In vivo* studies showed that after exposure to POPs, the chemicals are mainly detected in adipose tissue, liver and brain (P. R. S. Kodavanti et al. 1998; Szabo et al. 2010a). Studies in mice have shown that while exposure to POPs during gestation may lead to congenital effects (Curran et al. 2011), later exposure during brain development can cause disturbed spontaneous behaviour in adults (Alm et al. 2008; Per Eriksson et al. 2006; Viberg et al. 2003b).

1.3 The model contaminants

1.3.1 2,2',4,4'-tetrabromodiphenyl ether (PBDE-47)

Polybrominated biphenyl ethers (PBDEs) are chemicals used as a flame retardants in various consumer products, mainly in electrical equipment, plastics, furniture, food packaging and textiles as an additive in polyurethane foams, in resins and polyesters (Birnbaum and Staskal 2004a). As shown in figure 1.2 A, PBDEs are characterized by two phenyl rings joined by an oxygen bridge and contains 10 hydrogen atoms, each of which can be substituted with bromine giving different degree of bromination (Alaee et al. 2003b).

The positioning of the bromine atoms around the biphenyl ring can affect the three-dimensional structure of the PBDE. The PBDE of interest in this study is PBDE-47, which was chosen as it is one of the major congeners of the commercial mixture DE-71, and one of the more bioaccumulative and persistent, and therefore present at particularly high levels in biota including fish. It is characterised by four bromine atoms next to the ether linkage in both phenyl rings (2,2',4,4') causing the molecule to be non-planar. Figure 1.2 B.

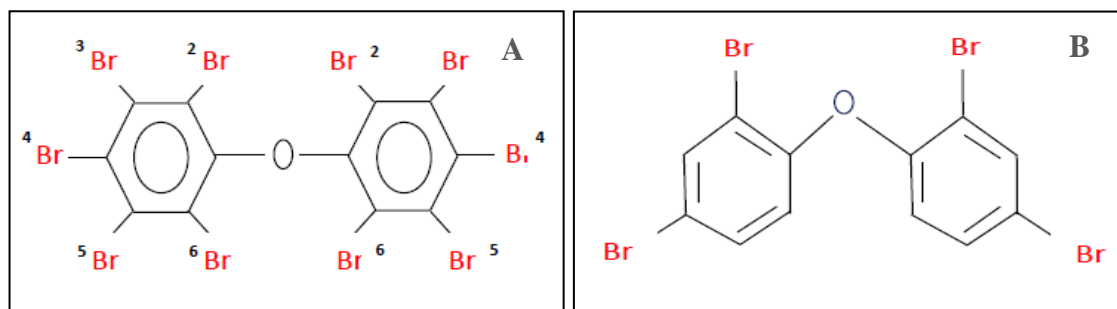


Figure 1.2: polybrominated biphenyl ether (PBDEs) chemical structure (Figure A). PBDEs are characterized by two phenyl rings joined by one oxygen bridge. The basic structure has 10 hydrogen atoms; each of them can be substituted for bromine giving different degree of bromination. **2,2',4,4'-tetrabromodiphenyl ether (PBDE-47) chemical structure (Figure B).** PBDE-47 is characterised by two phenyl rings and four bromines in position 2,2',4,4'.

PBDEs potentially involve 209 different congeners but the principal forms are Penta-BDE, Octa-BDE and Deca-BDE. The commercial mixtures DE-71 consists of over 20 different congeners and it is constituted primarily of 2,2',4,4'-tetrabromodiphenyl ether (PBDE-47; 38%) and 2,2',4,4',5-pentabromodiphenyl ether (PBDE-99; 49%); collectively these two congeners account for >80% of the mixtures (Coburn et al. 2008).

1.3.2 PBDEs in the environment, in biota and in humans

Most commercial PBDE-mixture are not chemically bonded to the material but simply blended with the polymers and therefore they are likely to leach out after the disposal of the consumer product at the end of its life-cycle. (Alaee et al. 2003b). PBDEs can also evaporate into the indoor environment from electronics and other PBDE-containing household or office products. Also materials containing PBDEs degrade with age and use, releasing PBDEs as they break down (NRDC, 2008). Since PBDEs are resistant to degradation, particularly the less brominated PBDEs, such as PBDE-47, they are now ubiquitous in the environment. In fact, PDBEs have been detected in soil, air and water (Birnbaum and Staskal 2004b).

Since the beginning of 2000, the level of PBDEs in the environment and in human samples has been increasing rapidly. As a consequence, in August 2004 the European Union banned the use of Penta and Octa-PBDE in all products, following earlier individual restrictions in Sweden, Denmark, Germany and the Netherlands. In 2007 also the Penta-PBDE mixture, DE-71, mainly constituted by penta and tetra-bde was banned.

In July 2006, the EU also banned Deca-PBDE for use in electronic products (BSEF, 2008). However, these restrictions do not inhibit the disposal of previously produced PBDE products which will continue to enter the environment by dumping and incomplete incineration.

The lower brominated PBDEs congeners (four to seven bromines) are more resistant to degradation and therefore more bioaccumulative and persistent. This is reflected by increasing concentrations of the smaller PBDEs, such as the penta and tetra PBDEs, in animals and in the food chain (Birnbaum and Staskal 2004b). PBDE-47 is the PBDE found at the particularly high levels in biota, which can be explained considering that PBDE-47 is the major congener of the DE-71 mixtures (Birnbaum and Staskal 2004b).

A study conducted on food samples from the US market showed that PBDEs are found at high levels in fish, with greater concentrations compared to those found in other food groups such as meat, eggs or dairy products (Schechter et al. 2006; Schechter et al. 2010b). Especially fatty fish, such as salmon, are reported to have very high concentration of POPs (Hites et al. 2004b). (Figure 1.3).

More recently, the European Food Safety Authority (EFSA) published a scientific Opinion on PBDEs in food, reporting data provided by 11 European countries on the analysis of 19 PBDE congeners in 3,971 food samples. Among the congeners, the highest dietary exposure was concluded to be PBDE-47 and -209. EFSA reported that the concentration of PBDEs in various food groups differ depending on the congeners (EFSA 2011a).

Alongside with the increase of PBDEs levels in the environment and in biota, also the levels in human tissue raised rapidly in the recent years (Hooper and McDonald 2000). In fact, in a recent study PBDEs have been detected in human milk and blood serum in US patients at much higher levels than what observed in the 1970s (Schechter et al. 2008). In the EFSA report, it was concluded that the average dietary human exposure to PBDE-47 across European countries is between 0.29 and 1.91 ng/kg b.w. per day (EFSA 2011a).

However, EFSA concluded that for the congeners PBDE-47, -153 and -209 current dietary exposure in the EU does not raise a health concern. For BDE-99 there is a potential health concern with respect to current dietary exposure. Also additional

exposure to PBDEs, such as through dust pollution, does not raise health concern (EFSA 2011a).

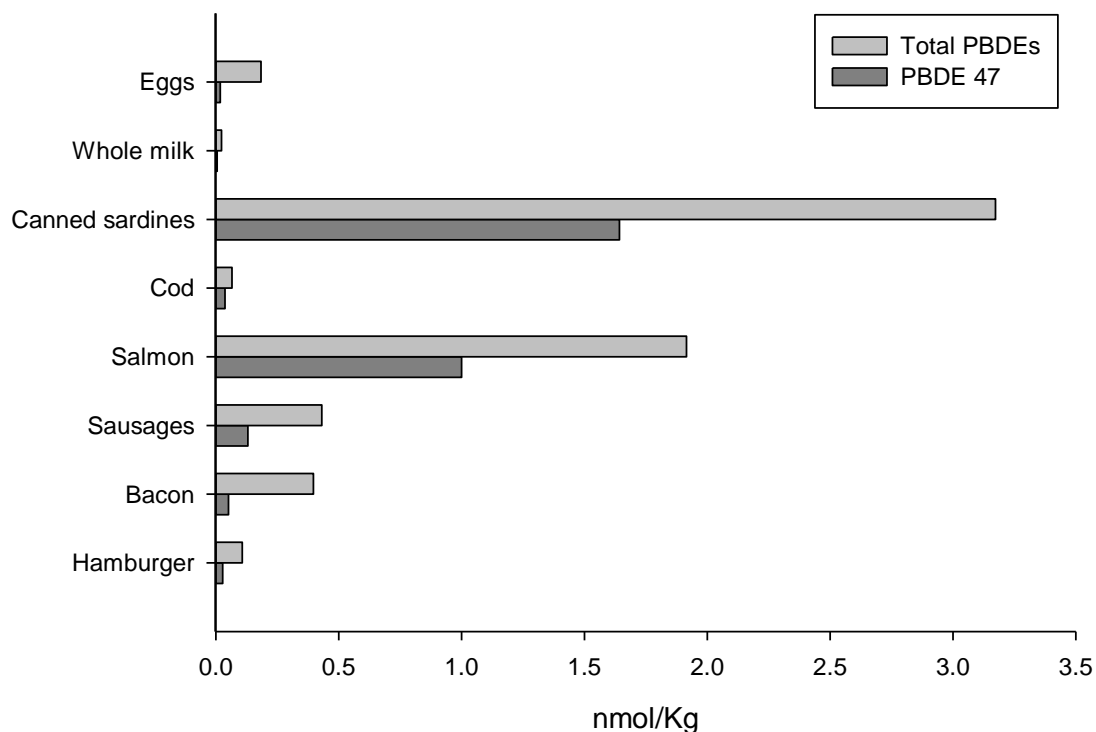


Figure 1.3: Amounts of total PBDEs and the individual PBDE congener, PBDE-47, in food groups from the US. PBDEs and PBDE-47 were measured in food samples from the US market. Both the fatty fish groups, canned sardines and salmon, are seen to have far higher levels of total PBDEs than any other food groups tested. PBDE-47 is clearly shown to be a dominant PBDE congener and represents over half the total PBDEs in all fish groups. Figure is drawn for presentation here from original data (Schechter et al. 2006; Schechter et al. 2010b).

1.3.3 PBDE toxic mechanisms

Early life exposure to PBDE has shown to cause neurological effects in rodents with effects on learning and memory functions and permanent aberrations in spontaneous behaviour (P. Eriksson et al. 2001). These effects have been associated with perturbation of calcium homeostasis and protein kinase C (PKC) signalling (Coburn et al. 2008; P. R. Kodavanti 2005) and with changes in levels of Arachidonic Acid (AA) and phospholipase A2 (P. R. Kodavanti and Derr-Yellin 2002). It has also been shown that exposure to PBDEs causes a reduction in the numbers of nicotinic cholinergic receptors in the mouse brain (Viberg et al. 2003c).

PBDE mixtures have been seen to affect circulating thyroid hormone levels (Birnbaum and Staskal 2004b; Darnerud et al. 2007) allegedly due to competitive binding to the thyroid hormone transport protein transthyretin (TTR). In fact it has been suggested that in particular hydroxylated PBDE metabolites, interfere with the thyroid hormone transport system preventing T4 from binding TTR and thus decreasing the circulating hormone level (Hallgren and Darnerud 2002b). The metabolite PBDE-47 has also been shown to disrupt thyroid hormone homeostasis with decrease of circulating T4 in mice studies. This decrease in the TH level coincided with the decrease of TTR in the plasma (Hallgren et al. 2001b; Hallgren and Darnerud 2002a).

PBDEs have been shown to affect cellular calcium homeostasis in *in vivo* and *in vitro* studies (Coburn et al. 2007; M. M. Dingemans et al. 2008a; P. R. Kodavanti 2005). PBDE-47 was seen to cause effects on calcium buffering and subsequent events such as alteration of PKC translocation in a concentration dependent manner (P. R. S. Kodavanti and Ward 2005). Previous work with DE-71 has demonstrated that in a cell-free preparation, this mixture at low concentrations is capable of inhibiting calcium uptake by microsomes and mitochondria (P. R. S. Kodavanti and Ward 2005). The same experiment was repeated for the congeners PBDE-47 which showed similar activity compared to the commercial mixture (Coburn et al. 2008).

Temporal Ca^{2+} oscillations in neurons may be stimulated by many factors leading to Ca^{2+} influx through plasma membrane bound ion channels and release from intracellular stores operated by inositol 1,4,5-triphosphate receptor (IP3R) and ryanodine receptor (RyR) (Coburn et al. 2008). PBDEs have similar chemical structure and physicochemical properties to some other POPs such as polychlorinated biphenyls (PCBs). In a recent study it was reported that PCB directly affects RyR, and the hypothesis that PBDE toxic activity on calcium homeostasis may be related to the same mechanism has been suggested (Pessah et al. 2010). The endoplasmic reticulum (ER) is considered as a focal point for possible calcium influx into the cytosol. (Pessah et al. 2010). Confirming this hypothesis, transcriptional changes associated with ER stress and with the unfolded protein response (UPR) have been seen after exposure of adrenocortical carcinoma cells to hydroxylated-PBDEs, suggesting that PBDE-47 effects on calcium homeostasis are a direct consequence of the disruption of ER processes (R. F. Song et al. 2009b).

Controversial opinions regarding the interaction between PBDE and the DNA binding receptor Aryl hydrocarbon receptor (AHR) have been reported in literature. AHR interacts with the dioxin responsive element (DRE) which results in the alteration of expression of a number of AHR dependent genes including cytochrome P450 enzymes from the CYP1A and CYP1B families (Chiaro et al. 2007). Activation of the constitutive androstane receptor (CAR) and pregnane X receptor (PXR) pathway may be also influenced by the AHR (Patel et al. 2007). The CAR/PXR pathways are known to be important in drug metabolism and have been previously associated with phenobarbital toxicity as well as with exposure to other xenobiotics (Waxman 1999). A POP with particularly strong affinity for the AHR is the dioxin 2,3,7,8-Tetrachlorodibenzo-p-dioxin (TCDD) and due to this characteristic it is used as a benchmark to which all dioxin-like (DL) toxicants are compared. This toxicity rating is termed the Toxic Equivalency Factor (TEF) and on its scale of zero to one, 2,3,7,8-TCDD has a TEF of one (Van den Berg et al. 2006). The ability for a toxicant to bind AHR is related to its chemical structure.

AHR has a strong affinity for co-planar hydrocarbons dioxins, which suggest that PBDE-47, as a non-planar congener, may act as a non dioxin-like compound. Little is known about the interaction of PBDE with the AHR, but an *in vivo* study in rats has shown that PBDE-47 is a weak inducer of the AHR related pathway, reporting a limited effect on the P450 enzymes CYP1A1, CYP2B1 and 2B2 (Richardson VM 2005). In the same study PBDE-47 was seen to induce PXR/CAR regulated genes and PBDE-47 showed to be more efficacious than the commercial mixture DE-71, indicating that PBDE-47 can cause both a weak dioxin-like effect and a phenobarbital-like/non dioxin-like effects (Richardson VM 2005). On the other hand, studies suggested that the effect on AHR activation caused by PBDE-47 could be due to trace of contaminants present in the compound (Luthe et al. 2008; Wahl et al. 2008a). In the study by Wahal et al (2008), analysis of the used PBDE-47 identified impurities such as 0.04% of 2,3,7,8-tetrabromo-dibenzofuran (TBDF) and 0.03% of 1,2,3,7,8-pentabromo-dibenzofuran (PBDF). In another study, similar concentrations of contaminant AHR agonists were detected in technical and commercial PBDE mixtures (Sanders et al. 2005). Especially TBDF is a known potent AhR agonist, which most likely was responsible for the observed activation of AHR (Wahl et al. 2008a).

PBDEs have been seen to have reproductive effects in both male and female rodents reducing sperm function (Tseng et al. 2006) and causing structural changes of the

ovaries (Talsness et al. 2005). Along with other PBDE congeners, PBDE-47 and its hydroxylated metabolites showed to have oestrogenic activity (Dang et al. 2007; Meerts et al. 2001).

The degree or order of effect of PBDE congeners actions or affinities to steroid hormone receptors appears to vary between studies and methodology employed, but a consensus across studies shows that PBDE-47 interacts with both oestrogen and androgen receptors (Dang et al. 2007; Meerts et al. 2001). Two *in vitro* studies using Chinese hamster ovary cells, showed PBDE-47 to have considerable oestrogen receptor agonist activity, reporting PBDE-47 to have the highest oestrogen receptor agonist activity of all congeners tested (Dang et al. 2007; Kojima et al. 2009). Both studies also found PBDE-47 to have androgen receptor antagonist activity although both placed PBDE-47 as a congener of lower activity here (Dang et al. 2007; Kojima et al. 2009)

In an *in vitro* studies in the SH-SY5Y neuroblastoma cell line, PBDE-47 was seen to cause oxidative stress with reactive oxygen species (ROS) formation and DNA damage (Ping He et al. 2007). In the same cell line, PBDE-47 was found to induce apoptosis at low micromolar concentration, and to increase the malondialdehyde (MDA) content, decrease glutathione peroxidase level and induce lactic dehydrogenase (LDH) leakage (W. H. He et al. 2008c). Apoptosis, ROS formation and effect on MDA were also confirmed by Zang et al (M. Zhang et al. 2007).

1.3.4 1,2,5,6,9,10-Hexabromocyclododecane–HBCD

1,2,5,6,9,10-Hexabromocyclododecane (HBCD) is a reasonably new class of brominated flame retardants, and due to the restriction imposed on other BFR such as PBDEs, its use at present is seen at very high level, especially in Europe. HBCD is mainly used in Expanded and Extruded Polystyrene (EPS and XPS), in thermal insulation foams in building and construction, as well in plastics and textiles (BSEF, 2008). The technical mixture produced for commercial use is typically made of up to eight of the sixteen different stereoisomer (Law et al. 2005), but three on these are dominant and labelled as α , β , and γ -HBCD. γ -HBCD is the principal isomer in mixtures contributing to 75-89% of the total content. The proportions of α and β -HBCD of total content are between 10–13% and <0.5–12%, respectively (Becher 2005).

HBCD is a brominated aliphatic cyclic hydrocarbon made of a ring of 12 carbon atoms with 6 bromines in the respective positions as shown in figure 1.4 (Covaci et al. 2006).

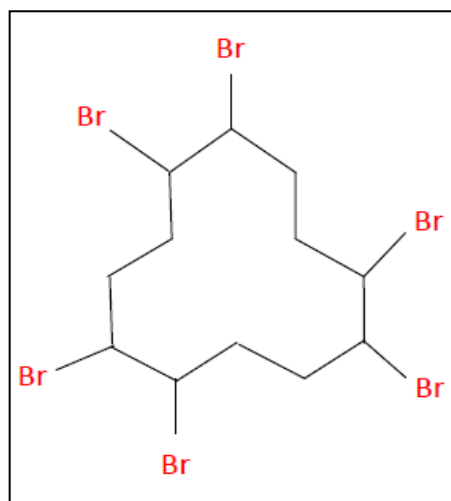


Figure 1.4: *1,2,5,6,9,10-HBCD chemical structure. HBCD consist of 12 carbon atoms with 6 bromine in position 1,2,5,6,9 and 10.*

1.3.5 HBCD in the environment, in biota and in humans

Like PBDEs, HBCD is not chemically bonded with the materials it is intended to protect, but instead mixed, so it readily leaches into the environment. Therefore, the main source of HBCD in the environment is the improper disposal of HBCD-containing goods (Covaci et al. 2006). As reported in figure 1.5, the use of HBCD in Europe represents a very high proportion of total BFRs when compared to both America and Asia, which is in accordance with the data reporting that Europe is the continent with the highest concentration of HBCD in the environment (Birnbbaum and Staskal 2004b; Law et al. 2005). In fact, HBCD has been detected in practically all the environment media such as urban and rural air, soil and water (Covaci et al. 2006; Heeb et al. 2005). However these data have to be consider just as an indication of the general usage of these chemicals, as more recent regulations, such as the prohibition of the usage and production of the Penta-PBDE mixture, may have altered the distribution of usage within these BFRs , with an increase in HBCD demand and production. However, the increasing in HBCD accumulation reflects the raise in usage of this POP.

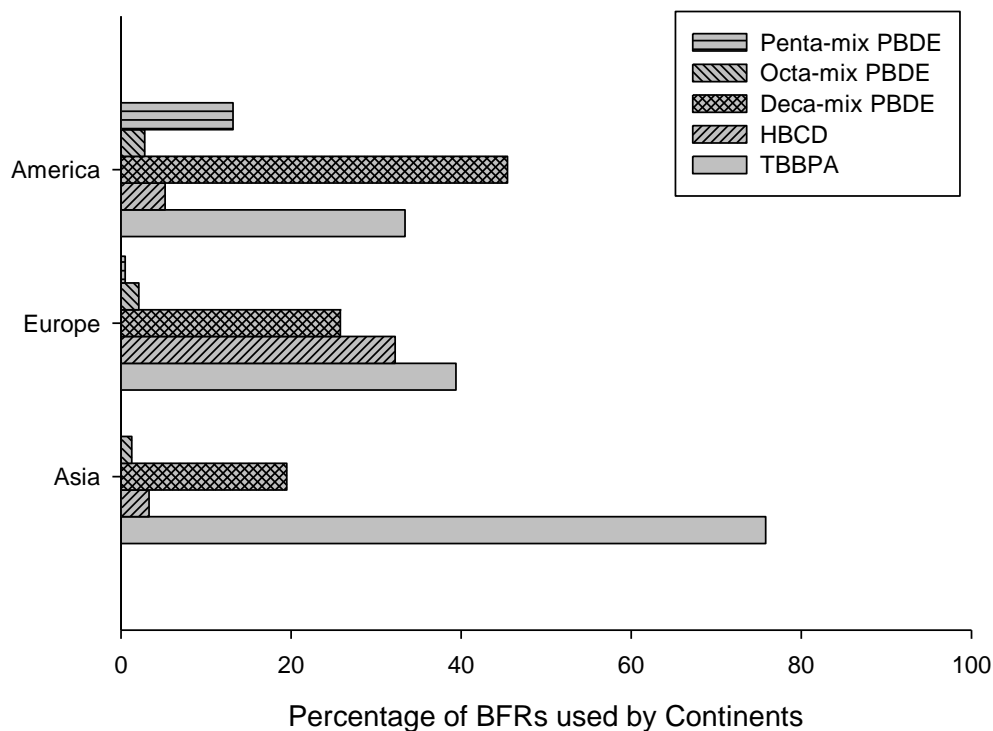


Figure 1.5: Usage of different brominated flame retardants as a percentage of total brominated flame retardant usage. Although Europe's major brominated flame retardant is TBBPA, HBCD use is greater than the proportional usage of HBCD in both America and Asia. In fact, HBCD level in the environment in Europe is higher than the one reported in America or Asia. Figure is drawn for presentation here from original data (Birnbaum and Staskal 2004b; Law et al. 2005).

HBCD is very lipophilic and largely insoluble in water, and therefore it is taken up by aquatic organisms and magnified as it moves upwards in the food-chain. Increased HBCD concentrations are not only found near point sources, but also in rural areas and in remote parts of the globe such as the Arctic, indicating that HBCD is subject to long-range transport (Heeb et al. 2005). In living biota it is detected with a predominance of the α -stereoisomer probably due to its higher hydrophilicity and resistance to degradation compared to the other stereoisomer (Law et al. 2005; Szabo et al. 2010b, 2011).

The main sources of HBCD for humans are dietary intake and indoor dust (Law et al. 2005) with consumption of fish indicated as the major route of exposure (Remberger et al. 2004). A study conducted in food samples from the US, reported that HBCD levels are higher in fatty fish than in other food sources (Schechter et al. 2010b). A

representation of the HBCD distribution in different food groups in USA can be seen in figure 1.6.

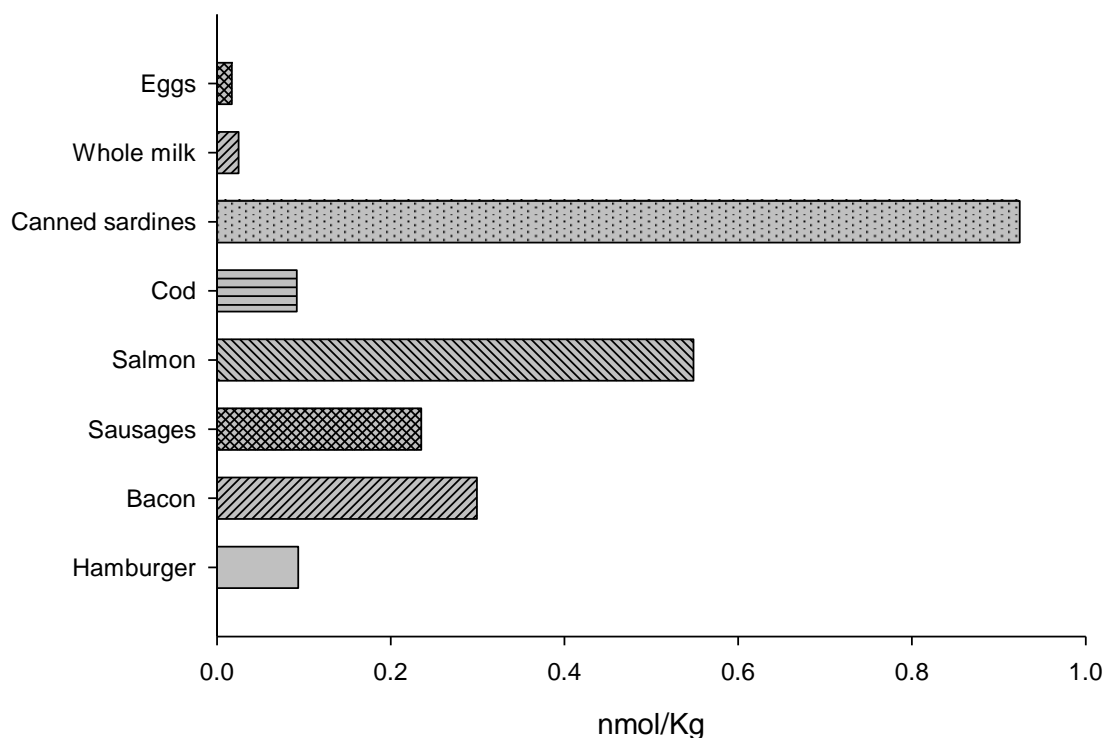


Figure 1.6: Amounts of HBCD in differing food groups in the USA. HBCD is shown to be at higher levels in the fatty fish than in any other food groups. Canned sardines and salmon are clearly shown to have the highest levels of all food groups. Figure is drawn for presentation here from original data (Schechter et al. 2010b)

Comparing these data with the estimated of the amount of PBDEs in food reported in section 1.3.2, it becomes evident that if we consider the amount of total PBDEs in food, HBCD is detected at roughly two to three times lower level in all the food groups, but comparing the concentration of HBCD in food with the single congener PBDE-47, the level of HBCD is higher in almost all food groups, excluding canned sardines and salmon in which PBDE-47 levels are slightly higher. In fact, since Penta-BDE commercial mixture, and thus PBDE-47, is no longer been produces, the demand and production of HBCD has been rapidly increased, and thus the amount detected in the environment and in biota has risen exponentially (Schechter et al. 2010a; Sellstrom et al. 2003).

As it did for PBDEs, EFSA recently published a scientific Opinion on HBCD on food, reporting HBCD concentration in food, based on data provided by seven European countries and covering the period from 2000 to 2010 (EFSA 2011b). In this publication it was estimated that for the food group of “Eggs and eggs products”, the lower bound (LB) and upper bound (UB) of the sum of the three individual stereoisomers are 0.14 and 0.54 ng/g fat. For the groups “Milk and dairy products” and “Meat and meat products”, the LB and UB were estimated to be 0.03 and 0.67 ng/g fat, 0.14 and 0.79 ng/g fat, respectively. “Fish and other seafood” was reported to be the highest contaminated among other food groups, with a range of total HBCD between 0.98 and 1.16 ng/g wet weight (EFSA 2011b).

However, it is important to consider that HBCD exposure is determined not only by the concentration in food, but also from the consumption amount itself. In regard to this concern, EFSA recently published the “Concise European Food Consumption Database (Concise Database)” in order to assess HBCD dietary exposure analysing the relative contribution of different food groups, taking in account HBCD concentration in each group (EFSA 2011a). The food groups considered in the database are “Eggs and egg products”, “Fish meat and products”, “Fish offal”, “Meat and meat products”, “Milk and dairy products”, “Water molluscs and Crustaceans”. EFSA established that the food group “Fish meat and products” is the main source of HBCD for humans, contributing in the range of the 83 to the 88.2 % to the median dietary intake. The contribution of the food group “Water molluscs and crustaceans” is about 1 %, whereas for “Fish offal” this is 0.5 %. Overall, the food groups ‘Fish meat and products’, ‘Fish offal’, and ‘Water molluscs and crustaceans’ together represent the main source of HBCD intake in the overall diet. The second highest source of dietary exposure to HBCD is the food group “Meat and meat products”, with a contribution ranging from 6.1 to 15.3 % for different age classes. The food group “Eggs and egg products” contributes in a range from the 1.3 to the 2.8 % to the overall HBCD intake, and for the food group ‘Milk and dairy products’, the contribution ranges from 2 to 5.1 % when the LB is considered, whereas considering the median UB the contribution ranges from 24.4 to 46 % within different age classes.

A limited number of studies have been conducted with the aim to estimate the concentration of HBCD in human specimens. HBCD has been detected in human milk of Swedish and Norwegian women, but in general the HBCD concentrations observed so far in human milk and blood have been lower compared to those of PBDEs (Covaci

et al. 2006; Heeb et al. 2005). EFSA estimated that the mean dietary exposure to HBCD across dietary surveys in European countries is in the range of 0.15 to 1.85 ng/kg body weight per day for children from three to ten years old. Total dietary exposure for adults was reported to be about half the exposure for children, with minimum LB and maximum UB of 0.09 and 0.99 ng/kg b.w. per day, respectively (EFSA 2011b). From a recent report, it appears that European intake of HBCD is comparable to what reported in America, where the dietary intake of HBCD has been estimated at 0.50 ng/kg/day (Schechter et al. 2010a).

The rapidly increasing concentration of HBCD in the environment and in living biota in the recent years, have raised attention to the hazard and possible health risk caused by accumulation of this contaminant. Currently, regulation with regards to production and demand of HBCD is limited. In 2007 HBCD was been classified as a Persistent, Bioaccumulative and Toxic (PBT) chemical according to the TC-NES (Technical Committee on new and existing substances under Regulation 793/93). On 1st June 2009, the European Chemicals Agency (ECHA) included HBCD in the list of substances to be subject to Authorisation as a priority. As a consequence, producers and users have started voluntary programmes to monitor, control and reduce HBCD emissions to the environment (BSEF, 2008).

However, more recently EFSA concluded that current dietary exposure to this toxicant in the European Union does not raise a health concern. It was also reported that additional exposure to HBCD from house dust is unlikely to raise a health concern (EFSA 2011b).

1.3.6 HBCD toxic mechanism

HBCD is a relatively new BFR and therefore the numbers of studies conducted to investigate its toxicity are limited. In studies conducted on rodents it appears that the acute toxicity of HBCD is very low with a $LD_{50} > 10$ mmol/kg body weight in mice and > 15 mmol/kg bodyweight in rats (Darnerud 2003a). Effects on the internal organs have been detected, particularly with changes in liver weight with microfoliar hyperplasia. Additionally, increased thyroid hormones in the serum with thyroid hyperplasia were noted. In these studies, HBCD indicated low foetotoxicity and teratogenicity, but mutagenicity results were negative (Darnerud 2003a).

In mice exposed to HBCD effects on memory and learning have been reported at concentration between 0.9 to 13.5mg/kg body weight, suggesting neurological effects caused by the toxicant (Per Eriksson et al. 2006). One study investigated the ability of HBCD to inhibit neurotransmitter uptake into isolated synaptosomes and vesicles, and showed that HBCD inhibited dopamine uptake with a half maximal inhibitory concentration (IC₅₀) of 4µM (Mariussen and Fonnum 2003). In the same study HBCD was also seen to inhibit glutamate uptake at concentration as low as 1µM, but it never achieved more than 50% inhibition (Mariussen and Fonnum 2003).

Effects of HBCD on calcium homeostasis and on neurotransmitter release have been investigated in a study on PC12 cells. Exposure to HBCD up to 20µM didn't cause any disruption in the basal intracellular calcium level or in the neurotransmitter release, but a dose-dependent reduction of a subsequent depolarization-evoked increase in cytosolic calcium concentration was found (M. M. L. Dingemans et al. 2009). In the same study, no specific voltage gated calcium channel could be related to the reduction of the depolarisation-evoked increase in calcium, suggesting that HBCD may non-specifically affect the cellular membrane and hence interfere with ion channels and their anchor proteins (M. M. L. Dingemans et al. 2009).

Studies of liver enzymes after exposure to HBCD showed activation of several cytochrome P450 enzymes. This effect has been linked to the activation of the CAR/PXR pathway in a AHR independent manner (Canton et al. 2008). Also, investigations of HBCD effects on liver gene expression have been conducted in both chicken embryonic hepatocytes (Crump et al. 2008) and by injection into chicken eggs (Crump et al. 2010). Induction of the chicken CYP2B1 and CYP3A1 orthologous, CYP2H1 and CYP3A37 were seen (Crump et al. 2008; Crump et al. 2010), but it has not conclusively been linked to CAR/PXR driven regulation.

Changes in thyroid hormone levels and effects on thyroid disruption have been also associated with HBCD exposure. In an *in vivo* study, HBCD was seen to affect the thyroid gland structure causing increase of the overall thyroid weight and activation of the thyroid follicle cells. Total serum T4 level was also seen decrease after exposure to HBCD. Effects on the pituitary gland were also observed. Increase of the pituitary weight and increasing levels of thyrotropin (TSH), a peptide hormone synthesized and secreted by thyrotrope cells in the anterior pituitary gland, were seen (van der Ven et al. 2006). An *in vitro* study on HeLa cells showed that HBCD exposure can affect the

thyroid hormone receptor (TR)-mediated gene expression at concentrations as low as 3.12µM (Yamada-Okabe et al. 2005). In addition, in a study in rainbow trout, HBCD was shown to cause alteration in thyroid size with a decrease in circulating T4 and increase in T3 levels (Palace et al. 2010).

A limited number of *in vitro* studies have been conducted showing some controversial preliminary results indicating the importance of further investigation to elucidate the toxic effects of HBCD. A study on cerebellar granule cells (CGC) showed evidence of an HBCD cytotoxic effect on a cellular level *in vitro* at micromolar concentration. After 24h exposure, HBCD induced death in CGC culture with a LC₅₀ of 3µM. No ROS formation was detected and no increase of intracellular calcium concentration was found. Morphological changes that are characteristic of apoptosis (chromatin condensation) were observed at low concentration of HBCD, but other hallmarks like caspase activation were absent, indicating an atypical form of apoptosis (Reistad et al. 2006a). A study on zebrafish embryos showed that HBCD induced an increase of superoxide dismutase (SOD) activities at the concentration of 0.1 mg/L (0.1µM), followed by a decline at higher concentrations. In the same study, increase in lipid peroxidation with increased MDA concentration and oxidative stress with over expression of the heat shock protein (HSP70), were also observed at concentration as low as 0.5 mg/L (0.8µM) (Hu et al. 2009). Finally, the effect of pure alpha-, beta-, and gamma-HBCD were investigated in Hep G2 cells, showing all the three stereoisomers lowered cell viability, increased LDH release and induced ROS formation from a concentration of 0.5µg/ml (0.8µM) upwards, indicating that the HBCD toxic mechanisms might include oxidative damage (X. L. Zhang et al. 2008).

1.4 Assessment of toxicology *in vitro*

1.4.1 Mechanistic Toxicology

The study of mechanistic toxicology aims to understand the mechanisms of adverse effects of chemical compounds on living organisms (Rietjens and Alink 2006). These investigations are expected to allow screening of chemicals for toxic effects and to provide mechanistic insight into outcomes associated with chemical exposures (Balbus 2005). In order to identify perturbation by chemicals on biological systems, *in vivo* studies are generally performed, but for better understanding of the mechanistic toxicity

and for risk assessment purposes, it is beneficial to also examine effects on a cellular level.

Mechanistic toxicity commonly employs functional genomics tools, such as transcript profiling, proteomics and metabolomics, to relate the induced phenotype with the observed changes in genes, proteins or metabolites. Transcript profiling technology allows quantitative measurement of the transcriptional activity of potentially thousands of genes in biological samples. The application of such technology to toxicology is referred as toxicogenomics which gives the ability to assess toxicity more comprehensively, potentially picking up more subtle changes than may be detected by other traditional detection methods (Balbus 2005).

However, concerns have been raised on the interpretation of the massive amount of data being monitored in gene and protein expression assays as changes in gene expression or protein levels may be mistakenly interpreted as related to adverse effects when in fact they may represent the activation of adaptive mechanism. In order to prevent misinterpretations, establishment of a relationship between toxicogenomics results and traditional toxicology tests outcomes has been suggested (Balbus 2005).

1.4.2 Toxicology effects on a genomic scale: gene expression analysis

Toxicological research into gene-environment interactions has developed particularly in the last decade. It is now possible to examine hundreds or thousands of genes simultaneously using microarrays, thus facilitating comparisons, for instance, between normal and diseased tissue, or between control and toxicant-treated cell lines (Vrana et al. 2003). Microarray technology provides a tool for the determination of gene expression at the level of messenger RNA (mRNA). The simultaneous measurement of large fractions of the genome facilitates the uncovering of specific gene expression patterns that are associated with the responses to a particular toxic substance (Vrana et al. 2003)

Microarrays can be divided into cDNA and oligonucleotide arrays, principally depending on the length of the probes. cDNA arrays typically contain small pieces of DNA sequence (usually 200 to 500 nucleotides long) selected from Expressed Sequence Tags (ESTs) libraries, while the oligonucleotide arrays are characterised by short probes complementary to the gene of interest (Brazma and Vilo 2000). In some platforms

multiple probes per gene are used as well as mismatch probes to determine the specificity of target-probe binding (Vrana et al. 2003).

cDNA microarrays are typically in house-printed array where the probes are spotted robotically onto the matrix surface. They can be one-colour arrays, where only one sample at a time is hybridized, or two-colour arrays, where samples and controls are labelled with different dyes, and hybridised on the same slide .Figure 1.7 shows in more detail how two-colour microarrays are deployed. After printing, samples and controls are labelled with different fluorescent dyes (typically Cy3 or Cy5) and both are hybridised to the same glass slide. By using competitive hybridization of separate targets to the same array, a major source of variability, hybridization, is eliminated. The slide is then scanned and the resulting fluorescence is measured (Vrana et al. 2003). The two fluorescent samples can then be normalised within and between arrays and, by the use of a reference sample or by a direct loop design, the arrays can be used to gain estimates of changes in gene expression for the conditions of interest (Hess et al. 2001a).

Oligonucleotide arrays have as well found a great deal of use in academic research (Hess et al. 2001a). These arrays contain probes that can potentially map all the exons within a genome. As the cDNA microarray, they can be spotted onto the matrix surface. However, oligonucleotide arrays can also be generated in situ on the surface of the matrix. To increase the specificity of this method, a series of oligonucleotides that differ by a one base mismatch from the gene-specific probe are also included on the array and can be used to determine the amount of mismatch hybridization, which can then be subtracted from the signal (Hess et al. 2001b). Internal control and multiple probes mapping the same gene guarantee the accuracy of the method (Hess et al. 2001b). Oligonucleotide arrays may be used for one or two-colour detection.

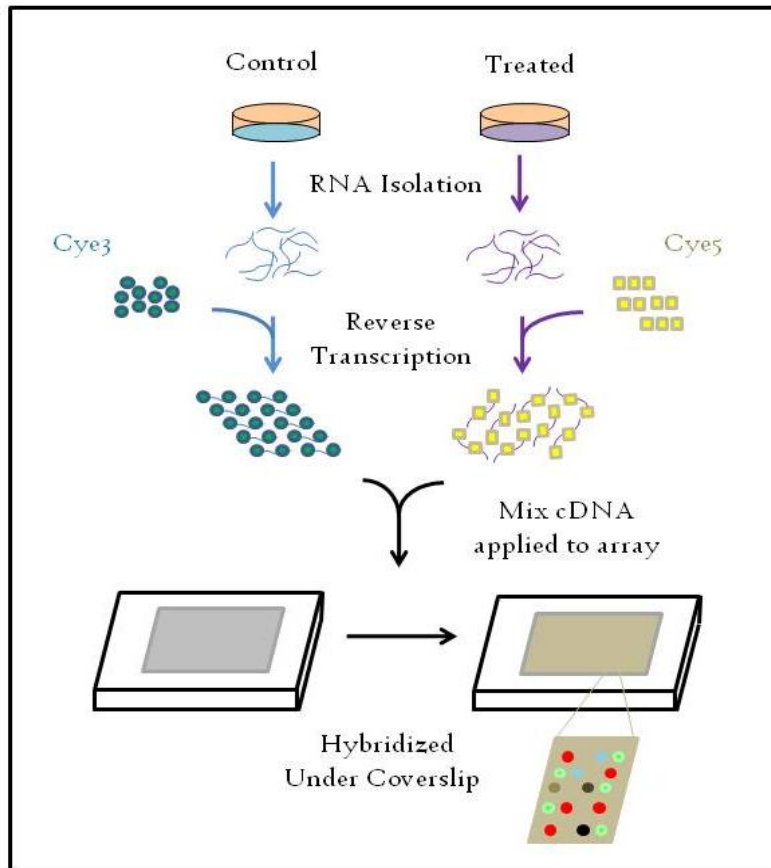


Figure 1.7: 2-colour microarrays. After RNA extraction from the treated sample and the control, the microarray slides are hybridized with samples labelled with one of the two fluorescent dyes. The slides are then scanned and the resulting fluorescence is measured. Normalisation within and between arrays is then possible and estimation of changes in gene expression is thus investigated.(Vrana et al. 2003).

Another commonly used method for investigating expression patterns is called digital transcriptomics. This technology is based on the counting of the number of reads generated by sequences of cDNA from different genes in the transcriptome, and from the reads it is possible to get an estimation of the expression level of these genes in the particular tissues sampled. A complementary approach is to scan publicly available databases of expressed sequence tags (ESTs) for the genes of interest. This technique has received a great deal of attention, but the use of these methods has been restricted in many species by the requirement of having a reference genome to evaluate and analyse the data (Ekblom et al. 2010; t Hoen et al. 2008).

Data analysis is a critical component of any transcript profiling technique particularly due to the large amount of data generated even in a single experiment. The most basic

goal of transcriptome data analysis is to identify genes that are differentially regulated. Many methods and software packages are being developed for this purpose, but to definitively demonstrate changes in gene expression, confirmation of the changes observed on hybridization arrays with other methods such as quantitative Q-PCR are still considered essential. A secondary goal of array experiments can be to characterise genes into functional groups and pathways or to look for groups of genes that behave similarly across a series of treatments (i.e. clustering analysis) and then identify common regulatory elements (Vrana et al. 2003). Several databases are freely available to test a set of genes in order to provide an analysis of perturbed pathway or to understand the relationship between regulated genes (Hess et al. 2001b). Some of the most well known examples of functional annotation tool include DAVID website, the Gene Ontology (GO) (Ashburner et al. 2000) and the Kyoto encyclopedia of Genes and Genomes (KEGG) (Kanehisa and Goto 2000).

1.5 Projects Aims

The aims of this study are to determine the mechanisms of toxicity of two BFRs in cultured neuronal cells. The two BFRs subjects of the study are 2,2,4,4-tetrabromodiphenyl ether (PBDE-47), one of the main POPs found in food especially in farmed salmon, and 1,2,5,6,9,10-hexabromocyclododecane (HBCD), a relatively new BFR whose presence in biota and in the environment is rapidly increasing.

The two cell lines selected for these studies are the mouse neuroblastoma (N2A) cell line and the mouse neuroblastoma x spinal cord (NSC-19) cell line. These cell lines will be used to act as stable neuronal-like models to investigate the mechanisms of action of the two toxicants considered.

Mechanistic toxicology will be investigated by performing biochemical assays and analysis of global gene expression to reveal potential genes and pathways involved in PBDE-47 and HBCD cytotoxicity. Moreover, investigation of the interactions between the two toxicants and seafood-enriched nutrients on the cellular machinery will be performed.

1.6 Hypothesis and Objectives

Persistent Organic Pollutants (POPs) are ubiquitous chemical compounds detected in all the environments and in living biota (de Wit et al. 2010). Increasing concentration of contaminants have been also measured in human milk and serum in the European and US population (Darnerud 2003a; Schechter et al. 2008). Since POPs have been proved to be able to pass the BBB and to accumulate into the brain (P. R. S. Kodavanti et al. 1998; Szabo et al. 2010a), adverse effect caused by these chemicals on neurological functions have been suggested.

POP mechanisms of action are still not fully understood, and we considered that transcriptomics analysis could be a very useful method to reveal the toxicity mechanisms of POP. The use of transcriptomics analysis is not dependent on any pre-formulated hypothesis, but is rather a powerful tool to investigate POP effects embracing all cellular systems. Adverse effects indicated through transcriptomics can then be further interrogated through specific hypothesis driven experiments.

Another aspect we wished to consider in the present study, is the effect of the diet on the modulation of POP toxicity. The food chain is one of the major route of exposure to POPs for humans, and among the various groups of food, fish is consider one of the main cause of contaminants accumulation (Schechter et al. 2006; Tornkvist et al. 2011). However, fish is a fundamental source of nutrients that may counteract the effects of dietary contaminants. We hypothesised that nutrients particularly enriched in fish, such as omega-3 fatty acids, can ameliorate the toxicity caused by HBCD. In a study using cultured neuronal cells it was found that pre-treatment of cells with Docosahexaenoic acid protected against metalmercury toxicity (Kaur et al. 2008). We wished to investigate if similar protective effects could be evidenced also in cells exposed to HBCD.

The two POPs tested in the present project, PBDE-47 and HBCD, have been chosen as they are two toxicant of recent concern and their levels in the physical environment and in living organisms have increased rapidly in recent years. In addition, the effects of these two POPs on the brain are not clear and their mechanisms of action have not been elucidated yet. Therefore, further study investigating PBDE-47 and HBCD toxicity mechanism were undertaken in the present project.

In order to assess PBDE-47 and HBCD toxicity, two neuroblastoma cell lines were exposed to the toxicants and a tolerance study performed. To investigate the mechanism of action of the two POPs, regulation of cellular gene expression was assessed using microarray technology. The evaluation of gene expression profiles evoked by the toxicants allowed for the identification of perturbed pathways and functions. To investigate if nutrients rich in fish, such as omega-3 fatty acid, can have ameliorative effects on the PBDE-47 or HBCD toxicity, the neuroblastoma cell lines were pre-treated with a pertinent omega-3 fatty acid. Toxicity markers were then tested, and the regulation of target genes determined, to be indicative of the two compounds' toxicities. Following evaluation of microarray results, effects of HBCD on metal homeostasis perturbation were investigated and the effect of HBCD exposure on cellular zinc concentration was measured.

2. Materials and Methods

2.1 Chemicals

2,2,4,4-Tetrabromodiphenyl ether (PBDE-47, 100% pure) was purchased from *LGC Promochem* and diluted in dimethyl sulfoxide (DMSO). A stock solution of 20.5 μ M was prepared and kept at room temperature.

1,2,5,6,9,10-Hexabromocyclododecane (HBCD) technical mixture with a purity of 99.2% was purchased from *Applied Biosystem* and reconstituted in DMSO to a final concentration of 32.7 μ M. The technical mixture was mainly constituted of α , β , and γ -HBCD. γ -HBCD contributed to 75-89% of the total content. The proportions of α and β -HBCD were between 10–13% and <0.5–12%, respectively.

For both the toxicants, working solutions were prepared by dilution of the stock solution into DMEM medium immediately before use. The final concentration of DMSO in the working solutions was <0.15% in all the experiments.

2.2 Cell Culture

In this project two cell lines have been selected as neuronal-like models: mouse neuroblastoma x spinal cord (NSC-19) and mouse neuroblastoma (N2A).

The neuroblastoma x spinal cord (NSC-19) cell line has been developed by fusing the aminopterin-sensitive neuroblastoma N18TG2 with mouse motor neuron-enriched embryonic day 12-14 spinal cord cells (Cashman et al. 1992). NSC19 display a typical neuronal phenotype and express properties expected from motor neurons such as generation of action potentials, expression of neurofilament proteins, and acetylcholine synthesis, storage, and release (Cashman et al. 1992)

Mouse neuroblastoma (N2A) derived from a spontaneous tumour in an albino strain A mouse. Cells produce microtubular protein which is believed to play a role in the contractile system giving axoplasmic flow in nerve cells.(Hpacultures 2008)

Both cell lines were cultured in Dulbecco's Modified Eagle's Medium (DMEM), with 110 mg sodium pyruvate. Media were supplemented with 100 units/ml penicillin, 100 units/ml streptomycin, and 10% fetal bovine serum (FBS). Cells were cultured at 37°C in a humidified atmosphere with 5% CO₂. Cells were maintained in T75 flasks (75 cm²), the media changed every two days and the cells split 1/3 every 3-4 days.

When cells were confluent, the medium was discarded and the cells washed with Phosphate-Buffered Saline (PBS). Trypsin solution (2.5% trypsin-EDTA) was added (1ml in a T75 flask) and incubated at 37°C for 1 minute. DMEM (5ml) was added to neutralise the trypsin action and the cells were collected in a 15ml Falcon tube. Cells were then centrifuged at 1500 RPM for 2 minutes, the supernatant then removed by aspiration and the pellet resuspended in 6ml of DMEM. The cells were split in three T75 flasks and more medium was added to achieve a volume of 15ml each flask.

2.3 Cell viability test

The MTT assay (SIGMA) was deployed to characterise the tolerance of N2A and NSC-19 cells to the toxicants PBDE-47 and HBCD. This viability test is based on the cleavage of the yellow 3-[4,5-dimethylthiazol-2-yl]-2,5-diphenyl tetrazolium bromide (MTT) to purple formazan crystal by metabolically active cells. (Mosmann 1983) Mitochondrial dehydrogenases of viable cells cleave the tetrazolium ring of MTT resulting in formation of purple formazan crystals. The amount of formazan is proportionate to the percentage of metabolically active cells (Mosmann 1983)

When the cells were confluent, they were harvested and seeded with a maximum number of 1×10^4 per well in a 96-well plate in 100 μ l of DMEM. Cells were then cultured in an incubator at 37°C and 5% CO₂ overnight. PBDE-47 and HBCD were diluted with serial dilution in culture media at concentrations between 100 to 0.39 μ M. The two compounds, reconstituted in dimethyl sulfoxide (DMSO), were added to the cells performing four replicates for each condition. A positive control and a DMSO control were also included. Cells were incubated for 48h in an incubator at 37°C and 5% CO₂. Following the 48h exposure to either toxicant, the cells were removed from the incubator into a sterile laminar flow hood and the medium was removed by aspiration. MTT salt was diluted 1 to 5 in DMEM and 100 μ l of the diluted solution was added to each well. Cells were incubated for 4 hours in incubator at 37° and 5% CO₂. After incubation, the cells were removed from the incubator and the MTT was aspirated. DMSO (20 μ l) was added to each well. The plate was left for 20 minutes on an agitator at room temperature to allow the purple formazan to dissolve. The absorbance was measured spectrophotometrically at a wavelength of 570 nm. The background absorbance measured at 650 nm was subtracted from the first measurement. Results were shown as a percentage of viable cells normalized to the positive control.

2.4 Assessment of Apoptosis

2.4.1 Caspase-3 assay

The caspase-3 assay (Invitrogen) was based on the cleavage properties of Caspase-3 and its high specificity for the amino acid sequence Asp-Glu-Val-Asp (DEVD). Rhodamine 110 bis-(*N*-CBZ-L-aspartyl-L-glutamyl- L-valyl-L-aspartic acid amide) (Z-DEVD-R110) is a substrate derived from rhodamine 110 (R110), containing the peptide DEVD covalently linked to each of R110's amino groups. After enzymatic cleavage, this bisamide non fluorescent substrate is converted into the fluorescent monoamide first, and then to the even more fluorescent R110. Both of these hydrolysis products have properties similar to fluorescein, with peak excitation and emission wavelengths of 496 nm and 520 nm, respectively.

To perform this assay, cells were harvested from a T75 flask and seeded in a 12-well plate. The number of cells used did not exceeding 1×10^6 per well in 2ml of media. The plates were then cultured in incubator over night at 37° with 5%CO₂.

PBDE-47 and HBCD were diluted in media from a stock solution to achieve four different concentrations: 1, 2, 4 or 8µM. The two compounds were added to the cells performing three replicates for each condition. A positive control and a DMSO only control were also included. Cells were incubated for 24h in incubator at 37° with 5%CO₂.

The cells were then removed from the incubator and placed into a sterile laminar flow hood where the medium was removed by aspiration. Cells were washed with PBS and treated for 1 minute with trypsin solution to allow the cells to detach from the plate. DMEM (500µl) was added to each well to neutralize the trypsin effect. Harvested cells were collected in a 1.5ml eppendorf tube. After 2 minutes of centrifugation at 1500 RPM, a PBS wash was performed. Cells were centrifuged again for 2 minutes at 1500 RPM and the PBS was removed by aspiration.

The 20X cell lysis buffer provided with the kit (1.5ml of 200mM TRIS, pH 7.5, 2M NaCl, 20mM EDTA, 0.2% TRITON™ X-100) was then diluted. To prepare the 1X buffer, 50µl of the 20X lysis buffer were added to 950µl of deionized water (dH₂O). 1X lysis buffer (50µl) was then added to each eppendorf tube. The cells were then lysed for

30 minutes in ice. A 5 minute centrifugation at 5000 RPM was performed and 50µl of the supernatant from each tube transferred to a 96 well plate. A black plate was used to enable fluorescence readings from individual wells. 1X cell lysis buffer (50µl) was used as a negative control to determine the background fluorescence of the substrate.

A 2X reaction buffer was prepared by mixing 400 µl of the 5X reaction buffer (20ml of 50mM PIPES, pH 7.4, 10mM EDTA, 0.5% CHAPS) provided with the kit, 10µl of 1M DTT and 590µl of dH₂O. The 2X substrate working solution was prepared by mixing 10µl of the 5mM Z-DEVD-R110 substrate provided, with 990µl of the 2X reaction buffer. The 2X substrate working solution (5µl) was added to each well and the plate was incubated in the dark at room temperature for 15 minutes. An R110 standard curve was also performed by diluting the appropriate amount of 5mM R110 stock solution provided, using 1X reaction buffer.

The fluorescence was read every 15 minutes for 6 times at an excitation/emission of 496/520 nm. The amount of fluorescent product generated was assumed to be proportional to the amount of caspase-3 activity present in the sample (Invitrogen 2011).

2.5 Toxicology assay lactate dehydrogenase (LDH) based

To assess the effect of HBCD on the membrane integrity, cytoplasmic lactate dehydrogenase (LDH) and LDH release into the medium were measured. LDH assay (SIGMA) is based on the reduction of NAD to NADH by the action of LDH. The product NADH is then used in the stoichiometric conversion of a tetrazolium dye, and the resulting coloured compound is measured spectrophotometrically (Decker and Lohmannmatthes 1988).

To evaluate the amount of LDH in the medium, cells were harvested from a T75 flask and seeded on to a 24-well plate, 4×10^4 cells in each well in 2ml of medium. The plate was then cultured in incubator over night at 37°C, 5%CO₂ and 95% of humidity.

Cells were then exposed to HBCD at the concentration of 1 or 2µM for 24 hours. Six replicates were performed; a positive control and a DMSO control were also included. Cells were incubated for 24h in an incubator at 37° C and 5% CO₂.

Following the exposure to the toxicant, the cells were removed from the incubator into a sterile laminar flow hood and an aliquot of 50µl of medium was transferred to a flat-bottom 96-well plate and the enzymatic analysis was performed. A LDH assay mixture was prepared by mixing equal amount of the Dye solution provided with the kit and the LDH Assay Substrate Cofactor previously prepared by adding 25ml of tissue culture grade water to the lyophilized cofactor provided with the kit. The assay mixture was added in an amount equal to 2X the volume of the medium to test (100µl each well). The plate was incubated at room temperature for 20-30 minutes protected from exposure to light. The reaction was then terminated by adding 1/10 volume of 1N HCl to each well and the absorbance measured in a plate reader at a wavelength of 490 nm. The background absorbance was also measured at a wavelength of 690 nm and subtracted from the primary measurement.

The cytoplasmic lactate dehydrogenase was also used to measure to assess the concentration of viable cells. A volume of 1/10 (200µl) of Assay Lysis Solution provided with the kit was added to the cells. The plate was transferred in the incubator for 45 minutes at 37°C, 5%CO₂ and 95% of humidity. Cells were then harvested and transferred to a 15ml tube. After centrifugation at 1500 RPM for 3 minutes, an aliquot of 50µl of medium was transferred to a flat-bottom 96-well plate and the enzymatic analysis was performed as described above. The amount of LDH released into the medium was calculated as a percentage of the total LDH (cytoplasmic LDH plus LDH in the medium).

2.6 Decosahexanoic acid (DHA) effects on HBCD toxicology

2.6.1 DHA solubility

In order to detect if DHA could mitigate the toxic effect of HBCD, cells were incubated with DHA, and then treated with HBCD.

To increase the solubility and facilitate the cellular uptake of DHA, the fatty acid was bound to a Fatty Acid Free-BSA (FAF-BSA). In order to perform this reaction, 7.76mg of DHA (1mg/ μ l) (SIGMA) was transferred in a glass test tube and 2.5ml of 96% ethanol were added. The alcohol was then evaporated under nitrogen gas. The test tube was placed on the heating block at 50°C and the subsequent procedure carried out in this condition. To get the DHA to the bottom of the tube, the wall was washed with chloroform, which was allowed to evaporate to dryness under nitrogen gas. The wash was repeated two times.

A KOH solution (2ml) at the concentration of 1mg/ml KOH in 90% ethanol was added. The test tube was filled with nitrogen gas, covered with parafilm and vortexed few seconds.

The solution was incubated in water bath at 37°C for 20min and vortexed every 5 minutes. After incubation, the ethanol was evaporated to dryness under nitrogen gas, and a brown layer on the side of the test tube was visible. An additional wash with 1000 μ L of ethanol was performed. The test tube was covered with parafilm under nitrogen gas, vortexed briefly and placed on a shaker table for an additional 10 min. The ethanol was then evaporated under nitrogen gas. 1.5 μ g/ml of FAF-BSA (SIGMA) solution in serum-free medium was prepared, and 2.5ml added to the tube, which was filled with nitrogen gas, covered with parafilm and vortexed for 30 seconds.

An additional 7.4 ml of the BSA solution was added to the tube and the volume was adjusted to 12.5ml with serum-free medium, obtaining a final concentration of 1.89mM of FFA-BSA-DHA. Prior to use, the mixture was sterilized using a 0.2 μ m filter. If necessary, the solution was stored under nitrogen gas at 4°C.

N2A cells were harvested from a T75 flask and 2×10^4 cells seeded in 24-wells plates in 2ml of medium. The plates were then cultured in incubator over night at 37°C, 5% CO₂ and 95% of humidity. The following day 30 or 90µM of FFA-BSA-DHA solution was added to the cells, which were incubated for 24 hours in the incubator. The solution was diluted in serum-free medium to keep the fatty acid profile unchanged. A negative control with FFA-BSA was also performed.

A study previously conducted on mouse neuronal cells showed that incubating cultured cells with DHA at a concentration of 90µM results in cellular DHA content between 19 to 24% of the total cellular fatty acids, which correspond to what is present in the brain (Kaur et al. 2008). However, in the present study DHA cellular uptake was not measured, therefore it was not possible to state the final DHA concentration after cellular exposure.

Cells were then exposed to HBCD at the concentration of 1 or 2µM for 24 hours. Six replicates were performed; a positive control and a DMSO control were also included. Cells were incubated for 24h in an incubator.

After exposure to HBCD, cytotoxicity was evaluated by measuring the release of LDH to the culture medium as described in section 2.5, and by concurrent analysis of expression of marker genes for HBCD effects on fatty acid metabolism using quantitative real-time polymerase chain reaction (qPCR).

2.7 Gene Expression Analysis

Microarrays were used to assess the global gene expression of cells exposed to HBCD or PBDE-47. In this assay, mRNA extracted from two samples is directly compared by labelling with spectrally distinct fluorescent dyes, and hybridisation to the same array. The relative gene expression is analysed by measuring the ratio between the fluorescence intensities of the two dyes (Eisen and Brown 1999). The major advantage of this technique is the possibility to measure the expression levels of thousands of genes simultaneously on a small glass surface (Shalon 1998).

In the present study, microarrays were used to analyse genome-wide gene expression profiles resulting from exposure of mouse N2A and NSC-19 cells to PBDE-47 or HBCD at different concentrations.

2.7.1 Preparation for Oligonucleotide Array Printing

2.7.1.2. Selection of Oligonucleotide Library

Oligonucleotide arrays were printed in house in the Kings College London Genomics Centre by Dr Thomas Carroll as described (Carroll 2011). The oligonucleotide libraries used for array printing was the Operon's Mus version 4 libraries. Operon Version 4 was chosen as it is characterised by a large gene coverage, having 36,232 probes and 21,357 annotated genes, resulting in a estimated gene coverage of about 84% (Verdugo and Medrano 2006). The processes used for the selection of probes to represent genes in the library sets was also considered, and after evaluation of the affordability, Operon Version 4 was considered the best candidate as oligonucleotide libraries to use for array printing.

2.7.1.3 Preperation of Operon's Mus Version 4 Library

The Operon library was stored at -20°C prior to resuspension of oligonucleotide probes. Oligonuceotides were used at the concentration of 0.50mg/ml or 500ng/ μl according to Corning recommendations (Corning 2005). Oligonucelotides were initially delivered at 600pm per well to reach a concentration of 500ng/ μl , 12 μl of solution were added.

In order to calculate concentration per well after resuspension in a known volume, a PERL program was written by Dr Carroll as described (Carroll 2011). This program, calculated the concentration in ng/ μl for a given volume while taking into account nucleotide base composition of the oligonucleotide 70mer as well as any modifications such a amines used to attach probes to array surface.

Oligonucleotides were resuspended in Pronto universal spotting solution (Corning 2005) to allow for a compact spot size, using a Biomek FX robot. The pipetting mixes performed by the Biomek FX robot were optimised by spectrophotometric assessment of the homogeneity of probe concentrations across randomly selected wells. In addition, for every run of the Biomek FX robot oligonucleotide resuspension, 24 wells were checked for their DNA concentration by measurement of absorbance using a NanoDrop. Concentrations were compared against those calculated by the PERL Oligoweigher.pl program and were found to be within the desired range. Following resuspension of the

oligonucleotide library, plates were centrifuged in a plate spinner in order to collect all probe suspension, and stored at 4°C.

2.7.1.4 Array Printing

Arrays were printed on a Genetix QARRAY2 robot. Array printing and array printing optimisation procedures were carried out on Corning Ultragaps slides using 48 Telechem printing tips. In order to reduce the time that the arrays were within the QARRAY2 robot and hence susceptible to degradation, and to produce spots with consistent and good morphology, array printing was first optimised for washing and printing procedures. Printing was carried out at room temperature at a constant humidity of 45% (considered optimal for Pronto printing (Corning 2005)) by Dr Carroll as described (Carroll 2011).

To access an ideal printing depth in order to produce reproducible spots for all tips, SYTO Red nucleic acid stain was used to produce a range of printing depths. Spot morphology and intensity were then assessed.

Once the printing was optimised, Ultragaps slides were loaded to the QARRAY2 robot and the plates containing the library were placed into the plate loader. Array printing was carried out over 3 days with ethanol, water and wastes replaced or removed as needed.

After printing, slides were treated with 300 mJ UV light to crosslink DNA. Final array quality was evaluated by staining with SYTO Red nucleic acid dye. Failed printtips were noted for removal from gene expression analysis at a later point. Arrays were then placed in a Corning 25 array holder and stored in a desiccator at room temperature until needed.

2.7.2 Sample Preparation

When N2A and NSC-19 cells were 70% confluent, the media were removed by aspiration and PBDE-47 or HBCD was added diluted in fresh media. PBDE-47 was used at concentration of 1 or 2µM and HBCD 0.5, 1 or 2 µM. DMSO control (>0.15% diluted in DMEM) and a positive control (DMEM, as used for cell culture) were also performed. The different concentrations were selected based on the previously

performed tolerance assay. Cells were then incubated for 12h in an incubator at 37° with 5% CO₂.

2.7.2.2 RNA Extraction

After 12h incubation with either of the two compounds, the medium was aspirated from the cells and 5ml of TRIZOL was added. Cells were incubated for 5 minutes at room temperature. Phase Lock Gel (PLG) Heavy tubes (Eppendorf) were pre-spun for 2 minutes at 1500g.

The cell homogenate was added to the PLG tubes and incubated for 5 minutes at room temperature. Chloroform (1ml) was added and the tubes were then vigorously shaken, by hand, for 15 seconds. After 3 minutes incubation at room temperature, the samples were centrifuged for 5 minutes at 1500 g. The PLG forms a gel barrier between the chloroform on the bottom, and the organic phase on the top. Carefully, the upper phase containing the nucleic-acid was transferred into a fresh Eppendorf tube. The same volume of ethanol 75% was added and the mixture applied to RNeasy Midi column (Qiagen).

The RNeasy Kit is based on a method that uses the selective binding properties of a silica-gel-based membrane to isolate all RNA molecules longer than 200 nucleotides. When the samples were applied, the column was placed in a 15ml tube supplied with the kit and centrifuged for 5 minutes at 3000-5000 g. The flow-through was discarded and 2.5ml of Buffer RPE (supplied with the kit) was added. The wash with Buffer RPE was repeated and an additional empty spin for 1 minute at 3000-5000 g was performed to eliminate any excess of buffer. To elute the RNA, the column was transferred to a new 1.5ml collection tube and 50µl of RNase-free water was added. The column was gently closed, left to stand for 1 minute and then centrifuged for 3 minutes at 3000-5000 g. The elution step was repeated twice to achieve a total final volume of 100µl.

2.7.2.3 RNA Analysis

To evaluate the RNA purity, the samples were analysed with a spectrophotometer (NanoSpec). A 260/280 ratio between 1.8 and 2.2 was considered acceptable quality RNA for use in the following steps (Corning 2005). RNA integrity was analysed by microcapillary electrophoresis using the Agilent 2100 Bioanalyser. This analysis

extracts an algorithm that describes RNA integrity based on RNA size distribution and calculates an RNA integrity number (RIN) and a RIN >7 was considered acceptable (Schroeder et al. 2006).

RNA was diluted from 25 to 500 μ M in RNase free water. The samples and the ladder were heated at 70°C for 2 minutes to allow them to denature. Gel (35 μ l) and dye (0.54 μ l) supplied with the kit (NanoReagent Agilent) were mixed together and centrifuged for 10 minutes at 13000g. The mix was loaded into the RNA Nano LabChip (supplied with the kit). The buffer provided (5 μ l) was also added and 1 μ l of sample was loaded in each well. The chip was mixed for one minute using a vortex machine and analysed in the Bioanalyser.

2.7.2.4 cDNA Synthesis and Aminoallyl Labelling

In order to prepare the samples for microarray analysis, fluorescently labelled deoxyribonucleotides were incorporated into the targets. To carry out the labelling, the first strand synthesis of cDNA was first performed containing amino-allyl-labeled nucleotides. Therefore, a covalent coupling to the NHS-ester of the appropriate Cyanine fluor was possible.

Random Hexamer Primer (Invitrogen) (1 μ l at 3 μ g/ μ l) and Anchored Oligo dT Primer (Invitrogen) (1 μ l at 2.5 μ g/ μ l) were added to 10 μ g of RNA previously extracted. The reaction volume was then brought to 17 μ l with RNase-free H₂O. After mixing the samples, a 10 minutes incubation at 70° in a PCR machine was performed. Samples were then chilled on ice for 30 seconds and centrifuged at maximum speed for one minute.

The labelling reaction master mix was prepared using an Invitrogen Kit. 5X Superscript II buffer (6 μ l), 3 μ l of 0.1M dithiothreitol (DTT), 0.6 μ l of dNTP mix (dATP 100mM, dCTP 100mM, dGTP 100mM, dTTP 100mM), 0.9 μ l aminoallyl-dUTP (2mM), 2 μ l of Superscript III RT (200U/ μ l) and 0.5 μ l RNase out (40U/ μ l) were added to prepare the master mix. This was then added to the samples followed by incubation at 46°C for 3h in a PCR machine. The tubes were removed from the machine and 10 μ l of 1M NaOH and 10 μ l 0.5M EDTA were added to each sample to stop the reaction. After incubation at 65°C for 15min, 10 μ l 1M HCl was added to neutralise the pH.

2.7.2.5 Clean up with Qiagen QIAquick PCR purification column

QIAquick column (Qiagen) is a system based on the selective binding properties of a silica membrane to purify cDNA and remove contaminants. cDNA binds to the silica gel, but unwanted impurities flow through the column and are discarded.

A Tris-free Phosphate buffer and a wash Phosphate buffer were prepared. Tris-free Phosphate buffer was prepared adding 1M KH_2PO_4 and 1M K_2HPO_4 . Wash Phosphate buffer was obtained by mixing 5% 1M KPO_4 , previously prepared by mixing 95% of 1M KH_2PO_4 and 5% of 1M K_2HPO_4 , and 95% ethanol. The pH was adjusted to 8.5-8.7 with 1M HCl.

The cDNA was mixed with 300 μl (5 times the previous reaction volume of 60 μl) buffer PB (provided with the kit). A QIAquick column was placed in a collection tube where the mix was transferred. The column was centrifuged for 1 minute at 14000rpm. A first wash with 750 μl of Phosphate wash buffer was performed. The column was then centrifuged at 14000 rpm for 1 minute. The wash was repeated and the column transferred to a fresh Eppendorf tube. To elute the cDNA, 30 μl of 4mM KPO_4 pH 8.5 (diluted 1/250 from the 1M buffer) was added and incubated for 1 minute. The samples were then centrifuged at 14000 rpm for 1 minute. Another 30 μl of 4mM KPO_4 pH 8.5 was added and the samples incubated for another minute and centrifuged again at 14000 rpm for 1 minute. The total final volume was thus 60 μl . The samples were then dried in a speed vacuum for ~45 minutes at 45°C.

2.7.2.6 Coupling the labelling cDNA to the Cy-Dye

The Cy-dyes Cytocain3 (Cy3) and Cytocain5 (Cy5) (Amersham Bioscience) were prepared by resuspending each dye in 54 μl of DMSO. Carbonate buffer (NA_2CO_3) at the concentration of 1M was prepared and adjusted to pH 9.0 with 10M HCl. The buffer was then diluted 1/10 to obtain a 0.1M solution.

The dried cDNA was resuspended in 4.5 μl of 0.1M carbonate buffer pH 9.0. The dyes were then added to the test and common reference samples. Cy3 (4.5 μl) was added to each test sample and Cy5 (4.5 μl) to each aliquot of the common reference (pool of all the samples). The labeling reaction was incubated for 2.5h in the dark at RT.

2.7.2.7 CLEAN UP II using QIAquick PCR purification column

After incubation in the dark, 35µl of 100mM NaOAc pH 5.2, diluted in dH₂O from a 3M stock, was added to each sample. PB Buffer (250µl), provided with the kit, was then added to the samples. A QIAquick Spin Column was placed in a 2ml collection tube and the mix was applied. The column was centrifuged for 60 seconds at 17900 g. The flow-through was then discarded and 750µl of Buffer PE added. The column was again centrifuged for 60 seconds at 17900 g. The flow-through was discarded and an empty spin was performed for 1min at 17900 g to rid of excess.

The column was placed in a new 1.5ml collection tube (supplied with the kit), and 50µl of EB Buffer was added to the centre of the column. A centrifugation for 1min at 17900g was then performed.

2.7.2.8 cDNA analysis

Labelled cDNA was analysed with a NanoSpec to measure the efficiency of the labelling reaction before the microarray hybridisation. Absorbance was measured at 260, 550 and 650nm to enable calculation of the total pmols/µl of Cy dyes incorporated into the cDNA. According to Corning Manual (Corning 2005), 150pmol of dye incorporation per sample is an optimal condition for hybridisation.

The Dye incorporation was calculated considering the total pmols per µl of Cy Dye, and it was calculated by two different methods: Frequency of Incorporation (FOI) and Nucleotide Incorporation (NI).

FOI is normally expressed as dye molecules per 1000 nucleotides, and it was calculated with the following formula:

$$[(\text{pmol/ng}) \times 324.5]$$

Equation 2.1: *Frequency of Incorporation (FOI) calculated considering the total pmols/µl of Cy dyes incorporated into the cDNA.*

The FOI range considered acceptable was between 20 to 50 (Corning 2005).

The NI number was obtained with the following formula:

$$[(ng/pmol) \times 3.08]$$

Equation 2.2: Nucleotide Incorporation (NI) calculated considering the total pmols/ μ l of Cy dyes incorporated into the cDNA

A NI between 67 to 22 was considered satisfactory (Corning 2005).

2.7.3 Microarray

2.7.3.1 Prehybridisation

Prehybridisation buffer was prepared containing: 5X SSC (0.3M sodium citrate, pH approx. 7.0 and 3M NaCl), 0.1% Sodium Dodecyl Sulfate (SDS), 1% bovine serum albumin (BSA). The microarray slides used were placed into a black box, filled with prehybridisation buffer and incubated at 42°C for 45min in an oven.

The slides were then washed by dipping twice in 0.1X SSC and incubated for 30 seconds at room temperature. The arrays were dried by centrifugation with slide-spinner for 1 min, stored in dust-clean environment till hybridisation. Coverslips used for hybridisation were washed with 0.1% SDS, rinsed in water and dipped in 99% ethanol. They were then blow-dried carefully in order to avoid creation of water marks.

2.7.3.2 Hybridisation

The samples were dried in a speed vacuum centrifuge for ~30 minutes at 45°C. A concentration of 150 pmol of dye incorporation per sample was used. Each sample was then resuspended in 45 μ l of hybridisation buffer containing: 50% formamide, 5X SSC and 0.1% SDS. The mixture was heated to 50°C for 3min in order to denature the cDNA. The samples were then centrifuged in a microcentrifuge for 1min at maximum velocity. The sample and the reference were pooled together and the mixture applied to the microarray slides. Slides were then covered with a 22mm X 60mm glass coverslip. The slides were then placed in a hybridisation chamber and 200 μ l of water was added to the chamber to avoid evaporation. The arrays were incubated at 42°C for 16-20h.

2.7.3.3 Arrays Washing

The slides were removed from the hybridisation chambers taking care not to disturb the coverslips. A low-stringency wash buffer containing 2X SSC and 0.1%SDS was pre-warmed at 42°C. The arrays were dipped in the solution and the coverslips were carefully removed. The slides were then transferred to a fresh buffer and gently shaken for 5 minutes at room temperature. The arrays were then washed for 5 minutes in a high-stringency buffer (0.1X SSC, 0.1%SDS) using an agitator at room temperature. High-stringency washing was followed by wash in a solution containing 0.1X SSC for one minute and this wash was repeated 6 times using fresh buffer each time. Slides were finally rinsed in 0.01X SSC for 10 seconds and dried using a centrifuge for 3 minutes.

2.7.3.4 Data collection, Normalisation and Analysis

The microarray slides were scanned with the Custom Array Scanner (ScanArray Express, Perkin Elmer) at 5 micron resolution. Custom Array Scanner is a simultaneous 2-color scanner which produces two images, one detecting Cy5 fluorescence at a wavelength of 670nm and the second one detecting Cy3 fluorescence at a wavelength of 570nm.

The images were then interpreted using BlueFuse (Blue Genome) software. BlueFuse is a software used to automate the process of microarray image analysis. It uses a Bayesian background correction to calculate actual spot intensities. It is also used to assess the spot quality and compare the consistency of replicates. BlueFuse uses a Gal file containing array information for each gene, its position on the array, and the record of positive and negative controls. (Cambridgebluegenome 2008)

The images obtained from the scanner, were downloaded into the software, which overlaid fluorescence from Cy5 and Cy3. The spots were first manually checked to exclude spots which were miss-aligned or areas with a very high background. Probe intensities were calculated by the program filtering out spots with low confidence ($P < 0.05$).

The Limma bioconductor package was used to analyse microarray data from both the HBCD and PBDE-47 experiments. Normalisations conducted were print-tip loess, median scaling, print-tip order and print-tip weighting. Low intensity spots were also filtered out of further analysis. Genes with at least two-fold change difference compared

to the control in at least one comparison were forwarded to statistical analysis. Gene expression profiles of the exposed groups were compared to that from the control, and the significant difference determined by ANOVA with Benjamini-Hochberg multiple testing correction (false discovery rate, FDR). FDR was set at 20%. Visualisations for microarray quality control were created with the LIMMA package.

2.8 Confirmation of differentially expressed genes with Real Time PCR (Q-PCR)

2.8.1 cDNA Synthesis

Synthesis of cDNA was performed using 5µg of RNA. Random Hexamer Primers (1µl; 200ng/µl) and 1µl of a 10mM dNTP mix (dATP 100mM, dCTP 100mM, dGTP 100mM, dTTP 100mM) was added to each sample. RNase-free water was added to bring the volume up to 12µl. The samples were mixed by vortexing and incubated at 65°C for 5 minutes in DNA Engine Thermal Cycler (ALS 1296, DYAD). They were then chilled on ice for 1 minute and centrifuged at maximum velocity for one minute. First Strand buffer (4µl; 5X), 1µl of 0.1M dithiothreitol (DTT), 2 µl of Superscript III RT (200U/ µl) and 1 µl RNase out (40U/ µl) were added to the samples. The reactions were then incubated in a thermal cycler for 10 minutes at 25°C, following by 60 minutes at 50°C. In order to deactivate the enzyme and therefore to stop the reaction, the samples were heated to 70°C for 15 minutes. After cDNA synthesis, RNase-free water was added to the samples up to 300µl and the cDNA was stored at -20°C.

2.8.2 Real time Q-PCR

Q-PCR was performed in order to confirm the expression of genes previously found by microarray analysis to be of particular interest. In cells exposed to HBCD, only the two highest exposure levels, 1 and 2µM, were included in Q-PCR validation assuming that any gene reliably regulated at the lowest concentration of 0.5µM would also be exposed at higher concentrations. Since DMSO was used as vehicle to dissolve HBCD, the effect of DMSO alone on gene expression was also tested by direct comparison against the negative control (medium-only).

The Q-PCR assay used deployed SYBR Green SuperMix-UDG from Invitrogen as a reporter. SYBR Green is a fluorescent dye that binds directly to double-stranded DNA. Therefore the fluorescent signal is proportional to the cDNA concentration. The SuperMix contains all the components needed to carry out the assay, except the primers; it contains SYBR Green, *Taq* DNA polymerase, Mg^{++} , uracil-DNA glycosylase (UDG) and deoxyribonucleotide triphosphates (dNTPs), with dUTP instead of dTTP. UDG and dUTP are included in the mixture to prevent the reamplification of carryover Q-PCR products between reactions.

To perform the assay, the tested primers were briefly spun to ensure that the mix was in the bottom of the tube. The primers were then reconstituted in 220 μ l of PCR-grade water and mixed by vortexing. The master mix was prepared adding 12.5 μ l of Platinum SYBR green, 0.5 μ l of ROX Reference Dye, 200nM (1 μ l) of the Primer tested and 6 μ l of water in each sample (Invitrogen). Samples were analysed in duplicate and a blank control was included.

The primers were tested in a 96-well plate. Master mix (20 μ l) was aliquoted into each well and 5 μ l of template, or water for the control, was added. The plate was then sealed and placed into an ABI PRISM 7700 machine.

The machine was programmed as shown below as recommended by Invitrogen:

50°C for 2 minutes

95°C for 2 minutes

40 cycles of: 95°C for 15 seconds

60°C for 1 minute.

A dissociation curve was also included to confirm primer specificity and to monitor the amplification of unspecific products. ROX Reference Dye was always added in each reaction to normalise the fluorescent reporter signal for non-PCR-related fluctuations in fluorescence between reactions

2.8.3 Primers tested

The primers used to assess gene expression levels were purchased from PrimerDesign or from QIAGEN. They were designed in order to have a Melting Temperature between 52 to 58°C, to produce short amplicons and to span at least one intron.

The tested primers from Primer Design and QIAGEN are listed in table 2.1 and 2.2 respectively.

Table 2.1: gene symbol and sequence of the primers tested in Q-PCR purchased from PrimerDesign

<i>Gene symbol</i>	<i>Sense primer</i>	<i>Anti-sense primer</i>
Acs14	AGAAAGTCAATCAGAATTCAACAAGA	TTCCCAGGTTTCAGTGCTACA
Bace2	TGCCTGGTATTAAATGGAATGGA	AAATGTCTGGAATCTTTGCTTGG
Edn1	GTTGCCTGTGGGTGACTAATC	AACGCTTCTGACTCGGACA
Egr1	GCCTTCGCTCACTCCACTA	GCTGGGATTGGTAGGTGGTA
Hspa5	ACTATTGCTGGACTGAATGTCATG	GTCAATGGTGAGAAGAGACACATC
Nfkb2	ATTGCACATGCCTGATTTTGGAG	GCTCCACAGTCAACTAACAGAT
Ngfr	GATACGGTGACCACTGTGATG	ATGGAGCAATAGACAGGAATGAG
Pak3	TGGATACATAGCAGCACATCAG	GGCGGAGGTTTCATTGTCATC
Park2	AAGGGGATTGCGACTCACT	CTTGGTGGTCTTCTTGATGGT
Pawr	GAGTGCTTAGATGAGTACGAAGAT	AGGTAGGATGTGCCTGGATC
Pnpl8	GCACCAACTCTCACTATTTAGGA	AGCAAACCTCCATCTTGATGAA
Prkcdbp	GTCCDGCTCTTCAAGGAGGA	AGAACTCTCTCCAACCTTCATCCT
Rara	CAGTCCCAGCTCCCACAGA	CCAGCAGGAAGGCAGAGAA

Table2.2: gene symbol, QIAGEN ID number and detected transcript of the primers tested in Q-PCR purchased from Qiagen.

<i>Gene symbol</i>	<i>QIAGEN ID</i>	<i>Detected Transcript</i>
Acsl4	QT00141673	NM_207625
Actb	QT01136772	NM_007393
App	QT00165060	NM_007471
Atp5b	QT00147210	NM_016774
Bace1	QT00493948	NM_011792
Camk2d	QT01062404	NM_023813
Cacna1c	QT00170632	NM_007578
Fgf2	QT00128135	NM_008006
Fos	QT00147308	NM-010234
Gapdh	QT01658692	NM_008084
Hip1	QT00160741	NM_146001
Homer1	QT01759261	NM_011982
Hspa5	QT00172361	NM_022310
Nmyc	QT00252196	NM_008709
Pink1	QT00111349	NM_026880
Pnpla8	QT00123375	NM_026164
Prkca	QT00146384	NM_011101
Rb1	QT00164255	NM_009029
Rbp4	QT01166193	NM_011255
Slc30a10	QT01537578	NM_001033286
Tbcb	QT00107289	NM_025548
Tg	QT00116592	NM-009375
Trip6	QT00256340	NM_011639
Ttr	QT00107485	NM_013697
Tubb2c	QT00139363	NM_146116

2.8.4 Housekeeping gene selection

During Q-PCR analysis the expression level of a gene under investigation is normalised against a housekeeping gene to correct for differences in CDNA concentration in the used samples. To ensure an accurate normalisation, the gene reference has to show minimum variances between different conditions and treatments.

To chose the most reliable and stable housekeeping gene for normalisation, a selection of six genes were tested using GeNorm reference gene selection kit (Primerdesign). GeNorm is an algorithm that calculates the gene expression stability from a panel of tested genes in various cDNA samples (Vandesompele et al. 2002). The six genes tested are reported in table 2.3.

Table2.3: gene symbol and accession number of the primers evaluated as candidate housekeeping genes.

<i>Gene symbol</i>	<i>Accession number</i>
Act-β	NM_007393
Ubc	NM_019639
Gapdh	NM_008084
Rpl13a	NM_009438
18S	NR_003278
Atp7a	NM_016774

Primers with a final concentration of 200 nM were added to the Platinum SYBR green and to the ROX dye as described in section (2.8.2), and a Q-PCR was performed according to the Invitrogen protocol for thermal-cycling as described in section 2.8.2. Melting curve analysis was also performed during real-time Q-PCR to analyse the specificity of the reaction and to verify the amplification of a single product.

Gene stability was then measure with GeNorm software which determined the gene-stability measure “*M*”. The gene with the lowest *M* values has the most stable

expression, and therefore is selected as housekeeping gene (Vandesompele et al. 2002). In the present study the gene *Gapdh* scored the lowest **M** value, and therefore was chosen as housekeeping gene

2.8.5 Efficiency test

Prior to Q-PCR assay, the primer efficiency was tested in each primer as well as in the housekeeping gene chosen.

Template of cDNA was diluted with 1/10 serial dilution, and 4 dilutions were deployed. Master mix was prepared as previously described in section 2.8.2 and a Q-PCR was performed according to the Invitrogen protocol for thermal-cycling as described in section 2.8.2.

The efficiency expressed in percentage was calculated by plotting the Ct value in scatter charts and the slope of the Ct values of the different dilutions of samples was included in the equation as follow:

$$Efficiency = \left(1 - \left(10^{-\frac{1}{slope}} \right) \right) * 100$$

Equation 2.3: primer's Efficiency expressed in percentage calculated from the slope of the Ct values of the 10 fold dilution samples.

With this method, the expected slope for a 10-fold dilution series of template is -3.32, when the corresponding efficiency is equal to 100%.

Efficiencies between 90 to 110% was considered acceptable according to ABI (AppliedBiosystems 2008) and, therefore, primers whose efficiency was in this range were used for further studies.

2.8.6 Analysis of Real Time PCR data

Q-PCR results were analysed with the REST (relative expression software tool) software. This software compares the Ct value of reference gene with target genes, and considering efficiency of primers, calculates the difference in gene expression (Pfaffl, Horgan et al. 2002). Statistical calculation of probability of differential expression is based on a randomisation of samples using the Pair Wise Fixed Reallocation Randomisation Test (Pfaffl et al. 2002). REST was set for a number of 1000 randomisations during this analysis.

2.8.7 Agarose gel Electrophoresis

PCR products were analysed by agarose gel electrophoresis to verify the amplification of a single product with the desired length. Based on standard methodology, 3% agarose gel was prepared and 5µl of Q-PCR product mixed with 2µl of loading buffer was then loaded. Gel was run at 80V for 30 minutes. A commercial 1000bp ladder was used for validation of specific product size.

2.9 Zinc regulation investigation

Effects of HBCD on intracellular Zn²⁺ release in the N2A cell line were investigated. Free and loosely bound Zn²⁺ was detected in the neuroblastoma N2A cell line using the fluorescent dye Zynpyr1 (Mellitech). Zynpyr1 is a zinc-specific cell permeable probe that emits fluorescence when it binds to Zn²⁺ (Kd = 0.7 ± 0.1nM).

The zinc assay was performed in cells grown on coverslips or in a 96-well plate, detecting the fluorescence with a fluorescence microscope or with a fluorescence plate reader at an excitation wavelength of 480nm and emission wavelength of 530nm, respectively.

2.9.1 Zinc assay on cells grown on coverslip.

N2A cell line was harvested from a confluent T75 flask and seeded in a 6cm Petri dish containing small rounded Poly-L-Lysine coated coverslips. Cells were cultured overnight in incubator at 37°C, 5%CO₂ and 95% of humidity to achieve a confluence above 60%. The following day cells were exposed to HBCD at concentrations of 1 or 2µM for

24 hours in an incubator. A DMSO control was also included. Coverslips were then removed from the dish and placed on microscope slides. Ringer buffer was prepared adding 3M NaCl, 2.7M KCl, 0.8M MgCl₂, 2M HEPES, 0.75M glucose, 1.8M CaCl₂, calibrated to pH 7.4 and used to maintain cells moisturised.

Cells were observed under microscope at 10X magnification, and once the confluence was checked, pictures of cells were taken. The Ringer buffer was then removed and 500µl of 5µM Zincpyr1 dye diluted in PBS was added. Cells were exposed to the dye for 10 seconds following by a wash with PBS for 20 seconds.

Coverslips were observed using fluorescence microscope Axioscop2 (Zeiss) and pictures were taken with Imagine Workbench (Axon Laboratory). Pictures were analysed counting the number of fluorescent cells and the total number of cells. Results were expressed as percentage of cells showing fluorescence.

2.9.2 Zinc assay using 96-wells plate.

To test a higher number of samples and multiple conditions, the zinc assay was also performed in 96-wells plate as described below.

2.9.2.1 Zinc assay in N2A cells exposed to HBCD

Cells were seeded in a 96-wells plate with a maximum number of 10⁴ per well in 100µl DMEM, and culture over night. Cells were then incubated for 24 hours with 1µM HBCD in <0.01% DMSO, or medium alone.

After the incubation period, the plate was removed from the incubator, the media was aspirated, and 100µl per well of 16µM Zincpyr1 dye diluted in PBS was added. After exposure to the dye for 30 seconds, cells were washed with PBS for 30 seconds. The fluorescence was measured with the plate reader Thermo Scientific Fluoroskan Ascent at an excitation wavelength of 480nm and emission wavelength of 530nm.

Fluorescence emission was normalized to the DMSO control in each row separately and the Zn²⁺-induced fluorescence expressed as percentage of the control.

2.9.2.2 Zinc assay in N2A cells exposed to HBCD and DEDTC

To confirm that the fluorescence detected was specific and it was representing zinc concentration perturbation, before incubation with HBCD, cells were incubated with the zinc chelator diethyldithiocarbamate (DEDTC).

DEDTC was diluted in DMEM to the concentration of 50µM and 100µl per well was added to the plate. Cells were then incubated for 2 hours in incubator at 37°C, 5% CO₂ and 95% of humidity. After exposure to the chelator, 1µM HBCD was added and cells were incubated for 24 hours. Zinc concentration was detected as previous described.

2.9.2.3 Zinc assay in N2A cells exposed to HBCD and to the NO donor Nitroprusside.

A positive control experiment using the nitric oxide (NO) donor Nitroprusside was also performed. After cells were seeded in a 96-well plate and cultured over-night in incubator, 100µl of 10µM of Nitroprusside was added to each well and the plate was incubated for 24 hours 37°C, 5% CO₂ and 95% of humidity. The following day the Zn²⁺ concentration was measured using Zincpyr1 dye as mentioned above.

2.9.2.4 Zinc assay in N2A cells exposed to HBCD and NAC

To investigate if the mechanism of action on the zinc homeostasis perturbation caused by HBCD involved oxidative stress, before exposure to the toxicant, N2A cells were incubated with the antioxidant, N-acetylcysteine (NAC).

After cells were seeded in a 96-well plate and cultured over night, 10µM of NAC diluted in DMEM was added. The plate was then placed in incubated for 1 hour and 1µM HBCD was added. Cells were cultured for an additional 24 hours in an incubator and intracellular Zn²⁺ was detected as described above.

2.9.2.5 Zinc assay in N2A cells exposed to HBCD and L-NAME

In order to investigate if the Zinc disruption caused from HBCD was caused by activation of the NO pathway, cells were treated with the NO pathway blocker L-NAME.

The N2A cell line was culture in a 96-well plate over night in an incubator. L-NAME (10 μ M) diluted in DMEM was added, and the cells incubated for 1 hour in an incubator. The cells were then exposed to 1 μ M HBCD for 24 hours. Following the incubation, intracellular Zn²⁺ was measured as described above.

2.10 Statistical analysis

Statistical analyses of microarray experiments are described under Section 2.7.3.4. Statistical testing of other experiments conducted was performed with SigmaPlot. Normality Test and Equal variance test were always performed on the data and statistical tests were carried out before conversion to ratios or percentages. Depending on the assay design, One Way ANOVA or Two Way ANOVA were used, and Multiple Comparison Procedures (Holm-Sidak method) was performed to compare different treatments.

3. PBDE-47 and HBCD
cytotoxicity assessment

3.1 Introduction

The molecular mechanisms involved in the toxicities of PBDE-47 and HBCD are still not well understood. Their ability to pass the blood-brain barrier (BBB) suggests that the accumulation of the two toxicants in the brain may cause neurotoxicity, as can be evidenced by developmental behavioural effects (Gee and Moser ; Lilienthal et al. 2009). In fact, in previous studies it was reported that acute exposure to PBDE-47 during postnatal development may produce subtle changes in the development of neuromotor systems that may alter adult behaviour (Gee and Moser 2008). In rats exposed to HBCD, effects on dopamine-dependent behaviour were observed (Lilienthal et al. 2009). Additionally, previous studies have shown that polychlorinated biphenyls (PCBs), which are chemically similar to PBDEs, cause neurotoxicity *in vivo* with manifestation of deranged spontaneous behaviour with learning and memory defects (Viberg et al. 2003c), suggesting that chemical with a similar structure may cause analogous effects.

The molecular mechanisms involved in the toxicities of the two compounds are difficult to deduce from animal experiments alone, suggesting the importance to investigate PBDE-47 and HBCD effects on neuronal cell lines. Thus, the mechanisms of cellular toxicity of the two toxicants were accessed in two neuroblastoma cell lines, N2A and NSC19. In this Chapter, the cytotoxicity of PBDE- 47 and HBCD to N2A and NSC19 cells are investigated. This provides a starting point for further studies into the mechanism of toxicity as expected in Chapter four and five.

Caspase-3, a cysteine protease, which is part of the caspases family, is a marker and irreversible point of apoptosis (Saraste and Pulkki 2000). Activation of the upstream caspases, such as caspases 2, 8, 9 and 10, by pro-apoptotic signals leads to proteolytic activation of the downstream or effector caspases 3, 6 and 7. The effector caspases actually cleave a set of vital proteins and thus, initiate and execute the apoptotic degradation phase including DNA degradation and the typical morphologic features (Saraste and Pulkki 2000). An approach to study the presence of apoptosis is to demonstrate the activation of downstream caspases, such as caspase-3, with an enzymatic assay (Saraste and Pulkki 2000). Thus, in the present study, caspase-3 activity was measured as a marker for apoptosis caused by PBDE-47 or HBCD exposure.

In order to assess the effect of HBCD on the membrane structure, Lactate Dehydrogenase (LDH) leakage from the intracellular space into the media was also measured as an indication of loss in membrane integrity and permeability. LDH is a cytosolic enzyme that catalyses the reversible reduction of pyruvate into lactate in the presence of NADH. LDH is normally very low in the medium of cultured cells, even at high cell densities. Its increase in the supernatant is an indicator of loss in cell viability and damage of cellular membrane integrity (Legrand et al. 1992).

3.1.1 Docosahexaenoic acid (DHA) and lipid regulation

Accumulation of PBDE-47 and HBCD has been reported in biota with biomagnification in the food chain (Covaci et al. 2006; Schechter et al. 2008). Studies conducted in food samples from the US, reported that PBDE-47 and HBCD levels are higher in fish, especially fatty fish such as salmon, than in other food sources (Hites et al. 2004b; Schechter et al. 2010b). High levels of PBDE-47 and HBCD have been also been reported in fish samples from the Swedish market, compared to other food groups (Tornkvist et al. 2011).

In the literature, it is largely agreed that consumption of fish is one of the main sources of pollutants for humans, with consequences in accumulation of food-born toxicants such as PBDE-47 and HBCD (Schechter et al. 2006; Tornkvist et al. 2011). On the other hand, fish is a fundamental source for nutrients, such as polyunsaturated omega-3 fatty acids, which plays an important role in the maintenance of normal neural functions (H. Y. Kim 2007), and in coronary heart disease prevention (Mozaffarian and Rimm 2006).

One of the most abundant polyunsaturated fatty acids in the human brain is docosahexaenoic acid (DHA). The main source of DHA for the organism is through the diet, especially with consumption of fish, and through maternal milk for infants. DHA biosynthesis does occur in the human liver where DHA is produced by desaturation and elongation of the precursor linolenic acid, a shorter chain *n*-3 fatty acid. DHA is then secreted in the blood stream, thus it reaches the brain where it is incorporated into membrane phospholipids (H. Y. Kim 2007). In the central nervous system, the supply of DHA principally depends on circulating plasma DHA derived from diet or from biosynthesis (H. Y. Kim 2007). In fact, among neural cells, only astrocytes have the capacity to synthesise DHA, neurons cannot produce it because of the lack of desaturase activity. When the DHA supply is inadequate, especially during foetal development,

astrocytes release DHA into the extracellular fluid providing a source for neuronal cells. The mechanism of neuronal DHA uptake is not clear but a diffusion of free fatty acid across the cell membranes has been demonstrated in cellular models (H. Y. Kim 2007).

In the literature, numerous studies report the role of DHA in brain development (Cao et al. 2009; Salem et al. 2001), especially in learning and memory (Boucher et al. 2011; Hashimoto et al. 2002). DHA has been also suggested to positively affect neuron survival and differentiation (Bazan 2005). In addition, studies on the ability of DHA to modulate methylmercury (MeHg)-induced neurotoxicity in primary astrocytes and neurons in rodents, showed that DHA has neuroprotective effect against MeHg toxicity *in vitro* (Kaur et al. 2007; Kaur et al. 2008).

The effect of DHA on lipid regulation and on membrane composition has also been largely investigated. Previous studies report that DHA has a role in lipid homeostasis regulation in brain. In fact, it has been shown that a DHA enriched diet can modify the lipid composition in brain and can decrease lipid peroxidation (Dalfo et al. 2007; Muntane et al. 2010; W. Zhang et al. 1995). It has also been suggested that DHA can affect membrane functions. DHA is mainly concentrated within the phospholipids in the cellular membrane and has a central role in maintaining the concentration of phosphatidylserine (PS), one of the main phospholipids components (Bazan 2005). Therefore, considering the fact that PS is the major negatively charged phospholipid class in many mammalian cell membranes and many of the signalling proteins such as protein kinases are influenced by PS, this alteration may have significant implications for cellular functions (Salem et al. 2001).

In literature, reports show that HBCD exposure can cause increasing levels of biomarker indicating lipid peroxidation and oxidative stress (Hu et al. 2009), with induction of reactive oxygen species (ROS) (Deng et al. 2009). Therefore, considering that DHA has a fundamental role in membrane functions and maintenance, potentially ameliorative effects of DHA on the membrane damage caused by HBCD are in this Chapter investigated.

3.1.2 Chapter objectives

The objectives of this Chapter were to:

1. assess the cytotoxicity of PBDE-47 and HBCD on the neuroblastoma cell lines, N2A and NSC19;
2. determine the effect on cell viability and on the activation of Caspase-3 as a marker of apoptosis, caused by the two toxicants;
3. investigate the effect of HBCD on the cellular membrane, with measurement of LDH leakage as a marker increased of membrane permeability and damage of membrane integrity;
4. establish if the role of the fatty acid DHA in membrane functions and maintenance can potentially lead to ameliorative effects on the membrane damage caused by HBCD.

3.2 Methods

All general methods performed in this chapter are described in Chapter 2.

3.3 Results

3.3.1 Effect on cell viability during exposure to PBDE-47 or HBCD

In order to characterise the tolerance of N2A and NSC-19 cells to the toxicants PBDE-47 and HBCD, the MTT assay (SIGMA), an method to measure metabolically active cells (Mosmann 1983), was performed. Cells were first incubated with a geometric range-finder series of concentration between 0.39 μ M to 100 μ M (data not shown), to narrow the concentrations to those resulting in dose dependent response (1.56 μ M to 35 μ M).

The initial response of the N2A and NSC19 cell lines exposed to PBDE-47 after 48 hours, presented similar effects in the measurement of metabolically active cells. The cell viability decreased linearly in a concentration-dependent manner. It was observed that cells incubated with concentrations between 1.56 to 3.15 μ M have decreased cell

viability between 20 and 30% for the N2A cell line, and between 30 to 40% for the NSC-19 cell line, relative to the DMSO control. Concentrations equal to or greater than 6.25 μ M PBDE-47 resulted in more than 50% reduction in cell viability for both the cell lines, and a complete quenching of metabolic activity was observed for concentration of 25 μ M or higher. The half maximal effective concentration (EC50) was estimated to be 4-5 μ M in both the cell lines and the EC10 about 1 μ M. Figure 3.1 A and B.

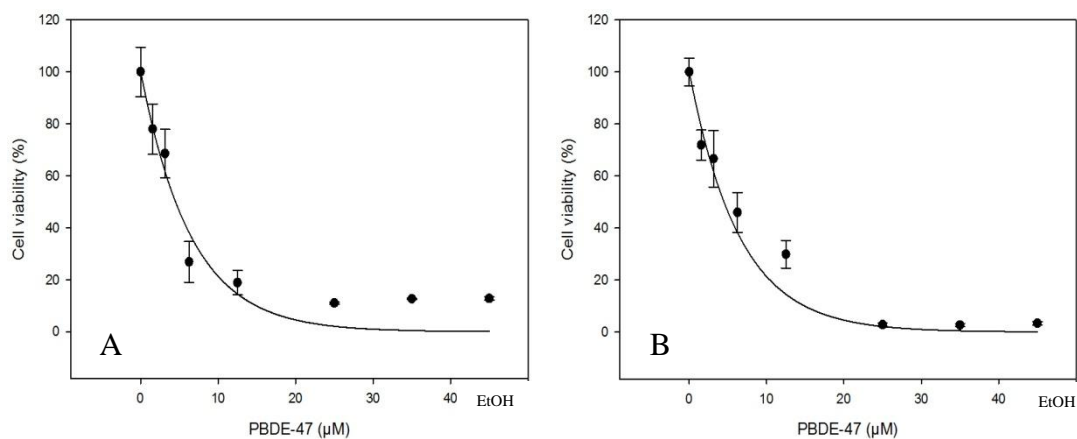


Figure 3.1: Cell viability of N2A cell line (figure A) and NSC19 cell line (figure B) exposed to PBDE-47. The two cell lines were incubated for 48 hours with a geometric series of concentration between 1.56 μ M to 35 μ M of PBDE-47. Cell viability was measured with the MTT assay. Viability decreased with increasing of PBDE-47 in a concentration-dependent manner. Three independent experiments were performed using eight replicates, and the average between replicates are reported (n=3). The regression curve “exponential decay” is also added. The cellular viability is express in percentage normalized to the DMSO control and the deviation standard is reported. Positive control (Ethanol) is also shown.

Cytotoxicity of N2A and NSC19 cells to HBCD was similar to that elicited by PBDE-47 treatment. Exposure to HBCD at concentrations between 1.56 to 50 μ M caused increasing degree of cytotoxicity as compared to the DMSO control. It was observed that cell viability was reduced by about 20-30% at concentrations between 1.5 to 3.15 μ M for N2A and NSC-19 cell lines as shown in figure 3.2 A and B. At concentrations greater than 6.25 μ M, cell viability decreased by more than 50% for both cell lines and up to 100% at concentration of 12.5 μ M for N2A cells and 25 μ M for NSC-19 cell line. The EC50 was estimated to be 5 and 6 μ M for the N2A and the NSC19 cell lines respectively, and the EC10 to be slightly more than 1 μ M in both the cell lines. Figure 3.2.

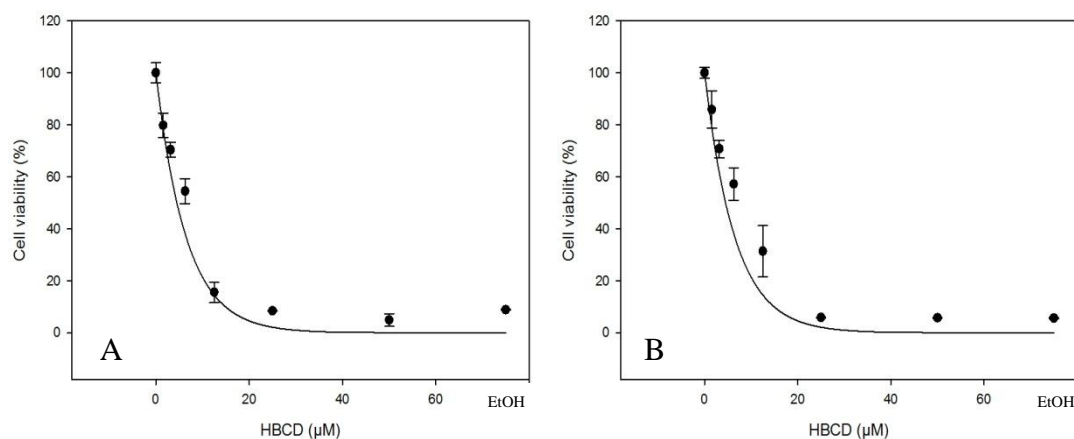


Figure 3.2: Cell viability of N2A cell line (figure A) and NSC19 cell line (figure B) exposed to HBCD. The two cell lines were incubated for 48 hours with a geometric series of concentration between 1.56 μ M to 35 μ M of HBCD. Cell viability was measured with the MTT assay. Viability decreased with increasing of HBCD in a concentration-dependent manner. Three independent experiments were performed using eight replicates, and the average between replicates are reported ($n=3$). The regression curve “exponential decay” is also added. The cellular viability is expressed in percentage normalized to the DMSO control and the deviation standard is reported. Positive control (Ethanol) is also shown.

3.3.2 Assessment of apoptosis in cells exposed to PBDE-47 or HBCD

A caspase-3 assay (Invitrogen) was performed in order to indicate if the cell viability loss due to the toxic effect of PBDE-47 and HBCD, previously demonstrated with the MTT assay, was caused by activation of the apoptosis pathway, with the induction of the caspase cascade. Caspase-3 was thus measured in N2A and NSC19 cell lines after incubation with PBDE-47 or HBCD at micromolar concentrations.

Based on the results of the MTT assay previously performed, a range of concentrations of PBDE-47 and HBCD causing a decrease of cell viability between 20 to 30% was selected for analysis of effect on caspase-3 activity. The cells were treated with four different concentrations: 1, 2, 4 or 8 μ M for 24 hours. As DMSO was used as a vehicle for the compounds, a DMSO only control was also included.

As illustrated in the figure below (figure 3.3, A), in the N2A cell line incubated with PBDE-47, at the concentrations of 2 μ M or 4 μ M caspase-3 enzymatic activity significantly increased compared the DMSO control ($p<0.05$). At the lower concentration of 1 μ M, the caspase-3 activity was not different from the control and also

at the highest PBDE-47 concentration (8 μ M), the caspase-3 activity showed no difference compared to the DMSO control.

In the NSC-19 cell line exposed to PBDE-47, caspase-3 activity showed similar regulation as reported for N2A cells. A significant increase ($p < 0.05$) was detected in cells exposed to PBDE-47 at the lowest concentration of 1, 2 or 4 μ M, compared to the DMSO control. Cells exposed to the higher concentration of 8 μ M, didn't show a significant difference in caspase-3 activity compared to the control. Results are reported in Figure 3.3, B.

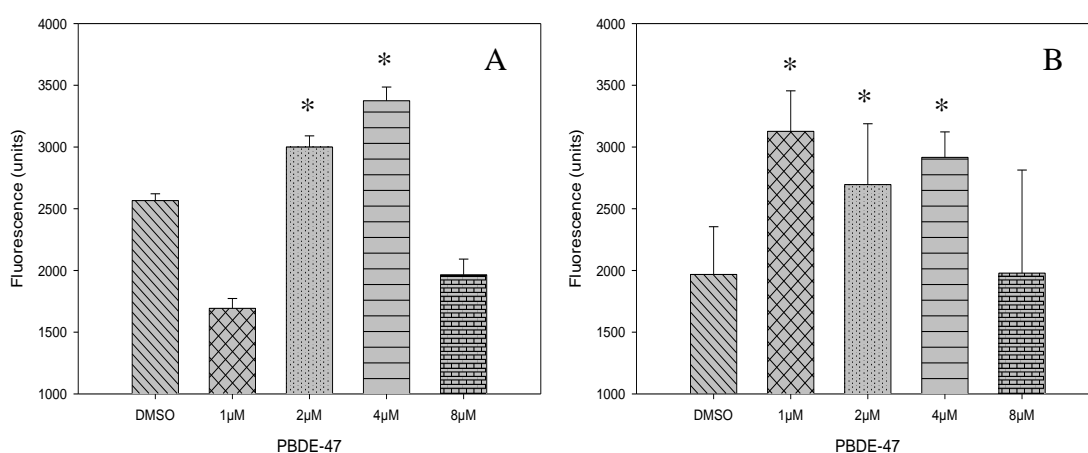


Figure 3.3: Caspase-3 activity in cells exposed to PBDE-47. A caspase-3 assay was used as indicator of apoptosis in the N2A cell line (A) and in the NSC19 cell line (B) exposed to PBDE-47. The two cell cultures were incubated for 24h with four different concentrations of PBDE-47 (1, 2, 4 or 8 μ M). A caspase-3 fluorescence assay was then performed and the fluorescence measured every 15 min in a microplate reader with 485nm excitation and 530nm emission, and is here expressed in arbitrary units. Three independent experiments were performed using eight replicates, and the averages between replicates are reported ($n=3$). Bars represent standard deviation and the asterisk represents a $p < 0.05$. A negative control (DMSO) is also included.

In cells treated with HBCD the results clearly show an increase in caspase-3 activity at the lowest concentration, 1 or 2 μ M for the N2A cell line (figure 3.4, A) and 1 μ M for the NSC-19 cell line (figure 3.4, B). As observed in cells exposed to PBDE-47, at concentrations higher than these, the caspase-3 activity drops dramatically and the value is lower than the negative control.

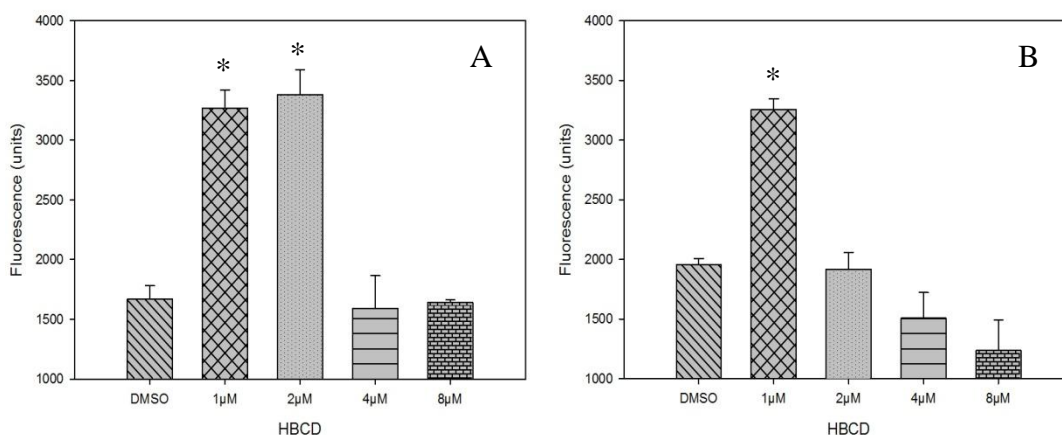


Figure 3.4: Caspase-3 activity in cells exposed to HBCD. A caspase-3 assay was used as indicator of apoptosis in the N2A cell line (A) and in the NSC19 cell line (B) exposed to HBCD. The two cell cultures were incubated for 24h with four different concentrations of HBCD (1, 2, 4 or 8µM). A caspase-3 fluorescence assay was then performed and the fluorescence measured every 15 min in a microplate reader with 485nm excitation and 530nm emission, and is here expressed in arbitrary units. Three independent experiments were performed using eight replicates, and the averages between replicates are reported (n=3). Bars represent standard deviation and the asterisk represents a $p < 0.05$. A negative control (DMSO) is also included.

3.3.3 Lactate Dehydrogenase (LDH) leakage as a marker of membrane permeability damage in cells exposed to HBCD

In order to investigate if the HBCD toxicity was leading to membrane damage, lactate dehydrogenase (LDH) leakage in the media was measured as a marker of membrane integrity. In this study, only one of the two toxicants was selected to be tested in the N2A cell line, at the concentration of 1µM only. This choice was necessitated by the time available limited, and therefore further studies are needed to investigate the effect on the LDH leakage caused by both the toxicants in both the cell lines used.

Exposure of the N2A cell line to 1µM HBCD for 24 hours demonstrated a significant increase in LDH leakage into the media compared to the DMSO control ($p < 0.05$). (Figure 3.5).

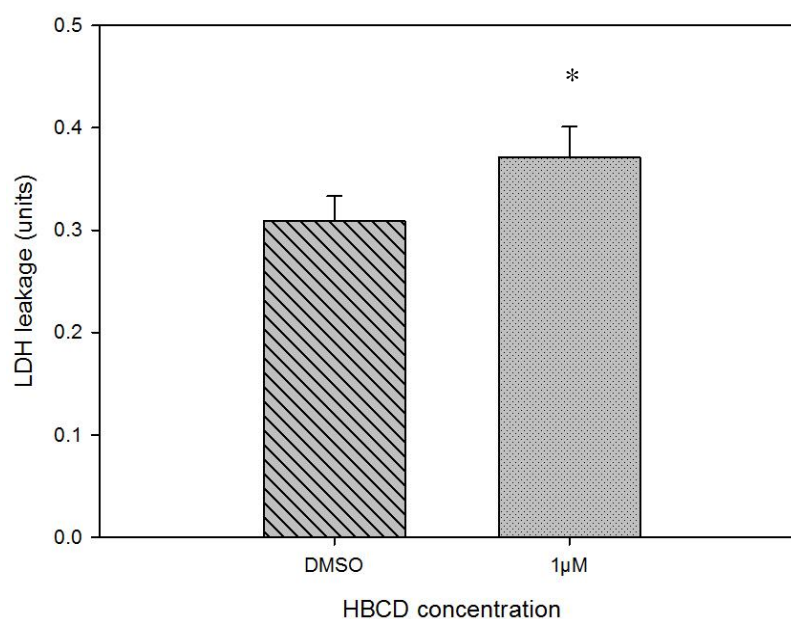


Figure 3.5: LDH leakage from N2A cells exposed to HBCD for 24 hours. The N2A cell line was incubated with 1µM of HBCD for 24 hours. LDH enzyme activity was measured in the media and in the cytoplasm. LDH leakage was calculated as the amount of the enzyme detected in the media compared to the total amount of LDH (medium + cytoplasm). Three independent experiments were performed using eight replicates, and the averages between replicates are reported (n=3). Bars represent standard deviation and the asterisk represents a $p < 0.05$. A negative control (DMSO) is also included.

3.3.4 Effect of the fatty acid DHA on LDH leakage caused by HBCD toxicity

In order to investigate if the fatty acid docosahexaenoic acid (DHA) could have a mitigate effect on the HBCD toxicity, LDH leakage in the media was measured in the N2A cell line treated with DHA and then exposed to HBCD. Because of true limitations, only one marker for toxicity was measured. LDH leakage was believed to be a relevant assay to investigate the effect of DHA on HBCD toxicity, based on the assumption that DHA can affect membrane structure and integrity, and that LDH leakage is a marker of membrane damage.

Cells were pre-incubated with 30 or 90µM of DHA for 24 hours, washed with PBS, and then exposed to 1µM of HBCD for 24 hours. DHA concentrations were selected based on a previous study analysing the fatty acid profile in C6-glia and B35-neuronal cell lines treated with a range of DHA concentrations (Kaur et al. 2007). In this study it was shown that cells treated with 90µM of DHA resulted in DHA constituting 19–24% of

the total fatty acids in the cultures, which is similar to what has been found in the gray matter of the brain (Kaur et al. 2007).

In the present study, the ration between cells exposed to HBCD and the control, in presence or absence of DHA, showed that a pre-incubation with 30 μ M of DHA was able to reduce the LDH leakage caused by HBCD, compared to the cells not treated with the fatty acid. A treatment with 90 μ M of DHA didn't cause any change in the LDH leakage compared to the not treated cells.

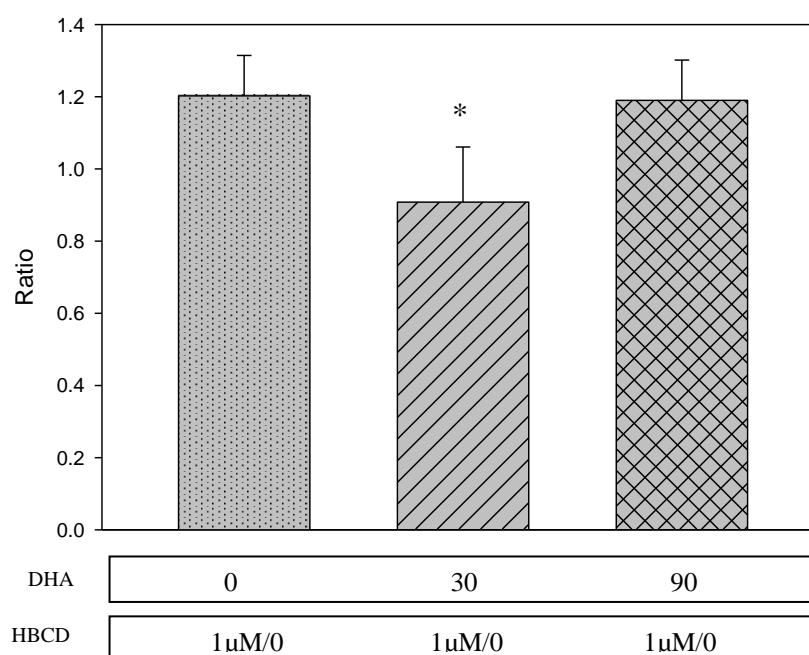


Figure 3.6: Effects of DHA on LDH leakage from N2A cells exposed to HBCD. The N2A cell line was exposed to HBCD (1 μ M) for 24 hours after a pre-incubation for 24 hours with 30 or 90 μ M of the fatty acid DHA. LDH enzyme was measure in the media and in the cytoplasm. LDH leakage was calculated as the amount of the enzyme detected in the media compared to the total amount of LDH (medium +cytoplasm). The figure represents the ratios between cells treated with HBCD and the control, in absence, or after incubation with 30 or 90 μ M of DHA. Three independent experiments were performed using eight replicates, and the average between replicates are reported (n=3). Bars represent standard deviation and the asterisk represents a $p < 0.05$.

3.4 Chapter discussion

In this Chapter, cytotoxicity of PBDE-47 and HBCD was characterised. Neuronal cells' susceptibility to the two BFRs was assessed and the results clearly indicated that PBDE-47 and HBCD are toxic for both the cell lines tested, causing cell viability loss, increasing of caspase-3 activity, and LDH leakage at single digit micromolar concentrations. We also established that the fatty acid DHA can ameliorate HBCD effect on membrane damage.

In the present study, the half maximal effective concentration (EC_{50}) for cells exposed to PBDE-47 was estimated to be 4-5 μ M in both the cell lines and the EC_{10} about 1 μ M. HBCD showed an EC_{50} of 5 μ M in the N2A cell line and 6 μ M in the NSC19 cell line and EC_{10} slightly more than 1 μ M. The potency of inducing cell death was very similar for both the toxicants and in both the cell lines tested. It is also comparable to what was found in a previous study on rat cerebellar granule cells exposed to the PBDE commercial mixture DE-71 or to HBCD which reported similar EC values with EC_{50} concentrations about 7 and 3 μ M for DE-71 and HBCD respectively (Reistad et al. 2006b). In the same study, in order to examine if the toxicity was due to the compound itself or a metabolite, the cells were incubated with the compounds together with rat liver post-mitochondrial S9 fraction. In this experiment the cell death was reduced by 58 and 63% for DE-71 and HBCD respectively, indicating that the parent compounds are the ultimate toxicant (Reistad et al. 2006b). PBDE-47 and HBCD EC_{50} were also shown to be very similar to what was previously observed for PCB, in fact Mariussen et al estimated that the EC_{50} value for the single PCB congener, PCB153, was 8 μ M, slightly less toxic than the BFRs tested here (Mariussen et al. 2002).

In our study, PBDE-47 and HBCD were also able to increase the marker for apoptosis, caspase-3, at micro molar concentrations. PBDE-47 was seen to cause increase of caspase activity at concentration as low as 2 μ M in the N2A cell line and as low as 1 μ M in the NSC19 cell line as can see in figure 3.3. Increasing in caspase -3 activity caused by HBCD was seen already at 1 μ M in both the cell lines as shown in figure 3.4. In both of the toxicants, increase in caspase-3 activity was seen at the lowest concentration tested, but in cells exposed to higher concentrations the enzyme activity suddenly dropped. This effect was probably caused by the loss of cell viability with reduction in the number of cells capable of mounting a caspase cascade after exposure to PBDE-47 or HBCD. In fact, reduction of caspase-3 activity was seen at concentrations higher then

4 μ M in cells exposed to PBDE-47 and 2 μ M for HBCD, and the MTT assay showed a reduction of cell viability of 50% at 4-5 μ M in both the toxicants. Even if this is the main hypothesis, it can also be argued that absence of caspase-3 activity at the highest concentration tested may as well be caused by onset of necrosis. However, in this specific experiment, the absence of an independent measure of viable cell number is a limitation to interpretation, therefore further studies are needed to better understand these data.

Investigation of HBCD effects on membrane integrity was conducted on the N2A cell line. It was seen that HBCD can cause increasing of LDH leakage in cells exposed to concentration as low as 1 μ M. LDH leakage is a direct consequence of cellular membrane damage with increasing of membrane permeability. A previous study already suggested that other structurally similar BFRs, such as PCBs, cause disruption of membrane structure, which alters the function of membrane proteins (Y. Tan et al. 2004a). It could be also hypothesised that the LDH leakage observed was a consequence of apoptosis, with membrane disruption and therefore increase of permeability. In fact, the MTT assay and the caspase-3 assay showed that HBCD can cause apoptosis at concentration as low as 1 μ M, with a loss of cell viability equal to the 10%. Therefore it is not possible to determine if the effect observed are a direct consequence of HBCD exposure on membrane integrity, or a secondary effect to necrosis.

Cellular membrane disruption can be also a consequence of lipid peroxidation due to the formation of reactive oxygen species (ROS) products. Increases in levels of ROS and lipid peroxidation (LPO), were previously seen as effects of HBCD exposure (Hu et al. 2009; X. L. Zhang et al. 2008). In the same study the positive correlation between the LDH release and ROS formation was suggested as indication that the toxic mechanism of HBCD might be mediated by oxidative damage (X. L. Zhang et al. 2008).

In the present study for the first time we investigated whether DHA supplementation can ameliorate the LDH leakage caused by HBCD exposure. DHA is the most abundant long-chain polyunsaturated fatty acid (LC-PUFAs) present in brain with essential roles in brain development and function. The main source of PUFAs for adult humans is via fish consumption, especially fatty fish such as salmon (Kaur et al. 2008). Fish is therefore an important supply of PUFAs as well as a source of contaminants, such as HBCD. The possible ameliorative effect of DHA on HBCD toxicity was therefore investigated.

In the N2A cell line exposed to HBCD in absence or presence of DHA, 30 μ M of DHA was able to reduce the LDH leakage elicited by HBCD. The higher concentration used, 90 μ M, didn't caused any variation in the LDH leakage, compared to the cells not treated with the fatty acid, suggesting that the lowest concentration used was more ideal for the cells used.

It could be argued that as DHA was added to the cells, the higher level of fatty acid in the medium could lead to the binding of the lipophilic HBCD to the fatty acid and, thus, reduced HBCD accumulation in cells. However, before DHA was added to the cells, it was bound to BSA to increase solubility and cellular uptake. Assuming that the uptake was indeed effective, the amount of DHA remaining in the medium after 24 hours of incubation would have been expected to decline. In addition, following the pre-treatment with DHA, the cells were washed with PBS before incubation with HBCD. Therefore, it is considered unlikely that any appreciable amount of DHA would be remaining in the medium during the HBCD exposure and it is therefore improbable that DHA treatment reduced the effective dose of HBCD received by the cells. Instead, the positive influence of DHA on cell tolerance to HBCD is proposed to be caused by the effects of DHA on the cells themselves.

Overall, the findings suggest a protective role of DHA against HBCD toxicity and possibly cell membrane damage, probably due to the ability of DHA to increase glutathione reductase activity and, therefore, to increase the antioxidant defence, to inhibit pro-inflammatory and pro-apoptotic signalling and to contribute to the formation and stability of membrane microdomains (Arnal et al. 2010; Kherjee et al. 2007). In fact, in previous studies in rats, it has been shown that DHA has the ability to increase the levels of reduced glutathione and raise glutathione reductase activity, and to suppress the increase in lipid peroxide and reactive oxygen species levels, suggesting an important role in the antioxidant defence (Hashimoto et al. 2002). In It has also been shown that DHA is the precursor of a biosynthetic product called neuroprotectin D1 (NPD1). NPD1 has been detected in human cells *in vitro* and in mouse *in vivo* (Bazan 2005). NPD1 has been shown to have neuroprotective bioactivity during oxidative stress and ability to inactivate pro-apoptotic and pro-inflammatory signalling (Kherjee et al. 2007).

It has also been suggested that PUFA incorporation into membrane phospholipids has effects on the formation and stability of membrane microdomains (Shaikh and Edidin

2006) and in maintaining the concentration of phosphatidylserine (PS) (Bazan 2005). Therefore, considering that most of the DHA is accumulated in the phospholipids of the cellular membrane and that PS influences many signalling proteins, such as protein kinases (Kaur et al. 2007; Salem et al. 2001), DHA could have protected or repaired the damage effects caused by HBCD on the cellular membrane structure.

3.5 Chapter conclusion

In this chapter the toxicities of the two POPs PBDE-47 and HBCD in neuroblastoma cell lines were investigated. The two toxicants were shown to affect cell viability at single digit micromolar concentrations, with EC₅₀ values of about 4-5µM for PBDE-47 and between 5 to 6µM for HBCD; EC₁₀ was about 1µM for both the toxicants. These findings are comparable to what was found in a previous study where rat cerebellar granule cells exposed to the PBDE commercial mixture DE-71 or to HBCD showed EC₅₀ values about 7 and 3µM for DE-71 and HBCD respectively. Increased caspase-3 activity, indicative of apoptosis, was also detected in cells exposed to either of the toxicants at a concentration as low as 1µM, which was the lowest concentration tested. At higher concentrations (>4µM) the activity of caspase-3 suddenly dropped indicating loss of functional cells. However, the limit of this method is the impossibility to determine the number viable cells, and therefore the percentage of cell loss. Without this variable the measurement of caspase-3 cannot be considered exhaustive.

Investigation into the effect of HBCD on the cell membrane integrity revealed that this toxicant can induce release of LDH enzyme into the medium of cells exposed at 1µM HBCD, indicating damage to the cell membrane. However, from the present data, it is not possible to establish if the effect on membrane permeability is a consequence of a direct effect of HBCD, or an indirect consequence of apoptosis or other cytotoxic mechanisms.

A pre-treatment with 30µM of the fatty acid DHA reduced LDH leakage induced by HBCD, suggesting a mitigating effect of DHA on HBCD toxicity. These results indicate that DHA has protective effects on the cell membrane damage caused by HBCD, possibly due to the ability of DHA to protect against oxidative stress, inhibit pro-inflammatory and pro-apoptotic signalling, produce NPD1, or to contribute to the formation and stability of membrane microdomains.

4. PBDE-47 and HBCD
gene expression profile

4.1 Introduction

In literature little is reported about the direct effect of PBDE-47 and HBCD on gene expression regulation (Canton et al. 2008; Crump et al. 2008; R. Song et al. 2009a; Van Boxtel et al. 2008; Yamada-Okabe et al. 2005). Therefore, to elucidate the toxicity targets of the two toxicants, for the first time we investigated the global gene expression profiles of the two neuroblastoma cell lines N2A and NSC19 exposed to PBDE-47 or to HBCD. Microarray was the technique used to analyse global gene regulation. This technology can be used to assay the relative expression of all genes in a genome, and so understand when each gene is or is not expressed, and how its expression changes with perturbations (Van Boxtel et al. 2008).

Previously, global gene expression profile after exposure to PBDE-47 has been assessed on zebrafish embryonic fibroblast (PAC2) (Van Boxtel et al. 2008), on liver of rats (Suvorov and Takser 2010), on rat hepatoma (Wahl et al. 2008b), and more recently on the brain of developing mice exposed during gestation and lactation to the toxicant (Haave et al. 2011b). Studies analysing the global gene expression profile after exposure to HBCD are more limited and restricted mainly to liver (Canton et al. 2008; Crump et al. 2010). In addition, effects of this toxicant have been tested on the expression of specific genes related to endocrine disruption (Yamada-Okabe et al. 2005).

In a previous study PAC2 cells exposed to PBDE-47 or to its metabolite OH-PBDE-47 showed that OH-PBDE47 significantly regulated genes involved in carbohydrate metabolism and proton transport, but results regarding the parent compound were not exhaustive (Van Boxtel et al. 2008). Microarray analysis has also been performed on the liver of rats exposed to PBDE-47 showing that oxidoreductase and transferase protein families were enriched, and genes involved in functions such as carbohydrate metabolism; electron transport; and lipid, fatty acid, and steroid metabolism were also affected (Suvorov and Takser 2010). Wahl et al conducted microarray experiments on rat hepatoma cells to compare changes in gene expression induced by either PBDE47 or the AhR agonist 2,3,7,8-tetrabromo-dibenzofuran (TBDF), showing that these two toxicants regulated different sets of genes (Wahl et al. 2008b). Gene enrichment after exposure to PBDE-47 has also been investigated testing specific genes or pathways rather than analysing the global gene expression profile using microarray. Thyroid hormone-mediated genes were seen to be differentially expressed in developing rat brain (Wang et al. 2011) and also in the pituitary and brain of minnows exposed to the

toxicant (Lema et al. 2008). In addition, regulation of CYP genes was investigated in juvenile Atlantic cod exposed to PBDE-47, which caused a significant reduction in abundance of mRNAs for CYP1A, CYP2C33 and CYP3C1 (Olsvik et al. 2009).

Microarray analyses on HBCD toxicity are very limited and mainly focus on liver. Gene expression analysis on rat liver showed that several specific pathways were affected by HBCD exposure, including PPAR-mediated regulation of lipid metabolism, triacylglycerol metabolism, cholesterol biosynthesis, and phase I and II pathways (Canton et al. 2008). In rat liver, HBCD was also seen to induce regulation of CYPs, such as CYP2B1 or CYP3A1 (Germer et al. 2006). Upregulation of CYPs was also seen in chicken hepatocytes exposed to HBCD (Crump et al. 2008)

Studies of specific genes showed that HBCD can increase the expression of the gene TFF1 in MCF-7 breast cancer cells causing oestrogen-like effects (Dorosh et al. 2011). In Purkinje cells HBCD was seen to suppress thyroid hormone receptor (TR)-mediated transcription (Ibhazehiebo et al. 2011). Effects on TR-mediated gene expression were also observed in HeLa cell line exposed to HBCD (Yamada-Okabe et al. 2005), and gene expression analysis in cultured hepatocytes derived from embryonic chickens showed transthyretin and liver fatty acid-binding protein to be downregulated (Crump et al. 2008).

These limited number of gene expression studies illustrate a shortage of investigations of the effects of PBDE-47 or HBCD in brain and also in neuronal cell models. Because some of the most sensitive endpoints of PBDE-47 and HBCD relate to neurological disturbances it is of importance to understand and characterise the molecular events that lead to these responses. For this reason, the global gene expression profile of two neuroblastoma cell lines exposed to PBDE-47 or HBCD was assessed in the present study. After microarray analysis, the resulting profiles were used to investigate molecular functions, biological processes and gene networks that were preferentially affected by PBDE-47 or HBCD.

Following the identification of enriched functions and pathways regulated by the two POPs, individual genes of interest were identified and their expression confirmed by Q-PCR.

In our laboratory, *in vivo* feeding trials exposing mice to either PBDE-47 or HBCD through the diet have been also conducted (Carroll 2011; Rasinger 2011). Gene and

protein expression profile in murine brains were generated using microarrays (Carroll 2011) and gel-based proteomics (Rasinger 2011) platforms. In these studies, the investigation of global gene expression in brain identified that PBDE-47 and HBCD exposure affect several fundamental cellular functions. Genes involved in protein folding and unfolded protein response were seen deregulated. Enrichment in genes related to calcium homeostasis and calcium signalling were also reported, perfectly fitting with the calcium homeostasis disruption previously seen in *in vivo* studies after exposure to either the toxicants (M. M. L. Dingemans et al. 2008b; M. M. L. Dingemans et al. 2009). Transcriptomic analysis revealed that HBCD also affected genes related to hormonefunctions, especially to Thyroid and Retinol activity (Carroll 2011). In addition, proteomics analysis detected markers of inflammation in the brain of mice exposed to either the toxicants. Considering that inflammation is a pathophysiological alteration that is commonly encountered in neurodegenerative disorders, such as Alzheimer's and Parkinson's disease, these results suggest that PBDE-47 and HBCD may contribute to neurodegeneration (Rasinger 2011).

Genes of interest found enriched in these animal trials were also chosen to be tested in the cell lines exposed to PBDE-47 and HBCD in order to clarify if the responses observed *in vivo* were caused by direct effects of the toxicants on the brain or indirectly through systemic responses.

4.2 Methods

All general methods performed in this chapter are described in Chapter 2.

4.2.1 Microarray analysis in cells exposed to PBDE-47 and HBCD

4.2.1.1 Data quality control, normalisation and filtering

Microarray analysis was performed in order to identify changes in global gene expression in N2A and NSC19 cells exposed to PBDE-47 or HBCD. The N2A or the NSC19 cell lines were exposed to PBDE-47 at 0.5, 1 or 2 μ M or to HBCD at 1 or 2 μ M for 24 hours performing three arrays for each conditions (n=3) and global gene

expression was assessed. Controls consisting of cells treated with DMSO only (<0.01%) or medium alone were also included.

Using the software BlueFuse (BlueGnome, Cambridge, UK), prior normalisation, all genes scoring less than 0.1 in their probability of biological signal in fluorescent channel scores (PCH01 or PCH02) were removed.

Analysis of microarrays data from cells exposed to HBCD or PBDE-47 was performed using the LIMMA bioconductor package. Arrays were normalised using print-tip LOESS, median scaling, print-tip order and print-tip weighting and testing. After normalisations, visualisations were created with LIMMA package to better assess arrays quality. LIMMA analysis, script and visualisation were carried out by Dr Thomas Carroll as described (Carroll 2011). The LIMMA script utilised in the microarray analysis and visualisation is reported in Appendix 1.

Plots created by LIMMA, representing fluorescence densities and the spread of \log_2 fold changes between arrays before and after normalisation, are shown in figure 4.1, 4.2 and 4.3 All the plot and visualisation created by LIMMA are reported in Appendix 2.

In figure 4.1 densities of Cy3 and Cy5 fluorescences are reported for each array, plotted against the respective intensities, for PBDE-47 and HBCD arrays. These plots allow for visualisation of the spreads of intensities between and within arrays. Furthermore mean signals from the two dyes showed more or less complete overlap (Fig 4.1)

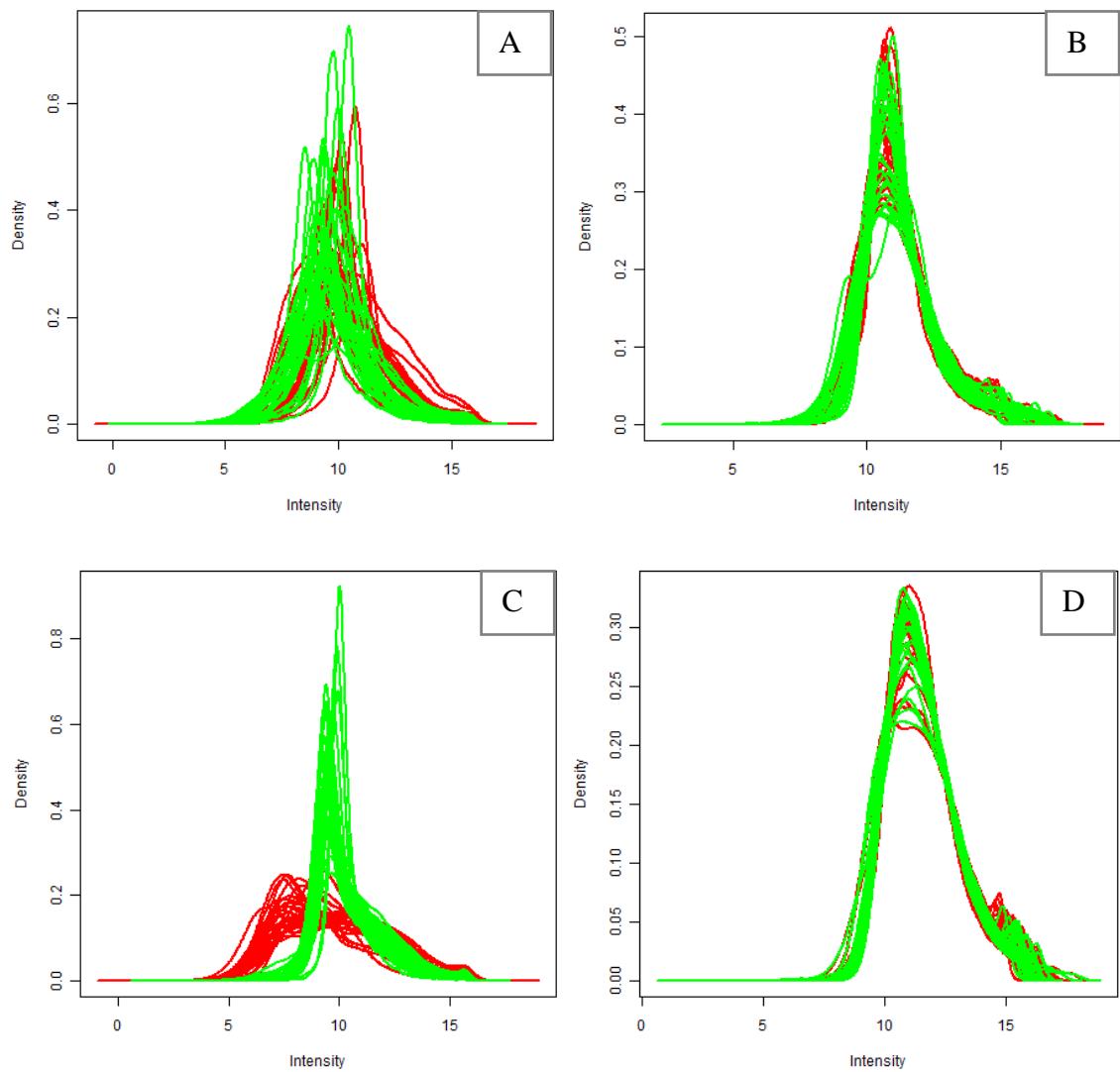


Figure 4.1: Visualisation of the spreads of intensities between and within arrays. The fluorescence intensity is compared with the densities of Cy5 (green) and Cy3 (red) fluorescence on all arrays. Red colour is associated with Cy5 and green colour with Cy3 dyes. Figure A and B represent fluorescence intensities for the PBDE-47 arrays before and after normalisation respectively. Figure C and D represent fluorescence intensities for the HBCD arrays before and after normalisation respectively. The densities are here expressed as percentiles and are homogeneous within and between arrays.

Data were also organised in a box plot to compare the spread of \log_2 fold changes between arrays and to confirm that the medians were centered on zero. After normalizations, the distribution of fold changes across the arrays appeared to be equally spread and all arrays were shown to have similar median (Figure 4.2 A-D).

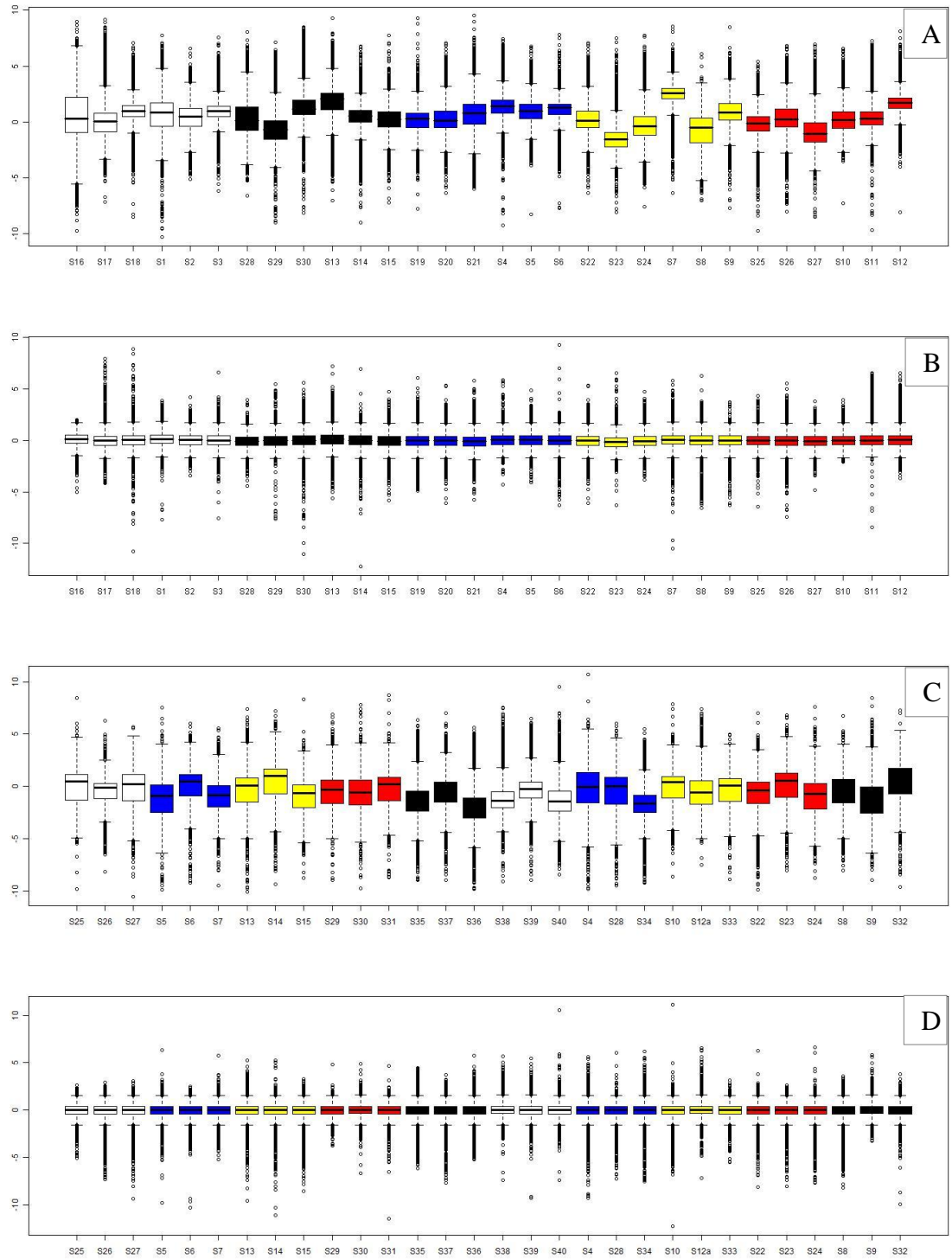


Figure 4.2: Comparison of the Log₂ fold change between arrays. In the graphs the Log₂ fold change is compared between arrays in microarray of cells exposed to PBDE-47 (figure A and B) and to HBCD (figure D and E) before and after normalisations respectively. After normalisations the fold change distributions appear equally spread and the medians show to be similar between arrays. In the graphs, boxes represent the lower and upper quartils of observations, respectively. The middle line represents the median. Whiskers illustrate 1.5 times the interquartile range outside the 25% and 75% quartiles with outliers outside these whiskers marked as points.

Once normalised, genes were filtered by fluorescence intensity using LIMMA software packages. Through an MA plot where M is the gene \log_2 fold change and A the average of fluorescence, it was possible to visualise that at low intensity of fluorescence, the number of genes with large fold-change was higher than at higher intensity. In order to remove low intensity dependent variance and following observations of the distribution of variance across intensity a non specific intensity filter was set to >9.7 . Therefore genes with lower intensity than this were excluded from further analysis. An example of an MA plot before and after normalisations is given in figure 4.3. The completed list of MA plot for PBDE-47 and HBCD arrays is reported in Appendix 3.

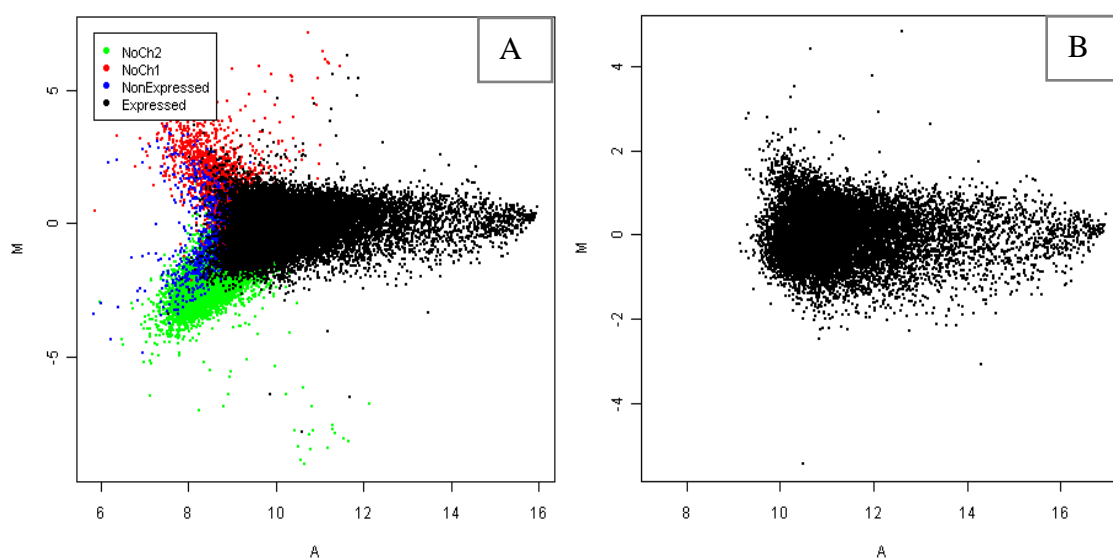


Figure 4.3: Fluorescence intensity within array. In the graphs genes \log_2 fold change (M) is plotted against the average of fluorescence (A) before (figure A) and after (figure B) normalisations respectively. An intensity filter was set to >9.7 . Therefore, genes showing low fluorescence intensity were not considered for further analysis.

After normalisations and filtering by probability of biological signal and fluorescence intensity, genes with equal or more then 2-fold change difference, compared to the control, were considered for further statistical analysis.

4.2.2 Statistical analysis

Linear models and weighted corrected t-statistics were used to calculate differential expression using the Limma Bioconductor packages. Fold changes between groups were calculated as the differences in the log₂ median gene expression between groups. Benjamini and Hochberg False Discovery Rate (FDR) was set at 20% to control for multiple comparisons.

4.2.3 Post-analysis: DAVID and IPA

After microarray analysis, the selected genes were analyzed for Gene Ontology and KEGG pathway enrichment using the DAVID website tool (DAVIDBioinformaticsResources). In this analysis the background used was the whole genome as recommended by DAVID website. DAVID can generate a list of enriched terms, to which is associated a specific p-value, but also it represents enriched terms as clast. Each cluster of familiar annotations is associated with an enrichment score value which indicates the overall enrichment considering all the terms belonging to the annotation cluster itself (DAVIDBioinformaticsResources). Therefore higher is the score and more significant is the function enrichment.

The Ingenuity Pathway Analysis (IPA) software was also used in order to identify relationships between significantly regulated genes in biological networks and functions. IPA is a software that analyzes a selected list of genes and detects interactions between focus genes and all other genes (and gene products) stored. IPA is used to identify pathways and functions that may be impacted due to a dysregulation induced by the differentially expressed genes. For each network generated, IPA associates a significance score, which indicates the likelihood of the perturbed pathway occurring by chance. The score is based on a hypergeometric distribution and is calculated with the one tailed Fisher's exact test. Within the software the score is provided as the negative base-10 logarithm of the p-value. Thus, a score of two indicates a p-value of 10^{-2} and is considered statistically significant

4.2.4 Chapter objectives

The objectives of the experiments described in this Chapter were to:

1. access the effect of PBDE-47 and HBCD on gene expression in neuronal cells, through the investigation of the global gene expression profile using microarray.
2. confirm the genes found differentially expressed with microarray analysis with Q-PCR.
3. identify relationships and interactions between significantly regulated genes in biological networks and functions.

4.3 Genes regulated in cells exposed to PBDE-47 of HBCD

One-way ANOVA was used to analyse both PBDE-47 and HBCD microarray, identified 679 genes enriched in the N2A cell line exposed to PBDE-47 and 494 in the NSC19 cells. In this analysis FDR was set at 20% and the gene expression was greater than 2-fold change compared to the control. The number of genes called significantly regulated by PBDE-47 are reported in Table 4.1.

Table 4.1: Number of genes significantly regulated in cells exposed to 1 or 2 μ M of PBDE-47. The two cell lines N2A and NSC19 were exposed to 1 or 2 μ M of PBDE-47 for 24h. Global expression of genes was then analysed by microarray and genes were called significantly regulated with greater than 2-fold change, compared with the control, and FDR of 20%. 3 arrays were performed in each conditions (n=3)

<i>Cells line</i>	<i>N2A</i>	<i>NSC19</i>
Numbers of genes regulated by PBDE-47	679	494

Performing one-way ANOVA on HBCD microarray enabled the identification of 790 genes regulated in the N2A cell line and 484 in the NSC19 cell line as reported in Table 4.2. The N2A cell line showed a higher responsiveness to the toxicants compared to the NSC19 cell line, reporting a higher number of differentially expressed genes for either

the compounds. In addition, the number of genes regulated by either the toxicants was very similar, in both the cell lines.

Table 4.2: Number of genes significantly regulated in cells exposed to 1 or 2 μM of HBCD. The two cell lines N2A and NSC19 were exposed to 0.5 1 or 2 μM of HBCD for 24h. Global expression of genes was then analysed by microarray and genes were called significantly regulated with greater than 2-fold change, compared with the control, and FDR of 20%. 3 arrays were performed in each conditions (n=3).

<i>Cells line</i>	<i>N2A</i>	<i>NSC19</i>
Numbers of genes regulated by HBCD	790	484

The numbers of genes that were commonly or uniquely changed in expression in the two cell lines, in response to either of the BFRs, are reported in Figure 4.4. PBDE-47 uniquely regulated 642 genes in the N2A cell line and 457 genes in the NSC19 cell line. HBCD was seen to regulate 690 genes uniquely in the N2A cell line and 384 in the NSC19 cells. While the majority of genes regulated by either of the toxicants were different in the two cell lines, there were 37 genes that showed changes in expression in both N2A cells and NSC cells and there were 100 genes regulated by HBCD independently of which cell line was used. The numbers of commonly regulated genes in the two cell types correspond to 3 and 10% of the total numbers of genes regulated by PBDE-47 and HBCD, respectively.

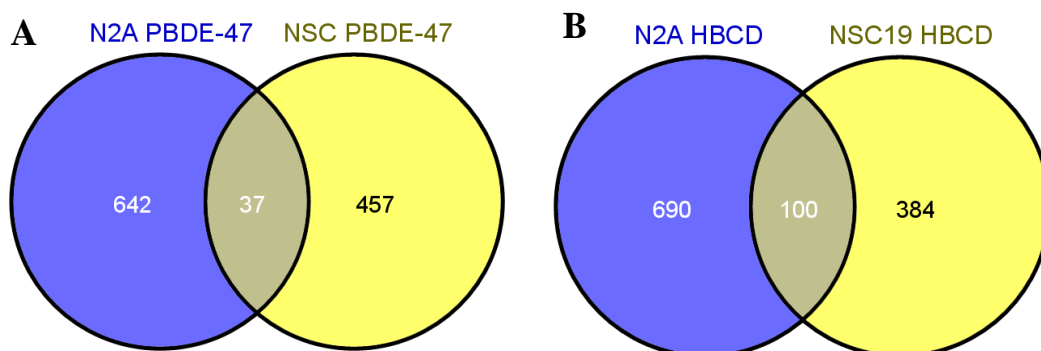


Figure 4.4: Commonality in gene expression responses to PBDE-47 or HBCD between N2A and NSC cells. The Venn diagram shows the numbers of genes that were uniquely regulated in N2A cells (Blue) and NSC cells (yellow) following exposure to (A) PBDE-47 or (B) HBCD.

The number of genes commonly or uniquely regulated in either of the cell lines exposed to PBDE-47 or to HBCD are shown in Figure 4.5. The number of genes that were changed in expression only in response to the PBDE-47 was 1021 genes and 1065 were regulated uniquely in response to HBCD. While the majority of genes regulated were toxicant specific, 114 genes (approximately 10% of the total), were commonly regulated.

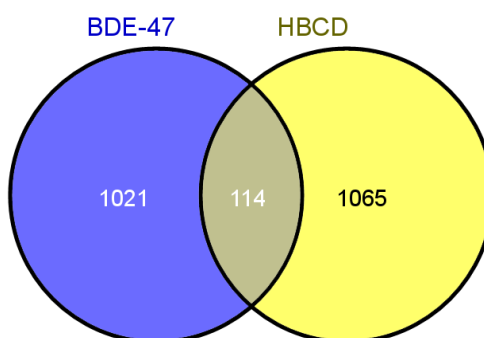


Figure 4.5: Commonality in gene expression responses from PBDE-47 and HBCD. The Venn diagram shows the numbers of genes that were commonly or uniquely regulated in either N2A or NSC cells exposed to PBDE-47 or to HBCD

4.3.1 Functional enrichment regulated by PBDE-47 or HBCD

Significantly regulated genes were analysed for enrichment of Gene Ontology (GO) terms using the DAVID online tools (DAVIDBioinformaticsResources). Between the functions enriched by PBDE-47 or HBCD, some of the most significant are reported in tables 4.2-5. Functions reported here are grouped for each toxicant and each cell line used. Each enriched term is represented alone along with its associated p-value, and also as part of groups of terms indicating similar functions. Each cluster of familiar annotations is associated with an enrichment score value which indicates the overall enrichment considering all the term belonging to the annotation cluster itself (DAVIDBioinformaticsResources). Therefore higher the score is and more significant is the function enrichment.

As shown in table 4.3 analysis of genes regulated by PBDE-47 in the N2A cell line showed the most significantly enriched functional annotation being “lipid and steroid synthesis” ($p < 5 \times 10^{-5}$). “Oxidoreductase” and “nucleotide binding” were also found to be highly significantly enriched functions. Three gene sets related to tubulin function, “tubulin/GTPase domain”, “tubulin” and “tubulin, conserved site”, were also among the main regulated functions. “Protein complex assembly” and set of genes related to “organelle membrane” and “mitochondrion” were also shown to be significant regulated. Two more functions among the enriched GO term were related to “fatty acid biosynthesis” and “endoplasmic reticulum membrane and part”.

Analysis to the genes regulated by PBDE-47 in the NSC19 cells revealed that, as observed in N2A cells, the annotations “steroid and lipid synthesis” was significantly enriched. Genes related to “transcription activity” were shown to be the most significantly enriched. Also three set of genes relating to neuronal development and differentiation or to neuronal signalling, such as “regulation of nervous system development”, “regulation of neuron differentiation” or “cell-cell signalling”, were among the significant GO terms. “Non-membrane-bounded organelle” and “metal ion binding” were also seen enriched gene sets (Table 4.3).

Table 4.3: Enriched Gene Ontology annotation terms among significant genes regulated by PBDE-47 in the N2A cell line. Enrichment analyses were performed with the DAVID online tool. Fisher Exact/EASE score test was performed to identify statistically significant bias for semantic annotations. The functional enrichment is expressed in $-\log(p\text{-value})$. GO terms belonging to the same group are indicated with the same colour.

Gene Ontology terms	$-\log(p\text{-value})$	Cluster of function
Lipid synthesis	9.77	Lipid and steroid synthesis
Steroid biosynthesis	9.30	
Lipid biosynthetic process	5.32	
Oxidoreductase	4.28	Oxidoreductase
Oxidation reduction	3.36	
Nucleotide binding	4.09	Nucleotide binding
Tubulin,GTPase domain	5.64	Tubulin function
Tubulin	4.46	
Tubulin, conserved site	3.96	
Protein complex assembly	3.52	Organelle
Organelle membrane	4.72	
Mitochondrion	3.33	
Fatty acid biosynthetic process	1.68	Fatty acid biosynthesis biosynthesis
Biosynthesis of unsaturated fatty acids	1.68	
Endomembrane system	4.02	ER membrane and part
Endoplasmic reticulum membrane	2.64	
Endoplasmic reticulum part	2.57	

Table 4.4: Enriched Gene Ontology annotation terms among significant genes regulated by PBDE-47 in the NSC19 cell line. Enrichment analyses were performed with the DAVID online tool. Fisher Exact/EASE score test was performed to identify statistically significant bias for semantic annotations. The functional enrichment is expressed in $-\log(p\text{-value})$. GO terms belonging to the same group are indicated with the same colour.

Gene Ontology terms	$-\log(p\text{-value})$	Cluster of function
Transcription repressor activity	3.68	Transcription activity
DNA-binding	3.31	DNA-binding
Regulation of transcription, DNA-dependent	3.31	
Cell-cell signalling	2.17	
Steroid biosynthesis	2.09	Steroid and lipid synthesis
Lipid Synthesis	1.74	
Lipid biosynthetic process	1.66	
Regulation of nervous system development	1.89	Neuronal development, differentiation and signalling
Regulation of developmental growth	1.85	
Regulation of neuron differentiation	1.36	
Mitochondrial membrane organization	2.42	Mitochondrial organization
Non-membrane-bounded organelle	1.59	Non-membrane-bounded organelle
Intracellular non-membrane-bounded organelle	1.59	
Cation binding	1.34	Metal ion binding
Metal ion binding	1.33	

As shown in table 4.5, some annotations found significantly enriched among genes regulated by PBDE-47 were also significantly overrepresented among genes regulated by HBCD. Annotation analysis of the genes enriched by HBCD in the N2A cell line revealed that the terms “non-membrane-bounded organelle” and “mitochondrial organisation”, showed significant overrepresentation among genes regulated by either of the toxicants. Sets of genes related to “Metabolic process”, to “DNA damage”, to “Cytoskeleton” and to “Synapse organisation” were among the more significantly enriched. Also the terms “Mitochondrial organization” and “Protein folding” were enriched among genes regulated by HBCD in the N2A cell line. Functions related to cell functions such as “Cell cycle process” and “Regulation of apoptosis” were also among the most significant enriched terms.

Significant genes regulated by HBCD in the NSC19 cell line showed similarity with those regulated in the N2A cell line, and also showed common functions enriched in the cells exposed to PBDE-47. In fact terms such as “non-membrane-bounded organelle”, “cytoskeleton” and cell cycle” were commonly enriched by HBCD in both the cell lines. The function related to “Endoplasmic reticulum membrane” was also seen regulated by PBDE-47 in the N2A cells. Uniquely regulated by HBCD in the NSC19 cell line were terms related to the “Actin organisation” and “DNA replication”. (Table 4.6).

Table 4.5: Enriched Gene Ontology annotation terms among significant genes regulated by HBCD in the N2A cell line. Enrichment analyses were performed with the DAVID online tool. Fisher Exact/EASE score test was performed to identify statistically significant bias for semantic annotations. The functional enrichment is expressed in $-\log(p\text{-value})$. GO terms belonging to the same group are indicated with the same colour.

Gene Ontology terms	$-\log(p\text{-value})$	Cluster of function
DNA metabolic process	5.08	Metabolic process
Cellular response to stress	3.96	
DNA damage	2.68	DNA damage
DNA replication	3.82	
Non-membrane-bounded organelle	4.33	Non-membrane-bounded organelle
Intracellular non-membrane-bounded organelle	4.33	
Cytoskeleton	1.77	Cytoskeleton
Cytoskeleton part	1.31	
Synaptogenesis	2.48	Synapse organisation
Synapse organisation	1.85	
Mitochondrion	3.45	Mitochondrial organization
Mitochondrial membrane	2.09	
Mitochondrial part	1.72	
Protein folding	1.85	Protein folding
Cell cycle	2.70	Cell cycle process
Cell cycle process	1.52	
Regulation of apoptosis	1.96	Regulation of apoptosis
Negative regulation of apoptosis	2.39	

Table 4.6: Enriched Gene Ontology annotation terms among significant genes regulated by HBCD in the NSC19 cell line. Enrichment analyses were performed with the DAVID online tool. Fisher Exact/EASE score test was performed to identify statistically significant bias for semantic annotations. The functional enrichment is expressed in $-\log(p\text{-value})$. GO terms belonging to the same group are indicated with the same colour.

Gene Ontology terms	$-\log(p\text{-value})$	Cluster of function
Non-membrane-bounded organelle	6.68	Non-membrane-bounded organelle
Cytoskeleton organization	6.02	Cytoskeleton
Cytoskeleton	3.48	
Cytoskeleton part	3.24	
Actin binding	6.02	Actin organisation
Actin cytoskeleton organization	3.24	
DNA replication initiation	4.22	DNA replication
DNA replication	2.08	
Endoplasmic reticulum membrane	1.68	Endoplasmic reticulum membrane
Protein polymerization	1.82	
Cell division	2.96	Cell cycle
Cell cycle	2.52	

4.3.2 Pathways analysis of genes regulated by PBDE-47 or HBCD

Pathway analysis was performed in order to identify relationships and networks between genes significantly regulated by PBDE-47 or HBCD. The proprietary software Ingenuity Pathway Analysis (IPA) was used to identify, from a set of genes, which genes were directly related to each other and which ones belonged to the same functional networks. Therefore, it was possible identify genes with central role in a specific pathway and essential to regulate particular functions.

Two of the main networks identified among genes regulated by PBDE-47 are reported in figures 4.6 and 4.7. The first network consists of three sub-networks. The first one presents genes involved in the ER stress and in the unfolded protein response (UPR). Among these genes is *Hspa5*, which corresponds to one of the chaperones reactive to endoplasmic reticulum (ER) stress (Chen et al. 2008), and *Xbp1*, a gene encoding for a protein that acts during ER stress by activating the UPR (Y. He et al.). *Xbp1* is directly linked to *S100a6*, a calcium sensor that contribute to cellular calcium signalling (Takata et al. 2010). The second sub-network shows genes encoding for proteins related to cytoskeleton structure and maintenance such as *Tubb2c* and *Tuba1a*. Both of these proteins are directly linked to *Camk2d*, a protein kinase known to have a range of roles in neurons, including maintaining synaptic plasticity and regulating calcium channels (Bradshaw et al. 2002). The third sub-network involves genes for proteins related to fatty acid synthesis. One of these genes, *Fasn*, is directly linked to *Lpin1*, which plays an important role in controlling the metabolism of fatty acids and in maintaining the lipid homeostasis (Miranda et al.).

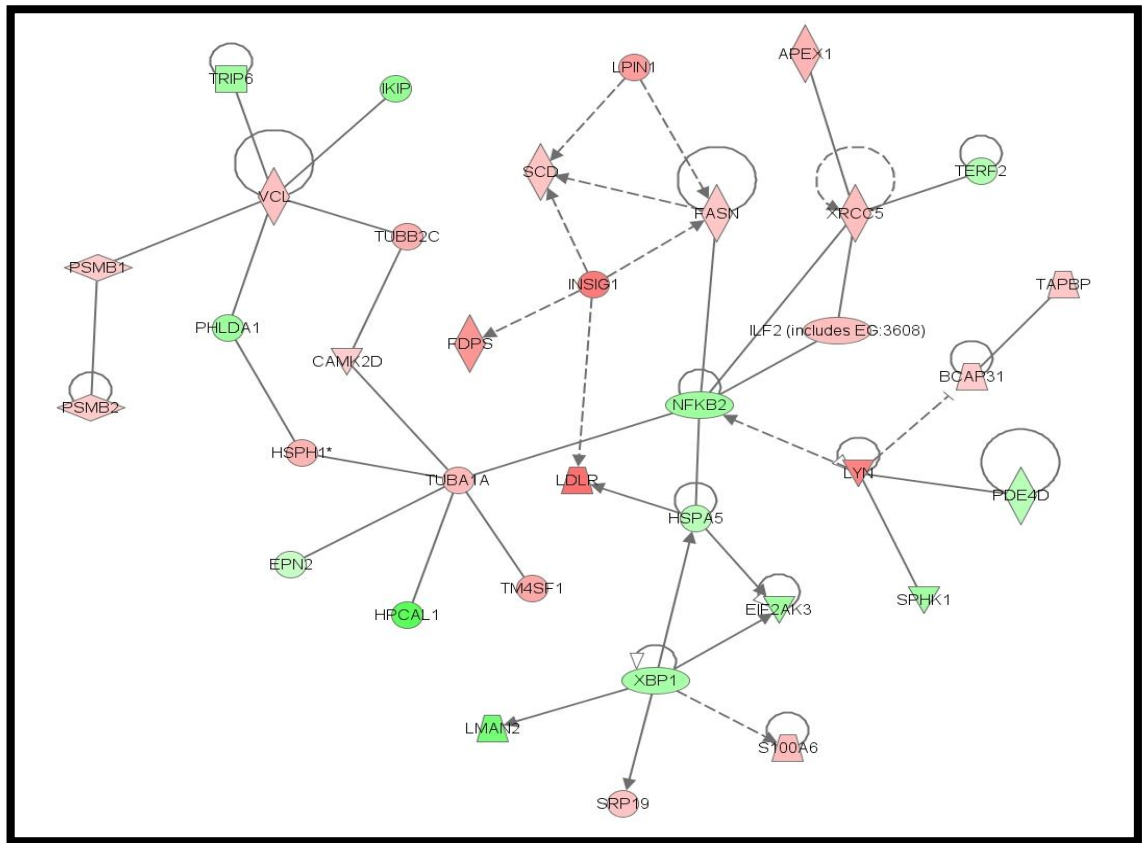


Figure 4.6: Lipid metabolism, small molecule biochemistry, cell death pathway. Pathway analysis was performed with IPA software in order to identify relationships and networks between genes significantly regulated by PBDE-47. In the figure genes up-regulated are represented in red and genes down-regulated in green. The density of colour represents the scale of differential gene expression. IPA SCORE=59.

The second network generated from analysis of genes regulated by PBDE-47, shows a main node with genes encoding proteins directly involved in calcium signalling and homeostasis, such as the calcium receptor, *Cacna1c* and *Homer1*, or genes that are regulated by calcium, like the protein kinase calcium dependent *Prkca*. A second sub-network is also present and its central regulatory protein is *Rb1* (retinol binding protein 1). *Rb1*, which appeared down-regulated in the pathway, is a transcription repressor with tumour suppressor activity (Binda et al. 2008). *Rb1* is directly linked to *Sirt1* which play a central role in its regulation (Binda et al. 2008).

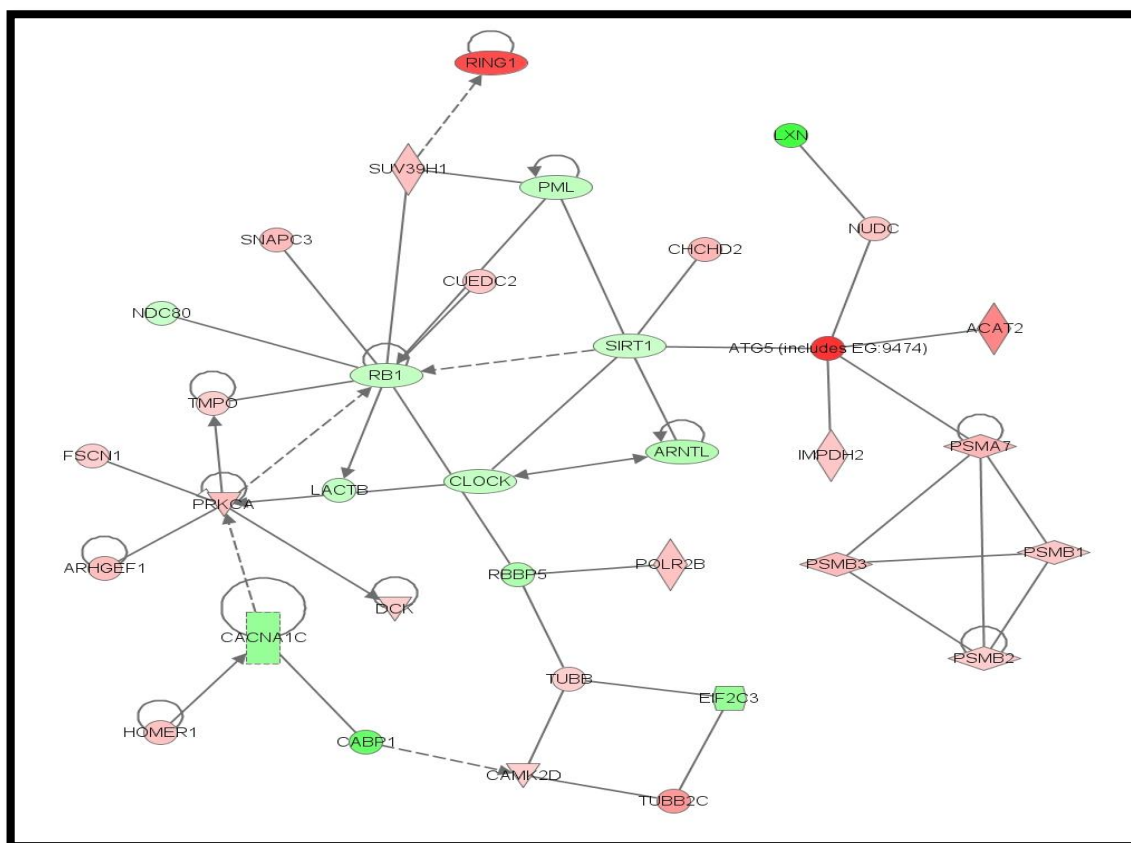


Figure 4.7: Immunological disease, cancer, connective tissue disorders pathway. Pathway analysis was performed with IPA software in order to identify relationships and networks between genes significant regulated by PBDE-47. In the figure genes up-regulated are represented in red and genes down-regulated in green. The density of colour represents the scale of differential gene expression IPA SCORE=52

Among the top networks regulated by HBCD in the NSC-19 cell line, IPA identified “lipid metabolism” and “neurological disease and cellular movement” pathways. The canonical pathway “biosynthesis of steroids” was also enriched. Analysis of genes regulated in the N2A cell lines revealed that the most significant enriched pathways were related to cells and nervous system functions, such as “behaviour, nervous system development and function, cell death” pathway.

Two of the main networks generated by the IPA analysis of genes regulated by HBCD are reported in figure 4.8 and 4.9. The first network, “Cellular function and maintenance, cell morphology, cell death”, consists in two main node of genes regulated by the main tumour suppressor *Rb1*, and by the gene *Cebpb*, encoding for the protein CCAAT/enhancer binding protein (C/EBP) beta.

Rb1, which was also seen regulated in cells exposed to PBDE-47, has a fundamental role in the induction of growth arrest and cellular senescence (Binda et al. 2008). *Cebpb*

encodes for a protein important in the regulation of genes involved in immune and inflammatory response (Gresa-Arribas et al. 2010), and has been shown to bind to the IL-1 (Interleukin-1 alpha response element). *Cebpb* also directly regulates the gene *Ppp1r15a*, encoding for the protein phosphatase 1 regulatory subunit 15A, which is a member of a group of genes whose are affected by inflammatory stimulation or DNA-damaging agents (Clavarino et al. 2012). *Ppp1r15a* is also linked with the gene involved in ER stress response and in UPR, *Hspa5* (Hsu et al. 2008).

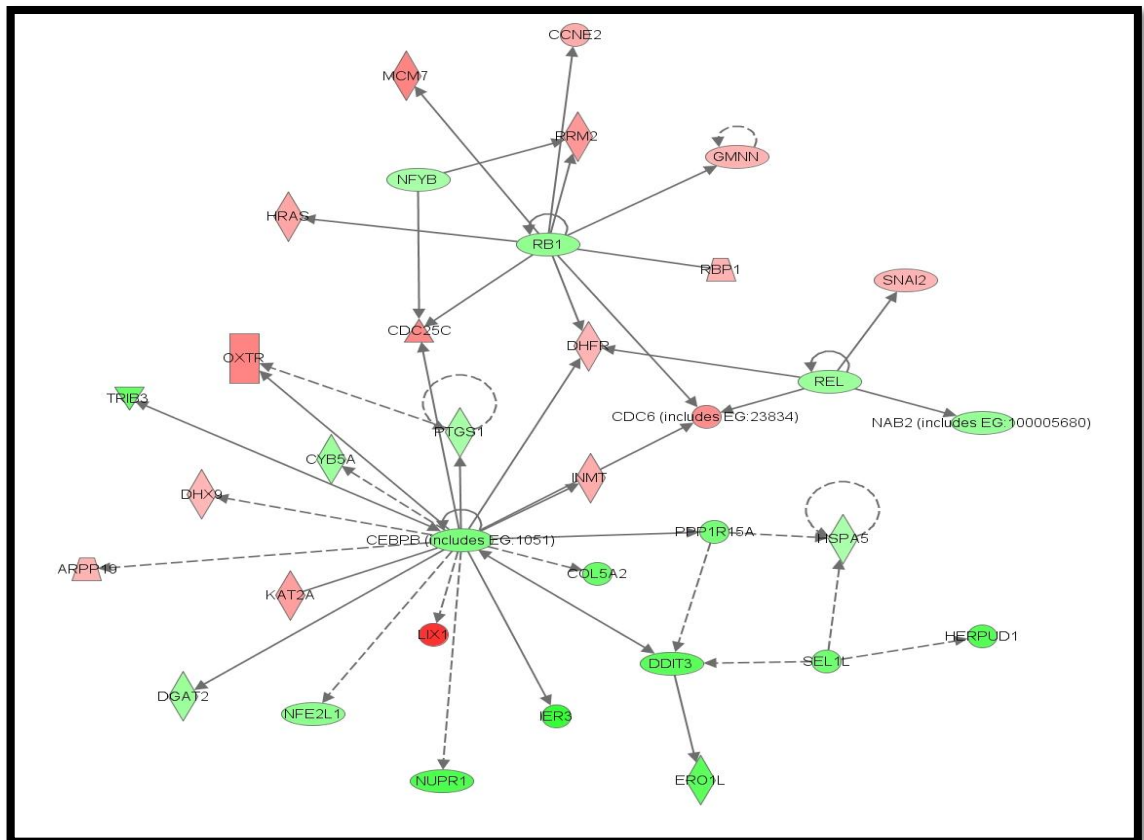


Figure 4.8: Cellular function and maintenance, cell morphology, cell death pathway. Pathway analysis was performed with IPA software in order to identify relationships and networks between genes significantly regulated by HBCD. In the figure genes up-regulated are represented in red and genes down-regulated in green. The density of colour represents the scale of differential gene expression. IPA SCORE=45

The second pathway generated from genes regulated by HBCD, Cellular growth proliferation, cancer, DNA replication, recombination and repair”, is shown in figure 4.9. In this network there are shown genes responsible for the regulation of cell

proliferation, differentiation, and transformation such as the cytokine IL5 or the gene ID2.

Another interesting gene in this network is the nerve growth factor receptor (*Ngfr*) gene, which has a fundamental role for the integrity and maintenance of the cholinergic neurons, which are known to atrophy in AD (Cuello et al.).

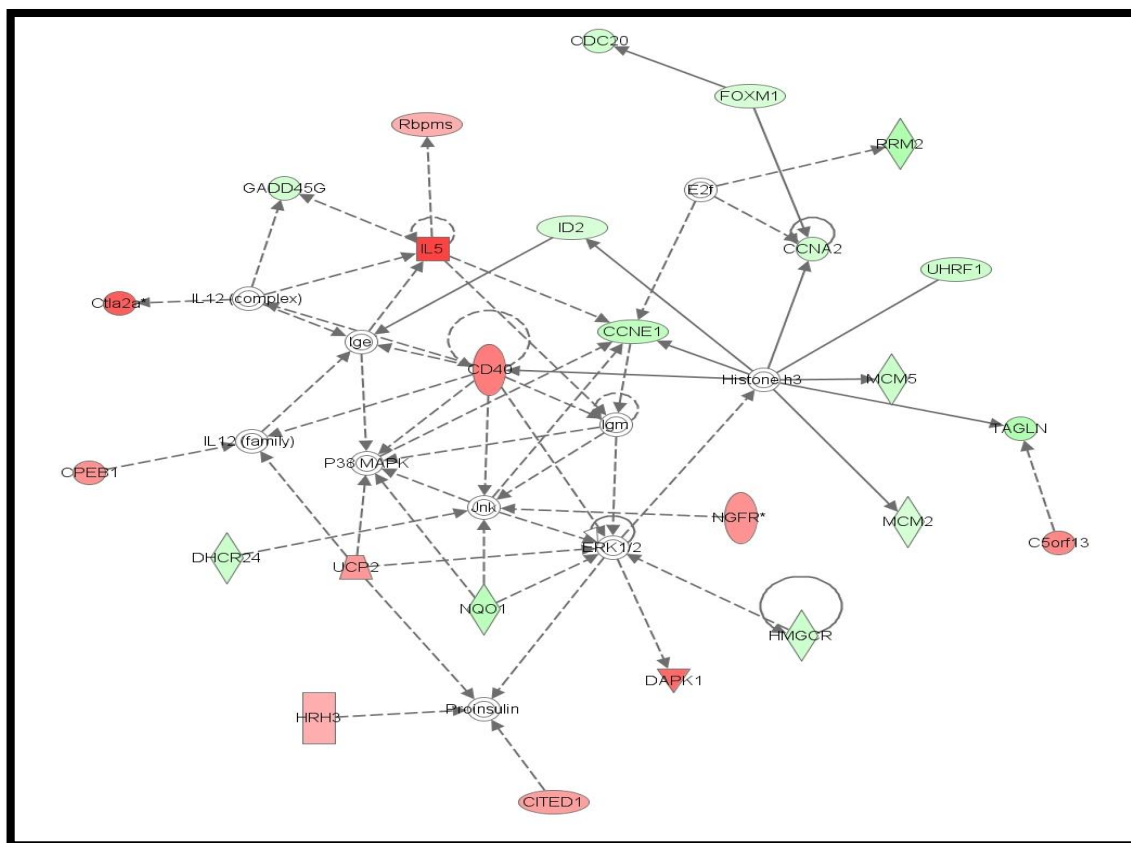


Figure 4.9: Cellular growth proliferation, cancer, DNA replication, recombination and repair pathway. Pathway analysis was performed with IPA software in order to identify relationships and networks between genes significantly regulated by HBCD. In the figure genes up-regulated are represented in red and genes down-regulated in green. The density of colour represents the scale of differential gene expression. IPA SCORE=37

4.4 Confirmation of significant genes regulated by PBDE-47 or HBCD using real-time PCR

Q-PCR was used in order to confirm the expression of genes of interest that were found significantly regulated in microarrays. To capture the most robust responses, Q-PCR analysis was focused on the two highest concentrations used (1 and 2 μ M). DMSO

effects were also tested by direct comparison between negative control (medium-only) and DMSO control genes expression, revealing that DMSO did not cause any change in the genes confirmed by Q-PCR (data not shown).

Q-PCR results were analysed with the REST software. This software compares the Ct value of reference gene with target genes, and considering efficiency of primers, calculates the difference in gene expression (Pfaffl, Horgan et al. 2002). Statistical calculation of probability of differential expression is based on a randomisation of samples using the Pair Wise Fixed Reallocation Randomisation Test (Pfaffl et al. 2002). Rest was set for a number of 1000 randomisations during this analysis.

4.4.1 Q-PCR analysis of genes regulated by PBDE-47

A summary of the genes regulated by PBDE-47 and chosen to be analysed with Q-PCR is reported in table 4.7 for the N2A cell line and in table 4.8 for NSC19 cells. In the tables, fold change seen in microarray is compared against fold change measured by Q-PCR. Among the genes regulated by HBCD in the N2A cell line, two of them, *Bace1* and *Ttr*, were not found differentially expressed in microarray, but still selected for Q-PCR analysis. *Bace1* has been selected because, even if not significantly regulated in microarray, it was a central gene in the pathway “neurodegenerative disorders” regulated by HBCD. *Ttr* has been selected because it was found regulated by PBDE-47 and therefore it was also of interest test the effect of HBCD on its expression. A number of genes found differentially expressed in microarray, were not confirmed to be significant in the Q-PCR analysis. The low confirmation rate may in part be explained by the relatively high FDR of 20% accepted for microarray data.

Table 4.7: fold change of genes regulated by PBDE-47 in the N2A cell line and confirmed with Q-PCR. The table reports fold change in microarray analysis compared to Q-PCR. Standard Error (in brackets) and p-value are also reported. P-value in blue are significant with a value <0.01 and p-value in red are significant with a value <0.05. P-value marked as <0.001 are below the minimum reported by Rest 2008 software.

PBDE-47 in the N2A						
MICROARRAY			Q-PCR			
Gene Symbol	Fold Change 1μM	Fold Change 2μM	Fold Change 1μM	p-value	Fold Change 2μM	p-value
BACE1	1.7	2	-1.5 (-2 to -1.2)	0.034	-1.9(-2.5to-1.4)	0.004
TTR	<±2	<±2	-4.2(-12.5to-1.1)	0.049	-4.2(-12.5to-1.1)	0.049
RB1	-2.2	<±2	-1.4(-2 to 1)	0.20	-1.4 (-2 to -1.1)	<0.001
HOMER1	2.5	<±2	1.2(1 to 1.6)	0.237	1.3 (1.1 to 1.5)	<0.001
TUBB2C	2.8	4.9	2.4(1.5 to 3.7)	<0.001	1.9 (1.3 to 2.9)	0.05
TRIP6	-3.2	<±2	-1.3(-4.3to-1.2)	0.077	-1.3(-4.3to-1.2)	0.077
TBCB	2.4	1.6	1.9(1.1 to 4.1)	0.095	1.25(1.4 to 1.8)	0.495
PINK1	<±2	-2.5	1.3(-1.4 to 2)	0.298	1.1(-1.6 to 1.8)	0.695
CACNA1C	<±2	-4.0	1.0(-1.6 to 1.3)	0.835	1.1 (-1.4 to1.5)	0.531
TG	<±2	-4.2	1.3(-1.4 to 2.1)	0.318	1.1 (-1.6 to1.8)	0.736
HSPA5	-2.4	-2.3	-1.2(-2.5 to1.2)	0.895	-1.4(-2.5 to1.4)	0.304
Egr1	<±2	-2.3	-1.4(-3.3 to2.7)	0.668	-1.8(-5.0 to1.9)	0.495
PRKCA	<±2	2.6	-1.0(-1.6 to1.5)	0.965	-1.2(-2 to 1.6)	0.748
CAMK2D	2.1	2.1	-1.1(-1.4 to1.1)	0.532	1.1(-1.6 to 1.8)	0.932

Table 4.8 reports the list of genes regulated by PBDE-47 in the NS19 cell line, selected for Q-PCR analysis. Among the genes tested, App was not regulated in microarray, but still selected for Q-PCR analysis as it covers a central role in the pathway “neurodegenerative disorders” regulated by PBDE. Among the genes tested, App only was confirmed to be differentially expressed by Q-PCR.

Table 4.8: fold change of genes regulated by PBDE-47 in the NSC19 cell line and confirmed with Q-PCR. The table reports fold change in microarray analysis compared to Q-PCR. Standard Error (in brackets) and p-value (in red when significant (<0.05)) are also reported). p-value marked as <0.001 are below the minimum reported by Rest 2008 software.

PBDE-47 in the NSC19						
Gene Symbol	MICROARRAY		Q-PCR			
	Fold Change 1µM	Fold Change 2µM	Fold Change 1µM	p-value	Fold Change 2µM	p-value
APP	1.6	1.3	1.5(1.0 to 2.1)	0.034	1.5(1.0 to 2.1)	0.034
HIP1	<±2	1.6	1.0(-1.6 to 1.3)	0.949	-1.1(-1.6 to 1.5)	0.954
NMYC	-3.4	-2.7	1.4(-1.1 to 2.0)	0.191	1.0(1.0 to 2.1)	0.202
FOS	-2.9	-2.9	1.5(-1.4 to 2.5)	0.374	1.0(-2.5 to 1.5)	0.789
FGF2	-2.9	-3.4	1.0(-1.4 to 1.3)	0.863	1.4(-1.7 to 1.5)	0.509

Genes regulated by PBDE-47 in both the two cell lines used, and confirmed to be significant with Q-PCR, are shown in figure 4.10. Genes linked to neurodegenerative disease, especially to Alzheimer's disease, were found significantly regulated (p<0.05). *App*, precursor of the amyloid peptide, linked to the formation of amyloid plaque in Alzheimer patients, was up-regulated by 1.5 fold change compared to the control in both of the concentrations tested. *Bace1*, gene encoding for the protein responsible for the cleavage of *App* to amyloid-beta (Aβ) protein, was down-regulated in both the concentrations. Genes related to thyroid hormone homeostasis, such as *Trip6* and *Ttr* were tested and found down-regulated by 1.3 and 4.2 fold change respectively, compared to the control in both the conditions tested. The *Rb1* gene, one of the main tumour suppressors, appeared to be significantly down-regulated in cells exposed to 1 or 2µM of PBDE-47, but this was only significant in cells exposed to 2µM of PBDE-47 (p<0.05). Genes related to calcium homeostasis and signalling were also tested. The gene *Homer1*, a main regulator of calcium signalling, was found to be significantly up-regulated in cells exposed to 2µM, but not in the 1µM condition. Cytoskeleton structure and maintenance functions were also investigated, and the gene *Tubb2c*, the major constituent of microtubules, was confirmed to be up-regulated by 2.4 fold change in cells exposed to 1µM and by 1.9 fold change in the 2µM condition, compared to the control. In addition, expression of *Tbcb* was 1.9 fold higher in cells treated with 1µM of

PBDE-47 compared with the control. *Tbcb* was statistically significant with a p-value < 0.1 (p=0.095).

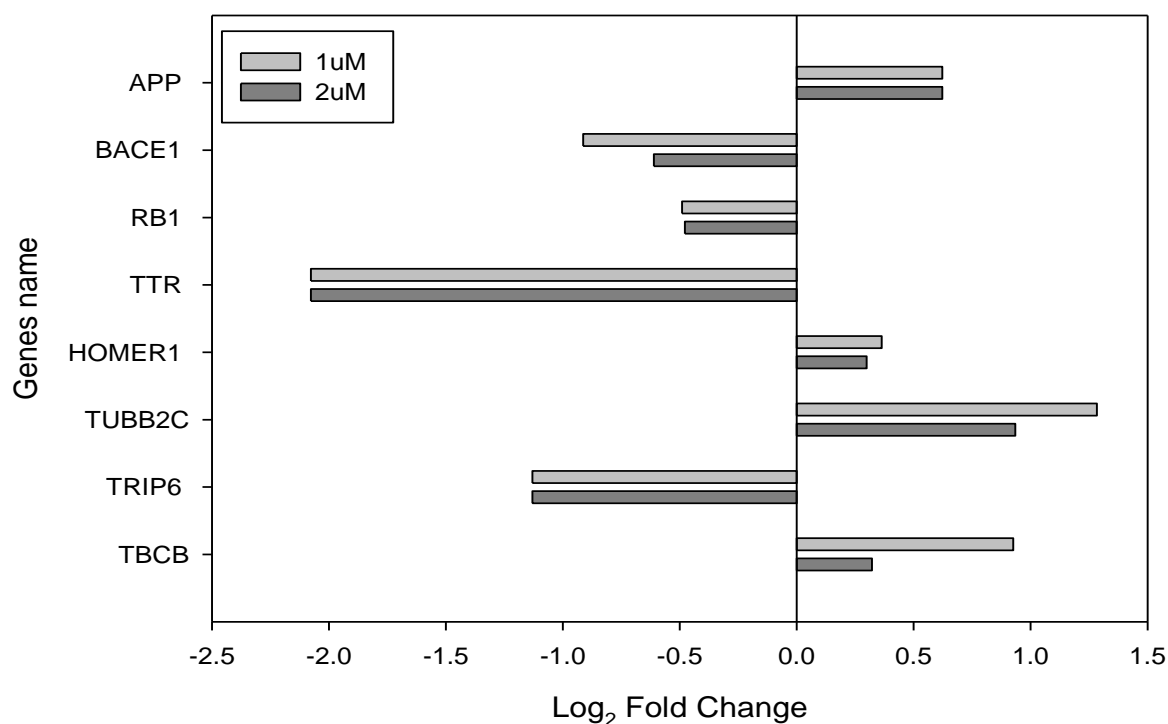


Figure 4.10: Log₂ fold change of genes regulated by PBDE-47. Gene expression was analysed with Q-PCR. Light blue represents gene expression in cells exposed to 1µM PBDE-47 and dark blue in cells exposed to 2µM PBDE-47. APP was regulated in the NSC19 cell line and the other genes in the N2A cell line.

4.4.2 Q-PCR analysis of genes regulated by HBCD

The set of genes selected from the ones regulated by HBCD and tested with Q-PCR are shown in table 4.9 for the N2A cell line, and in table 4.10 for the NSC19 cell line. Also compared in both the tables are the expressions of genes as assessed by microarray, and Q-PCR. Among the genes tested in the N2A cells, *Rbp4* was not found differentially expressed in microarray, but it was confirmed with Q-PCR analysis as it was regulated in brain of mice by HBCD in animal trials conducted in our laboratory. As a gene linked to hormone activity, *Rbp4* expression in cells exposed to HBCD could give a better understanding of the cytotoxic target of this toxicant. Among the genes tested in the N2A cell lines, all the genes were found to be significantly differentially expressed.

Table 4.9: fold change of genes regulated by HBCD in the N2A cell line and confirmed with Q-PCR. The table reports fold change in microarray analysis compared to Q-PCR. Standard Error (in brackets) and p-value (in red when significant (<0.05)) are also reported. p-value marked as <0.001 are below the minimum reported by Rest 2008 software.

HBCD in the N2A cell line						
Gene Symbol	MICROARRAY		Q-PCR			
	Fold Change 1μM	Fold Change 2μM	Fold Change 1μM	p-value	Fold Change 2μM	p-value
RBP4	<+2	<+2	-1.3(-1.4to-1.1)	<0.001	-1.3(1.5to-1.2)	0.034
HSPA5	1.5	-2	-1.2(-2.5 to 1.2)	0.773	-2 (-4.0 to -1.3)	0.031
NFKB2	<+2	-3.3	1.0(-2.3to 2.2)	0.967	-5.5(-6.6to4.4)	0.038
ACSL4	<+2	-2.2	-1.2(-1.3 to 1.1)	0.488	-1.7(-2.2to-1.3)	0.031
PNPLA8	<+2	-3.2	-2.5(-3.7to-1.7)	0.030	-5.1 (-8.3to3.5)	0.014

Genes considered being significant with Q-PCR analysis are reported in figure 4.11. Among the genes regulated in the N2A cell line, the gene coding for retinol hormone *Rbp4* was found down-regulated by 1.3 fold change compared to the control in both HBCD concentrations. The transcriptional factor *Nfkb2* was found to be down-regulated in cells treated with 2μM of HBCD. In cells treated with 1μM, *Nfkb2* was not shown to be differentially expressed. Genes linked to lipid biosynthesis and fatty acid regulation, were tested. The genes *Acsl4* (responsible for synthesis and degradation of cellular lipid) and *Pnpla8* (a phospholipase which cleaves fatty acid from phospholipids) were found down-regulated in both the HBCD concentrations tested. The gene *Acsl4*, was found significantly regulated only in cells exposed to 2μM (p<0.05). The *Hspa5* gene, encoding for a protein involved in the UPR and link with ER stress response (Chen et al. 2008), was significantly down-regulated in cells exposed to 2μM.

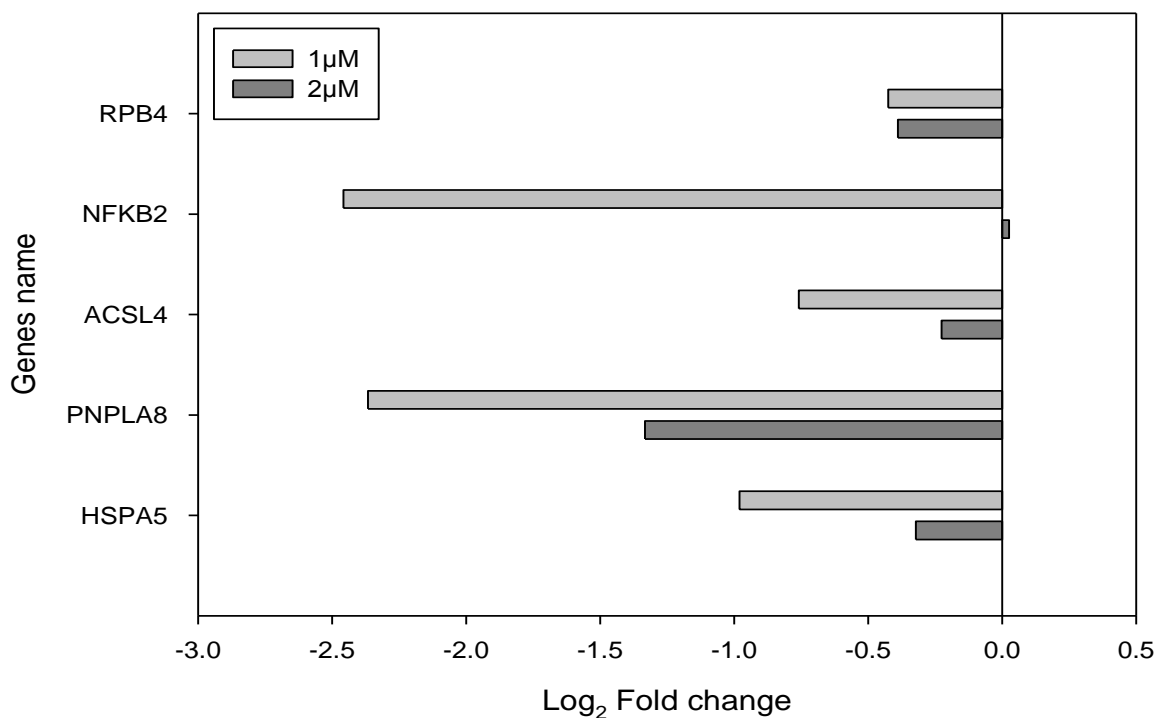


Figure 4.11: Log₂ fold change of genes regulated by HBCD in the N2A cell line. Gene expression was analysed with Q-PCR. Light blue represents gene expression in cells exposed to 1µM PBDE-47 and dark blue in cells exposed to 2µM PBDE-47.

Table 4.10 reports the list of genes regulated by HBCD in the NSC19 cell line. Gene fold change seen in microarray and in Q-PCR is compared. The genes *Rbp4*, *Ttr*, *Homer1* and *Pawr*, even if not differentially expressed in microarray, were selected for Q-PCR analysis as previously found regulated by HBCD in the N2A cell line or by PBDE-47, and also previously seen regulated in the animal trial conducted in our laboratory. All genes regulated by HBCD in the NSC19 cell line selected for Q-PCR analysis, were confirmed to be significant.

Table 4.10: fold change of genes regulated by HBCD in the NSC19 cell line and confirmed with Q-PCR. The table reports fold change in microarray analysis compared to Q-PCR. Standard Error (in brackets) and p-value (in red when significant (<0.05)) are also reported. p-value marked as <0.001 are below the minimum reported by Rest 2008 software.

HBCD in the NSC19 cell line						
Gene Symbol	MICROARRAY		Q-PCR			
	Fold Change 1μM	Fold Change 2μM	Fold Change 1μM	p-value	Fold Change 2μM	p-value
RBP4	<±2	<±2	3.5 (2.9 to 4.1)	<0.001	3.2 (2.4 to 4)	0.041
TTR	<±2	<±2	2.8 (1.4 to 4.7)	<0.001	1.9 (1.1 to 3)	0.202
HOMER1	<±2	<±2	2.5 (1.3 to 3.9)	0.023	1.5(1.2 to 1.7)	0.041
PAWR	<±2	<±2	3.2 (1 to 5.1)	0.031	2.1 (1.5 to 3.2)	<0.001
EGR1	-3.0	<±2	-1.6(-2 to -1.3)	0.047	-2.6(-3.7 to -1.6)	0.041
NGFR	1.9	2.7	8.6(5.7 to 13.9)	0.031	4.9(2.9 to 7.5)	0.023
BACE2	1.7	2.2	5.3(2.7 to 12)	0.031	3.4(2.6 to 4.6)	0.043

In the set of genes regulated by HBCD in the NSC19 cell line, genes related to retinol and thyroid hormones were tested and the *Rbp4* gene and the *Ttr* gene were found up-regulated in both the conditions tested. *Rbp4* was regulated in both of the cell lines, but in opposite directions. The transcriptional regulator *Egr1* was also found significantly down-regulated by 1.6 fold change in the 1μM condition and by 2.6 fold change in the 2μM condition compared to the control. Genes linked with neurodegeneration, especially Alzheimer's disease, were tested. All the three genes tested were up-regulated compared to the control. *Ngfr* was up-regulated by 8.6 and 4.9 fold change in cells treated with 1 and 2μM of HBCD, respectively. *Pawr*, encoding for a pro-apoptotic protein associated with the dopaminergic neuron loss in the Parkinson disease (Anantharam et al. 2007), was found up-regulated by more than 2 fold change. As also shown in cells treated with PBDE-47, the gene related to cellular calcium regulation *Homer1*, was also up-regulated in both the conditions tested. Gene expression is represented in figure 4.12.

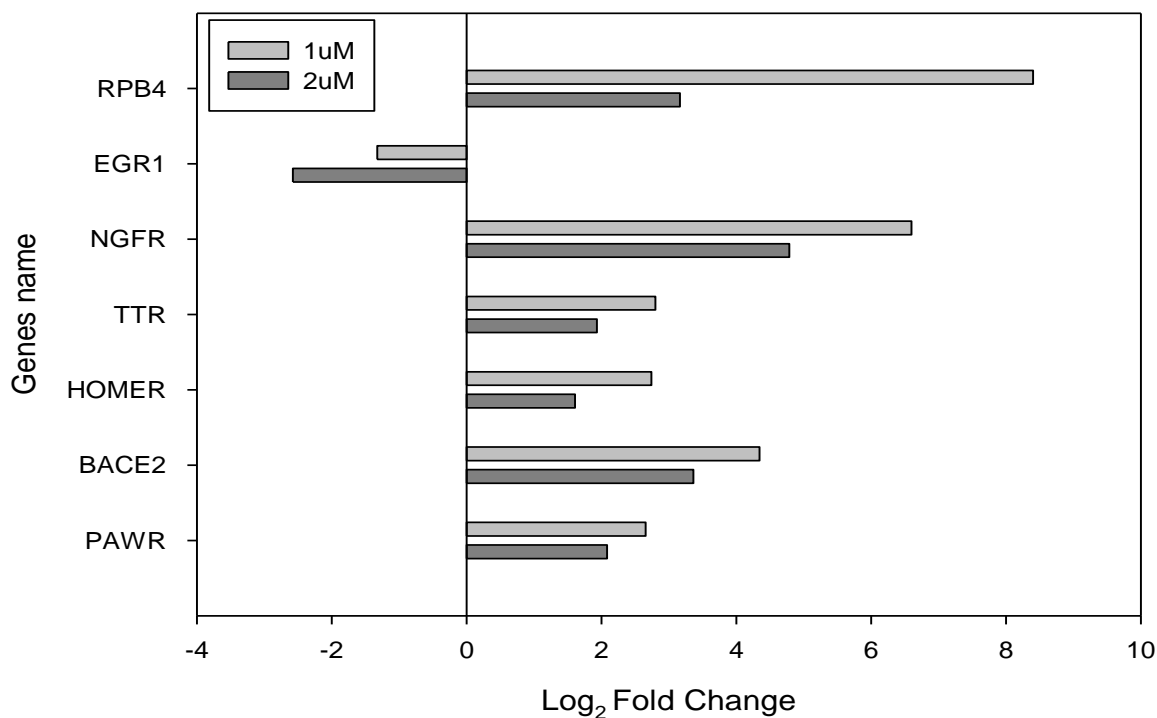


Figure 4.12: Log₂ fold change of genes regulated by HBCD in the NSC19 cell line. Gene expression was analysed with Q-PCR. Light blue represents gene expression in cells exposed to 1 μM PBDE-47 and dark blue in cells exposed to 2 μM PBDE-47.

4.5 General discussion

In this chapter for the first time the effect of the exposure to either PBDE-47 or HBCD has been evaluated on the global gene expression profile in cells of neuronal origin. Using microarray analysis we established that PBDE-47 and HBCD affect the expression of genes related to neurodegenerative disorders, especially to Alzheimer's and Parkinson's diseases. We also showed that the two toxicants affect genes related to calcium homeostasis and lipid metabolism, which could explain the spontaneous behaviour derange and the motor activity alteration previous reported in mice exposed to PBDE-47 or to HBCD (Per Eriksson et al. 2006; Gee and Moser 2008). Furthermore, the two toxicants affected thyroid hormone homeostasis genes, which may be related to the decrease in plasma T₄ level seen in previous in vivo studies after exposure to these two BFRs (Darnerud et al. 2007; Palace et al. 2010). Finally we established that exposure to either PBDE-47 or HBCD regulate the expression of genes related to membrane structure, with potentially effects on cytoskeleton structure and on ER functions.

4.5.1 Gene expression profile

Two-colour microarray analysis was deployed to identify changes in gene expression in N2A and NSC19 cells. Statistical analysis, using one way ANOVA with the LIMMA package (Bioconductor), on gene expression data from cells exposed to PBDE-47 resulted in 679 significant genes ($p < 0.05$, FDR 20%) with at least 2-fold change relative to the control, compared to the 494 genes for the NSC19 cell line ($p < 0.05$, FDR 20%). The N2A cell line clearly showed to be more responsive to the toxicant compared to the NSC19 cell line. Higher sensitivity by the N2A cell line to this toxicant was already seen in the cytotoxicity assay previously performed and reported in Chapter 3. A similar quantitative difference in response was seen in cells exposed to HBCD. LIMMA analysis showed that 790 genes ($p < 0.05$, FDR 20%) were differentially expressed in the N2A cell line and 484 ($p < 0.05$, FDR 20%) in the NSC19 cells with 2-fold change in expression in at least one of the three conditions used. Therefore, HBCD appeared to have likewise overall effect on gene expression in cells compared to PBDE-47.

In addition, comparison of genes regulated by PBDE-47 or HBCD showed that approximately the 10% of the regulated genes were in common, indicating that not only the two toxicants have overlapping regulatory effects, but can also affect distinct cellular functions. However, false positives (type II error) in the statistical analyses may also have contributed to the limited degree of shared genes between cell lines and toxicants.

Although regulated genes between the two toxicants were mostly different, some of the affected functions and cellular systems were overlapping. In fact, after GO analysis it was seen that both PBDE-47 and HBCD affect common sets of biological functions such as “endoplasmic reticulum membrane”, “non-membrane-bounded organelle” or “mitochondrial organisation”, and also functions distinct to either toxicant. Furthermore, PBDE-47 was seen to affect a function in common between the two cell lines, “steroid and lipid synthesis”. Other impacted functions were specific for each cell line. In the N2A cell line PBDE-47 caused changes in expression of genes related to functions such as “oxidoreductase”, “nucleotide binding” or “tubulin function”. In the NSC19 cell line, enriched terms related to ‘transcription regulation’, ‘neuronal development, differentiation and signalling’, and ‘metal ion binding’ were also present. The majority of children annotations under ‘metal ion binding’ related to zinc proteins and zinc homeostasis.

HBCD toxicity also appeared to affect specific target functions with enriched terms in common or distinct for each cell line. In both of the cell lines was seen enrichment in terms related to “non-membrane-bounded organelle”, “cell cycle process” and “cytoskeleton”. In the N2A cell lines terms related to “metabolic process”, “DNA damage”, “synapse organisation” “mitochondrial organisation”, “protein folding” and “regulation of apoptosis” were also seen enriched. In the NSC19 cells, changes in expression of genes involved in “actin organisation”, “DNA replication” and “endoplasmic reticulum membrane” were evident. Such pathways are often found in cancerous cells, although there is little evidence that HBCD is a carcinogen (Darnerud 2003a).

Among these enriched functions various terms such as “cytoskeleton”, “metal ion binding” or “DNA replication”, were for the first time seen to be enriched by PBDE-47 or HBCD. Other target functions could be instead related to previous *in vivo* or *in vitro* studies. For instance, effects on the endoplasmic reticulum membrane or on protein folding have been previously reported (Treiman 2002), as well as oxidoreductase unbalance after exposure to either the toxicants (W. H. He et al. 2008c; X. L. Zhang et al. 2008)

What is more, in previous animal studies conducted in our laboratory, proteomic and genomic analysis shared some of the functions enriched by PBDE-47 or HBCD in the present cellular study. According with what observed in this present study, protein folding related pathways were seen enriched in the *in vivo* work in both PBDE-47 and HBCD groups (Carroll 2011; Rasinger 2011). In the same study genomic analysis showed also enrichment for endoplasmic reticulum related genes after exposure to either the toxicants, as well as effects on metal responsive genes (Carroll 2011) specifically related to zinc proteins and zinc homeostasis, according with the present study.

4.5.1.1 Neurodegenerative disorders

In the present study, microarray analysis clearly showed that both PBDE-47 and HBCD exposure regulate genes involved in neurodegeneration. There are reports from behavioural studies indicating that PBDE-47 and HBCD neonatal exposure can cause permanent alteration in spontaneous behaviour and developmental behavioural defects (Per Eriksson et al. 2006; Viberg et al. 2003b). *In vivo* studies also showed that PBDE-

47 and HBCD have effects on neurological functions, particularly in memory and learning (Kuriyama et al. 2005; Viberg et al. 2003a; Viberg et al. 2003d). The causes for these effects and alterations are still unknown and, even if neurobehavioural effects in early life reported in vivo are not directly related to neurodegenerative diseases, the ability of the two toxicants to regulate the expression of genes related to neurodegeneration may contribute to the elucidation of the mechanism of action causing behavioural derange and neurological functions disruption. In fact some of the genes linked to neurodegenerative diseases regulated by PBDE-47 and HBCD are known to be linked also to behavioural dysfunctions, especially to memory and learning.

The gene for Amyloid Precursor Protein (*App*) was found to be up-regulated in cells exposed to PBDE-47. Proteolysis of the APP by beta- and gamma-secretases is known to lead to the production of amyloid-beta peptide ($A\beta$). $A\beta$ peptide deposition is found to be causing dementia progression in patients with Alzheimer's disease (AD), which is characterized by learning and memory impairment (W. Z. Li et al. 2012). $A\beta$ is the major component of the amyloid plaques in AD patient brain tissue (Hardy and Selkoe 2002) making its accumulation the primary cause of AD-associated neuropathology (McConlogue et al. 2007). In previous studies on hippocampal slices from mice that overexpressed APP, it has proved that an overexpression of $A\beta$ leads to the depression of synaptic transmission and therefore to the disruption of synaptic function (Kamenetz et al. 2003), suggesting that PBDE-47 exposure may lead to APP production with effect on synaptic activity.

PBDE-47 and HBCD were seen to regulate the two genes responsible for the cleavage of APP in $A\beta$. Among the secretase enzymes, β -secretases have a central role in the production of $A\beta$, and therefore in the induction of AD. The two β - secretases involved in the cleavage of APP have been identified as BACE1 (beta-site APP-cleaving enzyme 1) and BACE2 (Stockley and O'Neill 2007). While BACE1 activity as a β - secretases has been studied in some detail, BACE2 functions still not well characterised. Although it is known that both forms of BACE compete for the same substrate pool (Stockley and O'Neill 2007), *Bace2* function in $A\beta$ generation is controversial. Along studies suggesting an association between AD and *Bace2* (Myllykangas et al. 2005; Solans et al. 2000; Stockley and O'Neill 2007) differing finding are also reported. In humans studies it was suggested that BACE2 activity did not change significantly in the AD brain, and was not related to $A\beta$ concentration (Ahmed et al. ; Sun et al. 2005). Also, it has been shown that overexpression of *Bace2* does not lead to increased $A\beta$ production

(Bennett et al. 2000) and that BACE2 may even have an anti-amyloidogenic role (Basi et al. 2002). A more recent study, showed that *Bace2* overexpression in mice increased anxiety-like behaviour along with increased numbers of noradrenergic neurones, thus, suggesting an unexpected role of this protein (Azkona et al. 2010). These data suggest that BACE1 likely accounts for most of the A β produced in the human brain, and that BACE2 activity is not a major contributor. However, BACE2 activity remains unclear, and it should not be ignored when considering APP processing in AD.

In the present study, *Bace1* was found to be down-regulated by 1.5 fold in the NSC19 cell line exposed to PBDE-47. The down-regulation of this gene could be caused by a negative feedback as a consequence of *App* up-regulation. *App* over expression can lead to A β accumulation which could have caused a product inhibition on *Bace1* expression. In fact, inhibition of *Bace1* has been reported to abolish the production A β and therefore its accumulation (X. Luo and Yan 2010). *Bace2*, instead, was found to be upregulated by HBCD. Considering that *Bace2* has a minor activity in A β production, it can be speculated that it may act as a dominant negative for *Bace1* serving to slow down overall A β generation (Ahmed et al. ; Myllykangas et al. 2005).

Other genes related to neurodegenerative disease, especially Alzheimer's and Parkinson's diseases were shown to be regulated in cells exposed to HBCD. The gene *Pawr* also called *Park-7* was found to be up-regulated by more than two fold change in the NSC19 cell line. *Pawr* has been demonstrated to induce apoptosis and its over-expression confers enhanced sensitivity to apoptotic stimuli (Anantharam et al. 2007). *Pawr* is believed to be directly linked to Parkinson disease (PD) as this condition is characterised by dopaminergic neuron loss caused by apoptosis. Cell signalling events leading to apoptosis of dopaminergic neurons are not fully understood, but it is believed that oxidative stress is the major initiator of cell death in PD (Moore et al. 2005) (Rego et al. 2007). An *in vitro* study demonstrated that *Pawr* regulation is related to oxidative stress and its overexpression is caused by oxidative stimuli, suggesting *Pawr* as a gene related to PD neuronal loss (Anantharam et al. 2007).

The nerve growth factor receptor (*Ngfr*) gene, was regulated by HBCD in the NSC19 cell line. In cells exposed to 1 or 2 μ M of HBCD *Ngfr* was up-regulated by six and four fold change, respectively, as assayed by Q-PCR. The *Ngfr* gene encodes for P75^{NTR}, one of the two receptors specific for the nerve growth factor (NGF). Alteration of NGF signalling in the brain has been shown to contribute to a decline in cognitive function

such as memory and learning (Gibbs 1994; Terry et al. 2011). NGF has also a fundamental role for the integrity and maintenance of the cholinergic neurons, which are known to atrophy in AD (Cuello et al.). In AD patients it has been shown that increases in p75^{NTR} activity combined with signalling reduction of another receptor for NGF, contribute to neurodegeneration by enhancing the activation of pro-apoptotic mechanisms (Counts and Mufson 2005).

A graphic representation of the KEGG (Kyoto Encyclopaedia of Genes and Genomes) pathway “neurodegenerative disorders” is reported in figure 4.13. Genes regulated by either HBCD or PBDE-47 are present in the pathway and, as described above, are mainly related to Parkinson’s and Alzheimer’s diseases.

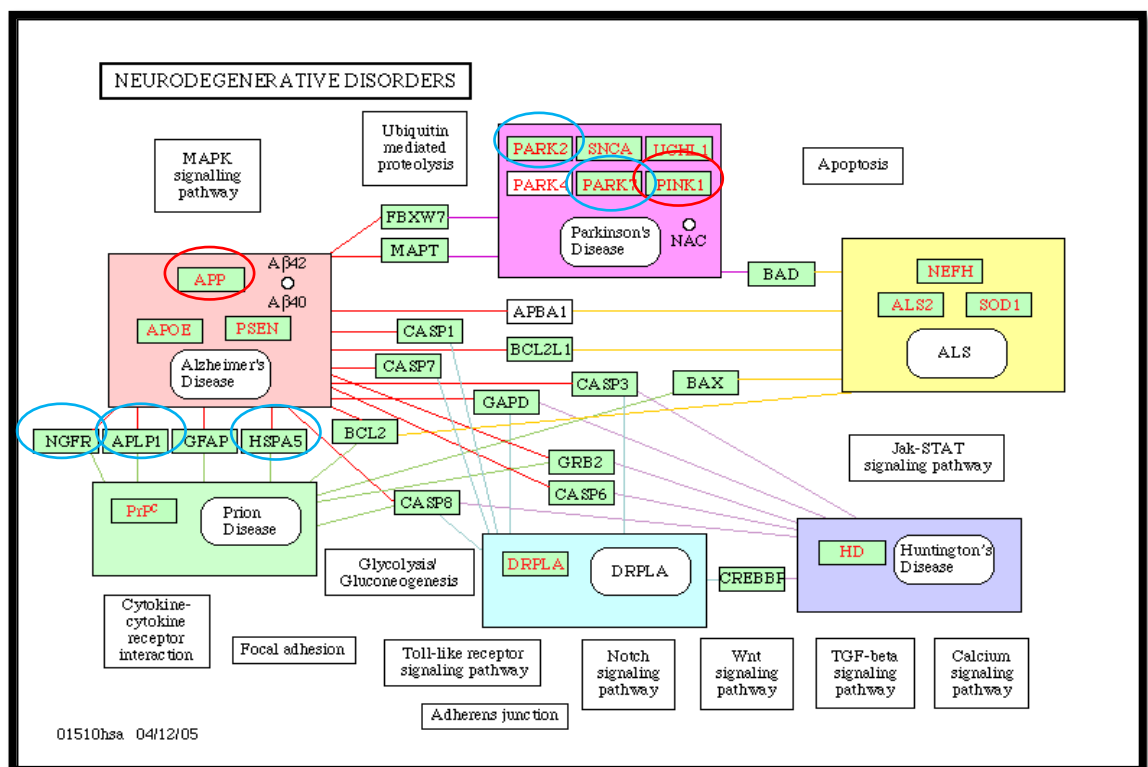


Figure 4.13: Representation of genes regulated by either PBDE-47 or HBCD linked to neurodegenerative disorders. In the picture genes circled in red are regulated by PBDE-47 and the ones in blue are regulated by HBCD. Both of the toxicants seem to regulate genes linked with Parkinson and Alzheimer’s disease.

These findings indicate that both PBDE-47 and HBCD exposure can cause regulation of genes responsible for the production and accumulation of Aβ in the brain such as *App*

and *Bace1* and *Bace2*. They also showed that the two toxicants can induce the expression of a gene responsible for the apoptosis of dopaminergic neuron such as *Pawr*, and inhibit the expression of the gene *Ngfr* fundamental to the integrity and maintenance of cholinergic neurons. The overall results suggest regulation of genes related to neuronal functions and maintenance caused by either PBDE-47 or HBCD.

4.5.1.2 Calcium homeostasis

Evidence of regulation of genes related to calcium homeostasis disruption was found after exposure to PBDE-47 or HBCD. Genes related to calcium signalling and homeostasis were found differentially expressed in both microarray and Q-PCR.

Previous finding *in vitro* have shown that, at concentration relevant to levels in the human brain tissue, PBDE-47 and HBCD can disrupt cellular calcium related processes (Coburn et al. 2007; M. M. L. Dingemans et al. 2008b; Mariussen and Fonnum 2003). The mode of action of calcium disruption is not well understood yet, but several ideas have been put forward. The two leading hypotheses involve direct interactions with the Ryanodine receptor (RyR) as has been suggested for dioxin-like POPs such as planar polychlorinated biphenyl (PCBs) (Pessah et al. 2010), or disruption of the plasma membrane with calcium changes as an indirect consequence (Y. S. Tan et al. 2004b). Non-dioxin-like PCBs have been also shown to interact with the RyR increasing its activity in isolated sarcoplasmic reticulum preparations (Wong and Pessah 1997). In the present study, the gene for the RyR itself was not seen to be regulated. However, effects on RyR activity may not necessarily be reflected in changes in its expression but rather in changes in the expression of genes downstream from RyR induced changes in cellular calcium status (Carroll 2011).

Calcium homeostasis disruption has been previously associated with effects on memory and learning, synaptic plasticity as well as changes in neurological function associated with ageing and Alzheimer's disease (Yu et al. 2009). The cytosolic calcium concentration is mainly regulated by ligand and voltage gated calcium channels in the neuron's plasma membrane, and from intracellular stores such as the smooth endoplasmic reticulum regulated by the action of Inositol Triphosphate (IP3) and Ryanodine interacting with the IP3 and RyR, respectively (Augustine et al. 2003).

One of the main proteins involved in calcium signalling is HOMER1. In the present study, the gene *Homer1* was found to be regulated by HBCD in the N2A cell line. HOMER1 acts as a bridge between the smooth endoplasmic reticulum (ER), containing the Inositol Triphosphate Receptor (IPR3) and the RyR, and the postsynaptic membrane containing the NMDA, the metabotropic glutamate receptor (mGluR) and the voltage-gated calcium channel. Therefore HOMER1 is a key element for calcium secondary messaging regulation and maintenance. The observed *Homer1* regulation by HBCD provides some insight into the mechanism of calcium homeostasis disruption and indicates that HBCD may have direct effects on HOMER1 as well as indirect effects operating via RyR.

4.5.1.3 Unfolded Protein Response (UPR) and Endoplasmic Reticulum (ER) stress

Exposure to either PBDE-47 or HBCD was seen to cause effects related to ER structure and proteins folding. GO analysis showed enriched terms such as “endoplasmic reticulum membrane” and “endoplasmic reticulum part” and “protein folding”. A number of genes related to ER stress and to unfolded protein response (UPR) were also seen regulated by either of the toxicants. Various factors can lead to ER stress such as oxidative stress, chemical insult, genetic mutation and even normal differentiation, but one of the main causes has been associated with calcium depletion (Rutkowski and Kaufman 2004; Treiman 2002). This observation accord with the calcium homeostasis disruption observed after PBDE-47 or HBCD exposure established in previous studies (Coburn et al. 2008; M. M. L. Dingemans et al. 2009), and also with the present transcriptomics results.

Calcium homeostasis disruption caused by either the toxicants can interfere with the folding pathway within the ER as many protein-folding proteins require calcium as a co-factor to correctly function. This can be a potential for cell injury through accumulation of misfolded protein aggregates (Treiman 2002). Accumulation of unfolded protein in the endoplasmic reticulum (ER) leads to the initiation of the UPR pathway, with the activation of chaperones that facilitate proper protein folding and prevent protein folding intermediates from aggregating. A well characterised sensor of UPR is the Heat Shock Protein 5, *Hspa5* (Lee 2005). *Hspa5* plays an important role in the ER stress and UPR as an ER stress signalling regulator and for its ability to maintain

the balance between cell survival and apoptosis in ER-stressed cells (Hsu et al. 2008). However, *Hspa5* was seen to be down-regulated by HBCD in the N2A cell line by almost two-fold change, suggesting that this sensor of UPR became disabled by HBCD exposure. Down-regulation of *Hspa5* caused by HBCD may therefore lead to accumulation of partially folded proteins in the ER with consequences in ER malfunctioning. In addition, accumulation of misfolded protein has been associated with neurodegenerative disorders such as Alzheimer's and Parkinson's diseases (Lee 2005), which fit with what was previously reported in the present transcriptomic study.

4.5.1.4 Lipid metabolism and mitochondrial function

Effects caused by PBDE-47 and HBCD on calcium regulation can also lead to secondary calcium dependent effects such as increase in arachidonic acid (AA) level by the activation of calcium-dependent phospholipases and effects on protein kinases (Draper et al. 2004). In fact, functions related to “lipid and steroid synthesis” and “fatty acid biosynthesis” were found to be preferentially regulated by PBDE-47. In addition, in the N2A cell line, HBCD down-regulated the genes related to fatty acid and lipid metabolism, *Acsl4* and *Pnpla8*. The gene *Acsl4* (acyl-CoA synthetase type 4 for long chain fatty acids) encodes for the ACSL4 protein which adds coenzyme A to long chain fatty acids. ACSL4 has a high substrate preference for arachidonic acid (AA), a polyunsaturated fatty acid particularly abundant in brain membranes (Melon et al. 2009). In a previous study it was shown that the absence of *Acsl4* protein results in mental retardation in humans (Piccini et al. 1998). Recently it was suggested that problems resulting from its absence may arise because of alterations in lipid metabolism (Melon et al. 2009). In fact, AA, *Acsl4* preferred substrate, is one of the most abundant polyunsaturated fatty acids in brain membranes and it has been related to important processes for normal brain development and function (Longo et al. 2003; Melon et al. 2009). Therefore *Acsl4* and *Pnpla8* down-regulation caused by PBDE-47 or by HBCD can contribute not only to lipid metabolism deregulation, but also to the alteration of brain development and functioning.

In recent years, a family of lipid hydrolases, designated patatin-like phospholipase domain containing (PNPLA), has attracted attention, as its members were found to serve critical roles in diverse aspects of lipid metabolism and signalling. These enzymes are generally important for many intra- and extra-cellular processes, including maintenance of membrane integrity, lipid signalling, and regulation of energy

homeostasis (Baulande and Langlois). One of the main members of these phospholipase is *Pnpla8*. *Pnpla8* gene was confirmed to be down-regulated by HBCD in the N2A cell line. A previous study showed that *Pnpla8* prevents and repairs lipid peroxidation induced by oxidative stress. It also participates in the removal of oxidized fatty acids from biological membranes to maintain membrane integrity (Kinsey et al. 2008). Studies showed that its decreased expression induces lipid peroxidation, impairs mitochondrial function, and decreases viability (Kinsey et al. 2008; Mancuso et al. 2007). Therefore the down-regulation of *Pnpla8* caused by HBCD, may lead to an increase in lipid peroxidation, with consequences on the membranes structure and permeability.

In addition, considering that the regulated gene *Acs14* has a high substrate preference for AA, its reduction in expression might result in an increase in free AA pool. Therefore it is possible that such an increase in free AA would lead to a regulation of phospholipase activity such as *Pnpla8* which was seen to be down-regulated in cells exposed to HBCD. Thus, *Pnpla8* down-regulation can be explained either as a consequence of a cellular compensatory mechanism or as a direct effect of HBCD exposure.

In addition, *Pnpla8* is located in the inner mitochondrial membrane and it is known that mitochondrial function decreases with decreased *Pnpla8* (Kinsey et al. 2008; Mancuso et al. 2007). These observations suggest that *Pnpla8* main function is in the maintenance of mitochondrial activity, specifically through tailoring mitochondrial membrane lipid metabolism and composition (Mancuso et al. 2007). Therefore, the down-regulation of *Pnpla8* caused by HBCD can lead to mitochondrial activity disruption.

Damage of mitochondrial functions can cause the excessive production of ROS, with consequent cellular oxidative damage (Lenaz 1998; Liu et al. 2000). In fact, the accumulation of ROS may lead to oxidative stress. The mitochondrial respiratory chain is one of the main sources of ROS in cells. Mitochondria also contain antioxidant enzymes, including superoxide dismutase, glutathione peroxidase, and lipid-soluble antioxidants such as vitamin E. Thus mitochondrial damage can prevent the natural cellular antioxidant activity.

In literature, oxidative stress as a target of HBCD toxicity has been previously reported. In Hep G2 cells, the three HBCD stereoisomers were seen to cause ROS formation at concentration between 0.5µg/ml to 5.0µg/ml depending on the stereoisomers (X. L. Zhang et al. 2008). Also, in zebrafish embryo, HBCD was shown to cause oxidative

stress with increase in SOD activities and in lipid peroxidation at concentration within the range of 0.002-10 mg/L. In the same study, an overexpression of *Hsp70* was also reported (Hu et al. 2009; X. L. Zhang et al. 2008).

Previous *in vitro* studies have revealed that also PBDE-47 can lead to oxidative stress damage. Studies on human neuroblastoma SH-SY5Y cells, showed that PBDE-47 can cause increase in ROS formation and in MDA content, decrease in GSH activity and in SOD activity at concentration of 4µg/ml (P. He et al. 2008b; M. Zhang et al. 2007).

In support of these findings, in the present study, GO analysis of genes regulated by PBDE-47 revealed enrichment of functions related to oxidative stress. Two of the highly significant enriched terms were “oxidoreductase” and “oxidation reduction” ($p < 0.0004$) supporting the idea that oxidative stress is also a PBDE47 toxicity target. In addition, analysis on genes regulated by HBCD showed that the toxicant can cause enrichment of annotations related to mitochondrial structure such as “mitochondrial part” and “mitochondrial membrane”, suggesting a direct effect on genes related not only to oxidative stress, but also to mitochondrial function.

4.5.1.5 Cytoskeleton regulation

In the present study, microarrays revealed that both PBDE-47 and HBCD affect the cytoskeleton structure and organisation. GO analysis in cells exposed to HBCD revealed enrichment of genes related to “cytoskeleton organisation” and “actin organisation”. Also cells exposed to PBDE-47 showed regulated genes related to “tubulin function” as enriched terms.

IPA analysis also reported genes with cytoskeleton structure and maintenance functions such as *Tubb2c* (tubulin, beta 2C), *Tuba1a* (tubulin, alpha 1a) and *Trip6* (thyroid hormone receptor interacting protein 6) to be in one of the main networks regulated by PBDE-47. *Trip6* was found to be downregulated by 1.3 fold in PBDE-47 exposed cells relative to the control in the N2A cell line. *Trip6* downregulation was previously associated with effect on the actin cytoskeleton regulation (Guryanova et al. 2004; Guryanova et al. 2005). Cytoskeleton structure maintenance has been also previously associated with Tubulin expression (Leandro-Garcia et al.), suggesting that PBDE-47 effects on *Tubb2c*, *Tuba1a* and on and *Trip6* may lead to cytoskeleton regulation disruption.

In literature, a limited number of studies have been conducted on the effects on POPs on cytoskeleton structure and functions. A study on primary cultures of fetal rat cortical cells showed that PBDE-99 can cause disruption of cytoskeleton organisation (Alm et al. 2008). A study conducted on muscles also showed that exposure to PBDEs can cause disturbance in microtubule subunit beta tubulin (Apraiz et al. 2006). In the present study substances with effects on cytoskeleton are extended to include PBDE-47 or HBCD.

An alternative hypothesis, parallel to a direct effect on gene expression, to explain PBDE-47 and HBCD effects on the cytoskeleton, is that the accumulation of AA, caused by the down-regulation of *Acs14* as previously illustrated, can lead to the regulation of AA-modulated cytoskeleton reorganization. A role of AA-modulated actin cytoskeleton remodelling in neuritogenesis in different neuronal models has been suggested before (Okuda et al. 1994). The actin cytoskeleton is known to have roles in many critical developmental processes including cell migration, proliferation and differentiation, and cytokinesis. In the central nervous system (CNS) it is also responsible for many functions including spine formation and synaptic regulation (L. Q. Luo 2002), suggesting that the effects caused by PBDE-47 and HBCD on the cytoskeleton structure and maintenance, may be one of the causes of the spontaneous behaviour derange observed in *in vivo* studies (Chou et al. 2010; Per Eriksson et al. 2006).

4.5.1.6 Hormone activity signalling

In the present study, PBDE-47 and HBCD were seen to affect the expression the two main retinol and thyroxin carriers, transthyretin (*Ttr*) and retinol binding protein4 (*Rbp4*). Regulations in the expression of these two genes, suggest that either the toxicants may affect hormone activity, especially thyroid hormone and retinoid regulations. Both *Ttr* and *Rbp4* were seen regulated in cells exposed to HBCD, when *Ttr* only was seen regulated after exposure to PBDE-47. In the *in vivo* study conducted in our laboratory, PBDE-47 and HBCD were seen to cause changes in the level of thyroid hormone concentrations, with a reduction of serum T4 level after exposure to HBCD, and a significantly ($p < 0.05$) reduction in serum T3 level after exposure to either PBDE-47 or HBCD (Carroll 2011; Rasinger 2011). In the same study, thyroid gland histology displayed a positive trend in foaming colloid in mice exposed to PBDE-47 (+66%), as well as a significantly ($p < 0.05$) increase occurrence of a reduction in the size of the follicular lumen. In addition, it was seen that both the toxicants caused increasing

of desquamation into follicular lumen, which is a marker of disruption of thyroid function, of the 14% and 71% for HBCD and PBDE-47 respectively, compared to control. In the same study, genomic analysis revealed that HBCD significantly regulate the expression of *Ttr* and *Rbp4* (Carroll 2011), which correlates with the finding in the present study.

Previous *in vivo* studies on rats and on the F1 animals reported that exposure to sublethal concentrations of HBCD reduce the level of apolar retinoids (van der Ven et al. 2006; van der Ven et al. 2009). Retinoid regulate the transcription of numerous target genes, consequently, they play vital roles in a multitude of processes such as nervous system development and maintenance in adult neurons. Therefore, disruption of retinol binding and signalling can lead to effects on nervous system and degeneration of motor neurons in adults (Maden 2007). These considerations relate to previous developmental neurotoxicity study in mice, where HBCD was seen to induce effects in spontaneous behaviour, learning and memory and alteration in locomotion behaviour (Chou et al. 2010; Per Eriksson et al. 2006).

Changes in *Ttr* and *Rbp4* expression, have been previously correlated with changes in serum thyroxin level (W. Zheng et al. 2001). Thyroxin, as well as retinol, is known to play an important role in neuron development and growth (Forrest et al. 2002).

The disruption of thyroid hormone homeostasis by persistent organic pollutants is well established. Thyroxin levels have been previously reported to decrease following HBCD (Darnerud 2003a) or PBDE-47 (Darnerud et al. 2007; Skarman et al. 2005) exposure . Also, an *in vitro* study showed that HBCD affects the expression of thyroid hormone receptor-regulated genes and therefore it represents a potential risk as endocrine disruptor (Yamada-Okabe et al. 2005).

In the present study either the toxicant were seen to affect the expression of *Ttr*. Regulation of *Ttr* by PBDE-47 and HBCD and of *Rbp4* by HBCD, supports the idea of thyroid hormone disruption as an important potential target of PBDE-47 and HBCD toxicity. Our main observation is that the regulation of retinol carrier proteins expression *in vitro*, raises the possibility that the decrease in thyroxin level ((Darnerud 2003a; Darnerud et al. 2007; Skarman et al. 2005) and the regulation of retinoid (van der Ven et al. 2006; van der Ven et al. 2009), reported in previous *in vivo* studies, is a secondary effect due to the direct effect of PBDE-47 and HBCD on the expression of the two carrier proteins.

However, we need to consider that in whole animal there will be metabolic reactions which cannot be appreciated in cultured cell line. In fact, the metabolism of thyroid hormones plays a substantial part on the regulation of circulating TH concentration. Metabolism of thyroid hormones is facilitated by two principal pathways, deiodination and conjugation (Klaassen and Hood 2001; Visser et al. 1993). During deiodination, thyroxine is converted to triiodothyronine, a more metabolically active hormone. Conjugation is instead a major pathway for biotransformation which involves sulfation and glucuronidation, functions to increase the water solubility of T₄ and T₃ and thus to facilitate excretion into bile and urine (Klaassen and Hood 2001; Visser et al. 1993). Glucuronidation of T₄ and T₃ is catalyzed by different species-specific hepatic UDP-glucuronosyltransferase (UGT) isoenzymes, which belong to the enzymes of phase II metabolism. Previous work with POPs indicated that PCB (M. O. James et al. 2008; Richardson and Klaassen 2010) and TCDD (Bank et al. 1989; Goon and Klaassen 1992) can act as UGT inducers, increasing T₄ glucuronidation, and consequently, evoking a decrease in blood level of thyroid hormones (Barter and Klaassen 1994; Gessner et al. 2011), suggesting that PBDE-47 and HBCD toxicity may involve the same mechanisms of action. In addition, a circulating thyroid hormone reduction, can lead to an alteration of the normal thyroid feedback loop, resulting in release of thyroid-stimulating hormone (TSH), which stimulates the thyroid gland to TH production, with consequence of thyroid gland hypertrophy and hyperplasia (Barter and Klaassen 1994), which accord with what previously observed in *in vivo* studies after exposure to PBDE-47 (Ferne et al. 2005; Lema et al. 2008) or HBCD (Palace et al. 2010).

Therefore we can conclude that several factors are involved in TH regulation, but for the first time we suggested a new approach to interpret changes in TH level in serum which can clarify POP effects on hormone regulation.

4.5.1.7 Transcriptional regulation and tumour suppression

Microarray analysis revealed that two of the most significant genes regulated by HBCD were the genes *Nfkb2* (nuclear factor of kappa light polypeptide gene enhancer in B-cells 2), and *Egr1* (early growth response 1), both seen regulated in the N2A cell line.

The immediate-early gene *Egr1* is known to be a positive regulatory nuclear factor (Khachigian et al. 1997; Ravni et al. 2008) with regulatory function on the expression of proteasome and related genes in neuronal cells with effects on brain plasticity and

synaptic function (A. B. James et al. 2006). The protein encoded by the *Nfkb2* gene, confirmed to be regulated in the NSC19 cell line, is also a well characterised transcriptional regulator (Keller et al. ; Savinova et al. 2009).

The observation of HBCD effects on the regulation of genes related to transcriptional regulation, fit well with the assumption that transcription factors can be HBCD toxicity targets.

In addition, the tumour suppressor *Rb1* (retinol binding protein 1) regulated by PBDE-47 has a central role in the main pathway affected by this toxicant as shown in figure 4.7. *Rb1* has been shown to play a role in the induction of growth arrest and cellular senescence via mechanisms involving transcriptional repression (Binda et al. 2008). *Rb1* is directly linked with the gene *Sirt1* (Sirtuin 1), a deacetylase which main function is epigenetic gene silencing (Binda et al. 2008). *Sirt1* was also found to be down-regulated in cells treated with PBDE-47, indicating direct and secondary effect by PBDE-47 on the expression of genes related to transcriptional mechanisms.

4.6 Chapter conclusion

In this Chapter, we established that exposure to PBDE-47 and HBCD cause regulation of genes related to fundamental cellular functions in cells of neuronal origin. We showed that both toxicants preferentially act on functions associated with neuronal activity such as neurodegeneration, calcium signalling, cytoskeleton structure or AA homeostasis. Regulation of genes related to these functions, perfectly fit with the phenotype profile seen in PBDE-47 or HBCD exposed mice, which displays spontaneous behaviour derange and effect on memory and learning (Chou et al. 2010; P. Eriksson et al. 2002; Per Eriksson et al. 2006). Furthermore, it was observed that the carrier proteins for thyroxin and retinol were regulated and this seems to perfectly fit with *in vivo* studies showing that exposure to the two toxicants cause decrease in T4 and in retinol level (van der Ven et al. 2009; W. Zheng et al. 2001).

Hence, in the present study we have found gene expression signatures that cast light on the molecular mechanisms underlying the major phenotypical manifestations of BFR toxicity. However, the low correlation between the results obtained using Q-PCR and with microarrays, is a limitation to be considered. Presumably, analysis made with Q-PCR are more reliable compared to the one implemented with microarrays, therefore

conclusions in the present study were mainly based on the data obtained with the former approach.

Comparing the effect on global gene regulation caused by exposure to the two toxicants, an approximately equal number of genes were regulated in cells exposed to either HBCD or PBDE-47. These results are consistent with findings reported in *in vivo* studies, where toxicity appears to be comparable with very similar oral LD₅₀ for both the contaminants. In a previous study, in rodents exposed to different PBDEs the oral LD₅₀ was in the range of 1-10mmol/kg body weight (Darnerud 2003b), likewise the LD₅₀ reported in rats following HBCD oral administration was 10 mmol/ kg body weight (Darnerud 2003b). In the same way, cytotoxicities of PBDE-47 and HBCD to the N2A and NSC19 cells analysed in the present study were also similar (Chapter 3). Therefore, it can be concluded that the toxicities of these two BRFs do not substantially differ.

In the present study, even if among the regulated genes the two toxicants did not appear to share a large number of affected genes, several of their toxicity targets, in terms of biological functions of regulated genes, were in common. Both of the toxicants were shown to cause effects on neurological functions regulating genes linked to neurodegenerative disease. PBDE-47 and HBCD regulated genes responsible for the formation of the amyloid peptide, a major component of the plaques in the brain in Alzheimer's disease, and genes responsible for the integrity and maintenance of neurons. These findings suggest that the effects in spontaneous behaviour derange seen in previous *in vivo* developmental studies after exposure to PBDE-47 or HBCD (Chou et al. 2010; Per Eriksson et al. 2006), are the consequence of the direct effects of these toxicants on specific molecular networks responsible for neuronal function as reflected in preferential changes in expression of genes within these systems.

The two toxicants were also causing effects on calcium signalling and homeostasis, with regulation of the gene, *Homer1*, which has an essential role in the activity of calcium channel receptors, including RyR and the IP3 receptor. Direct consequences of the cellular calcium disruption were seen in both cell lines exposed to PBDE-47 and HBCD. Interestingly, genes related to ER stress and UPR were also found enriched and effects on these genes could plausibly be explained by calcium deregulation. Considering that calcium homeostasis disruption can have consequences in memory and learning (Yu et al. 2009), we can speculate that the effect on memory and learning

caused by PBDE-47 or HBCD in previously *in vivo* studies (P. Eriksson et al. 2002; Per Eriksson et al. 2006), are the indirect consequence of calcium signalling disruption.

The two toxicants were also responsible for the regulation of genes related to lipid metabolism, which could be a consequence of the calcium disruption effects on the phospholipases activity. The phospholipase, *Pnpla8*, was in fact shown to be regulated by HBCD. This phospholipase has also a second important function, which is maintenance of mitochondrial activity. Therefore its down-regulation could lead to mitochondrial functions disruption. In further support of this finding, GO analysis revealed that HBCD affected expression of genes related to mitochondrial functions and structures.

PBDE-47 and HBCD also affected genes related to the cytoskeleton regulation. The effects observed could be direct to the cytoskeleton itself, or indirect as a consequence of calcium homeostasis disruption. In more details, calcium deregulation can lead to the activation of phospholipases with consequential increase in free AA (Draper et al. 2004). Accumulation of AA may lead to the regulation of genes related to the cytoskeleton structure and maintenance, and to the regulation of AA-modulated amyloid cytoskeleton remodelling, with consequences in cell migration, proliferation and differentiation (Okuda et al. 1994).

This study showed also that the two toxicants cause effects on hormone activity, with regulation of the two main retinol and thyroxin binding protein in plasma. These findings are in agreement with *in vivo* data showing that exposure to PBDE-47 or HBCD cause decrease in the plasma thyroxin level (Darnerud et al. 2007; Hallgren et al. 2001a; Palace et al. 2010). Therefore, we suggest that the effect on the expression of the two carrier proteins may influence circulating T4 level *in vivo*. However, *in vitro* studies don't reproduce metabolic functions that occur in an organism, such as glucuronidation of TH, which can also affect circulating T4.

HBCD was also seen to impact the expression of transcription factors which regulate genes in neuronal cells with effects on brain plasticity and synaptic function. PBDE-47, instead, was shown to regulate the main tumour suppressor *Rb1* which plays a role in the induction of growth arrest and cellular senescence via mechanisms involving transcriptional repression (Binda et al. 2008).

5. Post-transcriptomics
analysis

5.1 Introduction

In the present study, transcriptomics analysis was performed on cells exposed to either PBDE-47 or HBCD (Chapter4) in order to identify the effects on gene expression by these two toxicants. Analysis showed that PBDE-47 and HBCD affect a while range of vital functions such as neurodegeneration, ER membrane or hormone regulation, and in this Chapter effects noted in microarray analysis are further explored.

In Chapter 4 it has been largely discussed how HBCD exposure has the ability to influence the regulation of genes related to calcium homeostasis and signalling. One of the approach undertook in the present study was the investigation of the effect on calcium concentration after exposure of N2A cells to HBCD. In contrast to the usual response typically observed in the majority of cell types, N2A cells did not respond to treatment required to investigate calcium homeostasis. In fact, either ATP, Thapsigargin or Glutamate treatments could not trigger a rise in cellular Ca^{2+} concentration as expected. Therefore, the effect on calcium homeostasis was not further investigated.

Considering the relationship between calcium and zinc, which is a recently discovered second messenger (Yamasaki et al. 2007a), lead to the hypothesis that also zinc homeostasis could be affected by HBCD exposure. In fact the presence of zinc-containing neurons that sequester zinc in the presynaptic vesicles and release it in a calcium- and impulse-dependent manner has been demonstrated in the brain (Pan et al. 2011). What is more, in animal studies conducted in our laboratory, the gene *Mt1*, member of the Metallothionein family, was found to be regulated following exposure to either PBDE-47 or HBCD. *Mt1* is known to be a zinc responsive gene, which may be regulated by activated Metal Responsive Transcription Factor 1 (MTF1). This transcription factor binds the Metal Response Elements (MREs), in the 5' regulatory region of genes including *Mt1*. *Mt1* encodes for one of the main zinc binding proteins, fundamental for the zinc homeostasis and intracellular zinc concentration maintenance.

Moreover, a recent study performing gene transcription analysis on the hippocampus of mice exposed to either the three principal HBCD congeners, reported an enrichment of the canonical pathway “synaptic long term potentiation (LTP)”, with specific changes in proteins involved in glutamate receptor signalling and calcium homeostasis (Szabo DT 2011). In the brain most of the total zinc is bounded to metalloproteins, but ionic zinc is concentrated in zinc-containing glutaminergic neurons, specifically in glutamatergic

synaptic vesicles, where it acts as neuromodulator of several important receptors including the γ -amino butyric acid (GABA) and *N*-methyl-d-aspartate (NMDA) receptors (Pan et al. 2011; Takeda 2000). Thus it can be hypothesised that the observed changes in glutamate receptor are a direct consequence of the effect on zinc homeostasis disruption. These findings and considerations directed the investigation of the effect of HBCD exposure on zinc homeostasis and signalling.

A different approach undertaken to deeply explore HBCD effects observed in microarray in this present study, was the interactions between the omega-3 fatty acid, Docosahexaenoic acid (DHA), and HBCD, on gene expression. DHA is in fact the most abundant polyunsaturated fatty acid in the brain, and the main source for human is via fish consumption (H. Y. Kim 2007). Despite being rich in nutrients, fish is also one of the major routes of exposure to various environmental contaminants, especially POPs (Schechter et al. 2006; Schechter et al. 2010a) and its consumption can cause accumulation of toxicants. This bivalent characteristic raises concern regarding the benefit and risks related to fish consumption, although specific studies haven't been conducted to investigate the problem. Based on this consideration, for the first time the interaction between HBCD toxicity and possible moderating effects of DHA were evaluated on expression of genes identified as HBCD regulated, in the microarray experiment (Chapter 4).

5.1.1 Zinc and the brain

Zinc is an essential mineral that plays key roles in many vital biological functions (Brown et al. 2001). It is the second most abundant transition metal in the human body and is the constituent of an estimated 3,000 protein including enzymes of all classes (Andreini et al. 2006). In particular, zinc plays an important role in the folding of DNA-binding domains of many proteins, including the zinc finger domains of numerous transcription factors, such as nuclear receptors (Frederickson et al. 2000). Zinc has been also suggested to function as a second messenger (Yamasaki et al. 2007a). A study on mast cells showed that immunoglobulin E receptor stimulation induced an increase in intracellular free zinc, which was named zinc wave, originating in the region of the ER (Yamasaki et al. 2007a). In literature it is also reported that zinc function as a signalling molecule similarly to neurotransmitters (Hirano et al. 2008; Murakami and Hirano 2008; Smart et al. 2004). For example, a study on hippocampal mossy fibres, showed

that presynaptic stimulation caused zinc release from terminal vesicles into the synaptic cleft, suggesting a role in neurotransmission (Qian and Noebels 2005).

In the brain, zinc modulates neuronal post-synaptic excitability and synaptic plasticity, and is therefore implicated in the processes of learning and memory (Cuajungco and Lees 1997). It has been shown that deficiency or excess of zinc can cause alteration in behaviour, abnormal central nervous system development, and neurological disease. On the other hand, overabundance of zinc can be cytotoxic, inducing apoptosis and neuronal death. Therefore, zinc homeostasis maintenance has a critical role in normal functioning of the brain and the central nervous system (Bitanhirwe and Cunningham 2009). For this reason, intracellular zinc concentrations in different compartments are strictly controlled by zinc importers, exporters, and binding proteins such as metallothioneins (Mt) (Frederickson et al. 2000).

Considering these overall data, we hypothesised a potential effect of HBCD on zinc homeostasis, which seemed important to be elucidated. Disruption of cellular zinc homeostasis is recognised as a mechanism of action for other transition element, such as cadmium and mercury (Glover et al. 2009; Kawanai et al. 2009; Predki and Sarkar 1994) but its involvement in toxicity to organic POPs has not been previously studied.

5.1.2 Docosahexaenoic acid (DHA) and the brain

Long-chain polyunsaturated fatty acids (LC-PUFAs) have essential roles in brain function as they are required to maintain cellular functional integrity and overall they are essential for human health (Bazan 2005; Domingo 2007).

Docosahexaenoic acid (DHA) is the most abundant polyunsaturated fatty acid in the brain. In the nervous system astrocytes only have the ability to synthesise DHA and the main source of this fatty acid is through the diet, especially via fish and via maternal milk for infants (H. Y. Kim 2007). DHA is also biosynthesized in the liver from the precursor linolenic acid through chain elongation and desaturation processes. It is then secreted into the blood stream and transported to the brain where it is incorporated into membrane phospholipids (H. Y. Kim 2007).

DHA effects in brain have been investigated extensively with both *in vivo* and *in vitro* studies. DHA has been shown to contribute to brain functions and development with maintenance of neuronal survival and differentiation (Bazan 2005). Effects on neurite

growth and synaptogenesis in embryonic hippocampal neurons have also been reported, suggesting the importance of DHA for learning and memory functions (H. Y. Kim et al. 2011) Therefore, the loss of DHA or interference in its accumulation by nutritional deprivation or in pathological states, may diminish the protective capacity of the central nervous system, with significant implications for neuronal function (H. Y. Kim 2007). However, the beneficial effects of DHA on learning in humans are still controversial. Whilst several investigations have failed to find such an association (Delgado-Noguera et al. 2010; Hirayama et al. 2004), there are a few studies on humans suggesting that early dietary supply of DHA improves later cognitive development in infants (Birch et al. 2000; Boucher et al. 2011; Drover et al. 2009).

As mention above, the main source of DHA for human is via fish consumption. The current dietary guidelines recommend that healthy adults eat at least two servings of fish (particularly fatty fish) per week, or to consume about one gram of EPA+DHA per day (Domingo 2007). Because salmon is widely consumed by humans and contains notable quantities of PUFAs, it has been one of the marine species to which most attention has been paid in terms of being a good source of LC-PUFA (Domingo 2007). However, fish and seafood are potentially major sources of human exposure to various environmental contaminants. In recent years, a number of investigators have assessed the levels of various pollutants in several food groups, reporting that the levels of several POPs is higher in fish, especially in fatty fish, compared to other food sources (Schechter et al. 2006; Schechter et al. 2010a). In addition to the presence of legacy contaminants, accumulation of BFRs such as HBCD in marine animals including farmed fish has been reported to increase rapidly (Covaci et al. 2006; de Wit et al. 2010). Therefore, even if fish is a fundamental source for some essential nutrients, such as DHA, high consumption of fish and especially oily fish, may lead to increased exposure to HBCD, with consequent bioaccumulation into the organism.

Based on these assumptions, for the first time the possible interactions between DHA and HBCD on gene expression were investigated. In Chapter 4 it was reported that HBCD regulated the expression of genes related to biological processes and diseases, such as calcium homeostasis, hormone activity and neurodegenerative disorders. In Chapter 1 it was also shown that DHA has a protective role against HBCD effects on cell membrane structure and permeability. Therefore, six genes previously found regulated (Chapter 4) and linked to four functions affected by HBCD were selected, and DHA effects on HBCD induced expression of these genes was tested.

The genes selected were linked to neurodegenerative disorders, lipid metabolism, calcium homeostasis and cytoskeleton structure. These functions were chosen not only because target of HBCD toxicity, but also because based on literature it is known that DHA effects are related to these functions. In fact, reduced brain levels of essential PUFA, and especially DHA, have been reported in age-linked neurodegenerative conditions such as Alzheimer disease (AD) (H. Y. Kim 2007), with consequences in loss of synaptic contacts in neurons (Pomponi 2008; Quinn 2006). Also, APP/PS1 transgenic mice fed with diets supplemented with DHA show reduced β -amyloid plaque formation, one of the main causes of AD (Oksman et al. 2006).

There are reports from *in vivo* studies showing that a DHA enriched diet may modify brain lipid composition and susceptibility to oxidative damage (Muntane et al. 2010; W. Zhang et al. 1995). Dalfo et al (Dalfo et al. 2007) also showed that in transgenic mice used as a model for Parkinson's disease, lipid peroxidation was reduced by DHA. Moreover, it has been suggested that DHA affects membrane functions through the maintenance of phosphatidylserine (PS) concentration, one of the main phospholipids components (Bazan 2005; Salem et al. 2001).

Among genes regulated by HBCD in mouse neuronal cells (Chapter 4), there was an overrepresentation of genes with functions related to "lipid and fatty acid synthesis and metabolic processes". It was therefore of interest to investigate the influence of DHA on HBCD induced expression of genes within this category.

Previously studies have demonstrated that DHA has an important trophic function with induction of neurite growth, synapsin, and, particularly of interest for this study, glutamate receptor expression (Cao et al. 2009; H. Y. Kim et al. 2011). In Chapter 4 it was shown that HBCD regulated the gene expression of Homer1, a key protein in the calcium signalling with the main function to connect the glutamate receptors NMDA and mGluR and the voltage gated calcium channel in the postsynaptic membrane with IP3 and RyR in the endoplasmic reticulum (Tu et al. 2002). Considering the known effects of DHA on neuronal function in general and glutamate receptor expression in particular along with the main function of Homer1, the effect of DHA in modulating HBCD regulation of Homer1 expression was investigated.

Cytoskeleton structure was also a function in focus for analysis of DHA modulation of HBCD effects. In Chapter 4 it was reported that HBCD caused preferential regulation of genes with GO terms relating to cytoskeleton structure, including "cytoskeleton

organization” and “actin cytoskeleton organization”. Very little is known about the contribution of DHA in the cytoskeleton structure regulation. Considering that the cytoskeleton is connected to the cellular membrane and that DHA is one of the main components of neuron membrane, it is of interest to study the effect of DHA on the cytoskeleton structure and organization (Hasio et al. 2008).

5.1.3 Chapter objectives

The specific objectives of the study described in this Chapter were to:

- Investigate the effects of HBCD on cellular Zn^{2+} concentration in the neuroblastoma cell line N2A;
- Establish if the mechanisms leading to cellular Zn^{2+} increase involve oxidative stress, and/or activation of the NO pathway;
- Investigate the interactions between the omega-3 fatty acid, DHA, and HBCD on gene expression.

5.2 Methods

All general methods performed in this chapter are described in Chapter 2.

5.3 Results

5.3.1 Intracellular zinc response after exposure of cells to the nitric oxide (NO) donor Nitroprusside.

In order to validate the method used for this analysis and to verify that it could detect a $[Zn^{2+}]$ increase due to oxidative stress, zinc fluorescence detection was preliminarily tested with induction of intracellular zinc release, caused from the nitric oxide (NO) donor, sodium nitroprusside.

N2A cells grown on coverslip and then incubated with the NO donor sodium nitroprusside for 10 or 20 minutes showed little or no increase in $[Zn^{2+}]$. After 45 minutes of exposure, the intracellular concentration of Zn^{2+} significantly increased and was easily detectable with the fluorescence microscope, indicating that the method used

was sensitive enough to detect fluctuations in intracellular $[Zn^{2+}]$, and that the NO donor was reliable positive control for this study (Figure 5.1)

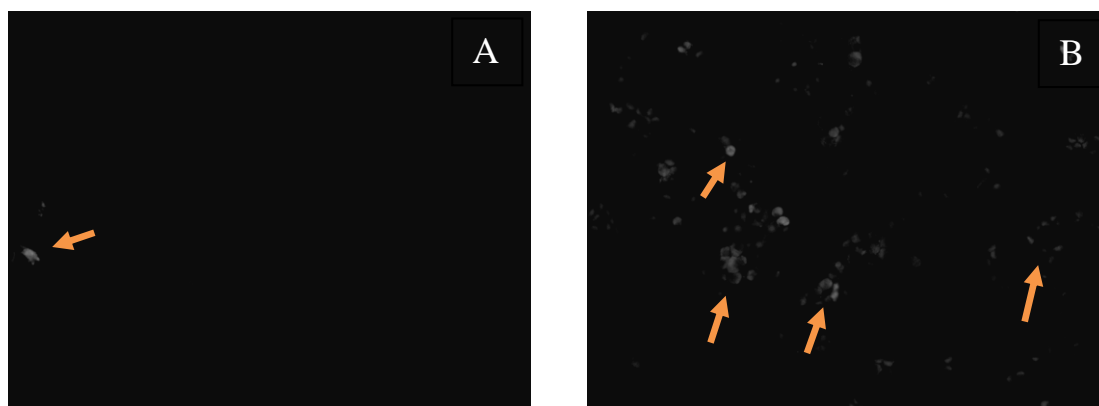


Figure 5.1: Preliminary method validation testing the intracellular zinc detection using the dye, Zynpyr1. N2A cells were grown on coverslips and then incubated for 10 minutes (picture A), 20 minutes (data not shown) or 45 minutes (picture B) with the NO donor nitroprusside to induce intracellular Zn^{2+} release. The fluorescent dye Zynpyr1 was used to detect $[Zn^{2+}]$.

Intracellular zinc release after exposure of cells to the NO donor was also detected using a plate reader to measure the fluorescence of Zynpyr1. N2A cells, cultured in a 96-well tissue plate, were incubated with $10\mu M$ of the NO donor nitroprusside for 24 hours. Like in experiments using the fluorescence microscope, the NO donor was found to significantly ($p < 0.05$) induce a 25% increase in $[Zn^{2+}]$ compared to the DMSO control (Figure 5.2).

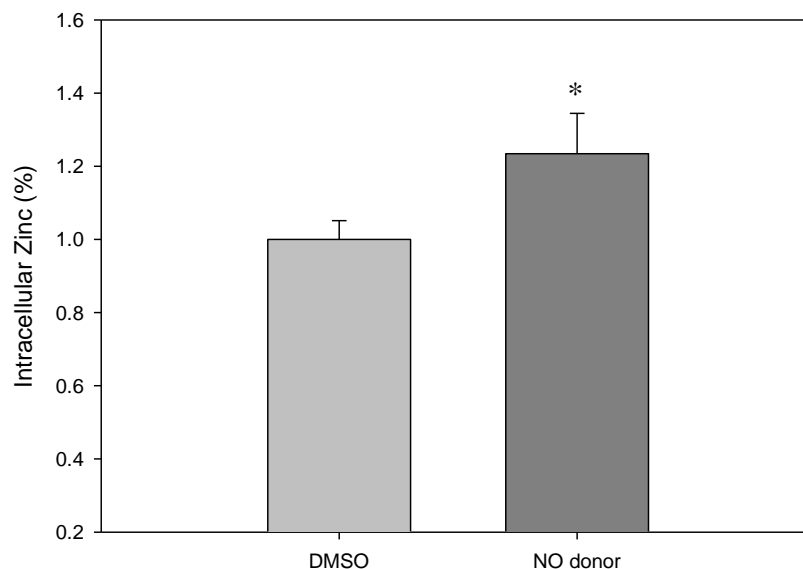


Figure 5.2: Intracellular zinc release in the N2A cell line exposed to a NO donor. Intracellular zinc was detected using the fluorescent dye Zynpyr1. The N2A cell line was incubated for 24h with 10µM of the NO donor nitroprusside. The experiment was repeated 3 times with an n=16 and the average of the measurements is reported. Intracellular Zn²⁺ concentrations are expressed as percentage of the DMSO control. Bars represent standard deviation and the asterisk represents a statistical significance at p<0.05.

5.3.2 Intracellular zinc response after cells exposure to HBCD

Once the detection method for increases in cytosolic [Zn²⁺] was optimized, N2A cells grown on coverslips were incubated with 1, 2, 5 or 10µM of HBCD for 24 hours, and the intracellular [Zn²⁺] was measured with Zinpyr-1. The number of fluorescent cells was divided by the total number of cells in a specific area and, thus, the proportion of fluorescent cells was calculated. Cells were also incubated with the vehicle DMSO as a control, which showed to not have any effect to the intracellular Zn²⁺ concentration (Figure 5.3 A and B).

Cells exposed to the two lower HBCD concentrations, 1 and 2µM, showed a significant release of [Zn²⁺] into the cytosol, with an evident increase in the dye fluorescence as shown in figure 3.12 (picture C, D ,E and F). The higher concentrations of HBCD, 5 and 10µM, didn't cause any significant increase in fluorescence, and therefore in zinc release, compared to the DMSO control. Figure 5.3 (picture G, H, I and J).

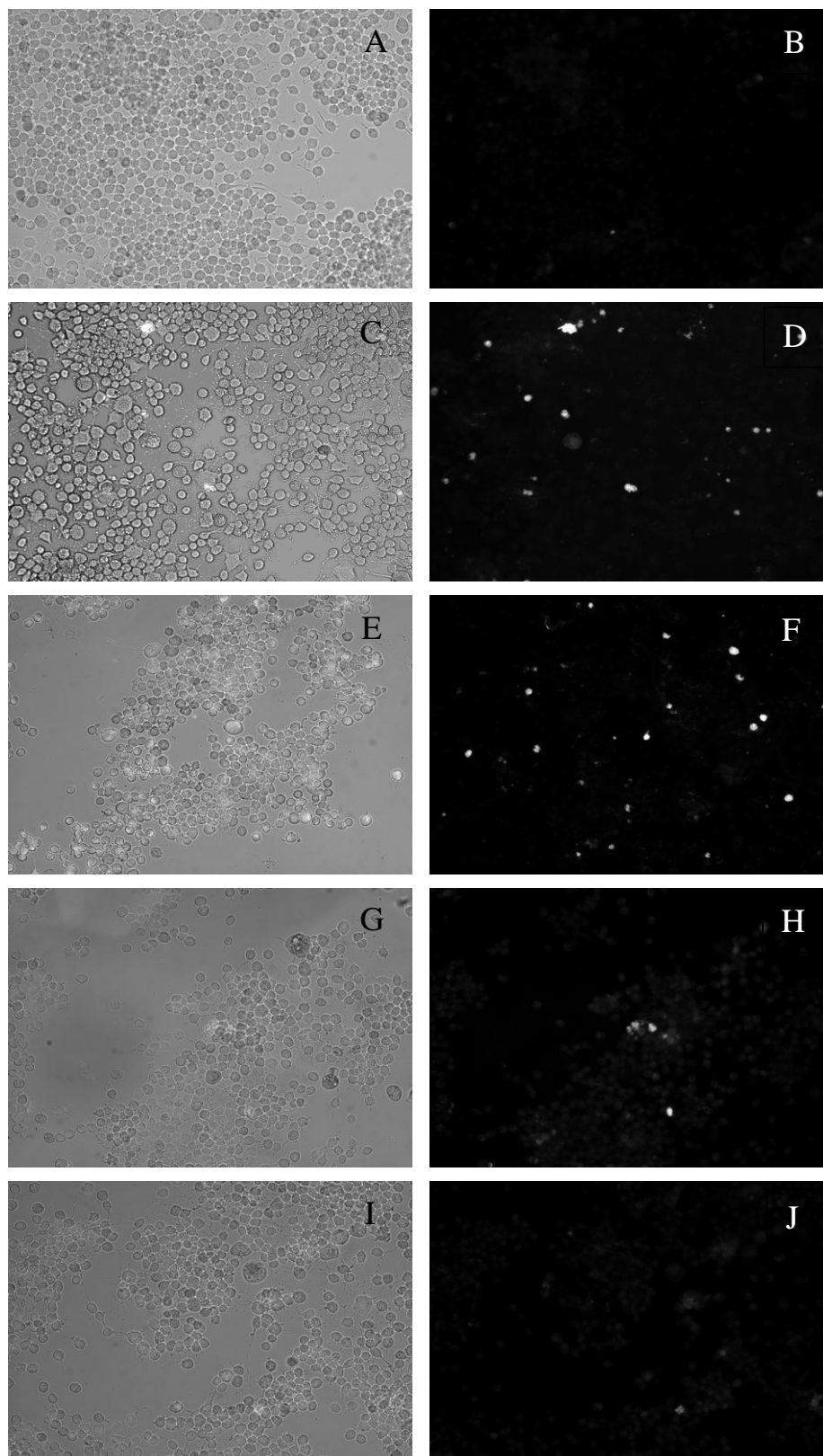


Figure 5.3: Intracellular zinc release detected with the fluorescent dye Zinpyr1. N2A cells were grown on coverslips and then incubated with 1 (Figure C and D), 2 (Figure E and F), 5 (Figure G and H), or 10 μ M (Figure I and J), of HBCD for 24h. Figure A and B show cells exposed to the vehicle DMSO. The fluorescent dye Zinpyr1 was used to detect [Zn²⁺] and the number of fluorescent cells divided by the total number of cells in a specific area. Thus, the proportion of fluorescent cells was calculated. The experiment was repeated 3 times with an n=4 and the average of the measurements is here reported.

A summary of the intracellular zinc release caused by HBCD is represented in the bar chart in Figure 5.4. As previously mentioned, N2A cells exposed to 1 or 2 μ M HBCD showed a significant release of intracellular zinc, but the higher HBCD concentrations, 5 and 10 μ M, didn't have any detectable effect on zinc homeostasis compared to the DMSO control.

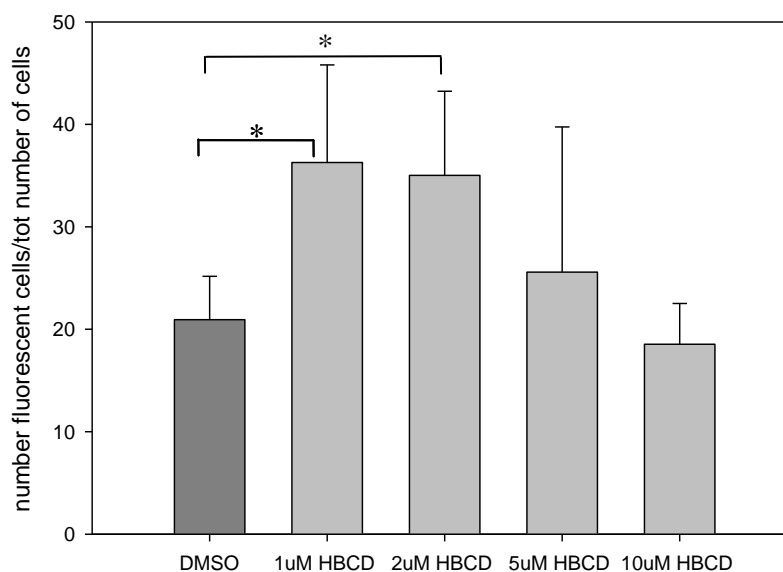


Figure 5.4: Intracellular Zinc in N2A cells exposed to HBCD for 24h. Summary bar chart of the intracellular zinc release in the N2A cell line incubated with 1, 2, 5 or 10 μ M of HBCD for 24h. The fluorescent dye Zynpyr1 was used to detect [Zn²⁺] and the number of fluorescent cells was divided by the total number of cells in a specific area. Thus the proportion of fluorescent cells was calculated. The experiment was repeated 3 times with an n=4 and the average of the measurements is here reported. Bars represent standard deviation and the asterisks represent a significant difference relative to the DMSO control at p<0.05.

A similar assay was repeated with cells cultured in 96-well tissue culture plates. The N2A cell line was exposed to 1, 2, 5 or 10 μ M of HBCD for 24 hours, and the intracellular zinc perturbation investigated measuring the relative [Zn²⁺] in the cells.

Confirming the previous study performed in cells grown on coverslips, cells incubated with 1 or 2 μ M of HBCD showed a significant (p<0.05) increased in intracellular [Zn²⁺] compared to the DMSO control. At the higher concentrations, 5 and 10 μ M, HBCD didn't induce any Zn²⁺ release. Results are reported in Figure 5.5.

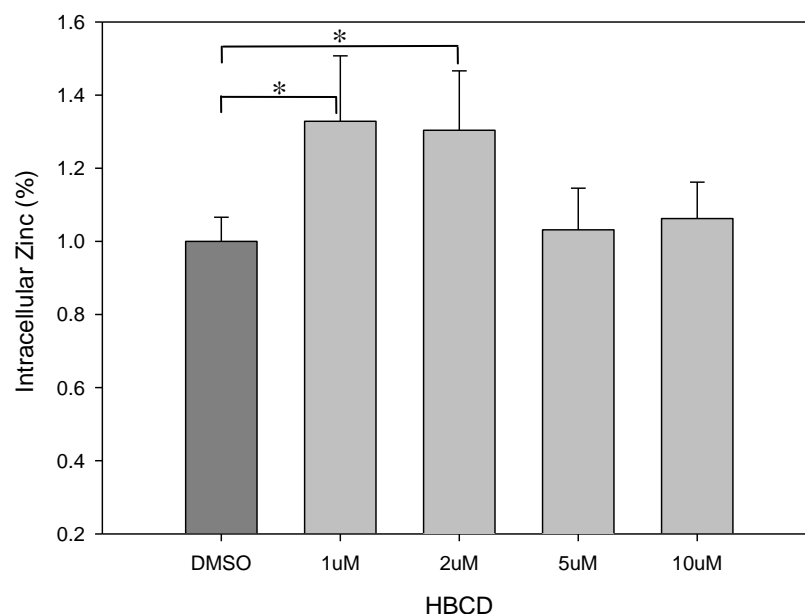


Figure 5.5: Intracellular zinc in N2A cells exposed to HBCD for 24 hours. N2A cells were exposed to 1, 2, 5 or 10 μM of HBCD for 24. Intracellular Zn^{2+} release was detected using the fluorescent dye Zynpyr1 and it is here expressed as percentage of responding cells. The experiment was repeated 3 times with an $n=16$ and the average of the measurements is here reported. Data are expressed as percentage of fluorescence measured in the DMSO control. Bars represent standard deviation and the asterisks represent a significant difference relative to the DMSO control at $p < 0.05$.

5.3.3 Investigation of the mechanism involved in the zinc release caused by HBCD

To confirm that the fluorescence detected in the previous experiment was specifically related to zinc and it was representing a perturbation in intracellular Zn^{2+} concentration, before exposure to HBCD, cells were incubated with the zinc chelator diethyldithiocarbamate (DEDTC). DEDTC is a specific chelator with a high affinity for zinc, able to block vesicular zinc ions in cells (Danscher et al. 1973).

Comparing the effect of HBCD in cells with or without DEDTC, it appeared that DEDTC efficiently chelated the intracellular Zn^{2+} because it abolished the increase in $[\text{Zn}^{2+}]$ caused by 1 μM HBCD. In fact, results reported in figure 5.6 show that the relative $[\text{Zn}^{2+}]$ in cells pre-incubated with DEDTC was lower than in the DMSO control, indicating a chelation of the cellular Zn^{2+} . The effect of HBCD on zinc release were also confirmed with an increase in $[\text{Zn}^{2+}]$ in cells exposed to 1 μM HBCD.

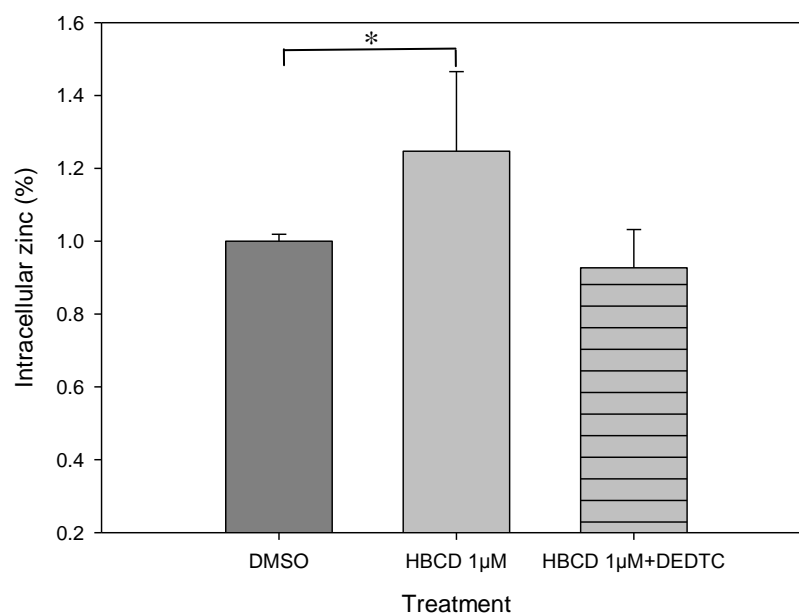


Figure 5.6: Intracellular zinc in the N2A cell line with or without DEDTC. Intracellular Zn^{2+} was detected using the fluorescent dye Zynpyr1. The N2A cell line was incubated for 24h with 1µM HBCD with or without 2 hours pre-incubation with 10µM of the zinc cheletor DEDTC. The experiment was repeated 3 times with an n=16 and the average of the measurements is here reported. Data are expressed as percentage of fluorescence measured in the DMSO control. Bars represent standard deviation and the asterisks represent a significant difference relative to the DMSO control at $p<0.05$

In order to determine if oxidation was the cause of the intracellular zinc perturbation following HBCD exposure, the N2A cell line was incubated for two hours with the antioxidant N-acetylcysteine (NAC) prior to HBCD exposure.

On evaluation of the effect of HBCD in presence or absence of NAC, it was revealed that the antioxidant has the ability to significantly ($p<0.05$) ameliorate the intracellular zinc release elicited by HBCD relatively to the DMSO control as shown in figure 5.7. A negative control exposing cells to HBCD with the zinc cheletor DEDTC was also added and it showed no increase in $[Zn^{2+}]$.

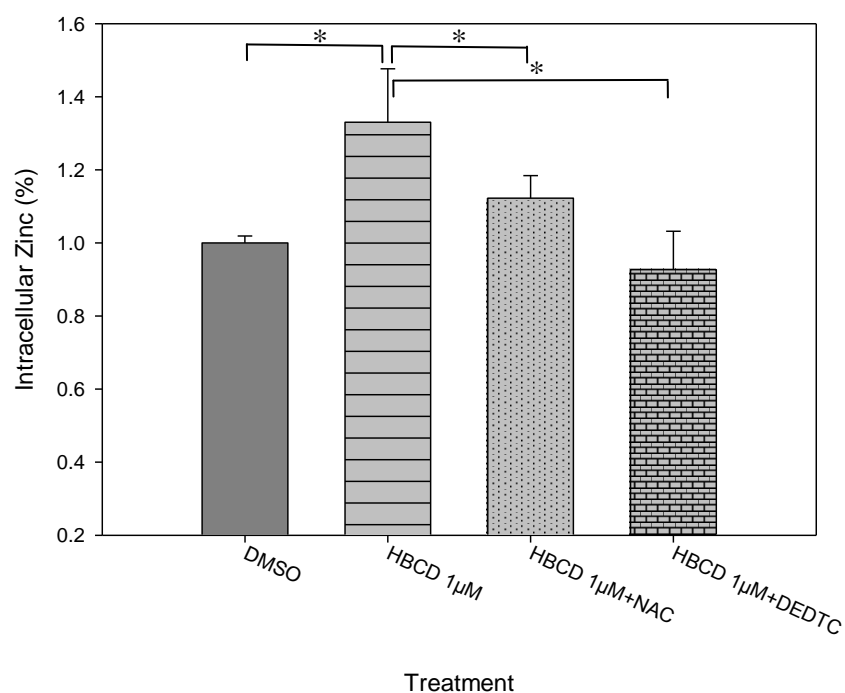


Figure 5.7: Intracellular zinc in the N2A cell line exposed to HBCD with or without NAC. Intracellular Zn^{2+} was measured using the fluorescent dye Zynpyr1. The N2A cell line was incubated for 24 hours with 1 μ M HBCD with or without 2 hours pre-incubation with the antioxidant NAC. The experiment was repeated 3 times with 16 technical replicates at each experiment. Data reported are the averages of values from the three experiments ($N=3$). Data are expressed as percentage of fluorescence measured in the DMSO control. Bars represent standard deviation and the asterisks represent a significant difference at $p<0.05$ relative to the treatment indicated with a bracket.

Considering that the NO pathway activation is one of the main causes of oxidative stress damage in cells, protein and lipids (Chung 2010), the Zn^{2+} concentration in cells exposed to HBCD following treatment with the NO pathway blocker L-NAME was investigated.

Intracellular zinc release was thus measured in N2A cells exposed to HBCD with or without L-NAME. In cells exposed to HBCD only, Zn^{2+} concentration was seen to increase by 35% compared to DMSO control. In cells pre-incubated with the NO pathway blocker for 2 hours, HBCD showed a small, but non-significant increase in the intracellular Zn^{2+} . Comparing the HBCD effect on Zn^{2+} release in cells treated or not with L-NAME, there was not a significant difference between cells treated with the NO pathway blocker and cells not treated, indicating that L-NAME didn't inhibit the release of Zn^{2+} caused by HBCD. A negative control exposing cells to HBCD with the

zinc chelator DEDTC was also added, and it showed a concentration of Zn^{2+} lower than the DMSO control. (Figure 5.8).

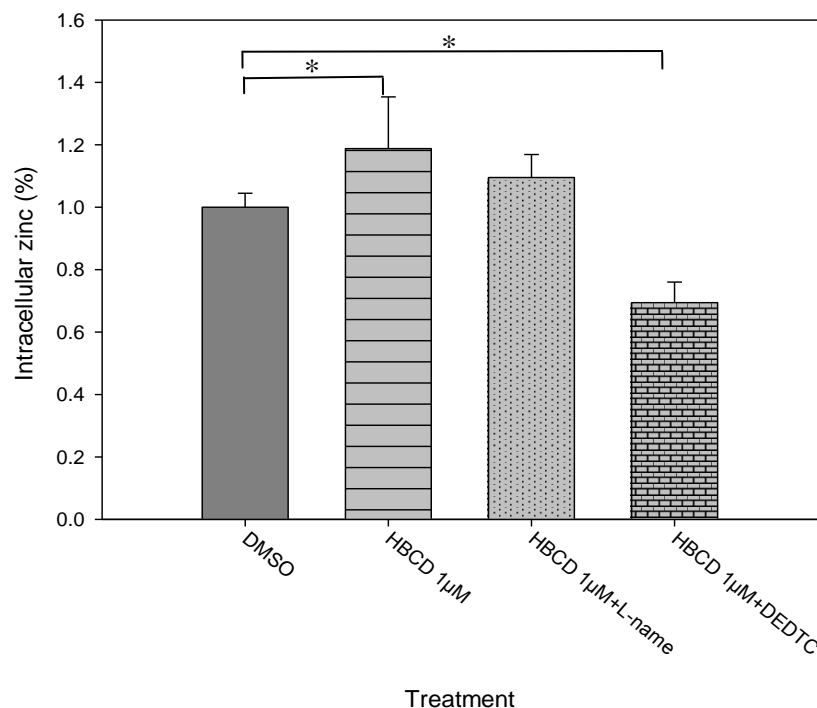


Figure 5.8: Intracellular zinc in the N2A cell line exposed to HBCD with or without L-NAME. Intracellular Zn^{2+} was measured using the fluorescent dye Zynpyr1. The N2A cell line was incubated for 24 hours with 1µM HBCD with or without 2 hours pre-incubation with the NO pathway blocker, L-NAME. The experiment was repeated 3 times with an n=16 and the average of the measurements is here reported. Data are expressed as percentage of fluorescence measured in the DMSO control. Bars represent standard deviation and the asterisks represent a significant difference relative to the DMSO control at $p < 0.05$

5.4 DHA and HBCD interactions on gene expression

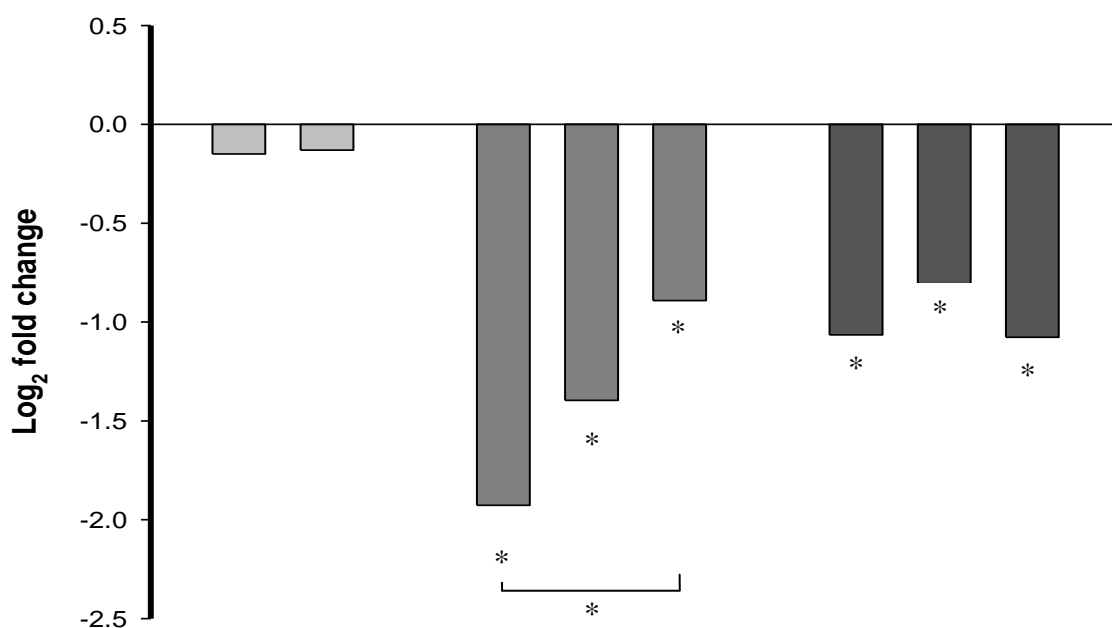
In order to investigate the effect of DHA on the HBCD toxicity, the neuroblastoma N2A cell line was treated for 24 hours with 30 or 90µM of DHA followed by 24 hours exposure to 1 or 2µM of HBCD. A previous study showed that incubating cultured mouse neuronal cells with DHA at a concentration of 90µM results in cellular DHA content between 19 to 24% of the total cellular fatty acids, which correspond to what is present in the brain (Kaur et al. 2008). A control with vehicle-only was also included. To increase DHA solubility and facilitate the cellular uptake, DHA was bound to a Fatty Acid Free-BSA (FAF-BSA). DMSO was used to dissolve HBCD as before. Thus, cells

incubated with FAF-BSA and then exposed to DMSO were used as a control. Differences in gene expressions in this chapter are expressed as \log_2 fold change relative to the control, and since \log_2 fold change of the control is zero, control expression is not shown in the graphs.

DHA treatment significantly altered the expression of all six genes tested (Figs 5.9 – 5.14). However, in contrast to the outcome of the experiment presented in Chapter 4, only one of the genes, *Pnpla8*, responded to HBCD only exposure. Three of the genes selected were previously seen to be regulated with microarray analysis by PBDE-47 in neuroblastoma cells and therefore were not expected to be enriched by HBCD, but the DHA effect on their regulation was nevertheless tested.

Gene expression analysis by Q-PCR showed that DHA alone altered the expression of all these genes tested. In the N2A cell line treated with 30 or 90 μ M of DHA, *Bace1*, *App* and *Hspa5* were significantly down-regulated compared to the control ($p < 0.05$).

Analysis on the *App* gene expression showed that DHA significantly ($p < 0.05$) reduced its mRNA levels at both concentrations tested. The largest effect on the gene expression was seen in cells exposed to 30 μ M of DHA. In this condition, HBCD was seen to affect DHA gene regulation. In fact, *App* down-regulation significantly decreased with the increasing of HBCD concentration ($p < 0.05$), suggesting a stimulation of *App* expression by this toxicant. Among cells treated with 90 μ M of DHA, *App* expression was seen to be down-regulated compared to the control. In this condition, HBCD didn't cause any effect on DHA gene regulation, and *App* expression was constant among the different HBCD treatment. As mentioned above, cells exposed to HBCD alone didn't show *App* regulation (Figure 5.9).

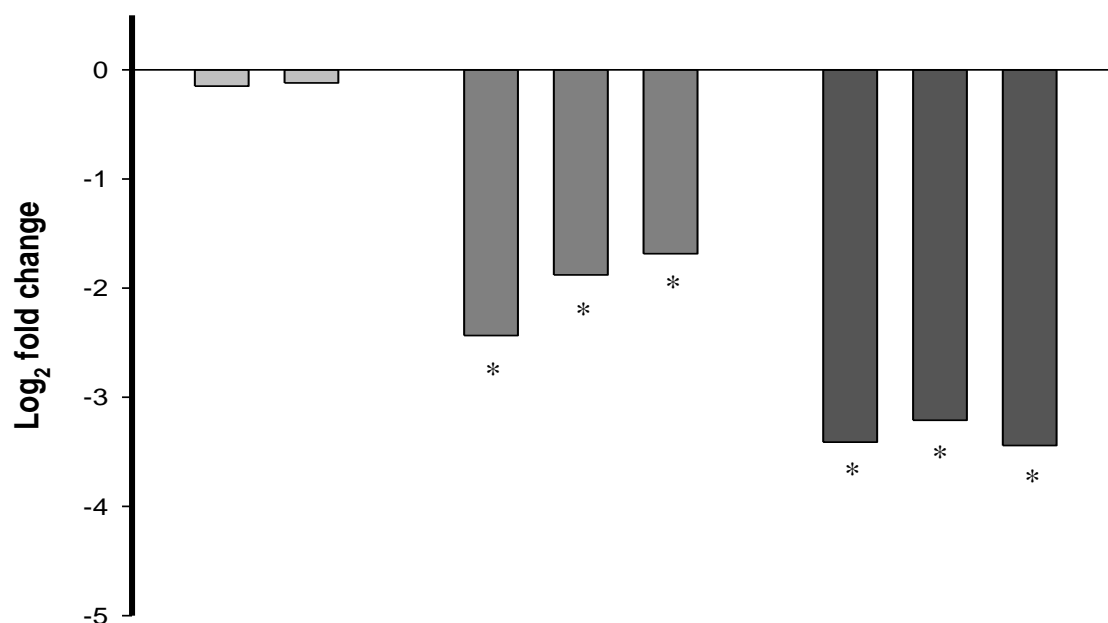


DHA (μM)	0	0		30	30	30		90	90	90
HBCD (μM)	1	2		0	1	2		0	1	2

Figure 5.9: DHA and HBCD interactions on expression of the *App* gene. N2A cells were treated with 30 or 90μM of the fatty acid DHA for 24 hours, washed in medium and then exposed to 1 or 2μM of HBCD. Gene expression was investigated by Q-PCR and reported as log₂ fold change values. Fold changes were calculated comparing expression values of the treated samples to the vehicle-only control (BSA and DMSO), which has assumed log₂ fold change=0 (not shown). The experiment was conducted with n=6. In the figure asterisk represents significant different gene expression compared to the control with a p-value <0.05.

As reported in Figure 5.10, DHA caused a down-regulation of the expression of the gene *Bace1* in both the concentrations tested. The major effect was reported at the highest concentration 90μM, but significant down-regulation was also present at 30μM. Considering the two DHA concentrations separately, among cells treated with 30μM DHA, the down-regulation of *Bace1* seemed to be slightly reduced with increasing concentrations of HBCD, as observed for *App* gene expression, but the difference was not significant. Among cells exposed to 90μM of DHA, HBCD didn't cause any

variation in *Bace1* expression. Cells exposure to HBCD alone also didn't affect the expression of *Bace1*, contrary to what seen in microarray analysis reported in Chapter4.

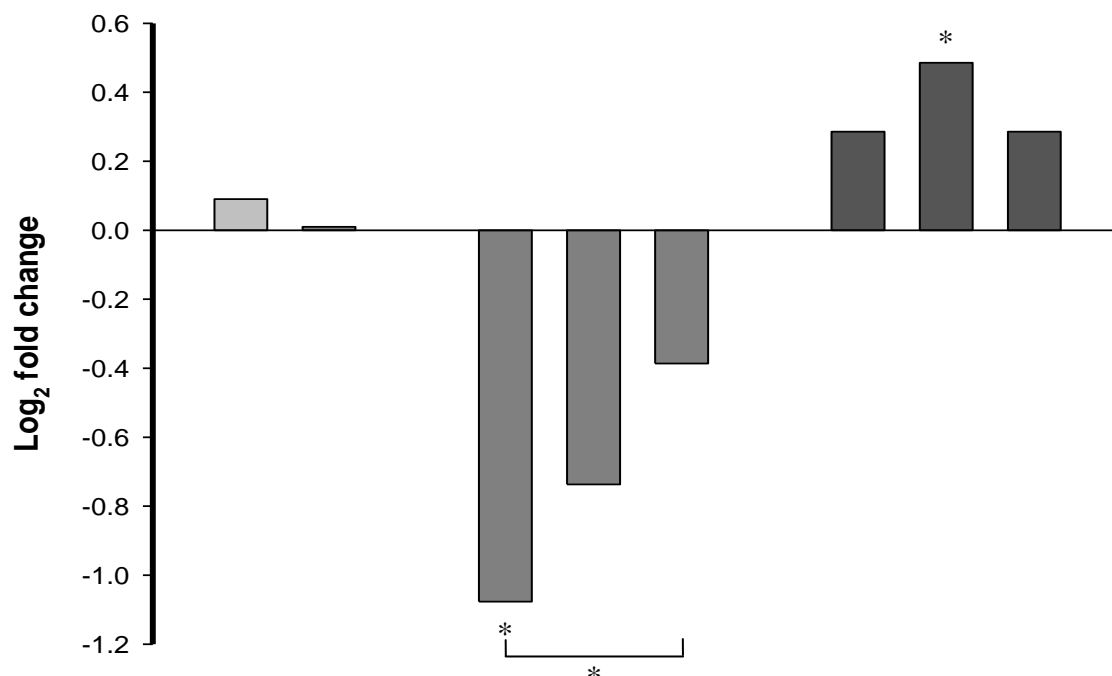


DHA (μM)	0	0		30	30	30		90	90	90
HBCD (μM)	1	2		0	1	2		0	1	2

Figure 5.10: DHA and HBCD interactions on expression of the *Bace1* gene. N2A cells were treated with 30 or 90μM of the fatty acid DHA for 24 hours, washed in medium and then exposed to 1 or 2μM of HBCD. Gene expression was investigated by Q-PCR and reported as log₂ fold change values. Fold changes were calculated comparing expression values of the treated samples to the vehicle-only control (BSA and DMSO), which has assumed log₂ fold change=0 (not shown). The experiment was conducted with n=6. In the figure asterisk represents significant different gene expression compared to the control with a p-value <0.05.

The *Hspa5* gene was also seen to be regulated in cells exposed to DHA. At the concentration of 30μM, DHA caused a significant decrease (p>0.05) in the *Hspa5* expression, but only in cells not treated with HBCD. In contrast, in cells treated with 30μM of DHA and then exposed to 1 or 2μM of HBCD, the toxicant stimulated *Hspa5* expression. In fact *Hspa5* expression in cells exposed to DHA only was significantly down-regulated compared to cells exposed to DHA and 2μM of HBCD. DHA at the concentration of 90μM caused a slight up-regulation of *Hspa5*. This regulation was

found significant in cells exposed to DHA and to 1 μM of HBCD ($p > 0.05$) but not in the cells exposed to DHA only or cells exposed to DHA and to 2 μM of HBCD. HBCD alone only didn't show any regulation in *Hspa5* expression (Figure 5.11).

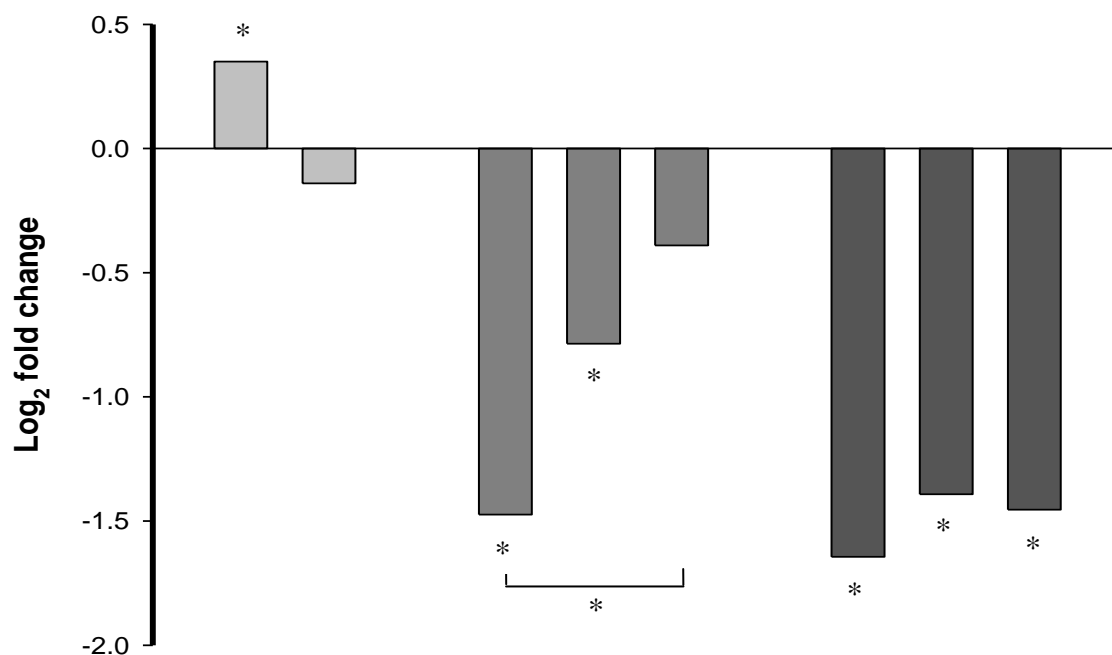


DHA (μM)	0	0		30	30	30		90	90	90
HBCD (μM)	1	2		0	1	2		0	1	2

Figure 5.11: DHA and HBCD interactions on expression of the *Hspa5* gene. N2A cells were treated with 30 or 90 μM of the fatty acid DHA for 24 hours, washed in medium and then exposed to 1 or 2 μM of HBCD. Gene expression was investigated by Q-PCR and reported as log₂ fold change values. Fold changes were calculated comparing expression values of the treated samples to the vehicle-only control (BSA and DMSO), which has assumed log₂ fold change=0 (not shown). The experiment was conducted with $n=6$. In the figure asterisk represents significant different gene expression compared to the control with a p -value < 0.05 .

The gene involved in lipid metabolism and signalling *Pnpla8* (patatin-like phospholipase) was also tested in the N2A cell line for DHA responsiveness. As shown in figure 5.12, DHA exposure down-regulated *Pnpla8* expression. In cells treated with 30 μM of DHA only, there was a significant ($p < 0.05$) down-regulation in *Pnpla8* expression. HBCD (1 μM) stimulated *Pnpla8* expression, and cells exposed to both 30 μM DHA and 2 μM HBCD *Pnpla8* expression was not seen significantly regulated

compared to the control. In addition, there was a significant difference between cells treated with DHA only and cells treated with DHA and 2 μ M of HBCD. Cell exposed to 90 μ M of DHA showed a clear down-regulation in *Pnpla8* expression and HBCD didn't seem to influence DHA effects at this concentration. HBCD alone caused an up-regulation in cells exposed to 1 μ M, but it didn't influence *Pnpla8* expression in cells exposed to 2 μ M. (Figure 5.12).

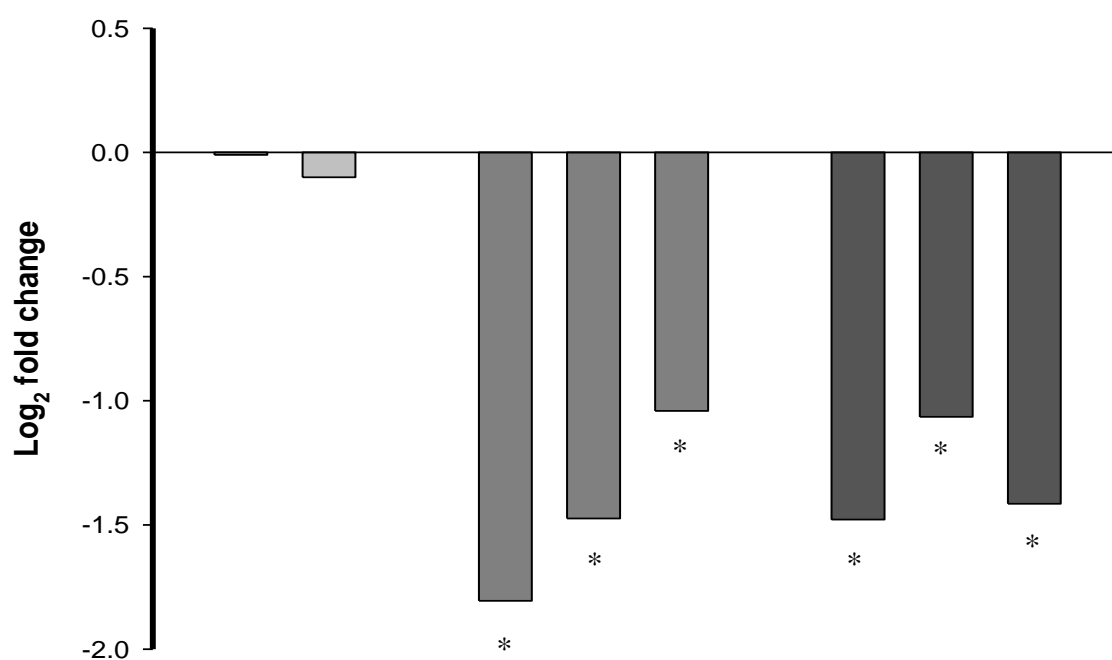


DHA (μ M)	0	0		30	30	30		90	90	90
HBCD (μ M)	1	2		0	1	2		0	1	2

Figure 5.12: DHA and HBCD interactions on expression of the *Pnpla8* gene. N2A cells were treated with 30 or 90 μ M of the fatty acid DHA for 24 hours, washed in medium and then exposed to 1 or 2 μ M of HBCD. Gene expression was investigated by Q-PCR and reported as log₂ fold change values. Fold changes were calculated comparing expression values of the treated samples to the vehicle-only control (BSA and DMSO), which has assumed log₂ fold change=0 (not shown). The experiment was conducted with n=6. In the figure asterisk represents significant different gene expression compared to the control with a p-value <0.05.

The function “calcium homeostasis” was also selected as possible target of DHA ameliorative effects, and the expression of a key gene in cellular calcium signalling, *Homer1*, was tested after DHA treatment and HBCD exposure. As reported in figure

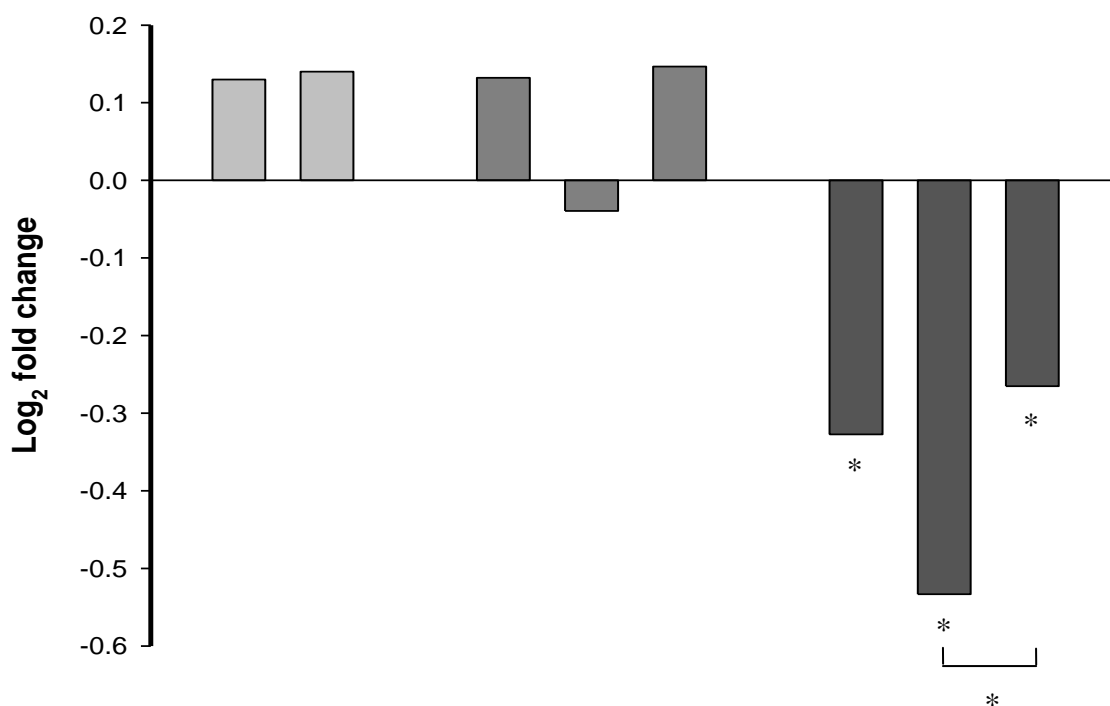
5.13 DHA caused significant ($p < 0.05$) down-regulation of the gene at both concentrations tested. In cells exposed to $30\mu\text{M}$ of DHA, HBCD had the tendency to dampen the effect of DHA on *Homer1* expression, although the difference between cells treated with DHA and exposed or not exposed to HBCD was not significant ($p = 0.068$). In cells exposed to $90\mu\text{M}$ of DHA, *Homer1* was significantly ($p < 0.05$) down-regulated by the fatty acid, and no difference in the gene expression was reported among the different HBCD treatments. HBCD also did not show any effect in *Homer1* expression in cells exposed to the toxicant only (Figure 5.13).



DHA (μM)	0	0		30	30	30		90	90	90
HBCD (μM)	1	2		0	1	2		0	1	2

Figure 5.13: DHA and HBCD interactions on expression of the *Homer1* gene. N2A cells were treated with 30 or $90\mu\text{M}$ of the fatty acid DHA for 24 hours, washed in medium and then exposed to 1 or $2\mu\text{M}$ of HBCD. Gene expression was investigated by Q-PCR and reported as \log_2 fold change values. Fold changes were calculated comparing expression values of the treated samples to the vehicle-only control (BSA and DMSO), which has assumed \log_2 fold change = 0 (not shown). The experiment was conducted with $n = 6$. In the figure asterisk represents significant different gene expression compared to the control with a p -value < 0.05 .

The gene related to cytoskeleton regulation *Tubb2c* (tubulin, beta 2C) was selected as a potential target of the DHA effects. Among the two DHA concentrations used, 30 μ M showed a slightly but not significant up-regulation in *Tubb2c* expression, with the exception for cells also exposed to 1 μ M of HBCD. In cells treated with 90 μ M of DHA, *Tubb2c* was significantly down-regulated. In the same condition, HBCD at the concentration of 2 μ M seemed to further affect *Tubb2c* down-regulation. Cells exposed to 1 μ M or 2 μ M of HBCD were significantly different in *Tubb2c* expression, but not different from cells exposed to 90 μ M of DHA only. HBCD alone did not significantly affect *Tubb2c* expression (Figure 5.14), contrary to what reported in transcriptomic study in Chapter 4.



DHA (μ M)	0	0		30	30	30		90	90	90
HBCD (μ M)	1	2		0	1	2		0	1	2

Figure 5.14: DHA and HBCD interactions on expression of the *Tubb2c* gene. N2A cells were treated with 30 or 90 μ M of the fatty acid DHA for 24 hours, washed in medium and then exposed to 1 or 2 μ M of HBCD. Gene expression was investigated by Q-PCR and reported as log₂ fold change values. Fold changes were calculated comparing expression values of the treated samples to the vehicle-only control (BSA and DMSO), which has assumed log₂ fold change=0 (not shown). The experiment was conducted with n=6. In the figure asterisk represents significant different gene expression compared to the control with a p-value <0.05.

5.5 Chapter discussion

In the present study targeted analysis were conducted in order to better interrogate the HBCD effects revealed by the genomic approach (Chapter 4). For the first time we showed that HBCD exposure increases the intracellular Zn^{2+} concentration in neuronal cells. We also established that the fatty acid DHA regulates genes previously seen to be regulated by HBCD or PBDE-47, and also that it can ameliorate the cytotoxicity caused by these toxicants.

5.5.1 HBCD effects on zinc homeostasis

In this Chapter, evidence is presented that perturbation of cellular zinc homeostasis can be elicited by exposure to a POP. Specifically, it was found that HBCD exposure of N2A cells causes an increase in the concentration of intracellular Zn^{2+} . It has recently been discovered that Zn^{2+} is a second messenger that is involved in regulation of various cellular events and participates in several signalling pathways, including BMP/TGF- β , PKC, AKT/GSK-3 β , and G-coupled receptor-mediated cAMP-CREB signalling (Fukada and Kambe 2011; Hogstrand et al. 2009; Yamasaki et al. 2007a). It is therefore possible that disruption of zinc signalling could significantly contribute to phenotypical effects observed during exposure to HBCD and possibly also other POPs.

Increased concentrations of intracellular Zn^{2+} may promote neuronal death by inhibiting cellular energy production, increasing cellular reactive oxygen species (ROS), changing the mitochondrial membrane potential, and reducing cellular ATP levels (Y. Li et al. 2010). Apoptosis in cortical cell culture induced by high concentrations of zinc has been previously reported (E. Y. Kim et al. 1999). Elevated levels of zinc may also induce cell death through inhibition of energy metabolism (Sheline et al. 2000). In fact a target for zinc toxicity is the mitochondrial respiration chain, with evidence that zinc dissipates the mitochondrial membrane potential (Dineley et al. 2003; Dineley et al. 2005). Zinc is also implicated in the pathogenesis of numerous neurological diseases such as Alzheimer's disease (AD). In patients with AD, accumulation of zinc in amyloid plaques has been detected and a role in the amyloid- β protein aggregation suggested (Bitanirwe and Cunningham 2009).

There are several possible explanations for the observed increase in cellular $[Zn^{2+}]$ upon HBCD exposure. (1) HBCD has been shown to generate reactive oxygen species

(ROS), which could cause zinc release from proteins, such as MT; (2) damage to plasma- or organelle-membranes could lead to increase diffusion of zinc into the cytosolic space; and (3) zinc influx into the cytosol could be stimulated as a secondary consequence of calcium disruption.

The increasing in intracellular $[Zn^{2+}]$ observed in cells exposure to HBCD could be a consequence of the oxidative stress caused by the toxicant with release of zinc from oxidized Zn^{2+} -binding proteins (Kroncke et al. 1994) and particularly from the main zinc storing protein metallothionein (MT) (Maret 2009; Spahl et al. 2003). In normal conditions total cellular zinc concentrations are a few hundred micromolar. Most zinc is bound to proteins with high affinity; therefore, the concentrations of cellular free Zn^{2+} ions are very low. Estimates put them in the picomolar range, but higher concentrations (up to 10nM) can occur during zinc signalling events or when oxidative stress releases zinc from proteins (Y. Li et al. 2010). Thus, exposing cells to oxidizing agents increases cellular free Zn^{2+} ion concentrations (St Croix et al. 2002; Turan et al. 1997).

HBCD effects on inducing oxidative stress have been previously reported. In a study on zebrafish embryos, HBCD was shown to cause oxidative stress and lipid peroxidation starting at the concentration of 0.1mg/L (0.16 μ M) (Hu et al. 2009). An *in vitro* study on Hep G2 cells confirmed that HBCD can induce the formation of reactive oxygen species (ROS) and lipid peroxidation with release of LDH enzyme at concentration as low as 0.5 μ g/mL (0.8 μ M) (X. L. Zhang et al. 2008).

The hypothesis that HBCD can cause oxidative stress with consequential $[Zn^{2+}]$ release was directly investigated with the use of the antioxidant N-acetylcysteine (NAC). NAC is an acetylated cysteine residue popular in experiments for its ability to minimize oxidative stress. The main role of NAC is the glutathione maintenance and metabolism because, as a source of cysteine, it is a substrate for biosynthesis of reduced glutathione (Kerksick and Willoughby 2005). Glutathione is itself the most abundant antioxidant in the cell and is able to minimize the damage caused by oxidative stress (Kerksick and Willoughby 2005). NAC is also used for other functions such as anti-inflammatory activity due to its ability to inhibit the transcription of the interleukin-6 (IL-6) and IL-8, or regulation of cell survival and apoptosis (De Flora et al. 2001).

Cells treated with NAC before being exposed to HBCD, did not show any significant increase in the intracellular $[Zn^{2+}]$, contrary to what was observed in cells not treated with the antioxidant, but instead exposed to HBCD only. The ability of NAC to mitigate

the HBCD cytotoxic effects on $[Zn^{2+}]$ is an indication that oxidative stress may be a cause of the $[Zn^{2+}]$ increase caused by HBCD. As both glutathione and its precursor NAC bind zinc, it could be argued that the observed effect was solely due to zinc chelation. However, while they possibly could influence the zinc-binding capacity of cells, reactive oxygen and nitrogen species would be able to dissociate zinc from these molecules, just as they do from MT.

Oxidative stress can also lead to lipid peroxidation and membrane integrity damage. A relation between lipid peroxidation and reactive oxygen species has been suggested before (Popova and Popov 2002). The peroxidative degradation of polyunsaturated fatty acids has been also found to produce changes in the fluidity of membranes and in other membrane functions (Popova and Popov 2002).

Recently it has been reported that the endoplasmic reticulum (ER) and mitochondria are essential stores for zinc (Sensi et al. 2003; Stork and Li 2010). Stork and Li showed that neuronal cells maintain a substantial concentration of zinc in ER-like storage, and zinc is released into the cytosol in an IP_3 -dependent manner (Stork and Li 2010). Mitochondria constitute another site of intracellular zinc sequestration. In previous studies it has been shown that, on strong cytosolic loading, zinc is taken up into these organelles, from which it can be subsequently released in a Ca^{2+} dependent manner (Sensi et al. 2003). Therefore, oxidative stress, or plasma- or organelle-membranes damage caused by lipid peroxidation, could also lead to diffusion of zinc into the cytosolic space.

Another mechanism that may play a role in the $[Zn^{2+}]$ increase caused by HBCD is related to the calcium-dependent release of zinc from cellular organellar stores. Yamasaki et al demonstrated that antigen binding to the high affinity IgE receptor in mast cells, can induce a release of free zinc from what appeared to be the ER, a phenomenon that has been called 'zinc wave'. In the same study it was shown that the zinc wave was dependent on calcium influx, and therefore it was suggested that zinc can act as an intracellular second messenger in a calcium-dependent manner. However, it was proved that calcium influx alone was not sufficient to induce the zinc wave, but that it also needed the activation of the MAPK/extracellular signal-regulated kinase (MEK) (Yamasaki et al. 2007a). In addition, it has previously been suggested that zinc can act as neuromodulator with an important role in the regulation of the excitability of the brain through its effect on voltage-gated calcium channels (Bitanhirwe and Cunningham 2009; Smart et al. 2004). Consequently, it can be suggested that calcium

has a fundamental role in zinc regulation, and eventually effects on calcium homeostasis caused by HBCD could lead to zinc activity disruption.

Very little is known about the effects of HBCD on calcium homeostasis and not many studies have been conducted on this subject. Calcium concentration disruption caused by HBCD has not been reported *per se*, but a study on PC12 cells showed that low concentrations of HBCD (2-20 μ M) can cause a dose-dependent reduction of a subsequent depolarization-evoked increase in calcium concentration (M. M. L. Dingemans et al. 2009). Further studies are needed to establish if any effect of HBCD on calcium regulation occurs upstream or downstream of the Zn^{2+} release observed in the present study.

In the light of the results obtained from the present study, activation of the NO pathway as a mechanism of oxidative stress caused by HBCD was hypothesised. The activation of the NO pathway is one of the main causes of oxidative stress damage in cells, especially to protein and lipids. In the brain, it has been shown that NO imbalance can cause protein nitration, lipid peroxidation and DNA damage (Chung 2010). It also has been proved to cause protein S-nitrosylation with damage to pro-survival and pro-death proteins (Chung 2010).

In order to inspect if HBCD effects on oxidative stress and therefore in zinc release were induced by activation of the NO pathway, the NO pathway blocker L-NAME was used to investigate if NO pathway inhibition could prevent the effect of HBCD on zinc release. L-NAME has the ability to block the NO pathway, thereby inhibiting the enzyme, inducible nitric oxide synthase (iNOS), the main catalyse responsible for the production of nitric oxide from L-arginine (Coskun et al. 2005). Cells incubated with L-NAME before exposure to HBCD showed a small but not significant decrease in zinc release compared to what was measured in cells exposed to HBCD only, indicating just a partial ameliorative effect on the HBCD induced zinc release. The mild effect of L-NAME on zinc release indicates that NO pathway activation may be one, but likely not the only pathway through which HBCD affects zinc homeostasis. Thus, further studies are needed to elucidate the exact mechanism of action of HBCD in $[Zn^{2+}]$ perturbation.

5.5.2 DHA effect on the gene expression

In this Chapter, we established that the fatty acid DHA regulates genes that were seen enriched by HBCD or by PBDE-47 in transcriptomics analysis conducted in the present work, and that HBCD can modulate the DHA effect on gene expression.

DHA effects on genes regulated by HBCD or PBDE-47 were investigated because one of the main sources of POPs for adults is via fish consumption (H. Y. Kim 2007), but in the other hand, fish is reached in nutrients, such as the fatty acid DHA, which are important for brain functions and growth (Bazan 2005). This consideration raised concern about the benefits and risks related to fish consumption, and it is for this reason that for the first time the effects of DHA on PBDE-47 and on HBCD toxicity targets have been investigated. DHA positive effects, especially in coronary heart disease prevention and in neurodevelopment are already known (Cohen et al. 2005; Mozaffarian and Rimm 2006). In literature, there are studies comparing positive effects of DHA and negative effects caused by POPs exposure (Mozaffarian and Rimm 2006; Rylander et al. 2009), but this is the first time that DHA effects are evaluated on the expression of genes regulated by HBCD or by PBDE-47.

One of the objectives of this present study was to investigate the capacity of DHA to ameliorate the gene expression deregulation caused by HBCD. However, in the light of the results we attained, we could not clearly established if DHA has the ability to modulate HBCD toxicity, as analysis failed to reproduce the effects of HBCD on the expression of most of the genes selected. Therefore, we could only established that DHA affects the expression of genes regulated by HBCD or PBDE-47, but to better understand the modulation of DHA on the two toxicants on gene expression regulation, further studies are needed.

The main reason why in this second study HBCD did not regulate the expression of most of the genes tested, is because in the previous study (Chapter 4), some of the genes were seen to be regulated by PBDE-47 or by HBCD in the NSC19 cell line rather than in the N2A cell line. However, we preceded selecting genes regulated by both the toxicants as our approach was in first place to investigate the effect of DHA on the expression of genes regulated by both the toxicants, and in second place to access the eventual modulation on DHA in both HBCD and PBDE-47 toxicity. The ability of DHA to modulate PBDE-47 toxicity was not been accessed because of time considerations. In addition, we need also to consider that gene expression may vary at

different time points as a consequence of cellular compensatory mechanisms, therefore the failure on the detection of HBCD effects on gene expression may be a consequence of this mechanism.

In the present study, among the functions preferentially regulated by HBCD or by PBDE in the microarray analysis reported in Chapter 4, four functions were selected as targets to investigate influence of DHA on gene expression. Based on previous publication, it is known that DHA has an important role in neuroprotection, in brain lipid regulation, and in trophic function and membrane structure (Bazan 2005; Muntane et al. 2010). Thus, among the GO annotation enriched by HBCD or PBDE-47 in microarray analysis, the effects of DHA were assessed on the expression of six genes related to neurodegenerative disorders, lipid metabolism, calcium homeostasis and cytoskeleton structure.

The direct effect of DHA on the expression of these genes was assessed, and in order to investigate the ability of this fatty acid to modify HBCD induced gene regulation, DHA effects on mRNA abundances were investigated also in cells exposed to HBCD. With the exception of the gene, *Pnpla8*, which was seen to be up-regulated in HBCD exposed cells, HBCD did not alter the expression of the genes exposed to the toxicant only. Furthermore, the ability of these two toxicant to regulate the expression of the genes in consideration was also confirmed in an *in vivo* animal trial conducted in our laboratory (Carroll 2011; Rasinger 2011).

5.5.2.1 DHA effect in neurodegenerative disorders

In the present study, we showed that DHA can affect the expression of genes related to neurodegenerative disorders previously seen regulated by HBCD or PBDE-47. DHA caused effect on the expression of the chaperone *Hspa5* gene encoding a protein involved in the unfolded protein reponse (UPR) and responsible for the prevention of partially folded proteins accumulation in the ER, and for maintenance of the ER functions itself (Lee 2005). DHA was seen to affect *Hspa5* expression in a complex manner. At the lower concentration (30 μ M), DHA down-regulated the chaperone *Hspa5*, but at the higher concentration (90 μ M), the fatty acid was seen to stimulate the expression of *Hspa5*. The reason of this opposite effect is not clear, not is the mechanism causing *Hspa5* down-regulation at the lower DHA concentration. However, DHA at the higher concentration stimulated *Hspa5* expression, suggesting that at this

concentration, DHA plays a protective role against misfolded protein accumulation and ER malfunctioning, which has been previously associated with neurodegenerative disorders such as Alzheimer's (AD) and Parkinson's disease (PD) (Lee 2005), and which can induce apoptosis (Hsu et al. 2008). An alternative explanation would be that at 90µM DHA, UPR might have been activated and *Hspa5* induced as a part of this response. However, this explanation might be questionable because N2A cells showed no direct signs of cytotoxicity in response to 90µM DHA.

In this present study it was not possible to conclude if DHA plays a protective role against HBCD toxicity, as the exposure to the toxicant alone, did not regulate *Hspa5* expression. Therefore, we could not establish an effect of DHA on the gene regulation caused by HBCD.

DHA was also seen to significantly down-regulate the expression of two genes closely associated with Alzheimer's disease (AD), *App* and *Bace1*, at both concentrations used. In this study, HBCD did not affect the expression of these two genes, making it impossible to clarify if DHA can ameliorate adverse effects caused by the toxicant. However, in the transcriptomics analysis reported in Chapter 4, PBDE-47 or HBCD were seen to stimulate the expression of *App* and *Bace1*, regulating the gene expression in the opposite way comparing to HBCD. This might be suggestive of a protective effect of this fatty acid against the natural aging process and also against POPs toxicity. In fact, APP and BACE1 are responsible for the formation and accumulation of amyloid-beta peptide (A β) in brain of AD patients and this is considered to be one of the main causes of the condition (X. Luo and Yan 2010; McConlogue et al. 2007). Thus, the down-regulation of *App* and *Base1* has the potential to abolish the production of A β and its accumulation in brain (Espeseth et al. 2004; X. Luo and Yan 2010), and therefore to decelerate the process of neurodegeneration.

5.5.2.2 DHA effect in lipid metabolism

Investigation of the effect of DHA in lipid metabolism revealed that this fatty acid regulates the expression of *Pnpla8*, a gene of importance for membrane integrity, lipid signalling and regulation of energy homeostasis (Baulande and Langlois). PNPLA8 has also been associated with removal of oxidized fatty acid from biological membrane and decrease lipid peroxidation (Kinsey et al. 2008). Because DHA seems to be a regulator of *Pnpla8* it can be argued that DHA is directly involved with membrane and lipid

maintenance. Previous studies already reported that DHA has effects on lipid metabolism and composition regulation in brain (Muntane et al. 2010; W. Zhang et al. 1995). It is also known that DHA plays an important role in maintenance of cellular membrane functions and in lipid peroxidation protection (Bazan 2005), probably due to its ability to increase reduced glutathione levels and glutathione reductase activity, and suppress the increase in lipid peroxide and reactive oxygen species (Hashimoto et al. 2002). DHA is also the precursor of a biosynthetic product called neuroprotectin D1 (NPD1) which has neuroprotective bioactivity in oxidative stress with the ability to inactivate pro-apoptotic and pro-inflammatory signalling (Kherjee et al. 2007). DHA regulation on *Pnpla8* expression, suggested also that this fatty acid can affect lipid regulation through the direct regulation of gene expression.

In the microarray experiment reported in Chapter 4, it was shown that HBCD affects the regulation of the phospholipase *Pnpla8* with a down-regulation of 2.5 fold change in cells exposed to 1 μ M and of 5 fold change in cells exposed to 2 μ M. Unexpectedly, in the present Q-PCR study, HBCD was seen to up-regulate *Pnpla8* expression in cells exposed to HBCD only, and also in the group treated with 30 μ M of DHA (Figure 5.12). What is more, DHA alone down-regulated the expression of the gene *Pnpla8* to the same extent to that observed after exposure to HBCD in Chapter 4. Variation of the directionality in the gene expression over time and doses is a well known phenomenon (D. Zheng et al. 2010). Changes in mRNA level are indication of an effect, but the gene expression directionality may vary over time presumably as function of cells trying to establish a new set point. In fact, gene regulation can be influenced by compensatory mechanism or by positive or negative cellular feedback. Gene expression directionality in this specific study has to be interpreted considering that it is concentrated on a single time-point. Thus to better understand the response in gene expression to the exposure to contaminants or nutrients, time-course studies of mRNA levels are needed also along with measurement of protein abundance (D. Zheng et al. 2010).

5.5.2.3 DHA effect in calcium homeostasis

In the present study we established that DHA can regulate the expression of the gene *Homer1*. *Homer1* has a fundamental role for calcium homeostasis maintenance as it acts as a bridge between the glutamate receptors and the VGCC in the postsynaptic membrane, and the IP3 receptor and RyR receptor in the ER (Tu et al. 2002). The ER is

known to be the main cellular calcium storage (Koch 1990) with the function to regulate and maintain the calcium secondary messaging. Thus, *Homer1* plays a main role in calcium signalling, and the DHA effect on its expression suggests the ability of this fatty acid to potentially influence cellular calcium regulation and/or signalling.

In the present study HBCD was not seen to regulate the expression of *Homer1*, contrary to what shown in the transcriptomics analysis reported in Chapter 4 where HBCD was seen to stimulate *Homer1* expression in the NSC19 cell line. Therefore we can not establish the direct effect of DHA on *Homer1* regulation caused by HBCD. However, in the two studies conducted, HBCD and DHA regulated the expression of *Homer1* in the opposite direction, suggesting a potential protective effect of DHA against HBCD toxicity.

We also speculate that the regulation of *Homer1* caused by DHA, could be a secondary consequence of the trophic effect of DHA on the glutamate receptor. In the literature, DHA trophic function with induction of neurite growth, synapsin, and glutamate receptor expression have been previously suggested (H. Y. Kim et al. 2011). Considering that *Homer1* activity is directly linked to the two main glutamate receptors, NMDA and mGluR, the effect of DHA seen on *Homer1* expression may be the secondary effect of the regulation on glutamate receptors.

5.5.2.4 DHA effect in cytoskeleton structure

Investigation of the DHA effect on cytoskeleton function, showed that this fatty acid, at the concentration of 90 μ M, has the ability to regulate *Tubb2c*, the gene for a tubulin that is fundamental for cytoskeleton structure maintenance (Leandro-Garcia et al.). Very little is reported in the literature about the effects of DHA on the cytoskeleton, but it is important to consider that the cytoskeleton is connected to the cell membranes, and DHA is one of the major components of the neuron membrane (Cao et al. 2009). It is also known that tubulin and actin are components of the cytoskeleton which is important in supporting nutrient transport by axons from the neuron cell body to the synapse, in maintaining the shape of the neuron, and in the growth of neurons (Schmitt et al. 1977). Therefore, we may hypothesise an effect of DHA on the cytoskeleton structure and organization through direct interaction with the cellular membrane and through the regulation of *Tubb2c*. In addition, we speculated that DHA may affect genes involved in the neuronal degeneration process in AD patient. In fact, it has been

suggested that neuronal degeneration in AD is in part caused by phosphorylated tau protein, a neuronal microtubule-associated protein and one of the components of the cytoskeleton (Hasio et al. 2008).

In the transcriptomics analysis reported in Chapter 4, PBDE-47 was seen to up-regulate *Tubb2c* expression by at least 2 fold change. In the following Q-PCR analysis, also HBCD slightly (1.12 fold change) but non-significantly up-regulated *Tubb2c* expression ($p=0.135$), therefore we cannot establish if DHA has ameliorative effect on HBCD toxicity, and further studies are needed.

5.6 Chapter conclusion

In the present study, for the first time we established that exposure to HBCD can lead to a rise in cellular free $[Zn^{2+}]$. This means that zinc disruption can be added to the list of potential modes of action of POPs. We also showed that the fatty acid DHA substantially changes the expression of six genes shown (in Chapter 4) to be regulated by PBDE-47 and/or HBCD. These genes represent functionalities that were identified to be among the most affected by PBDE-47 and HBCD (Chapter 4), plausibly explaining the observed decrease in LDH leakage caused by HBCD exposure in Chapter 3. In the present study we could not establish if DHA has ameliorative effect of HBCD toxicity on gene expression, as analysis failed to show regulation on genes expression after exposure to HBCD only.

HBCD exposure was seen to induce an increase in cellular free Zn^{2+} concentration in the N2A cell line at low micromolar concentrations. At higher concentration this perturbation in zinc was not seen probably due to a reduced cellular viability caused by HBCD toxicity. We hypothesised three different mechanisms responsible for the zinc release, which could act together in response to HBCD exposure. We suggested that, considering that HBCD can cause ROS formation with consequential cellular oxidative stress, it can lead to the release of zinc from the damage of Zn^{2+} -binding proteins and especially from the zinc storage protein MT. In support of this hypothesis, the effect of HBCD on zinc release was attenuated (but not abolished) by the antioxidant NAC. HBCD oxidative stress did not seem to involve NO pathway activation, as a pre-exposure with the NO pathway inhibitor L-NAME decreased only slightly the release of zinc caused by HBCD.

Another direct consequence of oxidative stress is lipid peroxidation which can lead to the loss of membrane integrity. HBCD toxicity effects on membrane damage and release of zinc from the zinc cellular stores, such as the ER and mitochondria, was also suggested. Release of zinc in a calcium-dependent manner as a secondary consequence from calcium homeostasis disruption caused by HBCD was also hypothesized.

Experiments of the effect of the fatty acid DHA on gene expression, showed that DHA can regulate genes shown to be regulated also by PBDE-47 or by HBCD in the earlier transcriptomic analysis reported in Chapter 4. Data presented in Chapter 3 also showed that DHA can ameliorate the effects of HBCD toxicity. DHA was seen to have positive effect on regulation of genes related to neurodegeneration. In fact, DHA stimulated expression of a chaperone fundamental in the unfolded protein response, and down-regulated the two main genes responsible for amyloid- β peptide formation and accumulation, one of the main causes of AD. The fatty acid was also seen to affect the expression of genes related to lipid metabolism, and membrane integrity and functions maintenance. DHA showed interaction on the gene *Homer1*, which encode for a protein with a key role in calcium signalling. DHA also affected genes related to cytoskeleton structure probably due to the connection between the cytoskeleton and the cellular membranes to which DHA is one of the major components.

It could be argued that the effects of DHA on gene expression were generally more marked than those of the BFRs. Influence of the diet on genes (Jayashankar et al. 2012) and proteins (Rasinger 2011) expression has been already shown to be more pronounced than what can be caused by some toxicants, even at environmental unrealistic levels. In fact, diet can affect the expression of genes associated with toxic stress in the same scale, or even more, than a toxicant itself.

6. General Discussion

6.1 PBDE-47 and HBCD cytotoxicity

In the present study for the first time we established that the two BFRs, PBDE-47 and HBCD, have the ability to directly affect vital cellular functions, and directly regulate gene expression in cells of neuronal origin. We showed that both of the toxicants can regulate the expression of genes associated with neuronal functions and with neurodegenerative diseases. These findings were confirmed by transcriptomic and proteomic studies in *in vivo* trials conducted in our laboratory, where common genes, or genes and proteins belonging to the same functions, were seen regulated. These results potentially explain the phenotype profile seen in PBDE-47 and HBCD exposed mice, which display spontaneous behaviour derange, and effects on memory and learning (Chou et al. 2010; P. Eriksson et al. 2002; Per Eriksson et al. 2006). We could also suggest that behavioural and systemic effects seen during *in vivo* exposures to PBDE-47 or HBCD are the consequence of direct effects on gene networks, rather than systemic feedback responses. We have also demonstrated that the gene expression regulation and the cytotoxicity caused by the two BFRs, are influenced by the fatty acid DHA, which is particularly abundant in fatty fish. Considering that fish is one of the main sources of BFRs, this finding may have implication on the risks associated with consumption of BFR-contaminated fish. They complicate the toxicological risk assessment, suggesting that BFRs toxicity is dependent on the diet and the nutritional status of the individual. Furthermore, we showed that HBCD exposure can cause increase of free Zn^{2+} in a neuronal cell line, indicating for the first time that zinc is a target of HBCD toxicity, and that zinc disruption is a POP toxicity mechanism.

In this PhD project, initially studies assessing the susceptibility to the two BFRs in two neuroblastoma cell lines, NSC19 and N2A, showed that PBDE-47 and HBCD cause cytotoxicity with cellular viability loss at low micromolar concentrations. EC_{50} was established to be about $4\mu M$ for PBDE-47 and between 5 to $8\mu M$ for HBCD depending on the cell line. EC_{50} seen in the present study is similar to previously reported in rat cerebellar granule cells exposed to the PBDE commercial mixture DE-71 or to HBCD, where the EC_{50} concentrations were about 7 and $3\mu M$ for DE-71 and HBCD respectively (Reistad et al. 2006b). EC_{50} observed in the present study is also comparable to what was previously found for the PCB congener, PCB153 (Mariussen et al. 2002).

Studies on humans on POPs level, reported that PBDE-47 is one of the predominant congeners detected in blood (Qiu et al. 2009). In samples collected from pregnant women living in the US and from their newborn babies, PBDE-47 concentration in the blood was in the average of 0.2nM in the fetal samples, and four time less concentrated in the maternal samples (Qiu et al. 2009). Also the HO-PBDE-47 metabolite detected in human blood taken from children living or working at a municipal waste disposal site in Managua, Nicaragua, was measured at concentration higher than in the US study, but also in the range on nanomolar (450 pmol/g lipid equal to 2nM) (Athanasidou et al. 2008). In comparison to PBDEs, much less information is available on the HBCD concentrations in human tissues (Covaci et al. 2006). One study reports that HBCDs were detected in Norwegian human blood at concentrations of 0.7pM (Covaci et al. 2006). It is therefore evident that the concentrations of the toxicants tested in the present study are at least 500 times higher than those that can be detected in human blood. However, this present study is focused on short-term effects, with the limit that it does not take in consideration the consequences of a long-term exposure, which would be more realistic in nature. In fact, the concentrations of toxicants measured in vivo tend to reflect long term steady state, not short term peaks. Whilst the compounds will sequester in fatty tissue, it is the free concentration that is available for interaction with critical cellular targets, and this will be in equilibrium with the plasma concentration. However, we need to consider that chronic exposure can also lead to a progressive accumulation and biomagnifications of toxicants in target tissues and organs, such as brain, which are difficult to measure in humans, and thus the precise concentration hard to know.

In the present study, the marker of apoptosis, caspase-3, was found to be increased by both of the toxicants at the lowest concentration tested of 1 μ M. Intriguingly, at higher concentrations (8 μ M) no activation of caspase-3 activity was observed, probably caused by a loss of cellular viability and therefore of metabolically active cells. In fact, the MTT assay indicated that PBDE-47 or HBCD can reduce cell viability of 50% at as low concentration as 4-5 μ M. Other explanations, such as onset necrosis or atypical apoptosis could also be considered as possible reasons to justify absence of caspase-3 activity at the highest concentration tested. In fact, Reistad et al already suggested that both the toxicants can induce abnormal apoptosis causing apoptotic cellular morphology and signs of DNA laddering in cells, but not other hallmarks of apoptosis like caspase activity (Reistad et al. 2006a). It is also known that certain causes, such as oxidative

stress or neurotoxins, can induce abnormal apoptosis in the nervous system (Sastry and Rao 2000).

In the present study, HBCD was seen to affect membrane integrity causing LDH leakage at concentrations as low as 1 μ M. This finding suggests that the alteration of membrane functions may be one of the mechanisms of action of the HBCD toxicity. Similar mode of action was observed for PCBs, which were seen to cause disruption of membrane structure and alteration of membrane proteins in cell line (Y. S. Tan et al. 2004b). Membrane damage could have been caused by lipid peroxidation due to the formation of reactive oxygen species (ROS) products. Confirming this hypothesis, a pre-incubation with 30 μ M of the fatty acid DHA was seen to significantly ameliorate the effect of HBCD toxicity with a reduction of the LDH leakage. In fact DHA is known to have the ability to increase the antioxidative defence, to inhibit pro-inflammatory and pro-apoptotic signalling (Hashimoto et al. 2002) and to produce neuroprotectin D1 (NPD1), which it is known to have a neuroprotective bioactivity in oxidative stress (Bazan 2005). These findings are of relevance for the benefit-risk assessment of fish consumption. In fact, fish is one of the major sources of many POPs for humans, but despite this, it is a fundamental source for nutrients important for brain development and functions. Nutrients rich in fish, such as fatty acid or vitamins and minerals, could also have ameliorative effects on the contaminants' toxicity. Because of the beneficial effects, especially associated with omega-3 fatty acid intake, several national and international expert groups have issued intake recommendation concerning number of fish meals per week (Strom et al. 2011). Typically 2–3 fish meals including at least 1 portion of oily fish per week are recommended (Strom et al. 2011). It is apparent that both benefits and risks need to be considered when fish consumption advisories are developed. In fact it is important to encourage fish consumption but at the same time to give advice as a preventive measure to limit intake of toxic agents.

6.2 Gene expression and functional enrichment terms

In this work, for the first time the global gene expression profile and associated functions of two neuroblastoma cell lines exposed to PBDE-47 or to HBCD, was evaluated. In the present study HBCD and PBDE-47 showed similar effects on gene expression regulation, affecting an approximately equal number of genes. Previously *in vivo* studies showed that PBDE and HBCD toxicity is similar (Darnerud 2003b). Oral

LD₅₀ in mice has been reported to be 10 mmol/kg body weight for HBCD (Darnerud 2003b), and in the range of 1-10 mmol/kg body weight for PBDE, depending on the congeners analysed (Darnerud 2003b), indicating that despite HBCD seems to have a greater influence on gene expression, the two toxicants toxicity do not substantially differ.

In the present study, despite the fact that approximately the 10% of the genes regulated were shared between the two toxicants, Gene Ontology (GO) analysis showed that some biological functions were affected by both PBDE-47 and HBCD, indicating that the two toxicants have similar regulatory effect but also that they can influence distinct functions.

An effect observed for both PBDE-47 and HBCD was related to neurodegenerative disorders. In previous *in vivo* studies both of the toxicant were seen to affect neurological functions especially memory and learning (Per Eriksson et al. 2006; Kuriyama et al. 2005) and to cause alteration in spontaneous behaviour (Per Eriksson et al. 2006; Viberg et al. 2003c). In our laboratory, a parallel *in vivo* experiment was conducted performing transcriptomic and proteomic analysis in the brain of mice exposed to PBDE-47 or HBCD within their diet for 28 days (Carroll 2011; Rasinger 2011). The gene expression changes and the proteomic results were then used to identify functions, pathways and phenotypes associated with these toxicants. An interesting but perhaps unsurprising phenotype gene set found to be associated with both PBDE-47 and HBCD treatment in the *in vivo* study was also “abnormal behavioural response to xenobiotics” (Carroll 2011). Investigation of this gene set showed that this phenotype was most associated with enrichment in the voltage-gated calcium channel (VGCC) activity, but effects on neurotransmitter binding activity and protein kinases regulation were also seen to contribute to its enrichment (Carroll 2011). In the same study, proteomics analysis revealed that the top scoring function associated with the cluster of proteins regulated by PBDE-47 or HBCD was “neurological disorder” (Rasinger 2011).

In the present study, neurodegenerative disorders related pathways were seen to be enriched in cells exposed to either of the contaminants. PBDE-47 and HBCD also regulated genes linked to Parkinson’s and Alzheimer’s disease. PBDE-47 was seen to up-regulate the gene *App*, which is responsible for the production of amyloid-beta peptide (A β). Deposition of A β in plaques in brain is considered to be the primary cause

of AD-associated neuropathology (McConlogue et al. 2007). The β -secretase *Bace1*, responsible for the APP cleavage in the A β formation, was also seen to be regulated by PBDE-47. *Bace1* was down-regulated by PBDE-47, which could be a cellular compensatory mechanism as a consequence of the observed *App* up-regulation. In fact inhibition of *Bace1* abolishes the production A β and therefore its accumulation (X. Luo and Yan 2010). HBCD was seen to up-regulate the expression of the second β -secretase involved in the formation of A β , *Bace2*. Even if less characterised, it is known that both forms of BACE compete for the same substrate pool, and therefore, even if *Bace1* has the major enzymatic role, small changes in *Bace2* activity could also have consequences for human disease (Ahmed et al. ; Myllykangas et al. 2005). HBCD has also shown to regulate other genes related to Alzheimer's (AD) and Parkinson's disease (PD) such as *Park-7*, encoding for a protein suggested to be responsible for the dopaminergic neuron loss in PD (Moore et al. 2005; Rego et al. 2007) and *Ngfr*, one of the two receptors specific for the nerve grow factor (NGF) which has been shown to contribute to neurodegeneration by enhancing the activation of pro-apoptotic mechanisms in AD patients (Counts and Mufson 2005).

Enrichment of genes related to calcium signalling were seen for both of the toxicants, suggesting effects on calcium homeostasis disruption. Previous *in vivo* studies showed that PBDE-47 and HBCD can disrupt cellular calcium related processes (Coburn et al. 2007; M. M. L. Dingemans et al. 2008b; Mariussen and Fonnum 2003). In addition, in the *in vivo* study conducted in our laboratory, it was observed an enrichment for differential expression within the "voltage gated calcium activity" gene set's gene members, or those in its' descendants, highlighting this cellular process as a target of possible neurotoxic effects of HBCD and PBDE-47 (Carroll, 2010). We can speculate that the effects caused by either the toxicants on calcium signalling have different explanations. Disruption of the plasma membrane, previously reported in cells exposed to HBCD, may lead to influx of calcium from the extracellular space and therefore to the perturbation of calcium-related functions as a secondary consequence (Y. S. Tan et al. 2004b). Change in calcium flux across the membrane of cellular calcium store such as the endoplasmic reticulum or mitochondria, have been also proposed (Pessah et al. 2010). A second possible mechanism would involve a direct interaction with the Ryanodine receptor (RyR), which would influence the calcium concentration through the regulation of calcium signalling in the endoplasmic reticulum. In support of this hypothesis, the gene interacting with the RyR *Homer1* was regulated in cells exposed to

HBCD, suggesting that HBCD has effects on a direct regulation of RyR activity, which can lead to release of calcium from the endoplasmic reticulum, and therefore to a calcium homeostasis disruption. *Homer1* was also seen regulated by the PBDE-47 and HBCD in an *in vivo* study performed in our laboratory (Carroll 2011). In the same study, Carroll also suggested that despite the fact that enrichment of regulated genes with functional annotation, “voltage-gated calcium channel activity” or its direct descendants, was seen in both PBDE-47 and HBCD groups, the effects on calcium homeostasis reported in previous *in vitro* studies (Coburn et al. 2008; M. M. L. Dingemans et al. 2008b; M. M. L. Dingemans et al. 2009) are not a consequence of a direct action through VGCCs (M. M. L. Dingemans et al. 2008b; M. M. L. Dingemans et al. 2009), but may be due to a regulatory relationship between RyR and VGCCs. The RyR has been proposed as a convergent target for non dioxin-like PCBs toxicity and their structural similarity to PBDEs may suggest a similar mode of action in this toxicant (Pessah et al. 2010). HBCD is structurally quite different from PBDEs and PCBs, thus its ability to affect Ryanodine receptor activity has yet to be established. Confirming what was found in the present *in vitro* study, the Ryanodine receptor interacting Homer 1 protein was also seen to be regulated in the *in vivo* experiment conducted in our laboratory in both HBCD and PBDE-47 groups (Carroll 2011). Therefore, these findings support the hypothesis that both toxicants are having effects on a direct regulator of Ryanodine receptor activity.

Calcium depletion is one of the major causes of ER stress (Treiman 2002). Enriched GO terms related to ER functions were evident in cells exposed to both PBDE-47 and HBCD. Calcium homeostasis disruption can also interfere with the protein-folding pathway within the ER, leading to accumulation of misfolded protein aggregates (Treiman 2002). Microarray analysis showed also that PBDE-47 and HBCD can cause direct effects on protein-folding related pathways as revealed from the enriched GO terms. ER stress and protein-folding perturbation may lead to the accumulation of unfolded protein and to the initiation of the unfolded protein response (UPR) pathway, with the activation of chaperones that facilitate proper protein folding and prevent protein folding intermediates from aggregating (Lee 2005). Effects on protein folding related pathways were also seen in the animal trial conducted in our laboratory in both PBDE-47 and HBCD groups (Carroll 2011; Rasinger 2011). Genomic analysis revealed that PBDE-47 and HBCD can lead to disruption of genes relating to protein folding (Carroll 2011). Also, IPA analysis of the differentially expressed proteins identified

after the exposure to HBCD, showed that the heat shock protein HSPA8, member of the HSP70 molecular chaperone machinery, occupied a central position in the pathway enriched by the toxicant (Rasinger 2011).

Another member of the HSP70 proteins, the chaperone *Hspa5*, was seen down-regulated in both the *in vivo* and *in vitro* genomic studies. *Hspa5* down-regulation can potentially lead to misfolded protein accumulation, which has been associated with neurodegenerative disorders such as Alzheimer's and Parkinson's diseases, as well as prion protein diseases (Lee 2005). If *Hspa5* down-regulation is the consequence of a direct effect of HBCD on gene expression, or if it is a secondary effect of the disruption of calcium homeostasis and ER functions, is still unknown. In addition, in the *in vivo* study PBDE-47 and HBCD were seen to regulate several protein disulphide isomerases (Carroll 2011). It is known that effects on protein folding often reflect an increase in endoplasmic reticulum stress (Schroder and Kaufman 2005). Genomic analysis in this *in vivo* study, in fact, showed enrichment for endoplasmic reticulum related genes, suggesting that both HBCD and PBDE-47 can induce a conserved effect on processes within the endoplasmic reticulum (Carroll 2011).

In the present study, PBDE-47 was seen to regulate lipid and fatty acid metabolism related pathways. Genes associated in Arachidonic acid related pathway were also enriched in the *in vivo* study conducted by Carroll in both PBDE-47 and HBCD group (Carroll 2011). In the same study an up-regulation of a calcium-dependent phospholipase suggested that arachidonic acid was being produced by a calcium-dependent mechanism (Carroll 2011).

In the present study, HBCD down-regulated the expression of the gene *Acs14*, which encodes for a protein involved in the fatty acid synthesis, with particularly affinity to the arachidonic acid (AA). The gene *Pnpla8*, linked with diverse aspects of lipid metabolism and signalling and prevention of lipid peroxidation, was also down-regulated by HBCD. Effects on lipid metabolism may be the direct consequence of HBCD membrane damage, or a secondary effect of the calcium homeostasis disruption. In fact, calcium homeostasis perturbation can lead to the increase of (AA) level by the activation of phospholipases (Draper et al. 2004). In addition, AA has been shown to be an activator of the RyR and through this interaction able to induce calcium release from the endoplasmic reticulum (Woolcott et al. 2006). Therefore increased AA release may affect the RyR activity and so act to further the disruption of the ER calcium status.

Increased AA can also lead to the regulation of AA-modulated cytoskeleton reorganization (Okuda et al. 1994). PBDE-47 and HBCD were seen to affect the regulation of cytoskeleton organisation and tubulin related functions. The effects of PBDE-47 on the cytoskeleton are probably the direct consequence of the interaction of the toxicant with the cellular membrane, which is directly connected to the cytoskeleton. Disruption of cytoskeleton organisation in response to PBDEs has previously been suggested (Alm et al. 2008). In muscles exposed to PBDEs it was observed a disturbance in the microtubule caused by damage of the microtubule subunit β -tubulin (Apraiz et al. 2006). Calcium homeostasis perturbation with AA release and modulation of the cytoskeleton reorganization are probably a contribution to the cytoskeleton effects caused by PBDE-47.

In the present study, we also established that HBCD exposure can cause effects on mitochondria, with enrichment of mitochondria structure related functions. The gene *Pnpla8*, above mentioned to be regulated by HBCD, is linked with lipid metabolism and lipid peroxidation prevention and it is also believed to maintain mitochondrial function (Mancuso et al. 2007). The down-regulation of *Pnpla8* may lead to disruption of mitochondrial function and thus to the production of reactive oxygen species (ROS) and oxidative stress. These findings indicate that HBCD directly affects mitochondrial activity with potential ROS formation and oxidative stress. Effects on mitochondria activity such as ROS formation and oxidative stress have been previously reported in cells exposed to either of the toxicants at concentration of 4 μ g/ml in cells exposed to PBDE-47, and at concentration between 0.5 μ g/ml to 5.0 μ g/ml for HBCD, depending on the congener (W. H. He et al. 2008c; X. L. Zhang et al. 2008). Confirming these results, in the present study, in cells exposed to PBDE-47, functions related to oxidative stress pathway were seen to be enriched, indicating that also PBDE-47 cytotoxicity mode of action involves oxidative stress damage.

Another function enriched by PBDE-47 and HBCD highlighted from our microarray and Q-PCR analysis was hormone activity disruption. Both of the toxicants were seen to cause preferential expression of genes related to thyroid hormone and retinoid regulations, such as the two main thyroxine and retinol carrier proteins *Ttr* and *Rbp4* for HBCD and *Ttr* only for PBDE-47. In previous *in vivo* studies both PBDE-47 and HBCD were seen to cause changes in retinol and thyroxine level in the blood (Darnerud 2003a; Darnerud et al. 2007; Skarman et al. 2005; van der Ven et al. 2009). In an *in vivo* study conducted in our laboratory PBDE-47 and HBCD were seen to cause changes in thyroid

hormone concentrations as well as thyroid gland histology (Carroll 2011). In this study both the toxicants showed increasing of desquamation into follicular lumen, which is a marker of disruption of thyroid function, of 14% and 71% for HBCD and PBDE-47 respectively, compared to control. In addition, in the same study the HBCD group had a significant enrichment of genes relating to retinol binding, and confirming what was found *in vitro*, the Retinol binding protein 4 (*Rbp4*) was seen differentially expressed by both toxicants (Carroll 2011).

Previously, it was suggested that the similar structure of PBDE-47, especially of the PBDE-47 hydroxylated metabolites, to T3 and T4 cause competitive binding to the thyroid hormone transport protein TTR, and therefore the prevention of T4 from binding the transporter protein cause a decrease in the circulating hormone level (Hallgren and Darnerud 2002a). HBCD is structurally not related to T3 or T4, but binding to TTR cannot be excluded. However, considering what was found in the *in vitro* and *in vivo* studies, we can suggest that HBCD and PBDE-47 act on processes controlling the expression of these genes directly and at least not exclusively through effects on thyroid hormone or release. Therefore the effect on circulating T4 and T3 seen *in vivo* may be secondary due to the direct effect of PBDE-47 and HBCD on the two carrier proteins.

Although this is the main hypothesis we support, we need to consider that metabolic reactions which occur *in vivo*, but cannot be appreciated in cultured cell line, will influence the regulation of thyroid hormone. Metabolic reactions such as glucorination, have the ability to increase T₄ and T₃ water solubility, and thus to facilitate excretion into bile and urine (Klaassen and Hood 2001; Visser et al. 1993), evoking a reduction of T₄ level in the blood. Previously other POPs such as PCB (M. O. James et al. 2008; Richardson and Klaassen 2010) and TCDD (Bank et al. 1989; Goon and Klaassen 1992) have been shown to have the ability to induce T₄ glucuronidation. Thus, we can't exclude that the *in vivo* effects on TH caused by PBDE-47 and HBCD are caused by the same mechanism.

In addition, HBCD was seen to regulate the expression of the immediate-early gene *Egr1*, which is known to affect brain plasticity and synaptic function (A. B. James et al. 2006), and of the transcriptional regulator *Nfkb2*, indicating that transcriptional regulation are HBCD toxicity targets.

Instead, the well characterised tumour suppressor *Rb1* (retinol binding protein 1) was seen to occupy a central role in pathways enriched by PBDE-47 and HBCD. *Rb1*, which plays a role in the induction of growth arrest and cellular senescence (Binda et al. 2008), is directly linked with the gene *Sirt1* (sirtuin 1), which main function is epigenetic transcriptional silencing (Binda et al. 2008) and which was also regulated by PBDE-47, indicating direct and secondary effect from this toxicant to gene expression related to transcriptional mechanisms. Studies on the carcinogenicity of PBDE are still limited with the focus of such studies being solely based on deca-PBDEs (Darnerud 2003a). Deca-PBDEs have been shown to induce cancers in mice and rats at really high doses, and IARC (1990) evaluates this compound not classifiable as to its carcinogenicity to humans (Darnerud 2003a). There are no studies investigating PBDE-47 carcinogenicity, but a study focused on assessing body burden among cancer patients living in the e-waste disassembly sites in China, reported a high level of POPs in the tissue samples. PBDE47 was reported to be the most predominant PBDE congener accounting for >17% of the total PBDEs observed in the collected samples (Zhao et al. 2009).

Considering the overall effects resulting from PBDE-47 or HBCD exposure, it could be argued that the observed gene expression patterns are the downstream consequences of oxidative stress with ROS formation, which can directly cause cell damage and apoptosis even before the secondary effects are triggered. However, the effects we observed in our study were measured at sub-lethal concentrations, and also, PBDE-47 and HBCD abilities to induce ROS formation have been always reported at higher concentrations than those used in the experiments described herein (P. He et al. 2008a; X. L. Zhang et al. 2008). Although in the present study some genes associated with oxidation were regulated there was little evidence of a NRF2 driven response, which would have been expected during oxidative stress. Thus, it is still unclear to what extent oxidative stress contributed to the overall gene expression response observed in the present study.

6.3 Microarray follow-up studies

6.3.1 HBCD effects on zinc homeostasis

In the present study, for the first time we established that HBCD exposure can cause increase in cellular free Zn^{2+} , indicating that zinc homeostasis disruption is a mechanism of action of POPs toxicity.

HBCD was seen to increase $[Zn^{2+}]$ in the N2A neuroblastoma cell line at concentration as low as 1 or 2 μ M (Figures 5.3 and 5.4). Higher concentrations were also tested, but zinc perturbation was not observed, probably due to the low cell viability caused by HBCD toxicity. We hypothesised three main explanations to motivate the $[Zn^{2+}]$ increase observed after HBCD exposure. The first one suggests that HBCD exposure can lead to ROS formation with release of zinc from oxidised Zn^{2+} -binding proteins (Kroncke et al. 1994). In the intracellular space most of the zinc is bound to proteins, especially to the main zinc storing protein metallothionein (MT), thus exposing cells to oxidizing agents may increase cellular free zinc ion concentration (Maret 2009; Spahl et al. 2003). Supporting this hypothesis, the ability of HBCD to cause oxidative stress and to induce ROS formation has been previously suggested. Studies in zebrafish embryo showed that HBCD can cause oxidative stress with ROS formation at low micromolar concentration (starting at 0.1mg/L) (Deng et al. 2009) and lipid peroxidation at as low concentration as 0.5 mg/L (Hu et al. 2009), concentrations similar to those tested in the present study.

According to these results and with our main hypothesis, in the present study the antioxidant N-Acetyl Cysteine (NAC) could mitigate the effect of HBCD exposure on zinc release, suggesting that oxidative stress may be the main cause of $[Zn^{2+}]$ perturbation caused by HBCD. Investigation of the mode of action of oxidative stress induced by HBCD revealed that it does not involve NO pathway activation as the antioxidant L-NAME did not decrease the release of zinc caused by this toxicant.

A second explanation speculates that increasing of $[Zn^{2+}]$ is caused by the damage of plasma- or organelle-membranes. Membrane damage may lead to increase diffusion of zinc into the cytosolic space from intracellular store such as the endoplasmic reticulum (ER) and mitochondria (Sensi et al. 2003; Stork and Li 2010). In more details, oxidative stress can lead to lipid peroxidation and membrane integrity damage resulting in efflux

of zinc from the cellular store to the cytosol (Hogstrand et al. 2009; Popova and Popov 2002; Stork and Li 2010).

The third mode of action suggested, is the influx of zinc in the cytosol in a calcium dependent manner. Yamasaki et al demonstrated that extracellular stimulus of the high affinity IgE receptor in mast cells, can induce a release of free zinc, dependent on calcium influx (Yamasaki et al. 2007a), suggesting that calcium may also play a role in the observed $[Zn^{2+}]$ increase (Yamasaki et al. 2007b). These findings are supported from the observations made in both the *in vitro* and *in vivo* experiment conducted in our laboratory (Carroll 2011). In these studies, we showed that HBCD affects genes linked to calcium signalling and to calcium related pathway, supporting the theory that calcium homeostasis perturbation may plays a role in HBCD toxicity, which can lead to perturbation the cellular $[Zn^{2+}]$.

6.3.2 DHA effect on gene expression and on HBCD cytotoxicity

As previously mentioned, HBCD is a ubiquitous contaminant found in all the environment media and in living biota (Covaci et al. 2006; Heeb et al. 2005). Recently it has also been detected at increasing concentration in human milk and serum (Covaci et al. 2006; Heeb et al. 2005). The main source of this contaminant for humans is through the food chain, especially through the consumption of fish (Remberger et al. 2004). Despite the fact that fish contains higher levels of HBCD compared to other food sources (Schechter et al. 2010a), it is also a great supplier of important nutrients fundamental for brain functions and growth. It is well known that fatty acids, such as DHA, that are abundant in fish, play a fundamental role in brain development and maintenance (Bazan 2005). In a recent *in vivo* study, PBDE-47 toxicity was investigated alongside with the potential ameliorating impact of seafood nutrients (Haave et al. 2011a). In this study mice were exposed to PBDE-47 with a casein or fish-based diet, and it was revealed that nutrients contained in fish have ameliorative effect on PBDE-47 gene expression changes, which were induced in the group fed with the casein-based diet, but not in the fish-based diet group (Haave et al. 2011a). In addition, DHA ameliorative effects have been previously reported in the methylmercury (MeHg)-induced neurotoxicity, where in cells treated with the fatty acid, it was observed a reduction of MeHg accumulation and a decrease in ROS formation (Kaur et al. 2008). At the present, no studies have been conducted on the DHA potentially ameliorative

effects on POPs toxicity. Therefore, using transcriptomic tools, we investigated the effect of DHA on HBCD toxicity.

In the present study, we established that DHA can regulate the expression of genes affected by PBDE-47 or HBCD exposure in transcriptomic experiments conducted in our laboratory. However it was not possible to determine if DHA can ameliorate the effect of HBCD toxicity, as analysis failed to reproduce the effects of this toxicant on gene expression, previously observed in our study (Chapter 4).

However, data on the effect of DHA on gene expression showed that this fatty acid can regulate the expression of genes linked to neurodegeneration, especially to Alzheimer's and Parkinson's diseases. DHA was seen to stimulate the expression of the chaperone *Hspa5* which was down-regulated by HBCD in both *in vivo* (Carroll 2011) and *in vitro* studies (present study) conducted in our laboratory. Thus, we could speculate that DHA, through the regulation of *Hspa5*, might maintain ER functions, facilitate proper protein folding and prevent partially folded proteins accumulation in the ER (Lee 2005). DHA was also seen to down-regulate the expression of the two genes responsible for the formation and accumulation of amyloid-beta peptide (A β) in brain plaques, one of the main causes of Alzheimer's disease (AD), *App* and *Bace1* (X. Luo and Yan 2010; McConlogue et al. 2007). The down-regulation of *App* and *Bace1* has been seen to abolish the production of A β and its accumulation (Espeseth et al. 2004; X. Luo and Yan 2010), suggesting that DHA may have a role in the prevention of neurodegeneration.

DHA was also seen to regulate the expression of the gene *Pnpla8*, which is responsible for lipid regulation and decrease in lipid oxidation, and also for membrane functions and integrity maintenance (Baulande and Langlois ; Kinsey et al. 2008). Thus, through the regulation of *Pnpla8*, DHA plays a role in membrane integrity and lipid maintenance. In Chapter 3 we already showed that DHA can ameliorate the effect of HBCD exposure on the cellular membrane. In fact DHA was seen to prevent the LDH leakage caused by HBCD, suggesting a protective role of DHA on membrane permeability and integrity (Figure 3.6). Thus, we could speculate that the observed ameliorative effect of DHA treatment, was related to its ability to increase the antioxidant defence, inhibiting pro-inflammatory and pro-apoptotic signalling (Hashimoto et al. 2002) and to produce neuroprotectin D1 (NPD1) which it is known to have a neuroprotective bioactivity during oxidative stress (Bazan 2005). DHA has been

also previously associated with lipid metabolism and composition regulation in brain (W. Zhang et al. 1995) and with lipid peroxidation protection (Bazan 2005). Thus, in the light of these new findings, the neuroprotective function of DHA against oxidative stress, may be a consequence of the direct effect of DHA on regulation of genes related to lipid metabolism and oxidation

DHA was also seen to regulate the gene related to cytoskeleton structure, *Tubb2c*. We speculated that *Tubb2c* regulation may be a secondary effect of the involvement of DHA in the cellular membrane structure. In more details, DHA is one of the major components of the neuron membrane (Cao et al. 2009), and the cytoskeleton is connected to the cellular membranes, therefore indirect effect from DHA on the cytoskeleton structure can be hypothesised.

We also showed that DHA can regulate the expression of the gene *Homer1*, one of the encoding proteins interacting with the RyR and involved in cellular calcium signalling (Tu et al. 2002). *Homer1* directly interacts with glutamate receptors on the cellular membrane (Tu et al. 2002). Considering that DHA has strong trophic effect on glutamate receptors, we could hypothesise that its effect on *Homer1* regulation may be caused indirectly through regulation on these receptors.

Considering the overall results we can't establish if DHA can ameliorate the effect caused by HBCD or PBDE-47 on the regulation of the genes above discussed, but we can observe that DHA affect the expression of genes related to protein folding and to the formation and accumulation of A β , to lipid regulation and calcium signalling, and that these genes are also target of HBCD or PBDE-47 toxicity. However, to establish if DHA has ameliorative effect on HBCD or PBDE-47 toxicity, and to investigate the eventually interaction of this fatty acid with the two toxicants, further studies are needed.

6.4 General conclusion and future prospective

In the present study, for the first time we have investigated the global gene expression in cell lines with neuronal origin, after exposure to two flame retardants, PBDE-47 and HBCD. Previously, global gene expression profile after exposure to these toxicants has been only assessed on zebrafish embryonic fibroblast, or on rat liver (Canton et al. 2008; Suvorov and Takser 2010; Van Boxtel et al. 2008), but never in a neuronal

model. For the first time, we compared genomic analyses conducted in an *in vitro* study with genomic and proteomic analyses performed in a parallel *in vivo* trial conducted in our laboratory. In this study, mice were exposed to PBDE-47 or HBCD within their diet for 28 days, the gene expression changes and the proteomic results were used to identify functions, pathways and phenotypes associated with these toxicants (Carroll 2011; Rasinger 2011). The overall results of the *in vitro* study have provided a better understanding of the possible conserved mechanisms by which these toxicants act *in vivo* and have proved that PBDE-47 and HBCD mechanism of action can be reproduced in a cellular model.

In this present study, implementing transcriptomics tools, we established that exposure to PBDE-47 or HBCD can affect specific but also common sets of biological functions. PBDE-47 and HBCD were seen to cause preferential regulation of genes involved in neurodegenerative disorders, such as Parkinson's (PD) and Alzheimer's disease (AD). These findings accord with what was seen in previous *in vivo* studies which demonstrated that both of the toxicants were able to induce aberrations in spontaneous behaviour (Per Eriksson et al. 2006; Viberg et al. 2003c), and to affect memory and learning functions (Per Eriksson et al. 2006; Kuriyama et al. 2005). The animal work conducted in our laboratory have also showed that a phenotype gene set associated with both PBDE-47 and HBCD treatment was "abnormal behavioural response to xenobiotics" (Carroll 2011). In the same study, also proteomics analysis revealed that the top scoring function associated with the cluster of proteins regulated by PBDE-47 or HBCD was "neurological disorder"(Rasinger 2011). Therefore, the overall findings clearly suggest a correlation between neurodegeneration and PBDE-47 or HBCD exposure.

In the present study, transcriptomics analysis showed that PBDE-47 regulates the expression of genes involved in the formation of Amyloid- β , the main component of the plaques in AD. The gene Amyloid Precursor Protein (*App*) and the β -secretase *Bace1*, were in fact seen regulated in cells exposed to PBDE-47. In addition, HBCD was seen to up-regulate the expression of the second β -secretase involved in the formation of A β , *Bace2*, and the expression of the gene *Park7*, believed to be responsible for the dopaminergic neuron loss in Parkinson Disease (PD), through apoptosis induction (Moore et al. 2005; Rego et al. 2007). HBCD was also seen to up-regulate the expression of one of the two receptors specific for the nerve grow factor (NGF), which

has been shown to contribute to neurodegeneration in AD patients (Counts and Mufson 2005)

Both the *in vitro* and *in vivo* studies conducted, demonstrated that PBDE-47 and HBCD affect calcium homeostasis, enriching functions related to calcium signalling in the neuroblastoma cell lines, and preferentially regulating expression within the “voltage gated calcium activity” gene set in the *in vivo* study (Carroll 2011). As previously suggested for polychlorinated biphenyls (PCBs) (Y. S. Tan et al. 2004b), exposure to PBDE-47 or HBCD can alter membrane components with consequence on the membrane structure and permeability. Membrane damage can lead to the flux of calcium across the membrane of cellular calcium store such as the endoplasmic reticulum or mitochondria, leading to calcium homeostasis and calcium related processes disruption. Indeed, a direct interaction of the two toxicants with the RyR and therefore regulation of calcium signalling in the endoplasmic reticulum was observed. In fact, the gene for a protein physically interacting with the RyR, Homer1, was regulated in either cell lines exposed to HBCD, and in the PBDE-47 and HBCD groups in the animal study (Carroll 2011).

Secondary effects as a consequence of calcium homeostasis disruption caused by PBDE-47 or HBCD exposure, were revealed by either genomic and proteomic analysis. ER stress and protein-folded functions were seen to be affected by either of the toxicants. Chaperons’ members of the HSP70 molecular chaperone machinery, which have protein folding and re-folding functions, were regulated by PBDE-47 and HBCD in either the *in vivo* or *in vitro* studies. Deregulation of the protein-folded functions can potentially cause malformed protein accumulation, which has been associated with neurodegenerative disorders such as Alzheimer’s and Parkinson’s diseases (Lee 2005). It is also known that protein-folding damage can lead to ER stress. In line with this observation, our genomic analysis in both the *in vitro* and the *in vivo* studies revealed enrichment for endoplasmic reticulum functions related genes.

We also established that PBDE-47 and HBCD can affect lipid and fatty acid metabolism regulating genes related to fatty acid synthesis, lipid metabolism and signalling, and prevention of lipid peroxidation. According to these findings, in the *in vivo* study, effects were reported on the arachidonic acid (AA) related pathway, and an up-regulation of a calcium-dependent phospholipase suggested that arachidonic acid was produced by a calcium-dependent mechanism (Carroll 2011). An increase in AA can in

turn lead to the regulation of AA-modulated cytoskeleton reorganization (Okuda et al. 1994). Indeed the genomics analysis performed in the *in vitro* study presented here supported these findings suggesting that both of the toxicants affect cytoskeleton organisation related functions.

PBDE-47 and HBCD effects on thyroid hormone signalling were also investigated. In the literature, thyroid hormone disruption caused by PBDE-47 or HBCD exposure has been quite extensively explored. Previous *in vivo* studies have showed that both PBDE-47 and HBCD affect retinol, T₃ and T₄ levels in the blood (Darnerud 2003a; Darnerud et al. 2007; Skarman et al. 2005; van der Ven et al. 2009). Transcriptomics analysis conducted in both the *in vitro* and *in vivo* studies conducted in our laboratory, revealed that both the toxicants affect the regulation of the two main thyroxine and retinol carrier proteins, *Ttr* and *Rbp4*. In previous studies, it has been hypothesised that the decrease in T₃ and T₄ levels in the blood is caused by competitive binding of the two toxicants with the thyroxine and retinol transporter proteins (Hallgren et al. 2001a; Hallgren and Darnerud 2002a). In the light of the results reported here and in mouse experiments from our laboratory, we can speculate that the effect on circulating T₄ and T₃ seen *in vivo*, may also be a consequence of the direct effect of PBDE-47 and HBCD on expression of the two carrier proteins. However we can't exclude that in the *in vivo* studies, the decrease in circulating T₄ levels could be a consequence of the increase in T₄ glucuronidation caused by the effects of the two toxicants on liver metabolic functions.

The present work has revealed for the first time that HBCD can cause increasing in cytosolic [Zn²⁺] in a neuroblastoma cell line. Never before has a flame retardant or any other POP been clearly associated with cellular [Zn²⁺] increase, and the implication of these findings have fundamental importance to better understand the mechanisms of action of HBCD and possibly on toxicity of other POPs. HBCD was seen to increase [Zn²⁺] at low micromolar concentrations, likely as a consequence of oxidative stress caused by the toxicant, with release of Zn²⁺ from oxidised Zn²⁺-binding proteins. In support of this hypothesis, the antioxidant N-acetyl cysteine partially quenched the [Zn²⁺] release. However, the effect observed was not mediated through NO signalling as the iNOS inhibitor L-NAME had no effect on the [Zn²⁺] release. As previously discussed, HBCD toxicity effects can lead to membrane damage and to calcium homeostasis disruption. Therefore, despite that our main hypothesis to explain [Zn²⁺] increase is an increase in oxidative stress, we could speculate that [Zn²⁺] perturbation is also, or partially, caused

by efflux of Zn^{2+} from cellular store as a consequence of organelle membrane damage, or as secondary effect of calcium homeostasis disruption.

A different aspect of the work was associated with a largely discussed topic regarding the role of fish consumption in a healthy diet. Many previous studies have reported the beneficial effects of the long chain n-3 polyunsaturated fatty acids (n-3 PUFAs), eicosapentaenoic acid (EPA) and docosahexaenoic acid (DHA), especially in coronary heart disease prevention and in neurodevelopment during gestation and infancy (Cohen et al. 2005; Mozaffarian and Rimm 2006). In contrast to these findings, concern has risen over the potential harm of POPs present in some fish species. Indeed, during the last decade the public has faced a conflict debate on the risks and benefits of fish intake, resulting in controversy and confusion over the health consequences of fish consumption. Previous evaluations on these issues have been largely discussed with focus on fish contamination with substances such as methylmercury, dioxins, and PCBs (Mozaffarian and Rimm 2006; Rylander et al. 2009). In these studies the positive effects of EPA and DHA have been contrasted to the toxic effects caused by the pollutants accumulated in fish (Mozaffarian and Rimm 2006; Rylander et al. 2009). Gene expression profile in brain of rodents after exposure to DHA through the diet has been also investigated, indicating that brain sensitively reacts to the fatty acid composition of the diet, and that DHA regulates the expression of genes related to energy household, lipid metabolism and respiration (Barcelo-Coblijn et al. 2003), but also to synaptic plasticity, cytoskeleton and membrane association, signal transduction, ion channel formation, energy metabolism, and regulatory proteins (Kitajka et al. 2002). However, never before the direct effects of the fatty acid DHA have been evaluated on the expression of genes deregulated by PBDE-47 or HBCD, and the potentially ameliorative effects of DHA have been investigated in the HBCD toxicity.

In the present study we established for the first time that DHA has the ability to alter the expression of several genes previously seen regulated by HBCD and/or PBDE-47. DHA was seen to affect the expression of genes linked to neurodegenerative disorders, up-regulating the chaperon *Hspa5* and down-regulating the two genes causing amyloid-beta peptide formation *App* and *Bace1*. The effect of DHA on the expression of a gene related to lipid metabolism and oxidation was also investigated. We showed that DHA can alter the expression of the gene *Pnpla8*, suggesting a direct role of this fatty acid in lipid metabolism regulation. DHA also regulated the gene responsible for the direct interaction with the RyR in the ER, *Homer1*, which has a fundamental function on

calcium homeostasis maintenance (Tu et al. 2002). Finally, we established that DHA play a role in the maintenance of membrane integrity and permeability. The fatty acid was in fact seen to reduce the LDH leakage caused by HBCD in a neuroblastoma cell line, suggesting that DHA can protect the cellular membrane against the damage caused by HBCD exposure. In addition, DHA regulated the expression of the gene related to cytoskeleton structure, *Tubb2c*.

The data obtained from the present work provides important and novel elucidations on the mode of action of environmental xenobiotics, with particular focus on mechanistic toxicology. It also contributed to reveal new toxicity targets and pathways affected by the two contaminants studied.

What is more, the present study adds valuable information for the planning of future studies that aim to assess toxicological effects of food-borne contaminants in relation to the nutritional status of the individual. Highlights also suggest the need to better assess the risk-benefit related to fish consumption, considering fish as a rich source of fatty acid, as well as vitamins and minerals.

APPENDECES

Appendix 1

LIMMA script utilised in the microarray analysis

```
#####  
#####  
#####  
#VALE'S HBCD ARRAY#  
  
#REQUIRES FUNCTION FILE TO BE RUN FIRST!!#  
#####  
#####  
#####  
  
## set the working directory where the files are stored and check  
## if they are really there  
#setwd("~/Dropbox/Work/NIFES/Aquamax/Aquamax Shared/Data/Cell  
Work/R HBCD files")  
setwd("C:/Users/jra/Dropbox/Work/NIFES/Aquamax/Aquamax  
Shared/Data/Cell Work/R HBCD files")  
getwd()  
dir()  
  
##Read in bluefuse files and extra columns  
targets <- SortAndReadTargets(targets="Targets.txt")  
autreOlumns <- c("CONFIDENCE","P ON CH1","P ON CH2")  
RG<- read.maimages(targets,source =  
"bluefuse",other.columns=autreOlumns)  
RG$genes <- readGAL()  
RG$printer <- getLayout(RG$genes)  
  
##Set Colours for different conditions  
Conditions <- c("CONTROL_N2A", "CONTROL_NSC19", "DMSO_N2A",  
"DMSO_NSC19", "HBCD_0.5mc_N2A", "HBCD_0.5mc_NSC19", "HBCD_1mc_N2A",  
"HBCD_1mc_NSC19", "HBCD_2mc_N2A", "HBCD_2mc_NSC19")  
Colours <-  
c("White","Blue","Yellow","Red","Black","White","Blue","Yellow","Re  
d","Black")  
Values4Colours <- cbind(Conditions,Colours)  
ConditionsIndex <- RG$targets  
ColourIndex <- setColours(ConditionsIndex,Values4Colours)  
  
##Set columns for probability of true biological signals in either  
channels and confidence  
Confidence <- RG$other$CONFIDENCE  
PofCh1 <- RG$other$"P ON CH1"  
PofCh2 <- RG$other$"P ON CH2"
```

```

##Create matrices showing positions(gene and array) of bad genes
based on them not being "Expressed"(pch > 0.05 in both channels)
statusPofCh2 <- which(PofCh2 < 0.1, arr.ind=TRUE)
statusPofCh1 <- which(PofCh1 < 0.1,arr.ind=TRUE)
statusPofBothCh1 <- which(PofCh2 < 0.1 & PofCh1 < 0.1,arr.ind=TRUE)
statusPofBothChOver <- which(PofCh2 >= 0.1 & PofCh1 >=
0.1,arr.ind=TRUE)

## Create Status Matrix for use with unfiltered data
status <- RG$other$CONFIDENCE
status[statusPofCh2] <- "NoCh2"
status[statusPofCh1] <- "NoCh1"
status[statusPofBothCh1] <- "NonExpressed"
status[statusPofBothChOver] <- "Expressed"

## Just of input/raw data
RGQuality(RG,prefix = "raw",status=status, RGplotcolours =
ColourIndex)

## Set weights to zero for bad genes based on them not being
"Expressed" (pch > 0.05 in both channels is fine)
RG.w <- RG
RG.w$weights <- RG$other$CONFIDENCE
RG.w$weights[statusPofCh1] <- 0
RG.w$weights[statusPofCh2] <- 0
RG.w$weights[statusPofBothCh1] <- 0
RG.w$weights[statusPofBothChOver] <- 1

## Set filter based on Being "Expressed" (pch > 0.05 in both
channels) in more than 75% of samples
#library(genefilter)
f1<- pOverA(0.75, 0)
ff <- filterfun(f1)
selected <- genefilter(RG.w$weights, ff)
sum(selected)

#####
#####
#####

##Subbed data only
RGsub <- RG[selected,]
RGQuality(RGsub, prefix = "SubOnly",RGplotcolours = ColourIndex)

## Whole set PTL
MA <- normalizeWithinArrays(RG)

## Whole set PTL then scaled
MA.normal <- normalizeBetweenArrays(MA, method = "scale")
RGQuality(MA.normal, prefix = "PTLthenBetween",RGplotcolours =
ColourIndex)

## Reset Status to Null (Status is now shorter than RG so messes up
quality plots)
Status <- NULL

```

```

## Whole set PTL then Subbed then scaled
MAsub <- MA[selected,]
MAsubBetween <- normalizeBetweenArrays(MAsub, method = "scale")
RGQuality(MAsubBetween, prefix = "PTLthenSubThenBetween",RGplotcolours = ColourIndex) =

## Sub then loess and scale
MAloesssub <- normalizeWithinArrays(RGsub,method = "loess")
MAloesssubBetween <- normalizeBetweenArrays(MAloesssub, method = "scale")
RGQuality(MAloesssub, prefix = "SubthenLoess",RGplotcolours = ColourIndex) =
RGQuality(MAloesssubBetween, prefix = "SubthenLoessthenBetween",RGplotcolours = ColourIndex) =

##Weights PTL
MA.w <- normalizeWithinArrays(RG.w)

##Weights PTL then subbed
MA.wsub <- MA.w[selected,]
RGQuality(MA.wsub, prefix = "WeightPTLthenSub",RGplotcolours = ColourIndex) =

##Weights PTL then Scaled then subbed
MA.wBetween <- normalizeBetweenArrays(MA.w, method = "scale")
MA.wBetweenSub <- MA.wBetween[selected,]
RGQuality(MA.wBetweenSub, prefix = "WeightPTLBetweenSub",RGplotcolours = ColourIndex) =

## Weights PTL then subbed then Scaled
MA.wSubthenBetween <- normalizeBetweenArrays(MA.wsub, method = "scale")
RGQuality(MA.wSubthenBetween, prefix = "WeightPTLthenSubBetween",RGplotcolours = ColourIndex) =

## Subbed then Weights Loess then Scaled
RG.wsub <- RG.w[selected,]
MA.wLoess <- normalizeWithinArrays(RG.wsub, method = "loess")
MA.wLoessBetween <- normalizeBetweenArrays(MA.wLoess, method = "scale")
RGQuality(MA.wLoessBetween, prefix = "SubthenWeightLoessthenBetween",RGplotcolours = ColourIndex) =
#####
#####
#####
#####
#####

#####
#####
#####
#####
#####

## SETTING UP FITS
design <- modelMatrix(targets, ref="REF")

## UnFiltered, PTL loess and then Scale with no Sub an with no weights

```

```

arrayWeightsPTLthenBetween <- arrayWeights(MA.normal, design)
fitPTLthenBetween <- lmFit(MA.normal, design)
fitPTLthenBetweenArrayWeights <- lmFit(MA.normal, design, weights =
arrayWeightsPTLthenBetween)

## Whole set PTL then Subbed then scaled with no weights
arrayWeightsPTLthenSubThenBetween <- arrayWeights(MAsubBetween,
design)
fitPTLthenSubThenBetween <- lmFit(MAsubBetween, design)
fitPTLthenSubThenBetweenArrayWeights <- lmFit(MAsubBetween, design,
weights =arrayWeightsPTLthenSubThenBetween)

## Sub then loess and scale with no weights
arrayWeightsSubthenLoessthenBetween <-
arrayWeights(MALoesssubBetween, design)
fitSubthenLoessthenBetween <- lmFit(MALoesssubBetween, design)
fitSubthenLoessthenBetweenArrayWeights <- lmFit(MALoesssubBetween,
design, weights = arrayWeightsSubthenLoessthenBetween)

## Weights PTL then subbed then Scaled
arrayWeightsWeightPTLthenSubBetween <-
arrayWeights(MA.wSubthenBetween, design)
fitWeightPTLthenSubBetween <- lmFit(MA.wSubthenBetween, design)
fitWeightPTLthenSubBetweenArrayWeights <- lmFit(MA.wSubthenBetween,
design, weights = arrayWeightsWeightPTLthenSubBetween )

## Subbed then Weights Loess then Scaled
arrayWeightsSubthenWeightLoessthenBetween <-
arrayWeights(MA.wLoessBetween, design)
fitSubthenWeightLoessthenBetween <- lmFit(MA.wLoessBetween, design)
fitSubthenWeightLoessthenBetweenArrayWeights <-
lmFit(MA.wLoessBetween, design, weights
arrayWeightsSubthenWeightLoessthenBetween)

## Plot fits
FitQuality(fitPTLthenBetween, prefix = "PTLthenBetween")
FitQuality(fitPTLthenSubThenBetween, prefix =
"PTLthenSubThenBetween")
FitQuality(fitSubthenLoessthenBetween, prefix =
"SubthenLoessthenBetween")
FitQuality(fitWeightPTLthenSubBetween, prefix =
"WeightPTLthenSubBetween")
FitQuality(fitSubthenWeightLoessthenBetween, prefix =
"SubthenWeightLoessthenBetween")
FitQuality(fitPTLthenBetweenArrayWeights, prefix =
"PTLthenBetweenArrayWeights", arrayWeightcols =
ColourIndex, arrayw=arrayWeightsPTLthenBetween)
FitQuality(fitPTLthenSubThenBetweenArrayWeights, prefix =
"PTLthenSubThenBetweenArrayWeights", arrayWeightcols =
ColourIndex, arrayw=arrayWeightsPTLthenSubThenBetween)
FitQuality(fitSubthenLoessthenBetweenArrayWeights, prefix =
"SubthenLoessthenBetweenArrayWeights", arrayWeightcols =
ColourIndex, arrayw=arrayWeightsSubthenLoessthenBetween)
FitQuality(fitWeightPTLthenSubBetweenArrayWeights, prefix =
"WeightPTLthenSubBetweenArrayWeights", arrayWeightcols =
ColourIndex, arrayw=arrayWeightsWeightPTLthenSubBetween)
FitQuality(fitSubthenWeightLoessthenBetweenArrayWeights, prefix =
"SubthenWeightLoessthenBetweenArrayWeights", arrayWeightcols =
ColourIndex, arrayw=arrayWeightsSubthenWeightLoessthenBetween)

```

```

#contrastsStuff
#####To be done
##Set Contrasts
contrast.matrix <- makeContrasts(DMSO_N2A-CONTROL_N2A,
                                HBCD_0.5mc_N2A-CONTROL_N2A,
                                HBCD_1mc_N2A-CONTROL_N2A,
                                HBCD_2mc_N2A-CONTROL_N2A,
                                DMSO_NSC19-CONTROL_NSC19,
                                HBCD_0.5mc_NSC19-CONTROL_NSC19,
                                HBCD_1mc_NSC19-CONTROL_NSC19,
                                HBCD_2mc_NSC19-CONTROL_NSC19,
                                levels=design)

##Make Contrast fits
fitPTLthenBetween2 <- contrasts.fit(fitPTLthenBetween,
contrast.matrix)
fitPTLthenBetween2 <- eBayes(fitPTLthenBetween2)
fitPTLthenSubThenBetween2 <-
contrasts.fit(fitPTLthenSubThenBetween, contrast.matrix)
fitPTLthenSubThenBetween2 <- eBayes(fitPTLthenSubThenBetween2)
fitSubthenLoessthenBetween2 <-
contrasts.fit(fitSubthenLoessthenBetween, contrast.matrix)
fitSubthenLoessthenBetween2 <- eBayes(fitSubthenLoessthenBetween2)
fitWeightPTLthenSubBetween2 <-
contrasts.fit(fitWeightPTLthenSubBetween, contrast.matrix)
fitWeightPTLthenSubBetween2 <- eBayes(fitWeightPTLthenSubBetween2)
fitSubthenLoessthenBetween2 <-
contrasts.fit(fitSubthenLoessthenBetween, contrast.matrix)
fitSubthenLoessthenBetween2 <- eBayes(fitSubthenLoessthenBetween2)
fitPTLthenBetweenArrayWeights2 <-
contrasts.fit(fitPTLthenBetweenArrayWeights, contrast.matrix)
fitPTLthenBetweenArrayWeights2 <-
eBayes(fitPTLthenBetweenArrayWeights2)
fitPTLthenSubThenBetweenArrayWeights2 <-
contrasts.fit(fitPTLthenSubThenBetweenArrayWeights,
contrast.matrix)
fitPTLthenSubThenBetweenArrayWeights2 <-
eBayes(fitPTLthenSubThenBetweenArrayWeights2)
fitSubthenLoessthenBetweenArrayWeights2 <-
contrasts.fit(fitSubthenLoessthenBetweenArrayWeights,
contrast.matrix)
fitSubthenLoessthenBetweenArrayWeights2 <-
eBayes(fitSubthenLoessthenBetweenArrayWeights2)
fitWeightPTLthenSubBetweenArrayWeights2 <-
contrasts.fit(fitWeightPTLthenSubBetweenArrayWeights,
contrast.matrix)
fitWeightPTLthenSubBetweenArrayWeights2 <-
eBayes(fitWeightPTLthenSubBetweenArrayWeights2)
fitSubthenLoessthenBetweenArrayWeights2 <-
contrasts.fit(fitSubthenLoessthenBetweenArrayWeights,
contrast.matrix)
fitSubthenLoessthenBetweenArrayWeights2 <-
eBayes(fitSubthenLoessthenBetweenArrayWeights2)

##Plot Contrasts
ContrastQuality(fitPTLthenBetween2,prefix = "PTLthenBetween2")
ContrastQuality(fitPTLthenSubThenBetween2,prefix
"PTLthenSubThenBetween2") =
ContrastQuality(fitSubthenLoessthenBetween2,prefix
"SubthenLoessthenBetween2") =

```

```

ContrastQuality(fitWeightPTLthenSubBetween2,prefix           =
"WeightPTLthenSubBetween2")
ContrastQuality(fitPTLthenSubThenBetween2,prefix           =
"fitSubthenLoessthenBetween2")
ContrastQuality(fitPTLthenBetweenArrayWeights2,prefix      =
"PTLthenBetweenArrayWeights2")
ContrastQuality(fitPTLthenSubThenBetweenArrayWeights2,prefix =
"PTLthenSubThenBetweenArrayWeights2")
ContrastQuality(fitSubthenLoessthenBetweenArrayWeights2,prefix =
"SubthenLoessthenBetweenArrayWeights2")
ContrastQuality(fitWeightPTLthenSubBetweenArrayWeights2,prefix =
"WeightPTLthenSubBetweenArrayWeights2")
ContrastQuality(fitPTLthenSubThenBetweenArrayWeights2,prefix =
"fitSubthenLoessthenBetweenArrayWeights2")
#####

# csv file of significant genes (FDR 20%) for 1mc and 2mc HBCD in
N2A and NSC19 Cells
sigGenes.HBCD_1mc_N2A.fitSubthenLoessthenBetweenArrayWeights2 <-
topTable(fitSubthenLoessthenBetweenArrayWeights2      ,number=100000,
coef=3, p.value=0.2, adjust="BH")
write.csv2(sigGenes.HBCD_1mc_N2A.fitSubthenLoessthenBetweenArrayWei
ghts2,
file="sigGenes_HBCD_1mc_N2A_fitSubthenLoessthenBetweenArrayWeights2
.csv")

sigGenes.HBCD_2mc_N2A.fitSubthenLoessthenBetweenArrayWeights2 <-
topTable(fitSubthenLoessthenBetweenArrayWeights2      ,number=100000,
coef=4, p.value=0.2, adjust="BH")
write.csv2(sigGenes.HBCD_2mc_N2A.fitSubthenLoessthenBetweenArrayWei
ghts2,
file="sigGenes_HBCD_2mc_N2A_fitSubthenLoessthenBetweenArrayWeights2
.csv")

sigGenes.HBCD_1mc_NSC19.fitSubthenLoessthenBetweenArrayWeights2 <-
topTable(fitSubthenLoessthenBetweenArrayWeights2      ,number=100000,
coef=7, p.value=0.2, adjust="BH")
write.csv2(sigGenes.HBCD_1mc_NSC19.fitSubthenLoessthenBetweenArrayW
eights2,
file="sigGenes_HBCD_1mc_NSC19_fitSubthenLoessthenBetweenArrayWeight
s2.csv")

sigGenes.HBCD_2mc_NSC19.fitSubthenLoessthenBetweenArrayWeights2 <-
topTable(fitSubthenLoessthenBetweenArrayWeights2      ,number=100000,
coef=8, p.value=0.2, adjust="BH")
write.csv2(sigGenes.HBCD_2mc_NSC19.fitSubthenLoessthenBetweenArrayW
eights2,
file="sigGenes_HBCD_2mc_NSC19_fitSubthenLoessthenBetweenArrayWeight
s2.csv")

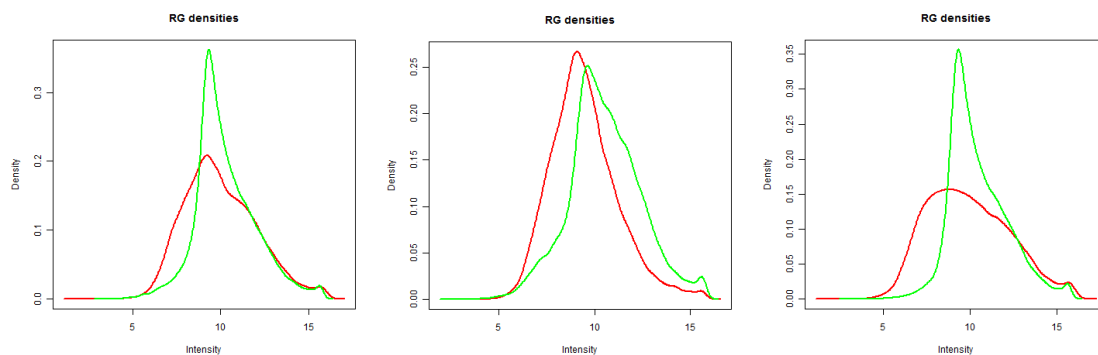
```


Appendix 2

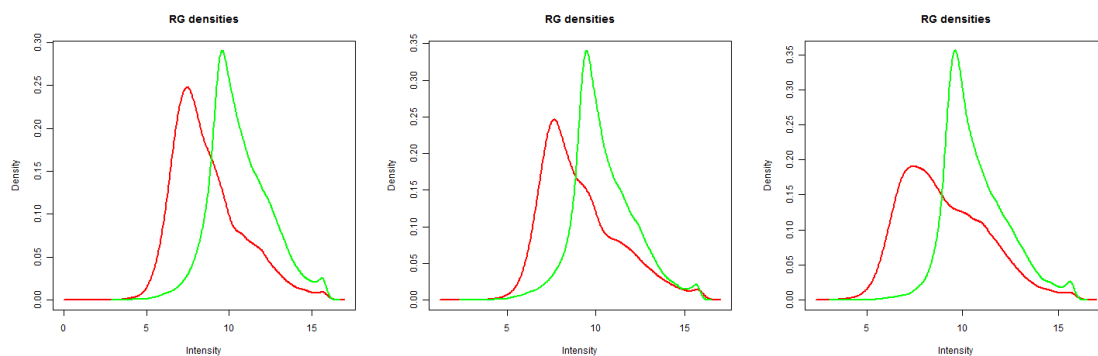
Plots created by LIMMA, representing fluorescence densities changes between arrays before and after normalisation

HBCD arrays. Samples before normalisation. Conditions were reproduced in triplicate.

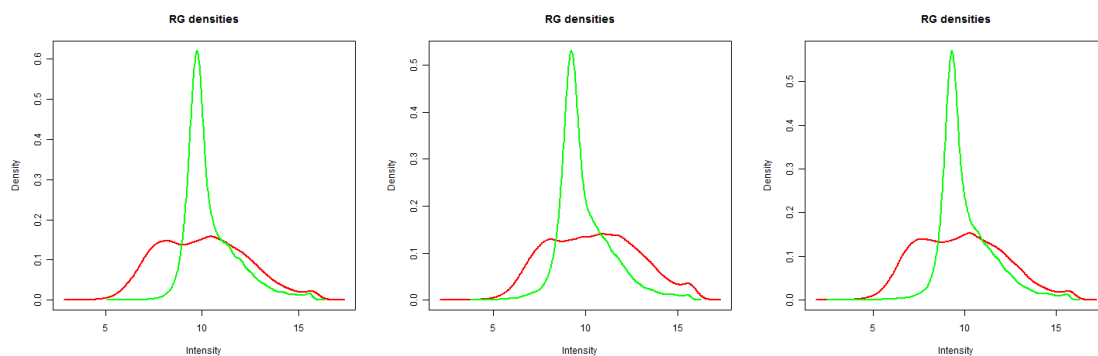
N2A cell line CONTROL



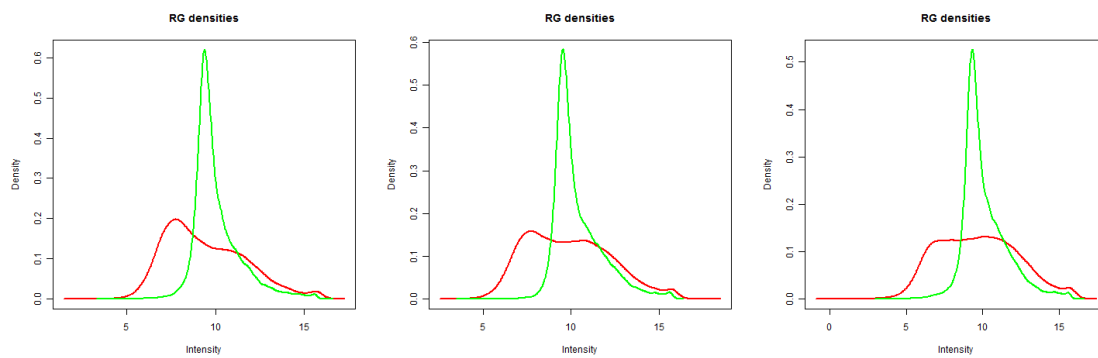
N2A cell line DMSO



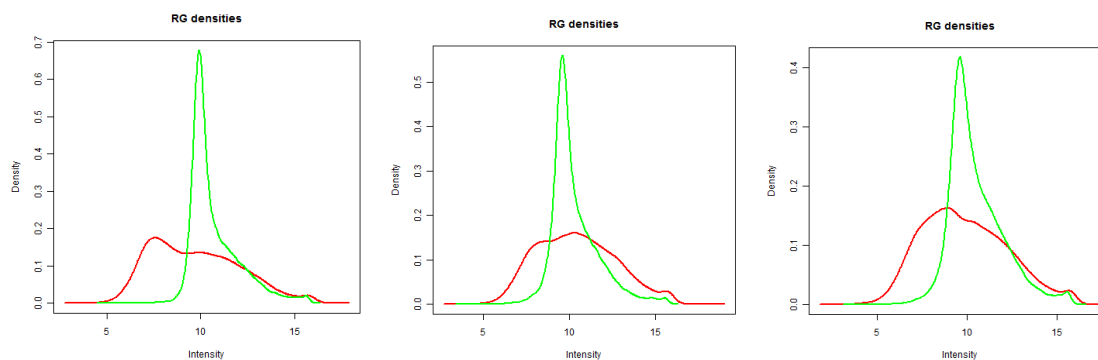
N2A cell line 1 μ M HBCD



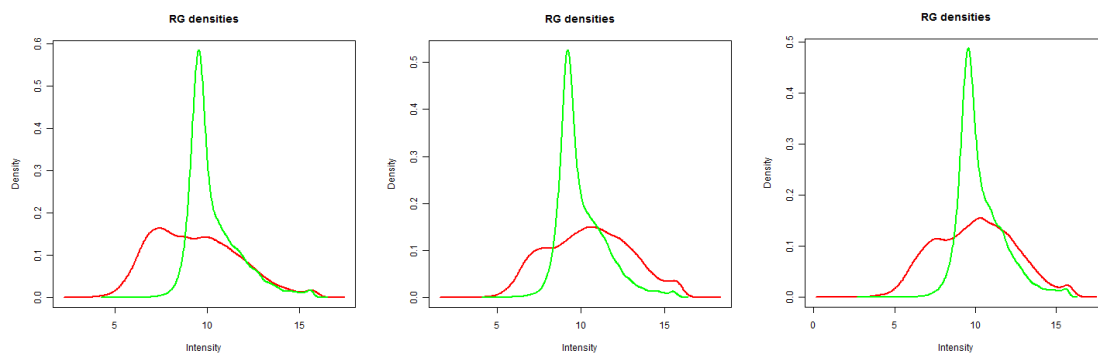
N2A cell line 2 μ M HBCD



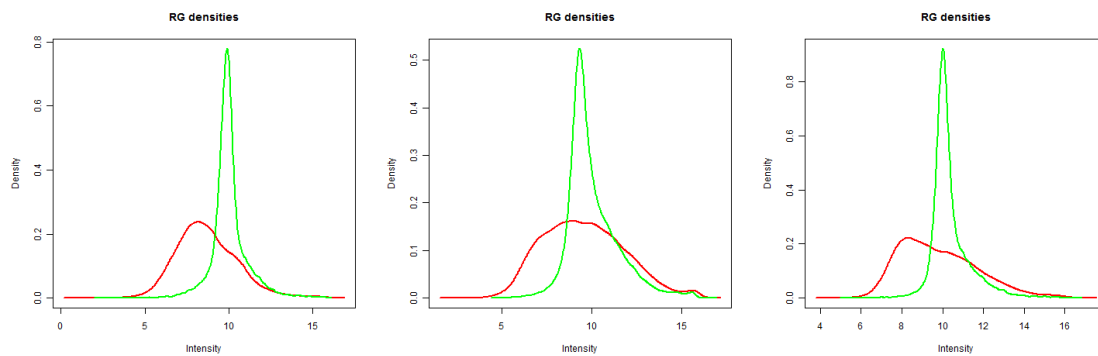
NSC19 cell line CONTROL



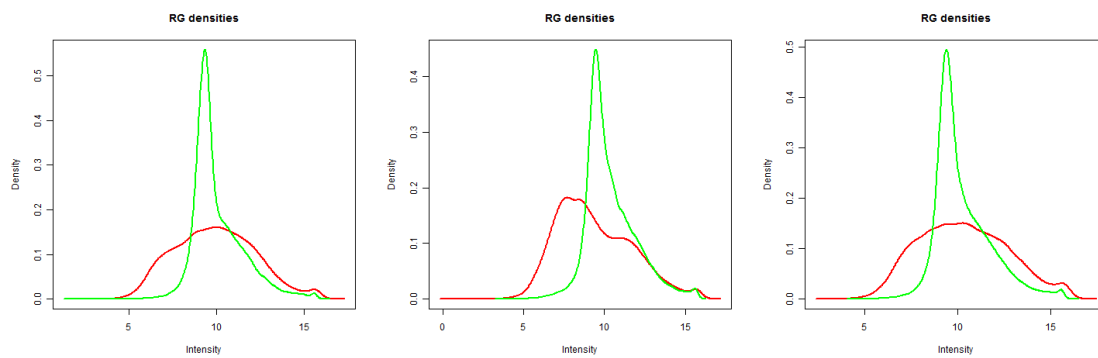
NSC19 cell line DMSO



NSC19 cell line 1 μ M HBCD

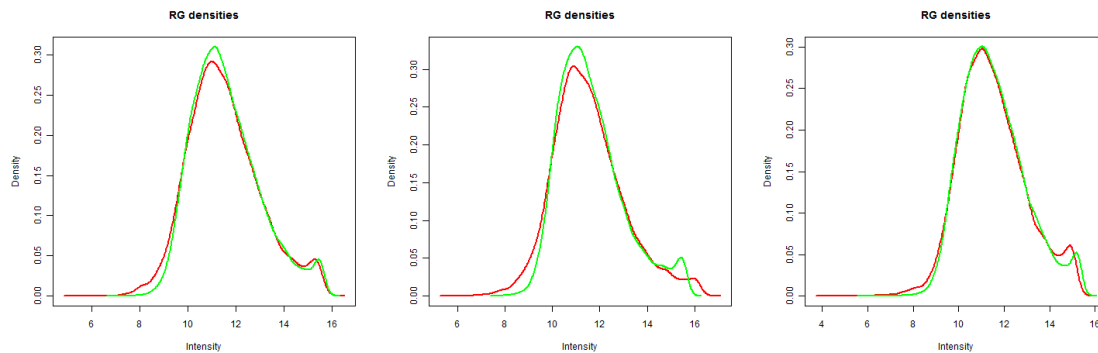


NSC19 cell line 2 μ M HBCD

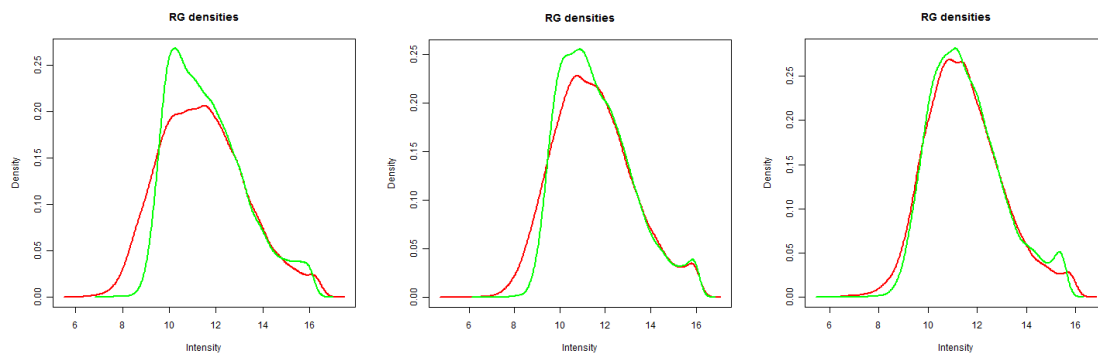


HBCD arrays. Samples after normalisation. Conditions were reproduced in triplicate.

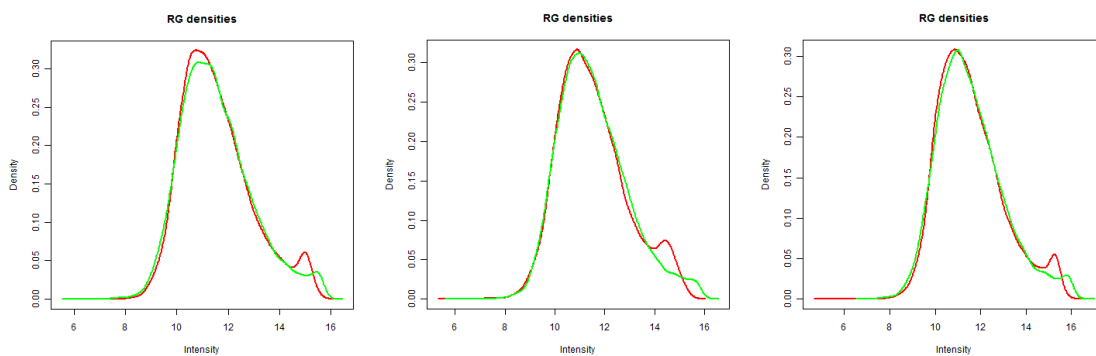
N2A cell line CONTROL



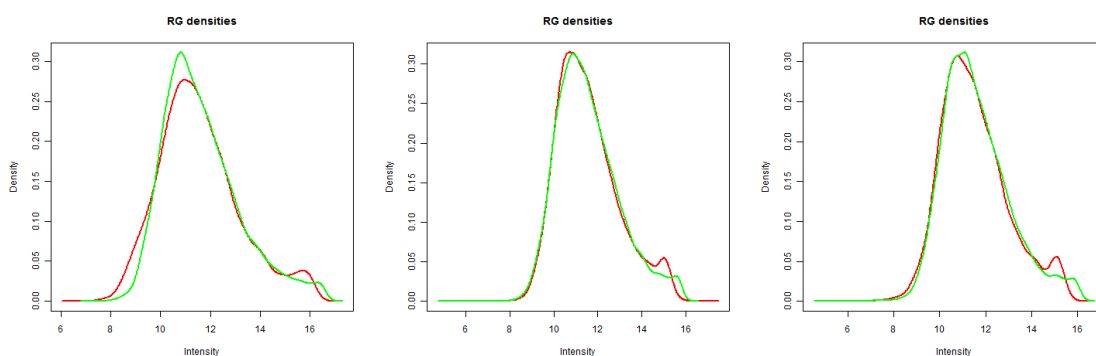
N2A cell line DMSO



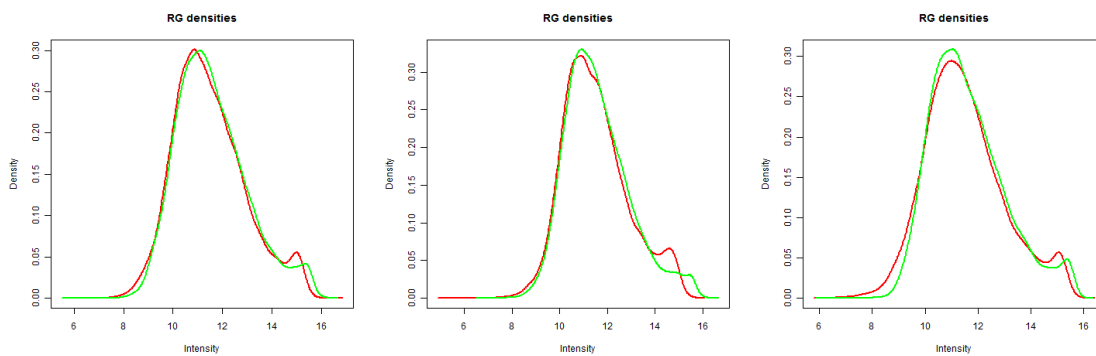
N2A cell line 1 μ M HBCD



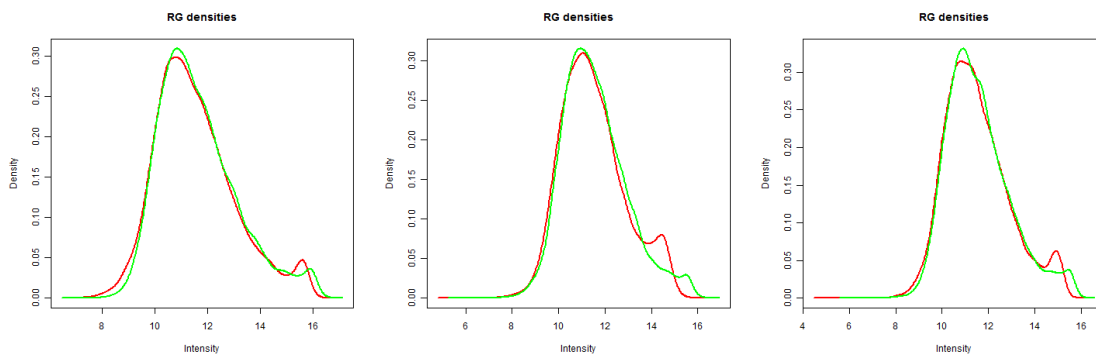
N2A cell line 2 μ M HBCD



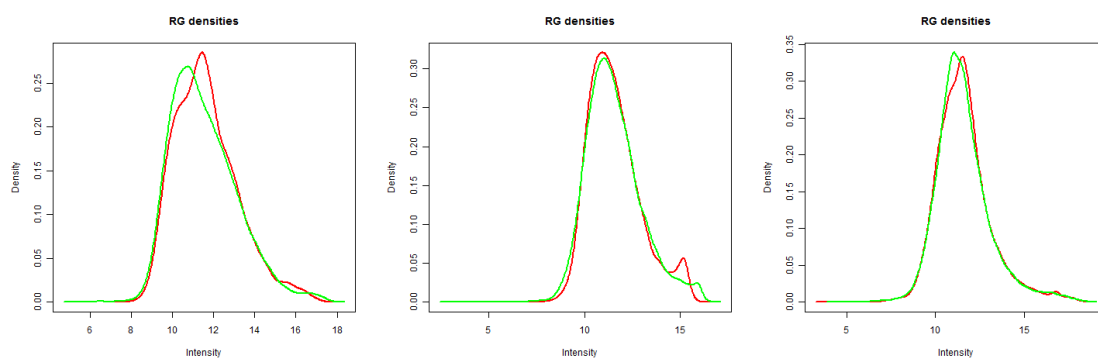
NSC19 cell line CONTROL



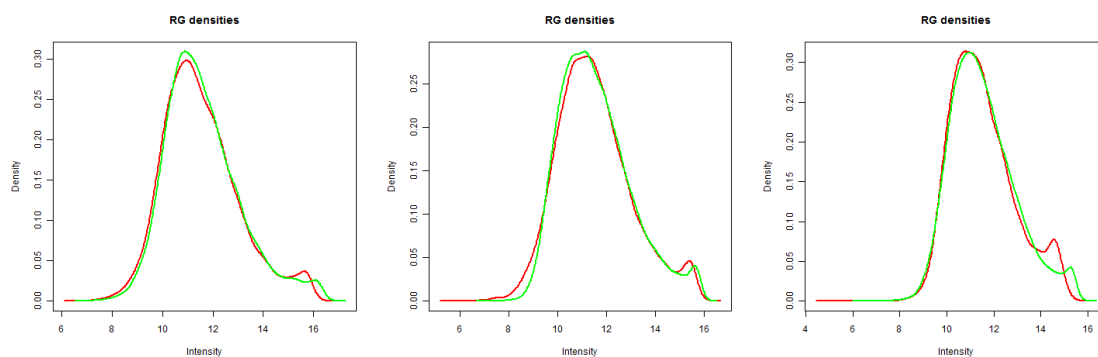
NSC19 cell line DMSO



NSC19 cell line 1 μ M HBCD

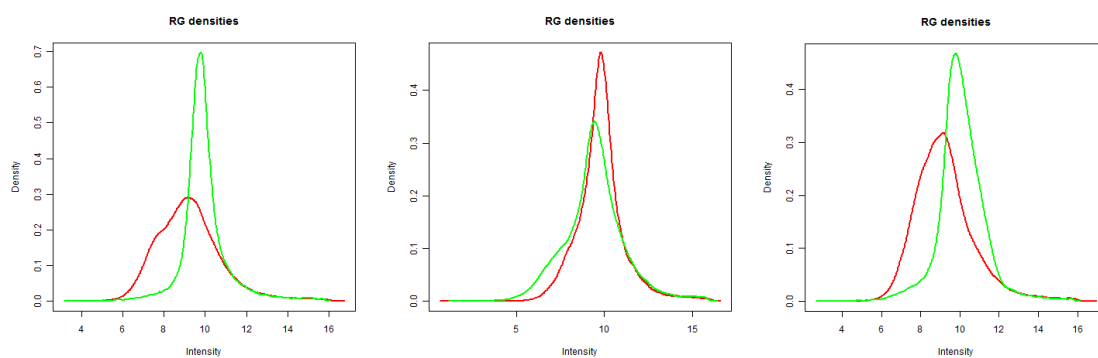


NSC19 cell line 2 μ M HBCD

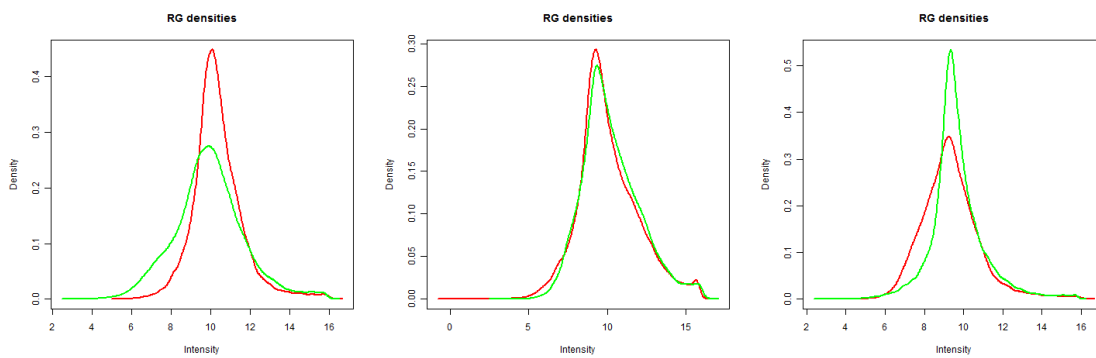


PBDE-47 arrays. Samples before normalisation. Conditions were reproduced in triplicate.

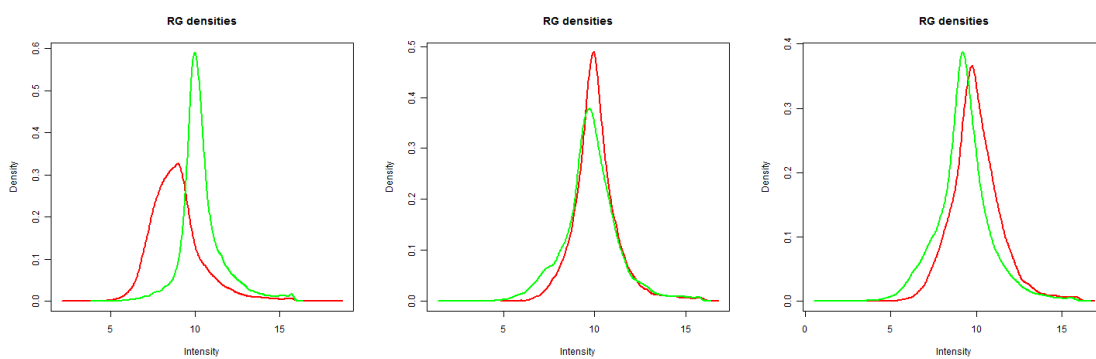
N2A cell line CONTROL



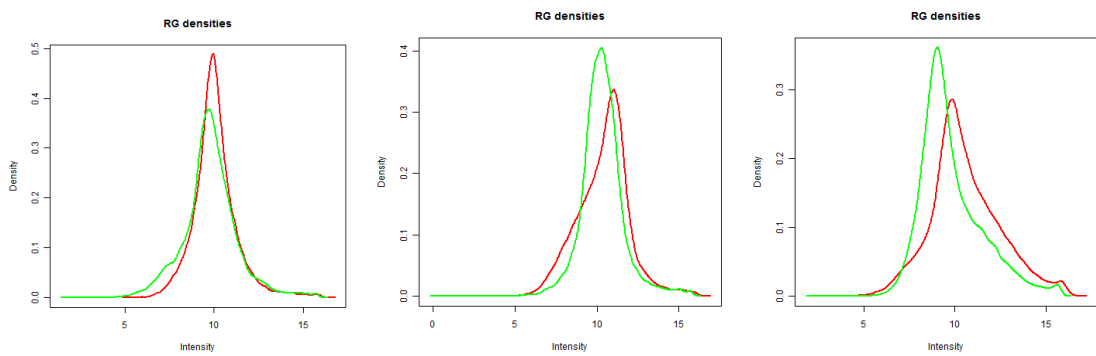
N2A cell line DMSO



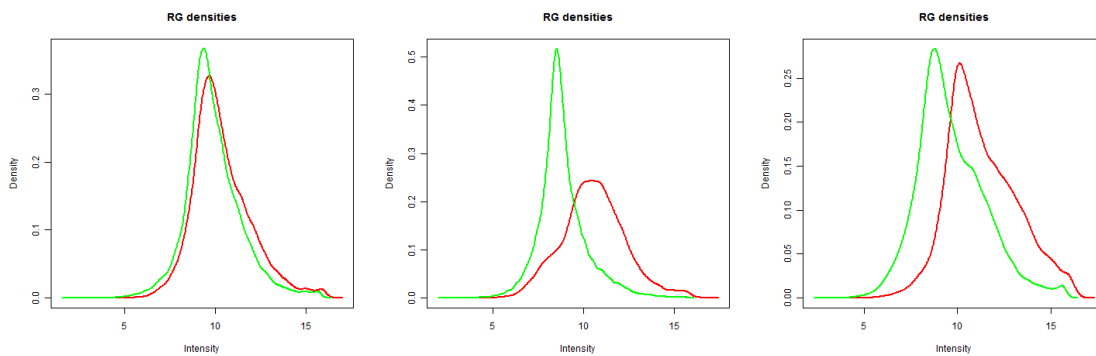
N2A cell line 1 μ M PBDE-47



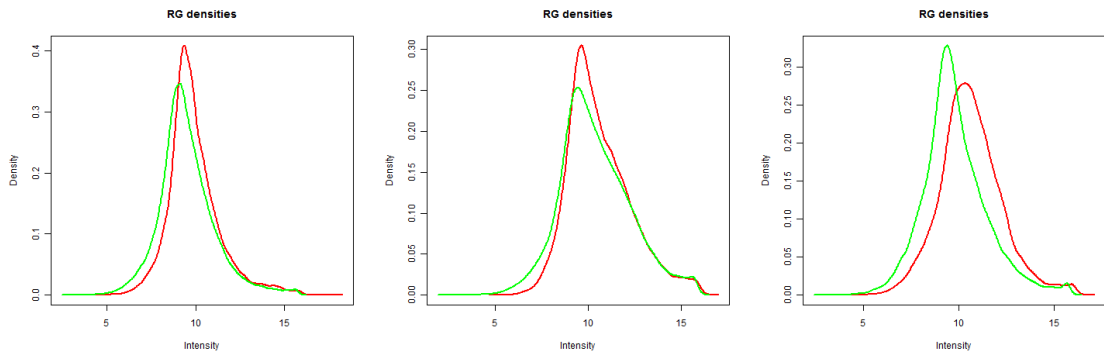
N2A cell line 2 μ M PBDE-47



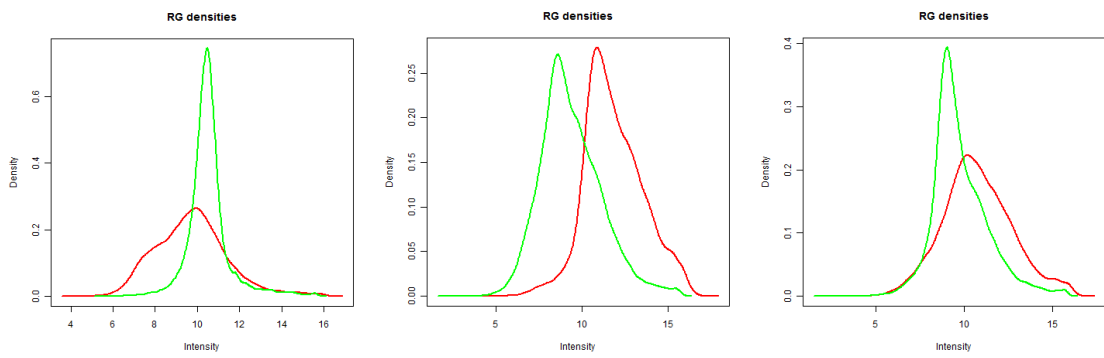
NSC-19 cell line CONTROL



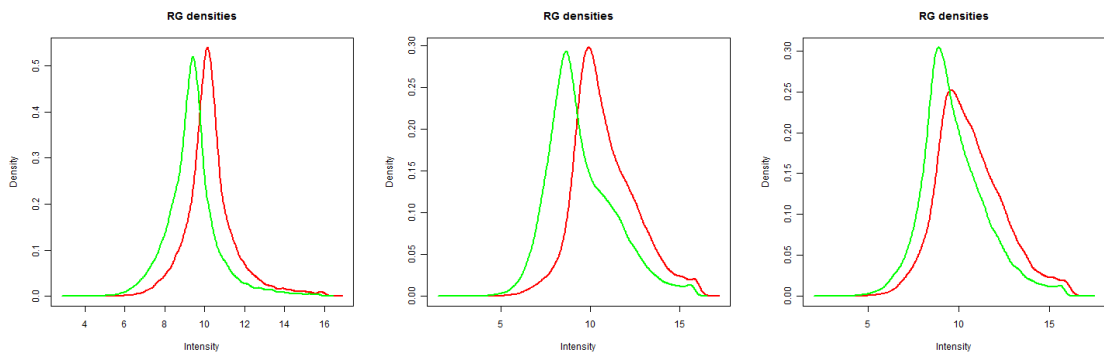
NSC-19 cell line DMSO



NSC-19 cell line 1 μ M PBDE-47

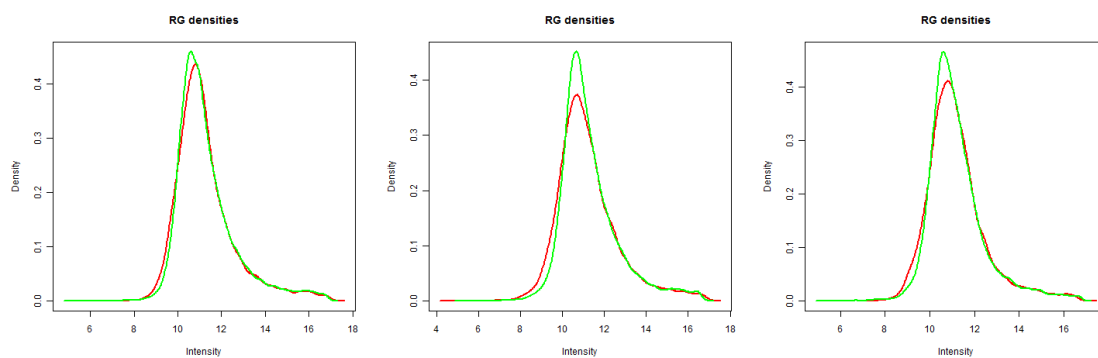


NSC-19 cell line 2 μ M PBDE-47

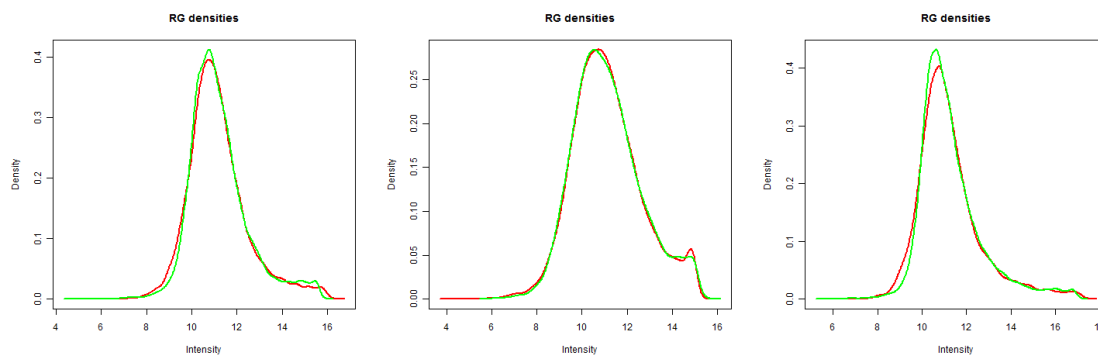


PBDE-47 arrays. Samples after normalisation. Conditions were reproduced in triplicate.

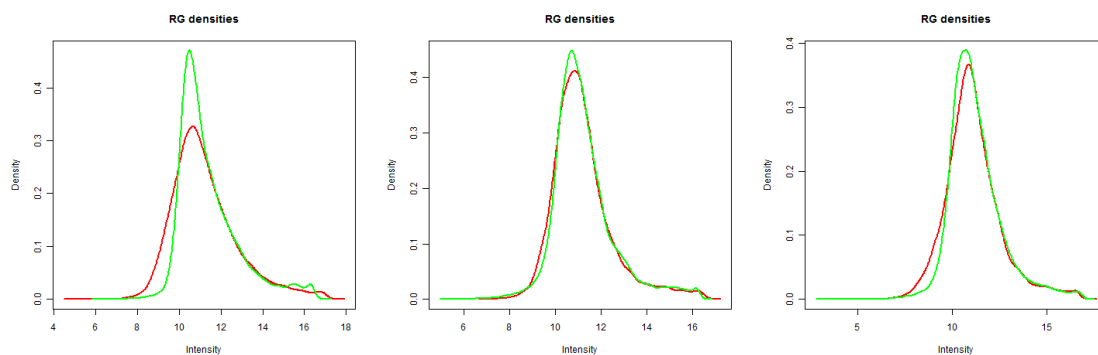
N2A cell line CONTROL



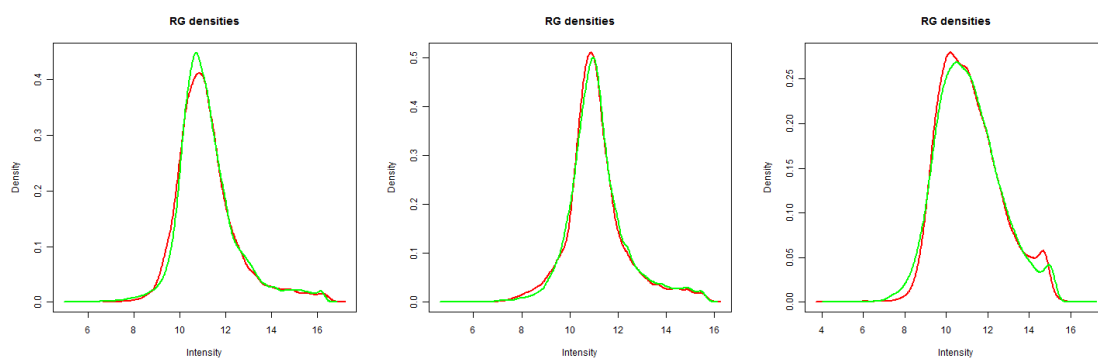
N2A cell line DMSO



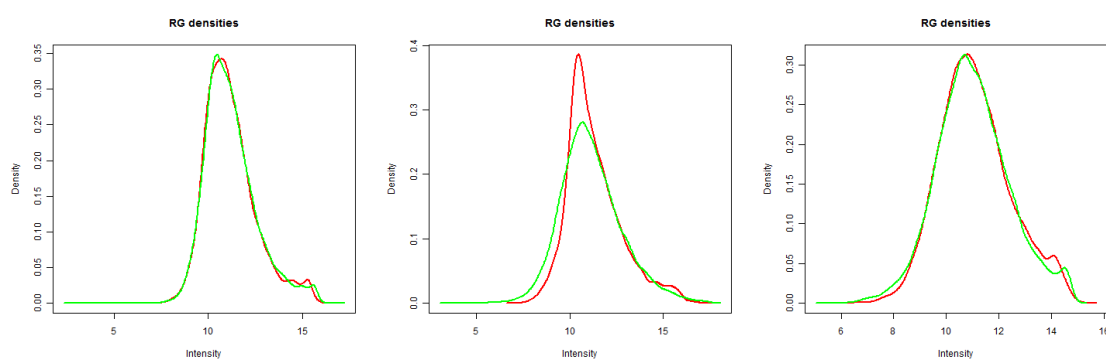
N2A cell line 1 μ M PBDE-47



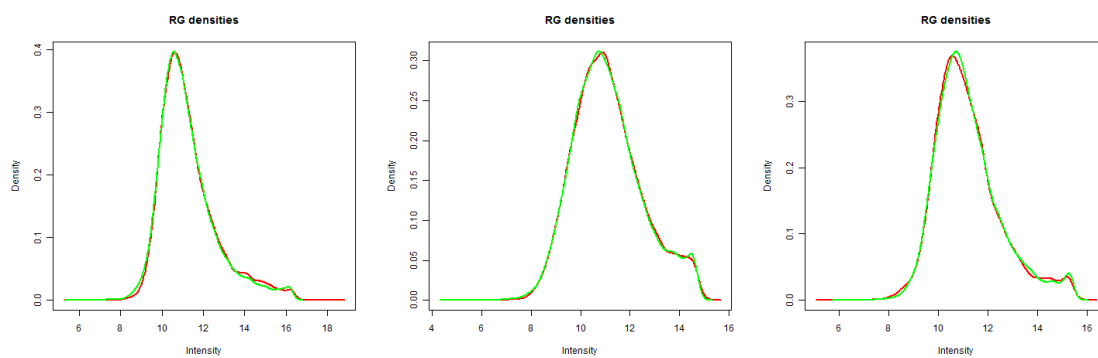
N2A cell line 2 μ M PBDE-47



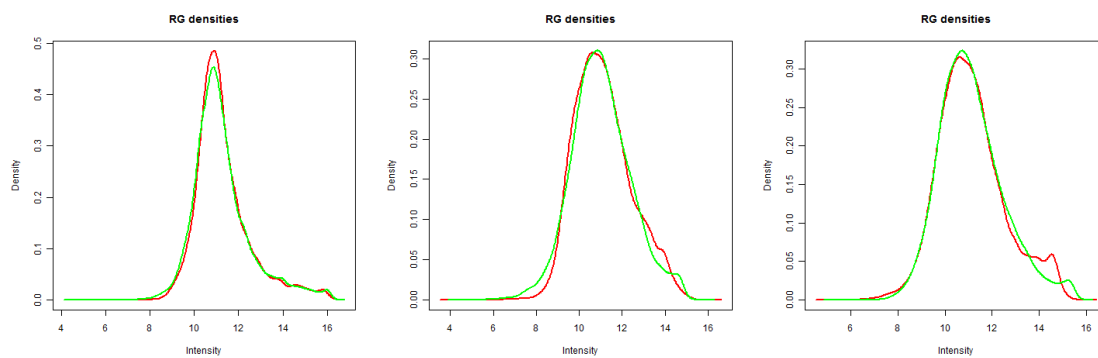
NSC-19 cell line CONTROL



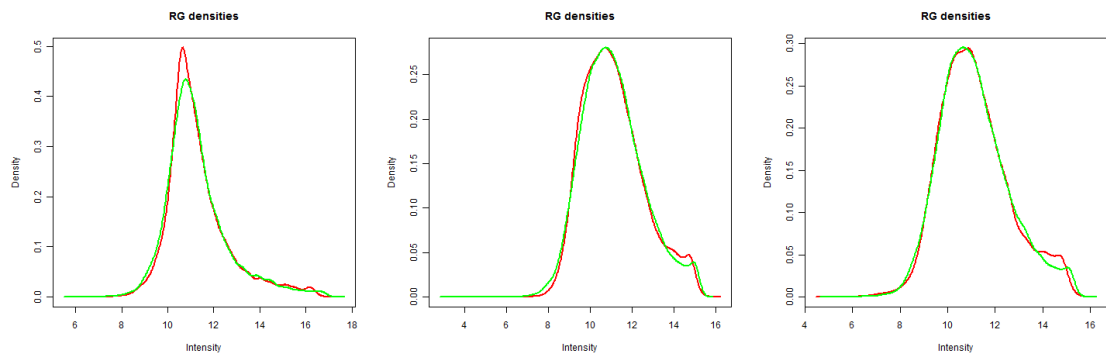
NSC-19 cell line DMSO



NSC-19 cell line 1 μ M PBDE-47



NSC-19 cell line 2 μ M PBDE-47

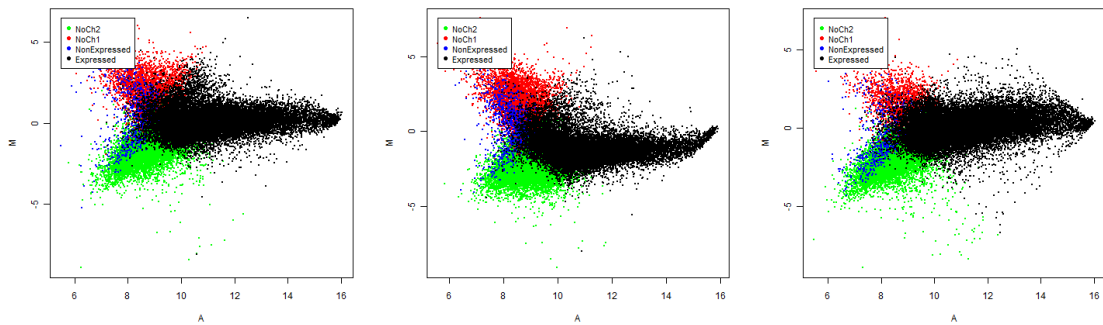


Appendix 3

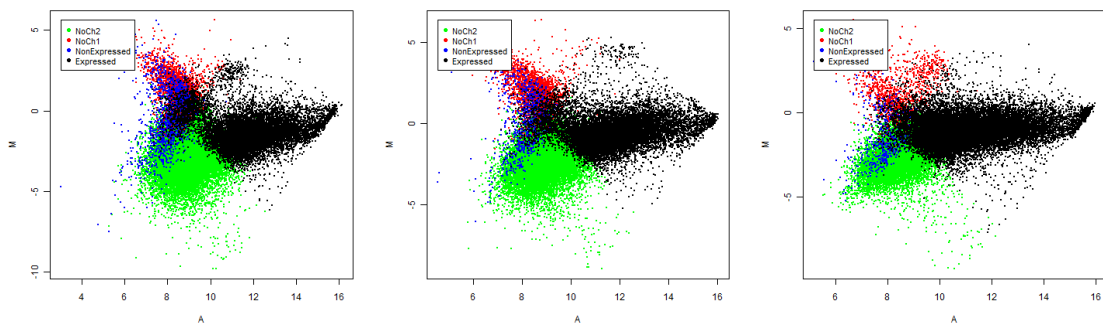
MA plots created by LIMMA before and after normalisation

HBCD arrays. Samples 1-24 before normalisation. Conditions were reproduced in triplicate.

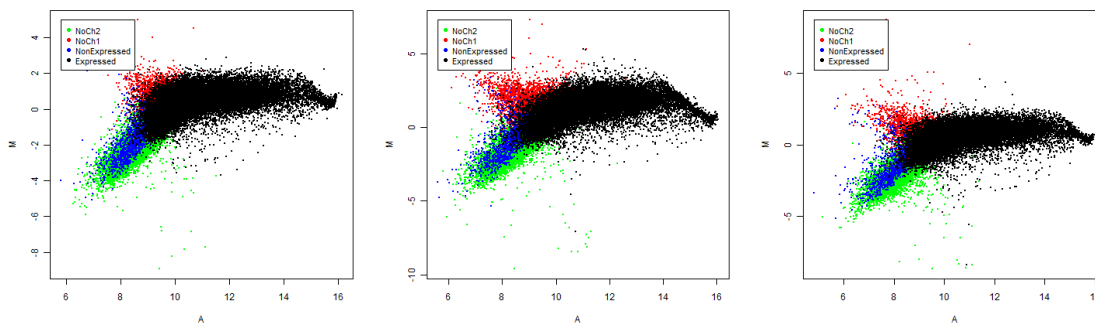
N2A cell line CONTROL



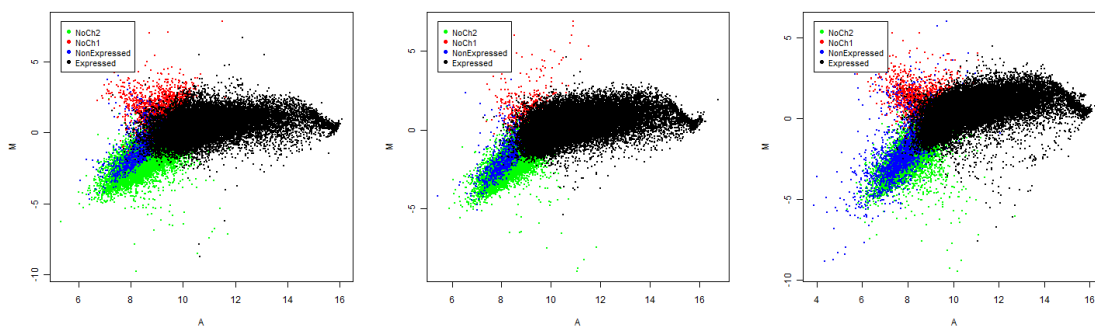
N2A cell line DMSO



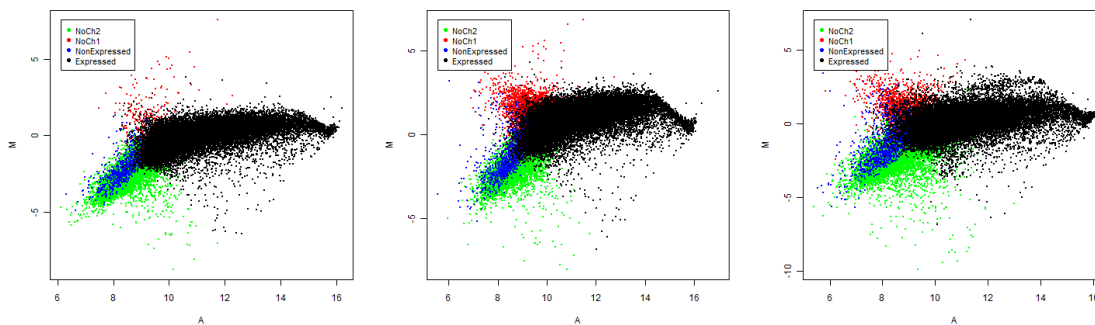
N2A cell line 1 μ M HBCD



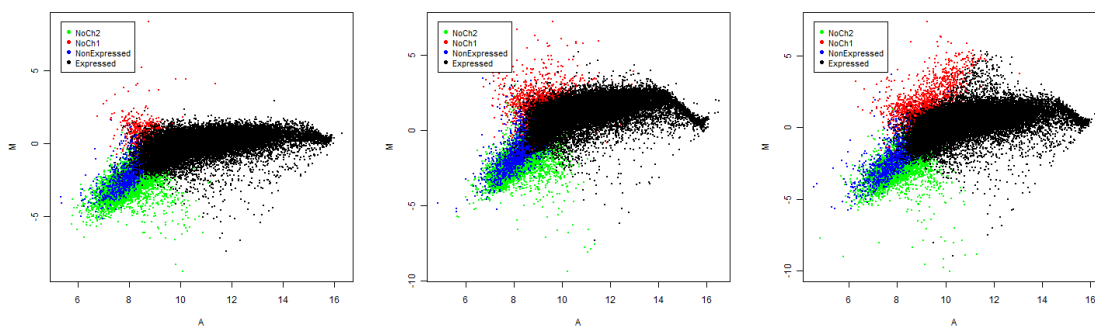
N2A cell line 2 μ M HBCD



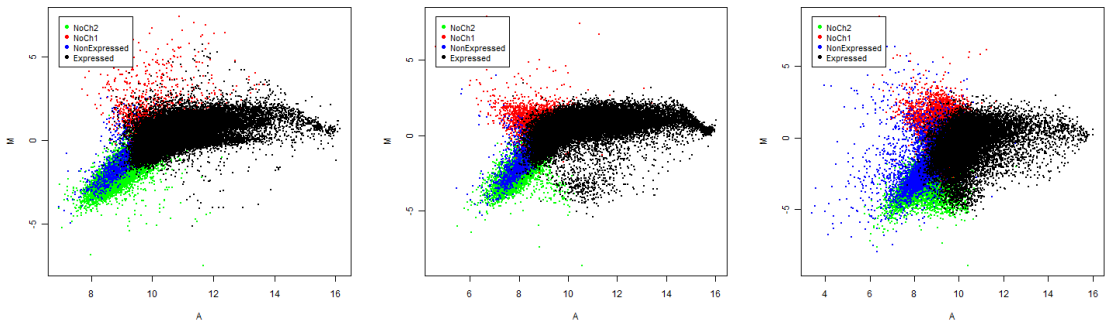
NSC-19 cell line CONTROL



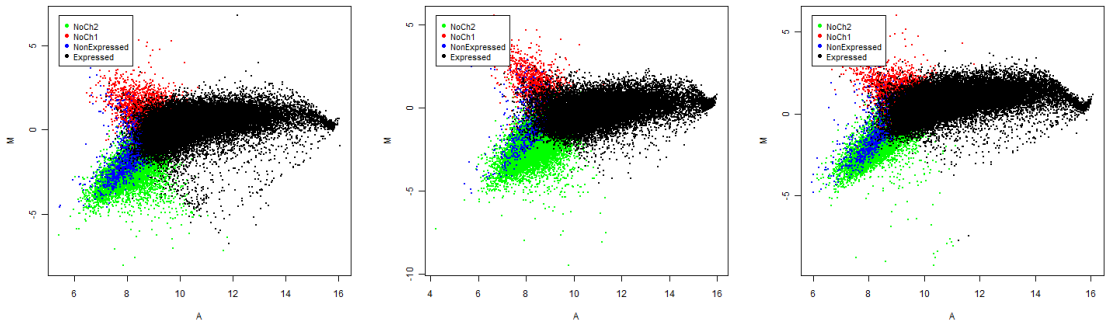
NSC-19 cell line DMSO



NSC-19 cell line 1 μ M HBCD

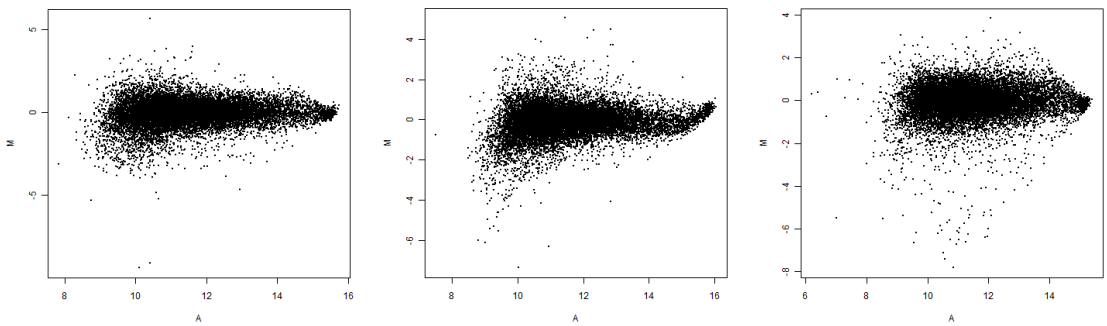


NSC-19 cell line 2 μ M HBCD

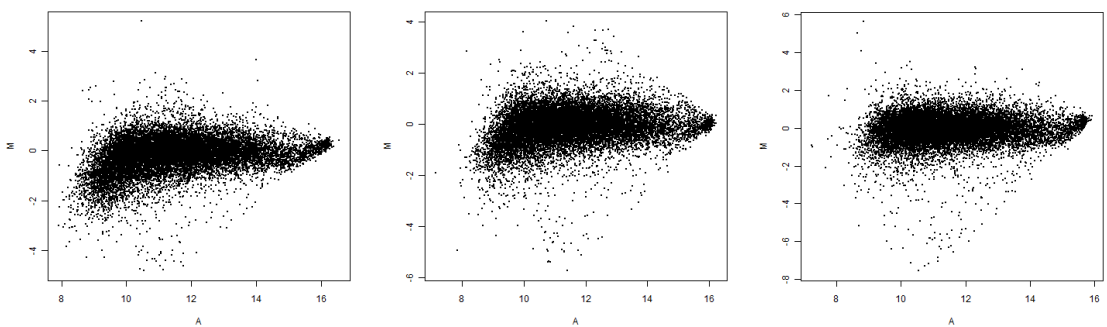


HBCD arrays. Samples 1-30 after normalisation. Conditions were reproduced in triplicate.

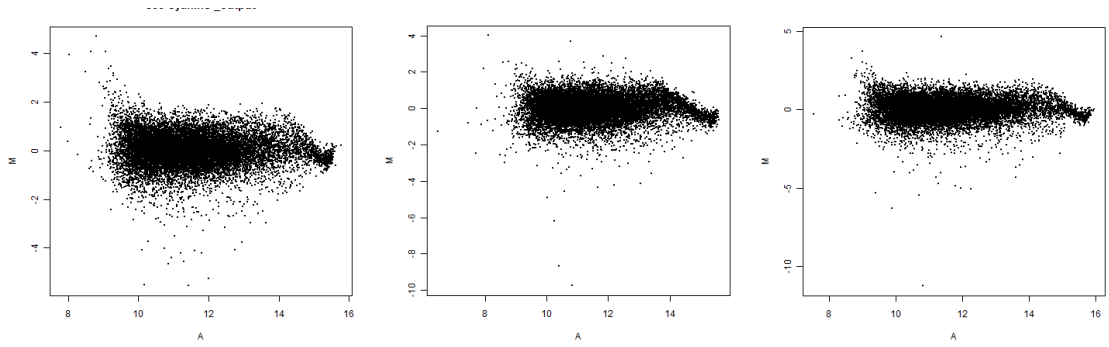
N2A cell line CONTROL



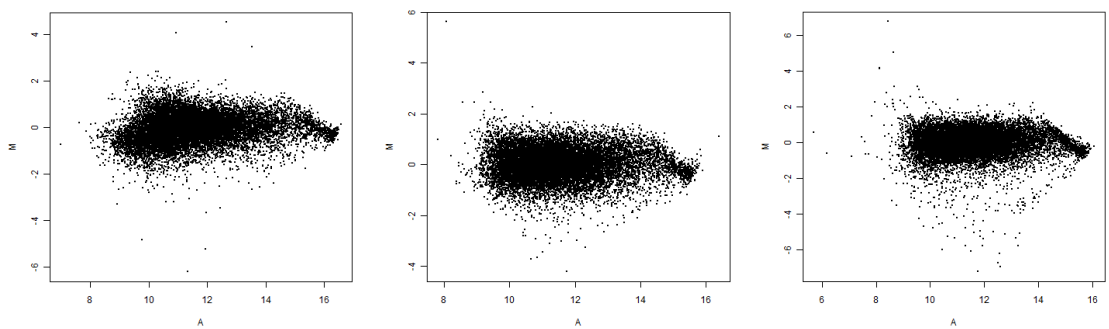
N2A cell line DMSO



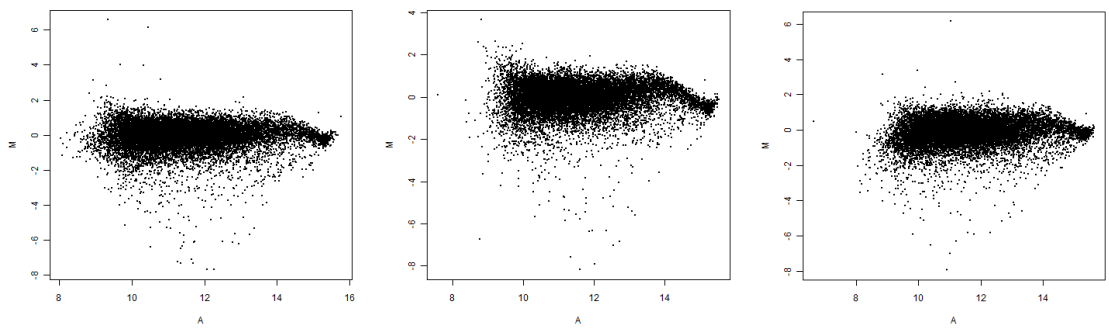
N2A cell line 1 μ M HBCD



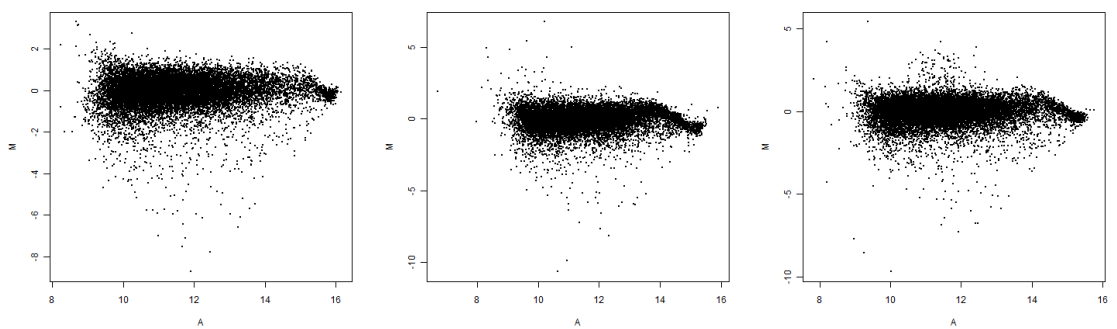
N2A cell line 2 μ M HBCD



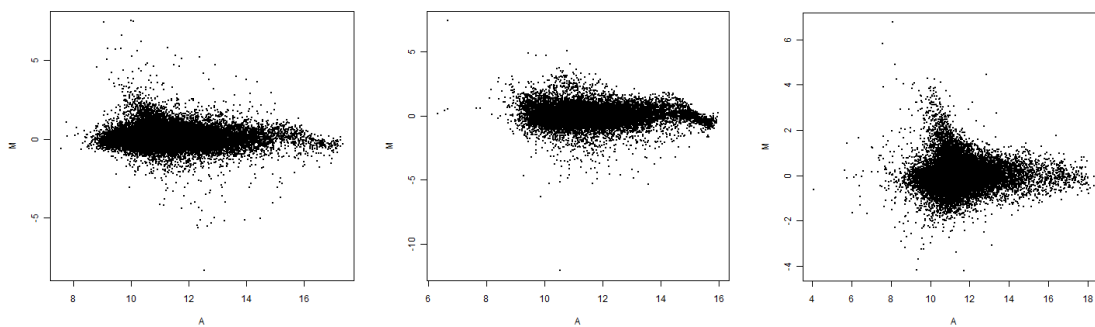
NSC-19 cell line CONTROL



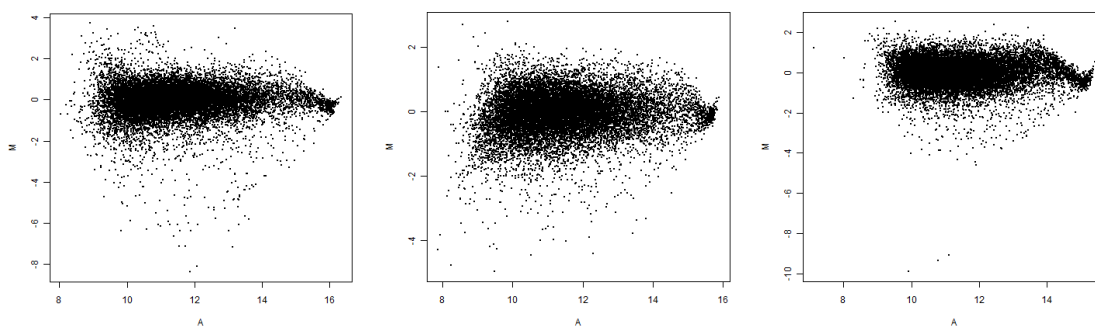
NSC-19 cell line DMSO



NSC-19 cell line 1 μ M HBCD

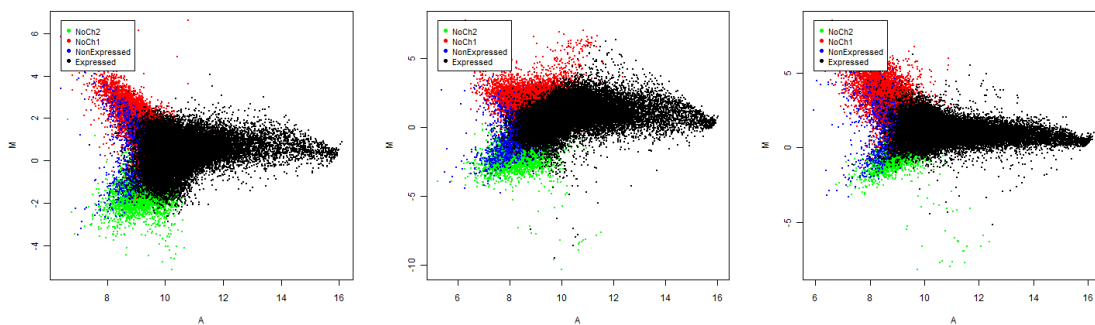


NSC-19 cell line 2 μ M HBCD

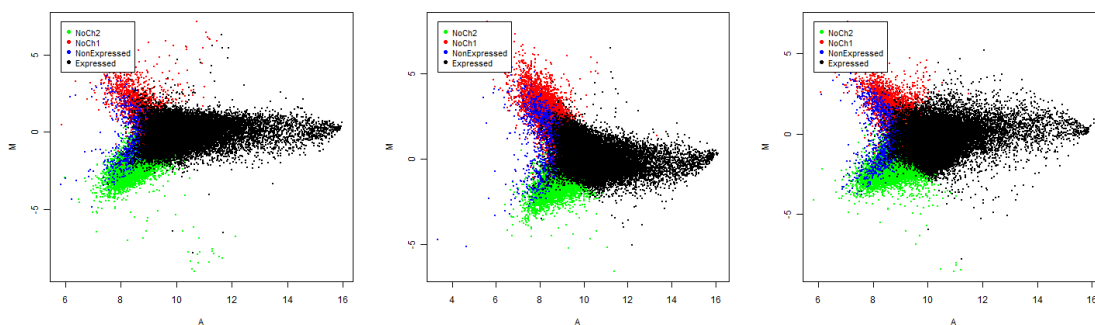


PBDE-47 arrays. Samples 1-30 before normalisation. Conditions were reproduced in triplicate.

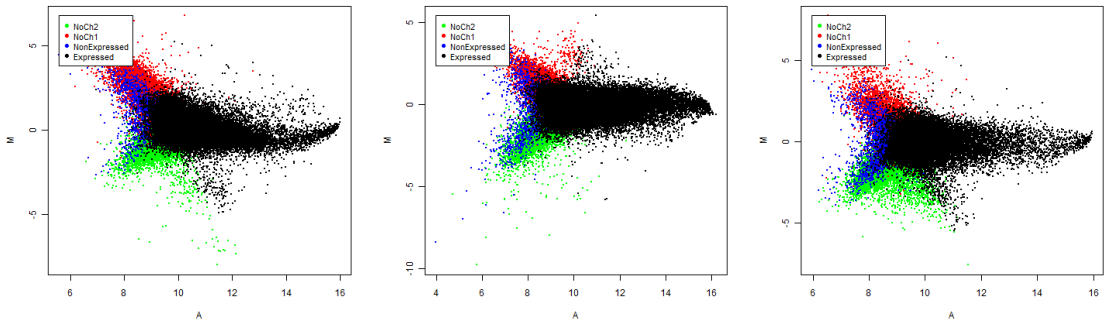
N2A cell line CONTROL



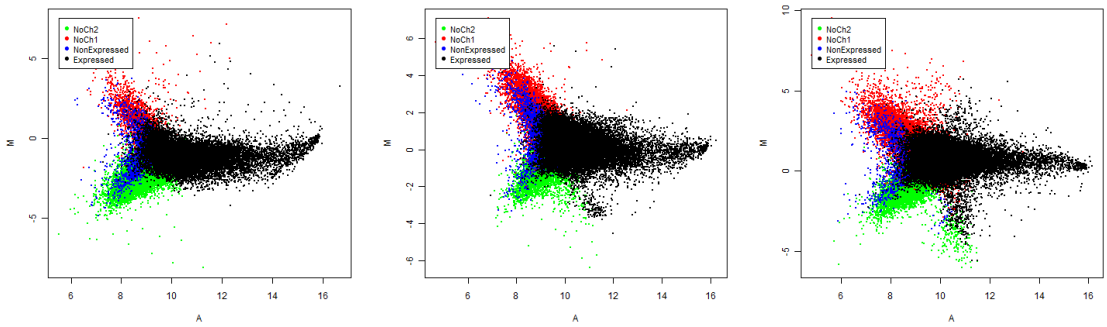
N2A cell line DMSO



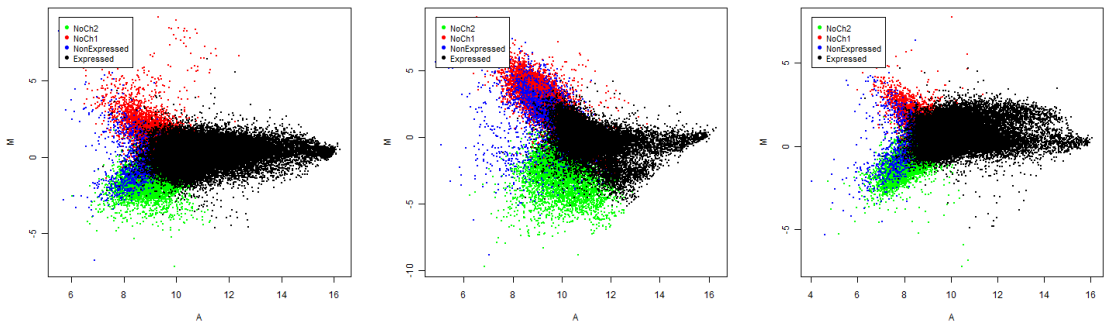
N2A cell line 1 μ M PBDE-47



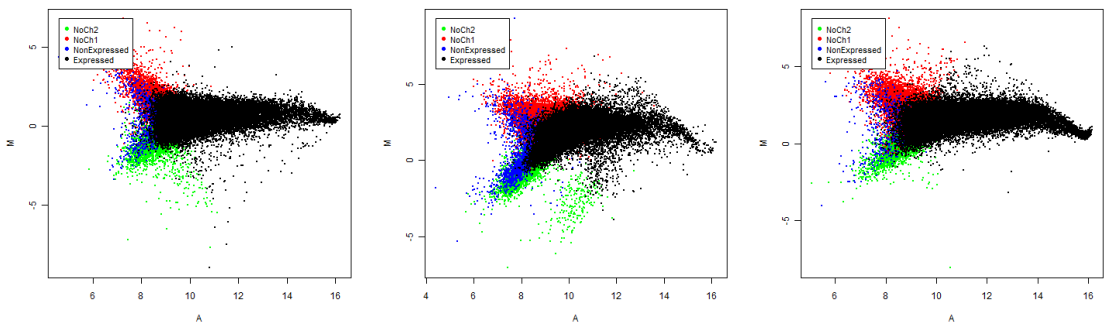
N2A cell line 2 μ M PBDE-47



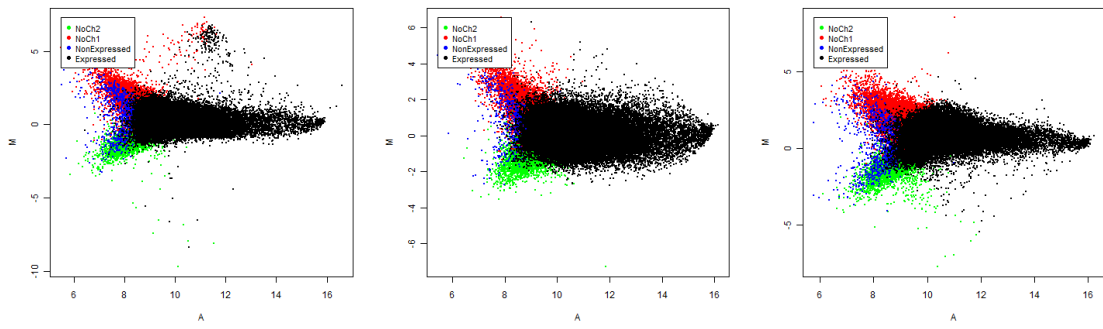
NSC-19 cell line CONTROL



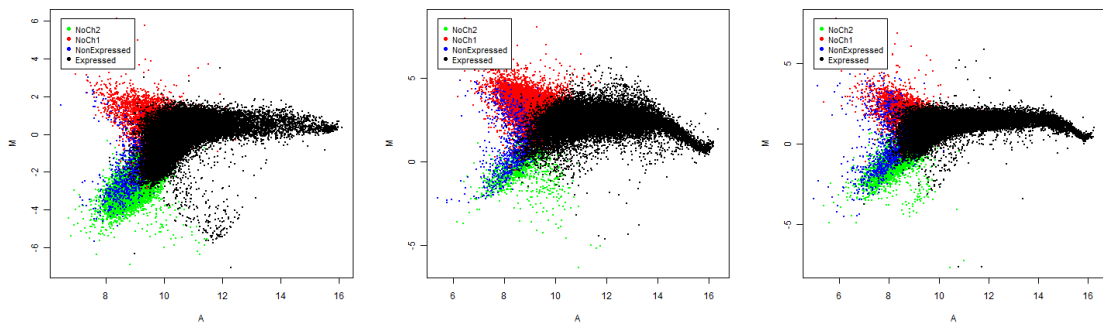
NSC-19 cell line DMSO



NSC-19 cell line 1 μ M PBDE-47

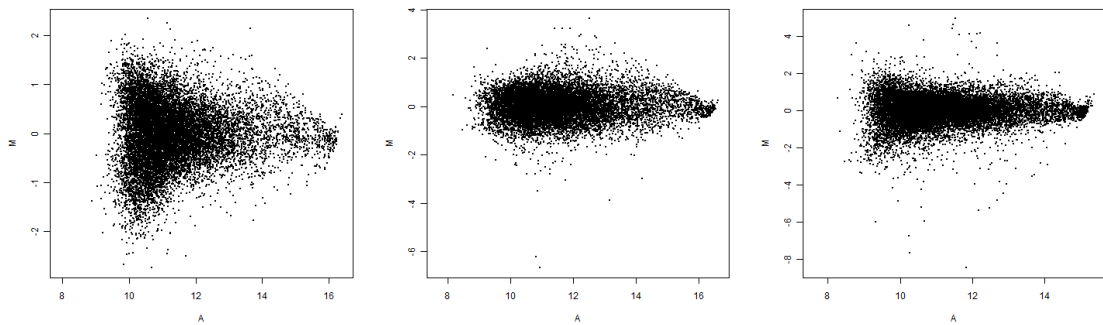


NSC-19 cell line 2 μ M PBDE-47

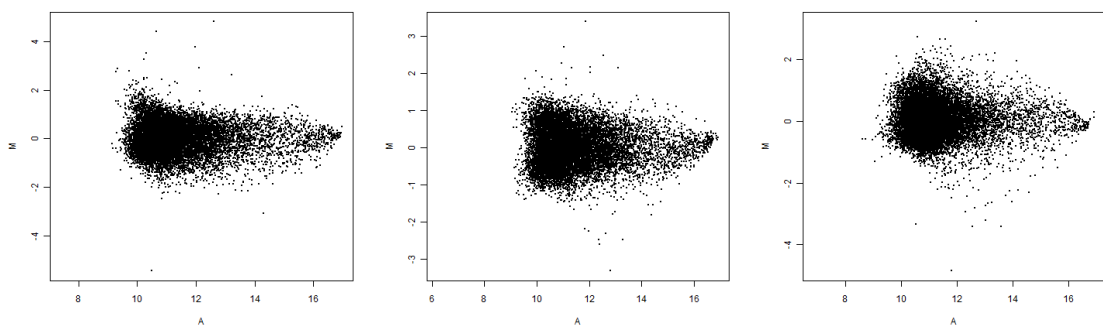


PBDE-47 arrays. Samples 1-30 after normalisation. Conditions were reproduced in triplicate.

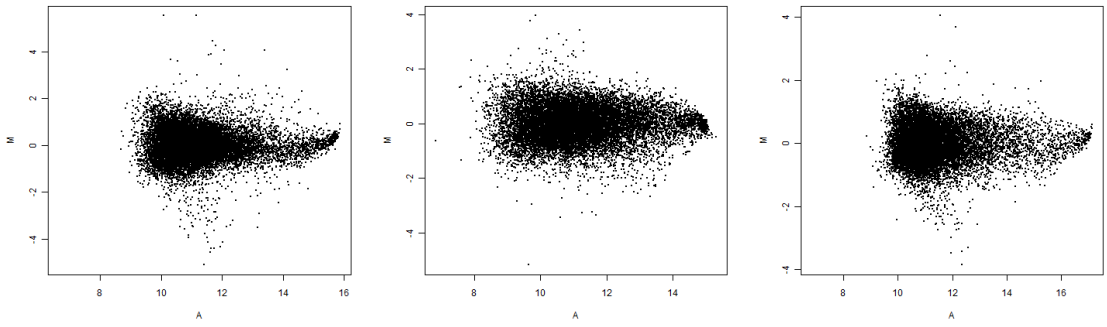
N2A cell line CONTROL



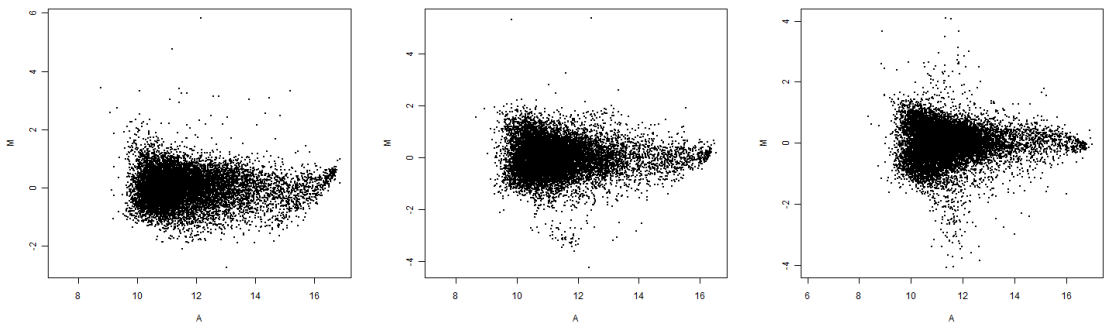
N2A cell line DMSO



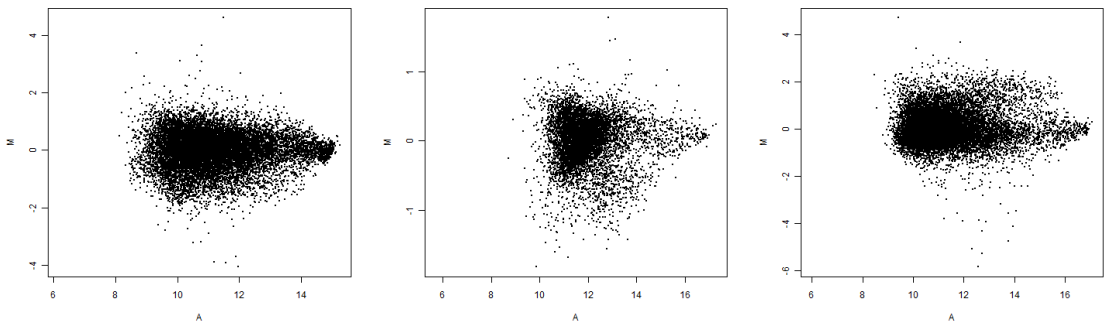
N2A cell line 1 μ M PBDE-47



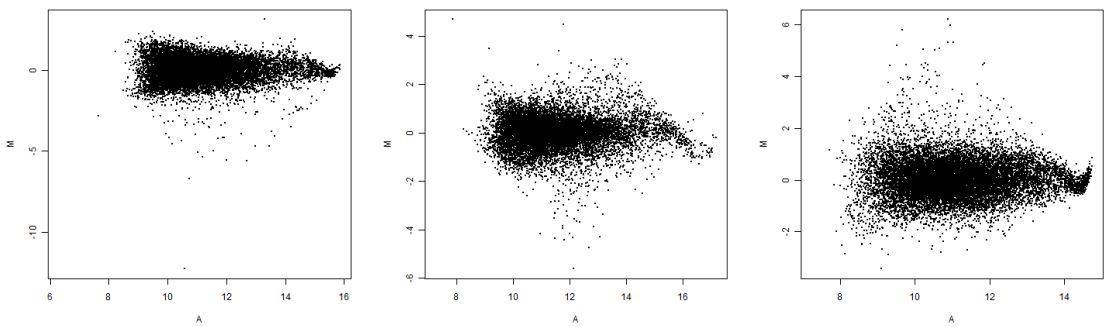
N2A cell line 2 μ M PBDE-47



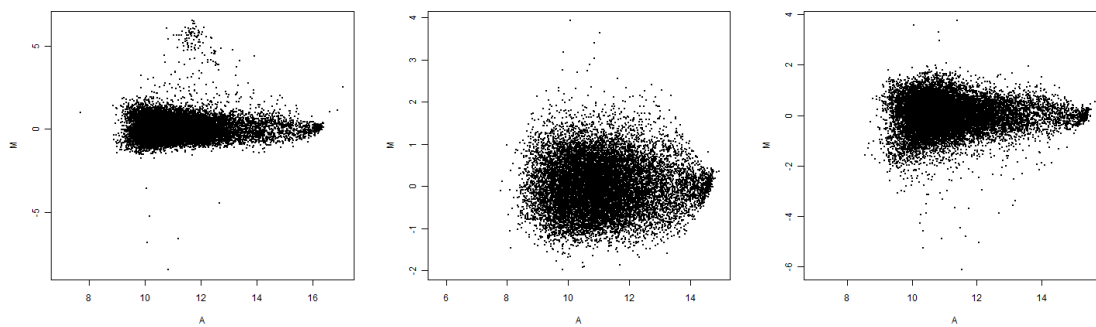
NSC-19 cell line CONTROL



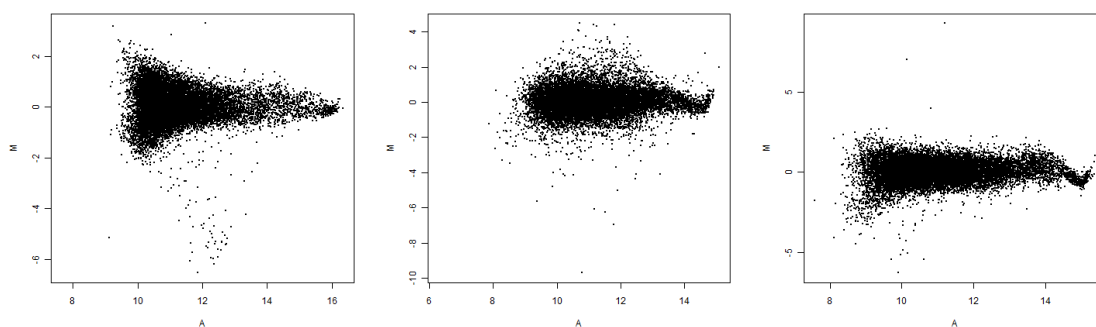
NSC-19 cell line DMSO



NSC-19 cell line 1 μ M PBDE-47



NSC-19 cell line 2 μ M PBDE-47



References

- Ahmed, R. R., et al. 'BACE1 and BACE2 enzymatic activities in Alzheimer's disease', *Journal of Neurochemistry*, 112 (4), 1045-53.
- Alaee, M., et al. (2003a), 'An overview of commercially used brominated flame retardants, their applications, their use patterns in different countries/regions and possible modes of release', *Environ Int*, 29 (6), 683-9.
- (2003b), 'An overview of commercially used brominated flame retardants, their applications, their use patterns in different countries/regions and possible modes of release', *Environment International*, 29 (6), 683-89.
- Alm, H., et al. (2008), 'Exposure to brominated flame retardant PBDE-99 affects cytoskeletal protein expression in the neonatal mouse cerebral cortex', *Neurotoxicology*, 29 (4), 628-37.
- Anantharam, V., et al. (2007), 'Microarray analysis of oxidative stress regulated genes in mesencephalic dopaminergic neuronal cells: Relevance to oxidation damage in Parkinson's disease', *Neurochemistry International*, 50 (6), 834-47.
- Andreini, C., et al. (2006), 'Counting the zinc-proteins encoded in the human genome', *J Proteome Res*, 5 (1), 196-201.
- Anonymous 'Liver defect likely cause of DHA deficiency in Alzheimer's patients', *Clinical Lipidology*, 5 (5), 612-12.
- AppliedBiosystems (2008), 'Real-Time PCR: Understanding C_T'.
- Apraiz, I., Mi, J., and Cristobal, S. (2006), 'Identification of proteomic signatures of exposure to marine pollutants in mussels (*Mytilus edulis*)', *Molecular & Cellular Proteomics*, 5 (7), 1274-85.
- Arnal, E., et al. (2010), 'Lutein and docosahexaenoic acid prevent cortex lipid peroxidation in streptozotocin-induced diabetic rat cerebral cortex', *Neuroscience*, 166 (1), 271-8.
- Ashburner, M., et al. (2000), 'Gene Ontology: tool for the unification of biology', *Nature Genetics*, 25 (1), 25-29.
- Athanasiadou, M., et al. (2008), 'Polybrominated diphenyl ethers (PBDEs) and bioaccumulative hydroxylated PBDE metabolites in young humans from Managua, Nicaragua', *Environ Health Perspect*, 116 (3), 400-8.
- Augustine, G. J., Santamaria, F., and Tanaka, K. (2003), 'Local calcium signaling in neurons', *Neuron*, 40 (2), 331-46.
- Azkona, G., et al. (2010), 'Characterization of a mouse model overexpressing beta-site APP-cleaving enzyme 2 reveals a new role for BACE2', *Genes Brain Behav*, 9 (2), 160-72.
- Balbus, J. M. (2005), 'Ushering in the new toxicology: Toxicogenomics and the public interest', *Environmental Health Perspectives*, 113 (7), 818-22.

- Bank, P. A., Salyers, K. L., and Zile, M. H. (1989), 'Effect of tetrachlorodibenzo-p-dioxin (TCDD) on the glucuronidation of retinoic acid in the rat', *Biochim Biophys Acta*, 993 (1), 1-6.
- Barcelo-Coblijn, G., et al. (2003), 'Gene expression and molecular composition of phospholipids in rat brain in relation to dietary n-6 to n-3 fatty acid ratio', *Biochim Biophys Acta*, 1632 (1-3), 72-9.
- Barter, R. A. and Klaassen, C. D. (1994), 'Reduction of thyroid hormone levels and alteration of thyroid function by four representative UDP-glucuronosyltransferase inducers in rats', *Toxicol Appl Pharmacol*, 128 (1), 9-17.
- Basi, G., et al. (2002), 'Cellular knock-out of endogenous BACE2 reveals its role in APP processing homeostasis of A beta production in cells co-expressing BACE1 and BACE2', *Neurobiology of Aging*, 23 (1), 668.
- Baulande, S. and Langlois, C. 'Proteins sharing PNPLA domain, a new family of enzymes regulating lipid metabolism', *M S-Medecine Sciences*, 26 (2), 177-84.
- Bazan, N. G. (2005), 'Neuroprotectin D1 (NPD1): A DHA-derived mediator that protects brain and retina against cell injury-induced oxidative stress', *Brain Pathology*, 15 (2), 159-66.
- Becher, G. (2005), 'The stereochemistry of 1,2,5,6,9,10-hexabromocyclododecane and its graphic representation', *Chemosphere*, 58 (7), 989-91.
- Bennett, B. D., et al. (2000), 'Expression analysis of BACE2 in brain and peripheral tissues', *J Biol Chem*, 275 (27), 20647-51.
- Binda, O., Nassif, C., and Branton, P. E. (2008), 'SIRT1 negatively regulates HDAC1-dependent transcriptional repression by the RBP1 family of proteins', *Oncogene*, 27 (24), 3384-92.
- Birch, E. E., et al. (2000), 'A randomized controlled trial of early dietary supply of long-chain polyunsaturated fatty acids and mental development in term infants', *Developmental Medicine and Child Neurology*, 42 (3), 174-81.
- Birnbaum, L. S. and Staskal, D. F. (2004a), 'Brominated flame retardants: Cause for concern?', *Environmental Health Perspectives*, 112 (1), 9-17.
- (2004b), 'Brominated flame retardants: cause for concern?', *Environ Health Perspect*, 112 (1), 9-17.
- Bitanhirwe, B. K. Y. and Cunningham, M. G. (2009), 'Zinc: The Brain's Dark Horse', *Synapse*, 63 (11), 1029-49.
- Boucher, O., et al. (2011), 'Neurophysiologic and neurobehavioral evidence of beneficial effects of prenatal omega-3 fatty acid intake on memory function at school age', *Am J Clin Nutr*, 93 (5), 1025-37.
- Bradshaw, J. M., Hudmon, A., and Schulman, H. (2002), 'Chemical quenched flow kinetic studies indicate an intraholoenzyme autophosphorylation mechanism for Ca²⁺/calmodulin-dependent protein kinase II', *Journal of Biological Chemistry*, 277 (23), 20991-98.

- Brazma, A. and Vilo, J. (2000), 'Gene expression data analysis', *Febs Letters*, 480 (1), 17-24.
- Brown, Kenneth H., Wuehler, Sara E., and Peerson, Jan M. (2001), 'The importance of zinc in human nutrition and estimation of the global prevalence of zinc deficiency', *Food and Nutrition Bulletin*, 22 (2), 113-25.
- Cambridgebluegenome (2008), '<http://www.cambridgebluegenome.com/bluefuse.htm>' (consulted 25September 2008)'.
- Canton, R. F., et al. (2008), 'Subacute effects of hexabromocyclododecane (HBCD) on hepatic gene expression profiles in rats', *Toxicology and Applied Pharmacology*, 231 (2), 267-72.
- Cao, D. H., et al. (2009), 'Docosahexaenoic acid promotes hippocampal neuronal development and synaptic function', *Journal of Neurochemistry*, 111 (2), 510-21.
- Carroll, T. (2011), 'Transcriptomic Analysis of the Neurotoxicity of Relevant Persistent Organic Pollutants in a Salmon-based Diet', *PhD thesis*
- Cashman, N. R., et al. (1992), 'NEUROBLASTOMA X SPINAL-CORD (NSC) HYBRID CELL-LINES RESEMBLE DEVELOPING MOTOR NEURONS', *Developmental Dynamics*, 194 (3), 209-21.
- Chen, C. M., et al. (2008), 'HSPA5 promoter polymorphisms and risk of Parkinson's disease in Taiwan', *Neuroscience Letters*, 435 (3), 219-22.
- Chiaro, C. R., et al. (2007), 'Evidence for an aryl hydrocarbon receptor-mediated cytochrome p450 autoregulatory pathway', *Mol Pharmacol*, 72 (5), 1369-79.
- Chou, C. T., et al. (2010), 'Chronic exposure of 2,2',4,4'-tetrabromodiphenyl ether (PBDE-47) alters locomotion behavior in juvenile zebrafish (*Danio rerio*)', *Aquat Toxicol*, 98 (4), 388-95.
- Chung, Kenny K. K. (2010), 'Modulation of pro-survival proteins by S-nitrosylation: implications for neurodegeneration', *Apoptosis*, 15 (11), 1364-70.
- Clavarino, G., et al. (2012), 'Protein phosphatase 1 subunit Ppp1r15a/GADD34 regulates cytokine production in polyinosinic:polycytidylic acid-stimulated dendritic cells', *Proc Natl Acad Sci U S A*, 109 (8), 3006-11.
- Coburn, C. G., Curras-Collazo, M. C., and Kodavanti, P. R. S. (2007), 'Polybrominated diphenyl ethers and ortho-substituted polychlorinated biphenyls as neuroendocrine disruptors of vasopressin release: Effects during physiological activation in vitro and structure-activity relationships', *Toxicological Sciences*, 98 (1), 178-86.
- (2008), 'In vitro effects of environmentally relevant polybrominated diphenyl ether (PBDE) congeners on calcium buffering mechanisms in rat brain', *Neurochemical Research*, 33 (2), 355-64.

- Cohen, J. T., et al. (2005), 'A quantitative analysis of prenatal intake of n-3 polyunsaturated fatty acids and cognitive development', *Am J Prev Med*, 29 (4), 366-74.
- Corning (2005), 'UltraGAPS coated slides, Instruction Manual. Corning Life Science '.
- Coskun, S., et al. (2005), 'The effect of L-NAME administrations after oral mucosal incision on wound NO level in rabbit', *Molecular and Cellular Biochemistry*, 278 (1-2), 65-69.
- Counts, S. E. and Mufson, E. J. (2005), 'The role of nerve growth factor receptors in cholinergic basal forebrain degeneration in prodromal Alzheimer disease', *Journal of Neuropathology and Experimental Neurology*, 64 (4), 263-72.
- Covaci, A., et al. (2006), 'Hexabromocyclododecanes (HBCDs) in the environment and humans: a review', *Environ Sci Technol*, 40 (12), 3679-88.
- Crump, D., et al. (2008), 'Effects of Hexabromocyclododecane and Polybrominated Diphenyl Ethers on mRNA Expression in Chicken (*Gallus domesticus*) Hepatocytes', *Toxicological Sciences*, 106 (2), 479-87.
- Crump, D., et al. (2010), 'Pipping Success, Isomer-Specific Accumulation, and Hepatic mRNA Expression in Chicken Embryos Exposed to HBCD', *Toxicological Sciences*, 115 (2), 492-500.
- Cuajungco, M. P. and Lees, G. J. (1997), 'Zinc metabolism in the brain: Relevance to human neurodegenerative disorders', *Neurobiology of Disease*, 4 (3-4), 137-69.
- Cuello, A. C., et al. 'Cholinergic Involvement in Alzheimer's Disease. A Link with NGF Maturation and Degradation', *Journal of Molecular Neuroscience*, 40 (1-2), 230-35.
- Curran, C. P., et al. (2011), 'In Utero and Lactational Exposure to a Complex Mixture of Polychlorinated Biphenyls: Toxicity in Pups Dependent on the Cyp1a2 and Ahr Genotypes', *Toxicological Sciences*, 119 (1), 189-208.
- Dalfo, E., et al. (2007), 'DHA reduces lipoxidative damage in a A53T mouse model of Parkinson's disease', *Parkinsonism & Related Disorders*, 13, S128-S28.
- Dang, V. H., Choi, K. C., and Jeung, E. B. (2007), 'Tetrabromodiphenyl ether (BDE 47) evokes estrogenicity and calbindin-D9k expression through an estrogen receptor-mediated pathway in the uterus of immature rats', *Toxicol Sci*, 97 (2), 504-11.
- Danscher, G., Haug, F. M. S., and Fredens, K. (1973), 'EFFECT OF DIETHYLDITHIOCARBAMATE (DEDTC) ON SULFIDE SILVER STAINED BOUTONS - REVERSIBLE BLOCKING OF TIMMS SULFIDE SILVER STAIN FOR HEAVY-METALS IN DEDTC TREATED RATS (LIGHT-MICROSCOPY)', *Experimental Brain Research*, 16 (5), 521-32.
- Darnerud, P. O. (2003a), 'Toxic effects of brominated flame retardants in man and in wildlife', *Environment International*, 29 (6), 841-53.

- (2003b), 'Toxic effects of brominated flame retardants in man and in wildlife', *Environ Int*, 29 (6), 841-53.
- Darnerud, P. O., et al. (2007), 'Plasma PBDE and thyroxine levels in rats exposed to Bromkal or BDE-47', *Chemosphere*, 67 (9), S386-S92.
- Darnerud, P. O., et al. (2009), 'POP levels in breast milk and maternal serum and thyroid hormone levels in mother-child pairs from Uppsala, Sweden', *Environ Int*, 36 (2), 180-7.
- DAVIDBioinformaticsResources 'DAVID Bioinformatics Resources 6.7 <http://david.abcc.ncifcrf.gov/>.'
- De Flora, S., et al. (2001), 'Mechanisms of N-acetylcysteine in the prevention of DNA damage and cancer, with special reference to smoking-related end-points', *Carcinogenesis*, 22 (7), 999-1013.
- de Wit, C. A., Herzke, D., and Vorkamp, K. (2010), 'Brominated flame retardants in the Arctic environment - trends and new candidates', *Science of the Total Environment*, 408 (15), 2885-918.
- Decker, T. and Lohmannmatthes, M. L. (1988), 'A QUICK AND SIMPLE METHOD FOR THE QUANTITATION OF LACTATE-DEHYDROGENASE RELEASE IN MEASUREMENTS OF CELLULAR CYTO-TOXICITY AND TUMOR NECROSIS FACTOR (TNF) ACTIVITY', *Journal of Immunological Methods*, 115 (1), 61-69.
- Delgado-Noguera, M. F., Calvache, J. A., and Bonfill Cosp, X. (2010), 'Supplementation with long chain polyunsaturated fatty acids (LCPUFA) to breastfeeding mothers for improving child growth and development', *Cochrane Database Syst Rev*, (12), CD007901.
- Deng, J., et al. (2009), 'Hexabromocyclododecane-induced developmental toxicity and apoptosis in zebrafish embryos', *Aquat Toxicol*, 93 (1), 29-36.
- Dineley, K. E., Votyakova, T. V., and Reynolds, I. J. (2003), 'Zinc inhibition of cellular energy production: implications for mitochondria and neurodegeneration', *Journal of Neurochemistry*, 85 (3), 563-70.
- Dineley, K. E., et al. (2005), 'Zinc causes loss of membrane potential and elevates reactive oxygen species in rat brain mitochondria', *Mitochondrion*, 5 (1), 55-65.
- Dingemans, M. M., et al. (2008a), 'Hydroxylation increases the neurotoxic potential of BDE-47 to affect exocytosis and calcium homeostasis in PC12 cells', *Environ Health Perspect*, 116 (5), 637-43.
- Dingemans, M. M. L., et al. (2009), 'Hexabromocyclododecane Inhibits Depolarization-Induced Increase in Intracellular Calcium Levels and Neurotransmitter Release in PC12 Cells', *Toxicological Sciences*, 107 (2), 490-97.
- Dingemans, M. M. L., et al. (2008b), 'Hydroxylation increases the neurotoxic potential of BDE-47 to affect exocytosis and calcium homeostasis in PC12 cells', *Environmental Health Perspectives*, 116 (5), 637-43.

- Domingo, J. L. (2007), 'Omega-3 fatty acids and the benefits of fish consumption: Is all that glitters gold?', *Environment International*, 33, 993-98.
- Dorosh, A., et al. (2011), 'Assessing oestrogenic effects of brominated flame retardants hexabromocyclododecane and tetrabromobisphenol a on mcf-7 cells', *Folia Biol (Praha)*, 57 (1), 35-9.
- Draper, D. W., et al. (2004), 'Calcium and its role in the nuclear translocation and activation of cytosolic phospholipase A(2) in cells rendered sensitive to TNF-induced apoptosis by cycloheximide', *Journal of Immunology*, 172 (4), 2416-23.
- Drover, J., et al. (2009), 'Three randomized controlled trials of early long-chain polyunsaturated Fatty Acid supplementation on means-end problem solving in 9-month-olds', *Child Dev*, 80 (5), 1376-84.
- EFSA (2011a), 'Scientific Opinion on Polybrominated Diphenyl Ethers (PBDEs) in Food'.
- (2011b), 'Scientific Opinion on Hexabromocyclododecanes (HBCDDs) in Food'.
- (2011a), 'Use of the EFSA Comprehensive European Food Consumption Database in Exposure Assessment. The EFSA Journal, 9(3):2097, 34 pp. Available from <http://www.efsa.europa.eu/en/efsajournal/doc/2097.pdf>'.
- Eisen, M. B. and Brown, P. O. (1999), 'DNA arrays for analysis of gene expression', *Cdna Preparation and Characterization*, 303, 179-205.
- Eklblom, R., et al. (2010), 'Digital gene expression analysis of the zebra finch genome', *BMC Genomics*, 11, 219.
- Eriksson, P., Jakobsson, E., and Fredriksson, A. (2001), 'Brominated flame retardants: a novel class of developmental neurotoxicants in our environment?', *Environ Health Perspect*, 109 (9), 903-8.
- Eriksson, P., et al. (2002), 'A brominated flame retardant, 2,2',4,4',5-pentabromodiphenyl ether: Uptake, retention, and induction of neurobehavioral alterations in mice during a critical phase of neonatal brain development', *Toxicological Sciences*, 67 (1), 98-103.
- Eriksson, Per, et al. (2006), 'Impaired behaviour, learning and memory, in adult mice neonatally exposed to hexabromocyclododecane (HBCDD)', *Environmental Toxicology and Pharmacology*, 21 (3), 317-22.
- Espeseth, A. S., et al. (2004), 'Inhibition of APP processing by substrate-binding compounds: A novel approach to amyloid lowering', *Neurobiology of Aging*, 25, S593-S93.
- FAO (2004), 'Food and Agriculture Organisation of the United Nations www.fao.org (consulted 2011)'.
- (2008), 'Food and Agriculture Organisation of the United Nations www.fao.org (consulted 2011)'.

- Fernie, K. J., et al. (2005), 'Exposure to polybrominated diphenyl ethers (PBDEs): changes in thyroid, vitamin A, glutathione homeostasis, and oxidative stress in American kestrels (*Falco sparverius*)', *Toxicol Sci*, 88 (2), 375-83.
- Foran, J. A., et al. (2005a), 'Risk-based consumption advice for farmed Atlantic and wild Pacific salmon contaminated with dioxins and dioxin-like compounds', *Environmental Health Perspectives*, 113 (5), 552-56.
- Foran, J. A., et al. (2005b), 'Quantitative analysis of the benefits and risks of consuming farmed and wild salmon', *Journal of Nutrition*, 135 (11), 2639-43.
- Forrest, D., Reh, T. A., and Rusch, A. (2002), 'Neurodevelopmental control by thyroid hormone receptors', *Current Opinion in Neurobiology*, 12 (1), 49-56.
- Frederickson, C. J., et al. (2000), 'Importance of zinc in the central nervous system: The zinc-containing neuron', *Journal of Nutrition*, 130 (5), 1471S-83S.
- Fukada, T. and Kambe, T. (2011), 'Molecular and genetic features of zinc transporters in physiology and pathogenesis', *Metallomics*.
- Gee, J. R. and Moser, V. C. 'Acute postnatal exposure to brominated diphenylether 47 delays neuromotor ontogeny and alters motor activity in mice', *Neurotoxicology and Teratology*, 30 (2), 79-87.
- (2008), 'Acute postnatal exposure to brominated diphenylether 47 delays neuromotor ontogeny and alters motor activity in mice', *Neurotoxicology and Teratology*, 30 (2), 79-87.
- Germer, S., et al. (2006), 'Subacute effects of the brominated flame retardants hexabromocyclododecane and tetrabromobisphenol A on hepatic cytochrome P450 levels in rats', *Toxicology*, 218 (2-3), 229-36.
- Gessner, D. K., et al. (2011), 'Increased plasma thyroid hormone concentrations in LDL receptor deficient mice may be explained by inhibition of aryl hydrocarbon receptor-dependent expression of hepatic UDP-glucuronosyltransferases', *Biochim Biophys Acta*.
- Gibbs, R. B. (1994), 'Estrogen and nerve growth factor-related systems in brain. Effects on basal forebrain cholinergic neurons and implications for learning and memory processes and aging', *Ann N Y Acad Sci*, 743, 165-96; discussion 97-9.
- Glover, C. N., et al. (2009), 'Methylmercury speciation influences brain gene expression and behavior in gestationally-exposed mice pups', *Toxicol Sci*, 110 (2), 389-400.
- Goon, D. and Klaassen, C. D. (1992), 'Effects of microsomal enzyme inducers upon UDP-glucuronic acid concentration and UDP-glucuronosyltransferase activity in the rat intestine and liver', *Toxicol Appl Pharmacol*, 115 (2), 253-60.
- Gresa-Arribas, N., et al. (2010), 'Inhibition of CCAAT/enhancer binding protein delta expression by chrysin in microglial cells results in anti-inflammatory and neuroprotective effects', *J Neurochem*, 115 (2), 526-36.

- Guryanova, O. A., Chumakov, P. M., and Frolova, E. I. (2004), 'TRIP6 down-regulation induces cytoskeleton changes and increases malignant phenotype', *Molecular Biology of the Cell*, 15, 1393.
- Guryanova, O. A., et al. (2005), 'Down-regulation of TRIP6 expression induces actin cytoskeleton rearrangements in human carcinoma cell lines', *Molecular Biology*, 39 (5), 905-09.
- Haave, M., et al. (2011a), 'Cerebral gene expression and neurobehavioural development after perinatal exposure to an environmentally relevant polybrominated diphenylether (BDE47)', *Cell Biol Toxicol*.
- (2011b), 'Cerebral gene expression and neurobehavioural development after perinatal exposure to an environmentally relevant polybrominated diphenylether (BDE47)', *Cell Biol Toxicol*, 27 (5), 343-61.
- Hallgren, S. and Darnerud, P. O. (2002a), 'Polybrominated diphenyl ethers (PBDEs), polychlorinated biphenyls (PCBs) and chlorinated paraffins (CPs) in rats - testing interactions and mechanisms for thyroid hormone effects', *Toxicology*, 177 (2-3), 227-43.
- (2002b), 'Polybrominated diphenyl ethers (PBDEs), polychlorinated biphenyls (PCBs) and chlorinated paraffins (CPs) in rats-testing interactions and mechanisms for thyroid hormone effects', *Toxicology*, 177 (2-3), 227-43.
- Hallgren, S., et al. (2001a), 'Effects of polybrominated diphenyl ethers (PBDEs) and polychlorinated biphenyls (PCBs) on thyroid hormone and vitamin A levels in rats and mice', *Archives of Toxicology*, 75 (4), 200-08.
- (2001b), 'Effects of polybrominated diphenyl ethers (PBDEs) and polychlorinated biphenyls (PCBs) on thyroid hormone and vitamin A levels in rats and mice', *Arch Toxicol*, 75 (4), 200-8.
- Hardy, J. and Selkoe, D. J. (2002), 'Medicine - The amyloid hypothesis of Alzheimer's disease: Progress and problems on the road to therapeutics', *Science*, 297 (5580), 353-56.
- Hashimoto, M., et al. (2002), 'Docosahexaenoic acid provides protection from impairment of learning ability in Alzheimer's disease model rats', *Journal of Neurochemistry*, 81 (5), 1084-91.
- Hasio, A. C., et al. (2008), 'Effect of brain DHA levels on cytoskeleton expression', *Asia Pacific Journal of Clinical Nutrition*, 17, 158-61.
- Hawkins, B. T. and Davis, T. P. (2005), 'The blood-brain barrier/neurovascular unit in health and disease', *Pharmacological Reviews*, 57 (2), 173-85.
- He, P., et al. (2008a), 'PBDE-47-induced oxidative stress, DNA damage and apoptosis in primary cultured rat hippocampal neurons', *Neurotoxicology*, 29, 124-29.
- (2008b), 'PBDE-47-induced oxidative stress, DNA damage and apoptosis in primary cultured rat hippocampal neurons', *Neurotoxicology*, 29 (1), 124-29.

- He, Ping, et al. (2007), '[Effects of 2,2', 4,4' -tetrabromodiphenyl ethers on oxidative stress and DNA damage in SH-SY5Y cells]', *Wei Sheng Yan Jiu*, 36 (3), 266-8.
- He, W. H., et al. (2008c), 'Effects of PBDE-47 on cytotoxicity and genotoxicity in human neuroblastoma cells in vitro', *Mutation Research-Genetic Toxicology and Environmental Mutagenesis*, 649, 62-70.
- He, Y., et al. 'Emerging Roles for XBP1, a sUPeR Transcription Factor', *Gene Expression*, 15 (1), 13-25.
- Heeb, N. V., et al. (2005), 'Structure elucidation of hexabromocyclododecanes - a class of compounds with a complex stereochemistry', *Chemosphere*, 61 (1), 65-73.
- Hess, K. R., et al. (2001a), 'Microarrays: handling the deluge of data and extracting reliable information', *Trends Biotechnol*, 19 (11), 463-8.
- (2001b), 'Microarrays: handling the deluge of data and extracting reliable information', *Trends in Biotechnology*, 19 (11), 463-68.
- Hirano, T., et al. (2008), 'Roles of zinc and zinc signaling in immunity: zinc as an intracellular signaling molecule', *Adv Immunol*, 97, 149-76.
- Hirayama, S., Hamazaki, T., and Terasawa, K. (2004), 'Effect of docosahexaenoic acid-containing food administration on symptoms of attention-deficit/hyperactivity disorder - a placebo-controlled double-blind study', *Eur J Clin Nutr*, 58 (3), 467-73.
- Hites, R. A., et al. (2004a), 'Global assessment of polybrominated diphenyl ethers in farmed and wild salmon', *Environmental Science & Technology*, 38 (19), 4945-49.
- Hites, R. A., et al. (2004b), 'Global assessment of organic contaminants in farmed salmon', *Science*, 303 (5655), 226-9.
- Hogstrand, C., et al. (2009), 'Zinc transporters and cancer: a potential role for ZIP7 as a hub for tyrosine kinase activation', *Trends Mol Med*, 15 (3), 101-11.
- Hooper, K. and McDonald, T. A. (2000), 'The PBDEs: An emerging environmental challenge and another reason for breast-milk monitoring programs', *Environmental Health Perspectives*, 108 (5), 387-92.
- Hpacultures (2008), 'www.hpacultures.org.uk consulted 15 September 2008'.
- Hsu, W. C., et al. (2008), 'Promoter polymorphisms modulating HSPA5 expression may increase susceptibility to Taiwanese Alzheimer's disease', *Journal of Neural Transmission*, 115 (11), 1537-43.
- Hu, J., et al. (2009), 'Assessing the Toxicity of TBBPA and HBCD by Zebrafish Embryo Toxicity Assay and Biomarker Analysis', *Environmental Toxicology*, 24 (4), 334-42.
- Ibhazehiebo, K., et al. (2011), '1,2,5,6,9,10-alphaHexabromocyclododecane (HBCD) impairs thyroid hormone-induced dendrite arborization of Purkinje cells and

- suppresses thyroid hormone receptor-mediated transcription', *Cerebellum*, 10 (1), 22-31.
- Invitrogen (2011), '<http://igene.invitrogen.com/iGene/browse/gene/CASP3/836> . April 2011.'
- James, A. B., Conway, A. M., and Morris, B. J. (2006), 'Regulation of the neuronal proteasome by Zif268 (Egr1)', *Journal of Neuroscience*, 26 (5), 1624-34.
- James, M. O., Sacco, J. C., and Faux, L. R. (2008), 'Effects of Food Natural Products on the Biotransformation of PCBs', *Environ Toxicol Pharmacol*, 25 (2), 211-7.
- Jayashankar, S., et al. (2012), 'Cerebral gene expression and neurobehavioural responses in mice pups exposed to methylmercury and docosahexaenoic acid through the maternal diet', *Environ Toxicol Pharmacol*, 33 (1), 26-38.
- Kamenetz, F., et al. (2003), 'APP processing and synaptic function', *Neuron*, 37 (6), 925-37.
- Kanehisa, M. and Goto, S. (2000), 'KEGG: Kyoto Encyclopedia of Genes and Genomes', *Nucleic Acids Research*, 28 (1), 27-30.
- Kaur, P., et al. (2007), 'Role of docosahexaenoic acid in modulating methylmercury-induced neurotoxicity', *Toxicological Sciences*, 100 (2), 423-32.
- Kaur, P., et al. (2008), 'Docosahexaenoic acid may act as a neuroprotector for methylmercury-induced neurotoxicity in primary neural cell cultures', *Neurotoxicology*, 29 (6), 978-87.
- Kawanai, T., et al. (2009), 'Methylmercury elicits intracellular Zn²⁺ release in rat thymocytes: its relation to methylmercury-induced decrease in cellular thiol content', *Toxicol Lett*, 191 (2-3), 231-5.
- Keller, U., et al. 'Myc suppression of Nfkb2 accelerates lymphomagenesis', *Bmc Cancer*, 10.
- Kerksick, Chad and Willoughby, Darryn (2005), 'The antioxidant role of glutathione and N-acetyl-cysteine supplements and exercise-induced oxidative stress', *J Int Soc Sports Nutr*, 2, 38-44.
- Khachigian, L. M., et al. (1997), 'Egr-1 is activated in endothelial cells exposed to fluid shear stress and interacts with a novel shear-stress-response element in the PDGF A-chain promoter', *Arteriosclerosis Thrombosis and Vascular Biology*, 17 (10), 2280-86.
- Kherjee, P. K. M., et al. (2007), 'Docosanoids are multifunctional regulators of neural cell integrity and fate: Significance in aging and disease', *Prostaglandins Leukotrienes and Essential Fatty Acids*, 77 (5-6), 233-38.
- Kim, E. Y., et al. (1999), 'Zn²⁺ entry produces oxidative neuronal necrosis in cortical cell cultures', *European Journal of Neuroscience*, 11 (1), 327-34.
- Kim, H. Y. (2007), 'Novel metabolism of docosahexaenoic acid in neural cells', *Journal of Biological Chemistry*, 282 (26), 18661-65.

- Kim, H. Y., et al. (2011), 'N-Docosahexaenoyl ethanolamide promotes development of hippocampal neurons', *Biochem J*.
- Kinsey, G. R., et al. (2008), 'Decreased iPLA₂γ expression induces lipid peroxidation and cell death and sensitizes cells to oxidant-induced apoptosis', *J Lipid Res*, 49 (7), 1477-87.
- Kitajka, K., et al. (2002), 'The role of n-3 polyunsaturated fatty acids in brain: modulation of rat brain gene expression by dietary n-3 fatty acids', *Proc Natl Acad Sci U S A*, 99 (5), 2619-24.
- Klaassen, C. D. and Hood, A. M. (2001), 'Effects of microsomal enzyme inducers on thyroid follicular cell proliferation and thyroid hormone metabolism', *Toxicol Pathol*, 29 (1), 34-40.
- Koch, G. L. E. (1990), 'THE ENDOPLASMIC-RETICULUM AND CALCIUM STORAGE', *Bioessays*, 12 (11), 527-31.
- Kodavanti, P. R. (2005), 'Neurotoxicity of Persistent Organic Pollutants: Possible Mode(s) of Action and Further Considerations', *Dose Response*, 3 (3), 273-305.
- Kodavanti, P. R. and Derr-Yellin, E. C. (2002), 'Differential effects of polybrominated diphenyl ethers and polychlorinated biphenyls on [³H]arachidonic acid release in rat cerebellar granule neurons', *Toxicol Sci*, 68 (2), 451-7.
- Kodavanti, P. R. S. and Ward, T. R. (2005), 'Differential effects of commercial polybrominated diphenyl ether and polychlorinated biphenyl mixtures on intracellular signaling in rat brain in vitro', *Toxicological Sciences*, 85 (2), 952-62.
- Kodavanti, P. R. S., et al. (1998), 'Congener-specific distribution of polychlorinated biphenyls in brain regions, blood, liver, and fat of adult rats following repeated exposure to Aroclor 1254', *Toxicology and Applied Pharmacology*, 153 (2), 199-210.
- Kojima, H., et al. (2009), 'Nuclear hormone receptor activity of polybrominated diphenyl ethers and their hydroxylated and methoxylated metabolites in transactivation assays using Chinese hamster ovary cells', *Environ Health Perspect*, 117 (8), 1210-8.
- Kroncke, K. D., et al. (1994), 'NITRIC-OXIDE DESTROYS ZINC-SULFUR CLUSTERS INDUCING ZINC RELEASE FROM METALLOTHIONEIN AND INHIBITION OF THE ZINC FINGER-TYPE YEAST TRANSCRIPTION ACTIVATOR LAC9', *Biochemical and Biophysical Research Communications*, 200 (2), 1105-10.
- Kuriyama, S. N., et al. (2005), 'Developmental exposure to low dose PBDE 99: effects on male fertility and neurobehavior in rat offspring', *Environ Health Perspect*, 113 (2), 149-54.
- Law, R. J., et al. (2005), 'Hexabromocyclododecane challenges scientists and regulators', *Environ Sci Technol*, 39 (13), 281A-87A.

- Leandro-Garcia, L. J., et al. 'Tumoral and Tissue-Specific Expression of the Major Human beta-Tubulin Isoforms', *Cytoskeleton*, 67 (4), 214-23.
- Lee, A. S. (2005), 'The ER chaperone and signaling regulator GRP78/BiP as a monitor of endoplasmic reticulum stress', *Methods*, 35 (4), 373-81.
- Legrand, C., et al. (1992), 'LACTATE-DEHYDROGENASE (LDH) ACTIVITY OF THE NUMBER OF DEAD CELLS IN THE MEDIUM OF CULTURED EUKARYOTIC CELLS AS MARKER', *Journal of Biotechnology*, 25 (3), 231-43.
- Lema, S. C., et al. (2008), 'Dietary exposure to 2,2',4,4'-tetrabromodiphenyl ether (PBDE-47) alters thyroid status and thyroid hormone-regulated gene transcription in the pituitary and brain', *Environ Health Perspect*, 116 (12), 1694-9.
- Lenaz, G. (1998), 'Role of mitochondria in oxidative stress and ageing', *Biochimica Et Biophysica Acta-Bioenergetics*, 1366 (1-2), 53-67.
- Li, W. Z., et al. (2012), 'Dexamethasone and Abeta(25-35) accelerate learning and memory impairments due to elevated amyloid precursor protein expression and neuronal apoptosis in 12-month male rats', *Behav Brain Res*, 227 (1), 142-9.
- Li, Y., et al. (2010), 'The relationship between transient zinc ion fluctuations and redox signaling in the pathways of secondary cellular injury: Relevance to traumatic brain injury', *Brain Research*, 1330, 131-41.
- Lilienthal, H., et al. (2009), 'Effects of the brominated flame retardant hexabromocyclododecane (HBCD) on dopamine-dependent behavior and brainstem auditory evoked potentials in a one-generation reproduction study in Wistar rats', *Toxicology Letters*, 185 (1), 63-72.
- Liu, L., Trimarchi, J. R., and Keefe, D. L. (2000), 'Involvement of mitochondria in oxidative stress-induced cell death in mouse zygotes', *Biology of Reproduction*, 62 (6), 1745-53.
- Longo, I., et al. (2003), 'A third MRX family (MRX68) is the result of mutation in the long chain fatty acid-CoA ligase 4 (FACLA) gene: proposal of a rapid enzymatic assay for screening mentally retarded patients', *Journal of Medical Genetics*, 40 (1), 11-17.
- Luo, L. Q. (2002), 'Actin cytoskeleton regulation in neuronal morphogenesis and structural plasticity', *Annual Review of Cell and Developmental Biology*, 18, 601-35.
- Luo, Xiaoyang and Yan, Riqiang (2010), 'Inhibition of BACE1 for therapeutic use in Alzheimer's disease', *Int J Clin Exp Pathol*, 3 (6), 618-28.
- Luthe, G., Jacobus, J. A., and Robertson, L. W. (2008), 'Receptor interactions by polybrominated diphenyl ethers versus polychlorinated biphenyls: a theoretical Structure-activity assessment', *Environ Toxicol Pharmacol*, 25 (2), 202-10.
- Maden, M. (2007), 'Retinoic acid in the development, regeneration and maintenance of the nervous system', *Nature Reviews Neuroscience*, 8 (10), 755-65.

- Mancuso, D. J., et al. (2007), 'Genetic ablation of calcium-independent phospholipase A2gamma leads to alterations in mitochondrial lipid metabolism and function resulting in a deficient mitochondrial bioenergetic phenotype', *J Biol Chem*, 282 (48), 34611-22.
- Maret, Wolfgang (2009), 'Molecular aspects of human cellular zinc homeostasis: redox control of zinc potentials and zinc signals', *Biometals*, 22 (1), 149-57.
- Mariussen, E. and Fonnum, F. (2003), 'The effect of brominated flame retardants on neurotransmitter uptake into rat brain synaptosomes and vesicles', *Neurochemistry International*, 43 (4-5), 533-42.
- Mariussen, E., et al. (2002), 'The polychlorinated biphenyl mixture aroclor 1254 induces death of rat cerebellar granule cells: The involvement of the N-methyl-D-aspartate receptor and reactive oxygen species', *Toxicology and Applied Pharmacology*, 179 (3), 137-44.
- McConlogue, L., et al. (2007), 'Partial reduction of BACE1 has dramatic effects on Alzheimer plaque and synaptic pathology in APP transgenic mice', *Journal of Biological Chemistry*, 282 (36), 26326-34.
- Meerts, I. A., et al. (2001), 'In vitro estrogenicity of polybrominated diphenyl ethers, hydroxylated PDBEs, and polybrominated bisphenol A compounds', *Environ Health Perspect*, 109 (4), 399-407.
- Melon, I., et al. (2009), 'THE XLMR GENE ACSL4 PLAYS A ROLE IN DENDRITIC SPINE ARCHITECTURE', *Neuroscience*, 159 (2), 657-69.
- Miranda, M., et al. 'Relation between human LPIN1, hypoxia and endoplasmic reticulum stress genes in subcutaneous and visceral adipose tissue', *International Journal of Obesity*, 34 (4), 679-86.
- Moore, D. J., et al. (2005), 'Molecular pathophysiology of Parkinson's disease', *Annual Review of Neuroscience*, 28, 57-87.
- Mosmann, T. (1983), 'Rapid colorimetric assay for cellular growth and survival: application to proliferation and cytotoxicity assays', *J Immunol Methods*, 65 (1-2), 55-63.
- Mozaffarian, D. and Rimm, E. B. (2006), 'Fish intake, contaminants, and human health: evaluating the risks and the benefits', *JAMA*, 296 (15), 1885-99.
- Muntane, G., et al. (2010), 'Modification of brain lipids but not phenotype in alpha-synucleinopathy transgenic mice by long-term dietary n-3 fatty acids', *Neurochemistry International*, 56 (2), 318-28.
- Murakami, M. and Hirano, T. (2008), 'Intracellular zinc homeostasis and zinc signaling', *Cancer Sci*, 99 (8), 1515-22.
- Myllykangas, L., et al. (2005), 'Chromosome 21 BACE2 haplotype associates with Alzheimer's disease: A two-stage study', *Journal of the Neurological Sciences*, 236 (1-2), 17-24.

- Oksman, M., et al. (2006), 'Impact of different saturated fatty acid, polyunsaturated fatty acid and cholesterol containing diets on beta-amyloid accumulation in APP/PS1 transgenic mice', *Neurobiology of Disease*, 23 (3), 563-72.
- Okuda, S., Saito, H., and Katsuki, H. (1994), 'ARACHIDONIC-ACID - TOXIC AND TROPHIC EFFECTS ON CULTURED HIPPOCAMPAL-NEURONS', *Neuroscience*, 63 (3), 691-99.
- Olsvik, P. A., et al. (2009), 'Transcriptional effects of nonylphenol, bisphenol A and PBDE-47 in liver of juvenile Atlantic cod (*Gadus morhua*)', *Chemosphere*, 75 (3), 360-7.
- Palace, V., et al. (2010), 'Altered thyroxine metabolism in rainbow trout (*Oncorhynchus mykiss*) exposed to hexabromocyclododecane (HBCD)', *Chemosphere*, 80 (2), 165-69.
- Pan, E., et al. (2011), 'Vesicular zinc promotes presynaptic and inhibits postsynaptic long-term potentiation of mossy fiber-CA3 synapse', *Neuron*, 71 (6), 1116-26.
- Patel, R. D., et al. (2007), 'Aryl-hydrocarbon receptor activation regulates constitutive androstane receptor levels in murine and human liver', *Hepatology*, 46 (1), 209-18.
- Pessah, I. N., Cherednichenko, G., and Lein, P. J. (2010), 'Minding the calcium store: Ryanodine receptor activation as a convergent mechanism of PCB toxicity', *Pharmacology & Therapeutics*, 125 (2), 260-85.
- Pfaffl, M. W., Horgan, G. W., and Dempfle, L. (2002), 'Relative expression software tool (REST (c)) for group-wise comparison and statistical analysis of relative expression results in real-time PCR', *Nucleic Acids Research*, 30 (9).
- Piccini, M., et al. (1998), 'FACLA, a new gene encoding long-chain acyl-CoA synthetase 4, is deleted in a family with Alport syndrome, elliptocytosis, and mental retardation', *Genomics*, 47 (3), 350-58.
- Pomponi, M. (2008), 'DHIA deficiency and Alzheimer's disease', *Clinical Nutrition*, 27 (1), 170-70.
- Popova, M. P. and Popov, C. S. (2002), 'Damage to subcellular structures evoked by lipid peroxidation', *Zeitschrift Fur Naturforschung C-a Journal of Biosciences*, 57 (3-4), 361-65.
- Predki, P. F. and Sarkar, B. (1994), 'Metal replacement in "zinc finger" and its effect on DNA binding', *Environ Health Perspect*, 102 Suppl 3, 195-8.
- Qian, J. and Noebels, J. L. (2005), 'Visualization of transmitter release with zinc fluorescence detection at the mouse hippocampal mossy fibre synapse', *J Physiol*, 566 (Pt 3), 747-58.
- Qiu, X., Bigsby, R. M., and Hites, R. A. (2009), 'Hydroxylated metabolites of polybrominated diphenyl ethers in human blood samples from the United States', *Environ Health Perspect*, 117 (1), 93-8.

- Quinn, J. (2006), 'Effects of docosahexaenoic acid (DHA) in slowing the progression of Alzheimer's disease', *Neuropsychopharmacology*, 31, S54-S55.
- Rasinger, J.D. (2011), 'Proteomic evaluation of the neurotoxic potential of model environmental contaminants commonly found in farmed salmon', *PhD Thesis*.
- Ravni, A., et al. (2008), 'A cAMP-dependent, protein kinase A-independent signaling pathway mediating neuritogenesis through Egr1 in PC12 cells', *Molecular Pharmacology*, 73 (6), 1688-708.
- Rego, Ana Cristina, Cardoso, Sandra Morais, and Oliveira, Catarina R. (2007), 'Molecular pathways of mitochondrial dysfunction in neurodegeneration: The paradigms of Parkinson's and Huntington's diseases', *Interaction Between Neurons and Glia in Aging and Disease*, 193-219.
- Reistad, T., Fonnum, F., and Mariussen, E. (2006a), 'Neurotoxicity of the pentabrominated diphenyl ether mixture, DE-71, and hexabromocyclododecane (HBCD) in rat cerebellar granule cells in vitro', *Archives of Toxicology*, 80 (11), 785-96.
- (2006b), 'Neurotoxicity of the pentabrominated diphenyl ether mixture, DE-71, and hexabromocyclododecane (HBCD) in rat cerebellar granule cells in vitro', *Arch Toxicol*, 80 (11), 785-96.
- Remberger, M., et al. (2004), 'The environmental occurrence of hexabromocyclododecane in Sweden', *Chemosphere*, 54 (1), 9-21.
- Richardson, T. A. and Klaassen, C. D. (2010), 'Disruption of thyroid hormone homeostasis in Ugt1a-deficient Gunn rats by microsomal enzyme inducers is not due to enhanced thyroxine glucuronidation', *Toxicol Appl Pharmacol*, 248 (1), 38-44.
- Richardson VM, Crofton KM, DeVito MJ. (2005), ' Effects of 2,2',4,4'-tetrabromodiphenyl ether on CAR and PXR regulated gene expression in weanling female rats. ', *Presented at Society of Toxicology Annual Meeting, New Orleans, LA. March 06 - 10*.
- Rietjens, I. M. and Alink, G. M. (2006), 'Future of toxicology--low-dose toxicology and risk--benefit analysis', *Chem Res Toxicol*, 19 (8), 977-81.
- Roosens, L., et al. (2010), 'Brominated flame retardants and perfluorinated chemicals, two groups of persistent contaminants in Belgian human blood and milk', *Environ Pollut*, 158 (8), 2546-52.
- Rutkowski, D. T. and Kaufman, R. J. (2004), 'A trip to the ER: coping with stress', *Trends in Cell Biology*, 14 (1), 20-28.
- Rylander, C., Sandanger, T. M., and Brustad, M. (2009), 'Associations between marine food consumption and plasma concentrations of POPs in a Norwegian coastal population', *J Environ Monit*, 11 (2), 370-6.
- Salem, N., et al. (2001), 'Mechanisms of action of docosahexaenoic acid in the nervous system', *Lipids*, 36 (9), 945-59.

- Sanders, J. M., et al. (2005), 'Differential expression of CYP1A, 2B, and 3A genes in the F344 rat following exposure to a polybrominated diphenyl ether mixture or individual components', *Toxicol Sci*, 88 (1), 127-33.
- Saraste, A. and Pulkki, K. (2000), 'Morphologic and biochemical hallmarks of apoptosis', *Cardiovascular Research*, 45 (3), 528-37.
- Sastry, P. S. and Rao, K. S. (2000), 'Apoptosis and the nervous system', *Journal of Neurochemistry*, 74 (1), 1-20.
- Savinova, O. V., Hoffmann, A., and Ghosh, G. (2009), 'The Nfkb1 and Nfkb2 Proteins p105 and p100 Function as the Core of High-Molecular-Weight Heterogeneous Complexes', *Molecular Cell*, 34 (5), 591-602.
- Schechter, A., et al. (2008), 'PBDE and HBCD Brominated Flame Retardants in the USA, Update 2008: Levels in Human Milk and Blood, Food, and Environmental Samples', *Epidemiology*, 19 (6), S76-S76.
- Schechter, A., et al. (2006), 'Polybrominated diphenyl ether (PBDE) levels in an expanded market basket survey of US food and estimated PBDE dietary intake by age and sex', *Environmental Health Perspectives*, 114 (10), 1515-20.
- Schechter, A., et al. (2010a), 'Polybrominated Diphenyl Ethers (PBDEs) and Hexabromocyclodecane (HBCD) in Composite US Food Samples', *Environmental Health Perspectives*, 118 (3), 357-62.
- Schechter, A., et al. (2010b), 'Polybrominated diphenyl ether levels in foodstuffs collected from three locations from the United States', *Toxicology and Applied Pharmacology*, 243 (2), 217-24.
- Schmitt, H., Gozes, I., and Littauer, U. Z. (1977), 'DECREASE IN LEVELS AND RATES OF SYNTHESIS OF TUBULIN AND ACTIN IN DEVELOPING RAT-BRAIN', *Brain Research*, 121 (2), 327-42.
- Schroder, M. and Kaufman, R. J. (2005), 'ER stress and the unfolded protein response', *Mutation Research-Fundamental and Molecular Mechanisms of Mutagenesis*, 569 (1-2), 29-63.
- Schroeder, A., et al. (2006), 'The RIN: an RNA integrity number for assigning integrity values to RNA measurements', *Bmc Molecular Biology*, 7.
- Sellstrom, U., et al. (2003), 'Temporal trend studies on tetra- and pentabrominated diphenyl ethers and hexabromocyclododecane in guillemot egg from the Baltic Sea', *Environ Sci Technol*, 37 (24), 5496-501.
- Sensi, S. L., et al. (2003), 'Modulation of mitochondrial function by endogenous Zn²⁺ pools', *Proceedings of the National Academy of Sciences of the United States of America*, 100 (10), 6157-62.
- Shaikh, S. R. and Edidin, M. (2006), 'Polyunsaturated fatty acids, membrane organization, T cells, and antigen presentation', *American Journal of Clinical Nutrition*, 84 (6), 1277-89.

- Shalon, D. (1998), 'Gene expression micro-arrays: a new tool for genomic research', *Pathol Biol (Paris)*, 46 (2), 107-9.
- Sheline, C. T., Behrens, M. M., and Choi, D. W. (2000), 'Zinc-induced cortical neuronal death: Contribution of energy failure attributable to loss of NAD(+) and inhibition of glycolysis', *Journal of Neuroscience*, 20 (9), 3139-46.
- Skarman, E., et al. (2005), 'Reduced thyroxine levels in mice perinatally exposed to polybrominated diphenyl ethers', *Environmental Toxicology and Pharmacology*, 19 (2), 273-81.
- Smart, T. G., Hosie, A. M., and Miller, P. S. (2004), 'Zn²⁺ ions: Modulators of excitatory and inhibitory synaptic activity', *Neuroscientist*, 10 (5), 432-42.
- Solans, A., Estivill, X., and de la Luna, S. (2000), 'A new aspartyl protease on 21q22.3, BACE2, is highly similar to Alzheimer's amyloid precursor protein beta-secretase', *Cytogenetics and Cell Genetics*, 89 (3-4), 177-84.
- Song, R., et al. (2009a), 'Cytotoxicity and gene expression profiling of two hydroxylated polybrominated diphenyl ethers in human H295R adrenocortical carcinoma cells', *Toxicol Lett*, 185 (1), 23-31.
- Song, R. F., et al. (2009b), 'Cytotoxicity and gene expression profiling of two hydroxylated polybrominated diphenyl ethers in human H295R adrenocortical carcinoma cells', *Toxicology Letters*, 185 (1), 23-31.
- Spahl, D. U., et al. (2003), 'Regulation of zinc homeostasis by inducible NO synthase-derived NO: Nuclear translocation and intranuclear metallothionein Zn²⁺ release', *Proceedings of the National Academy of Sciences of the United States of America*, 100 (24), 13952-57.
- St Croix, C. M., et al. (2002), 'Nitric oxide-induced changes in intracellular zinc homeostasis are mediated by metallothionein/thionein', *American Journal of Physiology-Lung Cellular and Molecular Physiology*, 282 (2), L185-L92.
- Stockley, J. H. and O'Neill, C. (2007), 'The proteins BACE1 and BACE2 and beta-secretase activity in normal and Alzheimer's disease brain', *Conference on New Approaches for Elucidating Protease Biology and Therapeutic Opportunities* (Cirencester, ENGLAND: Portland Press Ltd), 574-76.
- Stork, Christian J. and Li, Yang V. (2010), 'Zinc release from thapsigargin/IP3-sensitive stores in cultured cortical neurons', *J Mol Signal*, 5, 5.
- Strom, S., et al. (2011), 'Nutritional and toxicological aspects of seafood consumption--an integrated exposure and risk assessment of methylmercury and polyunsaturated fatty acids', *Environ Res*, 111 (2), 274-80.
- Sun, X., et al. (2005), 'Distinct transcriptional regulation and function of the human BACE2 and BACE1 genes', *FASEB J*, 19 (7), 739-49.
- Suvorov, A. and Takser, L. (2010), 'Global gene expression analysis in the livers of rat offspring perinatally exposed to low doses of 2,2',4,4'-tetrabromodiphenyl ether', *Environ Health Perspect*, 118 (1), 97-102.

- Szabo, D. T., et al. (2010a), 'Toxicokinetics of the Flame Retardant Hexabromocyclododecane Gamma: Effect of Dose, Timing, Route, Repeated Exposure, and Metabolism', *Toxicological Sciences*, 117 (2), 282-93.
- (2010b), 'Toxicokinetics of the flame retardant hexabromocyclododecane gamma: effect of dose, timing, route, repeated exposure, and metabolism', *Toxicol Sci*, 117 (2), 282-93.
- (2011), 'Toxicokinetics of the flame retardant hexabromocyclododecane alpha: effect of dose, timing, route, repeated exposure, and metabolism', *Toxicol Sci*, 121 (2), 234-44.
- Szabo DT, Shah R, Birnbaum LS (2011), 'Transcriptomics identifies molecular mechanisms involved in developmental neurotoxicity after acute *in vivo* exposure to HBCD stereoisomers in mice'.
- t Hoen, P. A., et al. (2008), 'Deep sequencing-based expression analysis shows major advances in robustness, resolution and inter-lab portability over five microarray platforms', *Nucleic Acids Res*, 36 (21), e141.
- Takata, M., et al. (2010), 'Regulation of nuclear localization signal-importin alpha interaction by Ca²⁺/S100A6', *Febs Letters*, 584 (22), 4517-23.
- Takeda, A. (2000), 'Movement of zinc and its functional significance in the brain', *Brain Res Brain Res Rev*, 34 (3), 137-48.
- Talsness, C. E., et al. (2005), 'Ultrastructural changes observed in rat ovaries following in utero and lactational exposure to low doses of a polybrominated flame retardant', *Toxicology Letters*, 157 (3), 189-202.
- Tan, Y., et al. (2004a), 'Ortho-substituted PCBs kill cells by altering membrane structure', *Toxicol Sci*, 80 (1), 54-9.
- Tan, Y. S., et al. (2004b), 'Ortho-substituted PCBs kill cells by altering membrane structure', *Toxicological Sciences*, 80 (1), 54-59.
- Terry, A. V., Jr., Kutiyawalla, A., and Pillai, A. (2011), 'Age-dependent alterations in nerve growth factor (NGF)-related proteins, sortilin, and learning and memory in rats', *Physiol Behav*, 102 (2), 149-57.
- Tornkvist, A., et al. (2011), 'PCDD/F, PCB, PBDE, HBCD and chlorinated pesticides in a Swedish market basket from 2005--levels and dietary intake estimations', *Chemosphere*, 83 (2), 193-9.
- Treiman, M. (2002), 'Regulation of the endoplasmic reticulum calcium storage during the unfolded protein response - Significance in tissue ischemia?', *Trends in Cardiovascular Medicine*, 12 (2), 57-62.
- Tseng, L. H., et al. (2006), 'Postnatal exposure of the male mouse to 2,2',3,3',4,4',5,5',6,6'-decabrominated diphenyl ether: Decreased epididymal sperm functions without alterations in DNA content and histology in testis', *Toxicology*, 224 (1-2), 33-43.

- Tu, J. C., et al. (2002), 'HOMER REGULATES GAIN OF RYANODINE RECEPTOR', *Society for Neuroscience Abstract Viewer and Itinerary Planner*, 2002, Abstract No. 746.1.
- Turan, B., Fliss, H., and Desilets, M. (1997), 'Oxidants increase intracellular free Zn²⁺ concentration in rabbit ventricular myocytes', *American Journal of Physiology-Heart and Circulatory Physiology*, 272 (5), H2095-H106.
- Van Boxtel, A. L., et al. (2008), 'Microarray analysis reveals a mechanism of phenolic polybrominated diphenylether toxicity in zebrafish', *Environmental Science & Technology*, 42 (5), 1773-79.
- Van den Berg, M., et al. (2006), 'The 2005 World Health Organization reevaluation of human and mammalian toxic equivalency factors for dioxins and dioxin-like compounds', *Toxicological Sciences*, 93 (2), 223-41.
- van der Ven, L. T. M., et al. (2006), 'A 28-day oral dose toxicity study enhanced to detect endocrine effects of hexabromocyclododecane in wistar rats', *Toxicological Sciences*, 94 (2), 281-92.
- van der Ven, L. T. M., et al. (2009), 'Endocrine effects of hexabromocyclododecane (HBCD) in a one-generation reproduction study in Wistar rats', *Toxicology Letters*, 185 (1), 51-62.
- Vandesompele, J., et al. (2002), 'Accurate normalization of real-time quantitative RT-PCR data by geometric averaging of multiple internal control genes', *Genome Biology*, 3 (7).
- Verdugo, R. A. and Medrano, J. F. (2006), 'Comparison of gene coverage of mouse oligonucleotide microarray platforms', *BMC Genomics*, 7, 58.
- Viberg, H., Fredriksson, A., and Eriksson, P. (2003a), 'Neonatal exposure to polybrominated diphenyl ether (PBDE 153) disrupts spontaneous behaviour, impairs learning and memory, and decreases hippocampal cholinergic receptors in adult mice', *Toxicol Appl Pharmacol*, 192 (2), 95-106.
- (2003b), 'Neonatal PBDE 99 exposure causes dose-response related behavioural derangements that are not sex or strain specific in mice', *Toxicological Sciences*, 72, 126-26.
- Viberg, H., et al. (2003c), 'Neurobehavioral derangements in adult mice receiving decabrominated diphenyl ether (PBDE 209) during a defined period of neonatal brain development', *Toxicological Sciences*, 76 (1), 112-20.
- (2003d), 'Neurobehavioral derangements in adult mice receiving decabrominated diphenyl ether (PBDE 209) during a defined period of neonatal brain development', *Toxicol Sci*, 76 (1), 112-20.
- Visser, T. J., et al. (1993), 'Glucuronidation of thyroid hormone by human bilirubin and phenol UDP-glucuronyltransferase isoenzymes', *FEBS Lett*, 324 (3), 358-60.
- Vrana, K. E., Freeman, W. M., and Aschner, M. (2003), 'Use of microarray technologies in toxicology research', *Neurotoxicology*, 24 (3), 321-32.

- Wahl, M., et al. (2008a), 'A technical mixture of 2,2',4,4'-tetrabromo diphenyl ether (BDE47) and brominated furans triggers aryl hydrocarbon receptor (AhR) mediated gene expression and toxicity', *Chemosphere*, 73 (2), 209-15.
- (2008b), 'A technical mixture of 2,2',4,4'-tetrabromo diphenyl ether (BDE47) and brominated furans triggers aryl hydrocarbon receptor (AhR) mediated gene expression and toxicity', *Chemosphere*, 73 (2), 209-15.
- Wang, F., et al. (2011), 'Interaction of PFOS and BDE-47 Co-exposure on Thyroid Hormone Levels and TH-related Gene and Protein Expression in Developing Rat Brains', *Toxicol Sci*.
- Waxman, D. J. (1999), 'P450 gene induction by structurally diverse xenochemicals: Central role of nuclear receptors CAR, PXR, and PPAR', *Archives of Biochemistry and Biophysics*, 369 (1), 11-23.
- Wong, P. W. and Pessah, I. N. (1997), 'Noncoplanar PCB 95 alters microsomal calcium transport by an immunophilin FKBP12-dependent mechanism', *Mol Pharmacol*, 51 (5), 693-702.
- Woolcott, O. O., et al. (2006), 'Arachidonic acid is a physiological activator of the ryanodine receptor in pancreatic beta-cells', *Cell Calcium*, 39 (6), 529-37.
- Yamada-Okabe, T., et al. (2005), 'Modulation at a cellular level of the thyroid hormone receptor-mediated gene expression by 1,2,5,6,9,10-hexabromocyclododecane (HBCD), 4,4'-diiodobiphenyl (DIB), and nitrofen (NIP)', *Toxicology Letters*, 155 (1), 127-33.
- Yamasaki, S., et al. (2007a), 'Zinc is a novel intracellular second messenger', *Journal of Cell Biology*, 177 (4), 637-45.
- (2007b), 'Zinc is a novel intracellular second messenger', *J Cell Biol*, 177 (4), 637-45.
- Yu, J. T., Chang, R. C. C., and Tan, L. (2009), 'Calcium dysregulation in Alzheimer's disease: From mechanisms to therapeutic opportunities', *Progress in Neurobiology*, 89 (3), 240-55.
- Zhang, M., et al. (2007), '[Effects of PBDE-47 on oxidative stress and apoptosis in SH-SY5Y cell]', *Zhonghua Lao Dong Wei Sheng Zhi Ye Bing Za Zhi*, 25 (3), 145-7.
- Zhang, W., et al. (1995), 'MODIFICATION OF FATTY-ACID DISTRIBUTION IN RAT-BRAIN LIPIDS BY DIETARY-FAT COMPOSITION', *Faseb Journal*, 9 (3), A463-A63.
- Zhang, X. L., et al. (2008), 'Cytotoxicity evaluation of three pairs of hexabromocyclododecane (HBCD) enantiomers on Hep G2 cell', *Toxicology in Vitro*, 22 (6), 1520-27.
- Zhao, G., et al. (2009), 'Burdens of PBBs, PBDEs, and PCBs in tissues of the cancer patients in the e-waste disassembly sites in Zhejiang, China', *Sci Total Environ*, 407 (17), 4831-7.

Zheng, D., et al. (2010), 'Dynamic transcriptomic profiles of zebrafish gills in response to zinc supplementation', *BMC Genomics*, 11, 553.

Zheng, W., et al. (2001), 'Transthyretin, thyroxine, and retinol-binding protein in human cerebrospinal fluid: Effect of lead exposure', *Toxicological Sciences*, 61 (1), 107-14.